Stem Cells International

Metabolic Control of Stemness and Differentiation

Lead Guest Editor: Viviana Moresi
Guest Editors: Athanassia Sotiropoulos, Giuseppina Caretti, and Alexandra Harvey

Metabolic Control of Stemness and Differentiation

Stem Cells International

Metabolic Control of Stemness and Differentiation

Lead Guest Editor: Viviana Moresi
Guest Editors: Athanassia Sotiropoulos, Giuseppina Caretti, and Alexandra Harvey

Editorial Board

Contents

Metabolic Control of Stemness and Differentiation
Viviana Moresi, Athanassia Sotiropoulos, Giuseppina Caretti, and Alexandra Harvey
Editorial (2 pages), Article ID 6865956, Volume 2019 (2019)

Oxygen Regulates Human Pluripotent Stem Cell Metabolic Flux
Jarmon G. Lees, Timothy S. Cliff, Amanda Gammilonghi, James G. Ryall, Stephen Dalton, David K. Gardner, and Alexandra J. Harvey
Research Article (17 pages), Article ID 8195614, Volume 2019 (2019)

Metabolic Phenotyping of Adipose-Derived Stem Cells Reveals a Unique Signature and Intrinsic Differences between Fat Pads
Camille Lefevre, Baptiste Panthu, Danielle Naville, Sylvie Guibert, Claudie Pinteur, Bénédicte Elena-Herrmann, Hubert Vidal, Gilles J. P. Rautureau, and Anne Mey
Research Article (16 pages), Article ID 9323864, Volume 2019 (2019)

Metabolism Is a Key Regulator of Induced Pluripotent Stem Cell Reprogramming
James Spyrou, David K. Gardner, and Alexandra J. Harvey
Review Article (10 pages), Article ID 7360121, Volume 2019 (2019)

Metformin Delays Satellite Cell Activation and Maintains Quiescence
Theodora Pavlidou, Milica Marinkovic, Marco Rosina, Claudia Fuoco, Simone Vumbaca, Cesare Gargioli, Luisa Castagnoli, and Gianni Cesareni
Research Article (19 pages), Article ID 5980465, Volume 2019 (2019)

Mitochondrial Dynamics: Biogenesis, Fission, Fusion, and Mitophagy in the Regulation of Stem Cell Behaviors
Wenyan Fu, Yang Liu, and Hang Yin
Review Article (15 pages), Article ID 9757201, Volume 2019 (2019)

The Emerging Role of Mesenchymal Stem Cells in Vascular Calcification
Changming Xie, Liu Ouyang, Jie Chen, Huanji Zhang, Pei Luo, Jingfeng Wang, and Hui Huang
Review Article (11 pages), Article ID 2875189, Volume 2019 (2019)

One-Carbon Metabolism Links Nutrition Intake to Embryonic Development via Epigenetic Mechanisms
Si Wu, Jun Zhang, Feifei Li, Wei Du, Xin Zhou, Mian Wan, Yi Fan, Xin Xu, Xuedong Zhou, Liwei Zheng, and Yachuan Zhou
Review Article (8 pages), Article ID 3894101, Volume 2019 (2019)

Mitochondrial Role in Stemness and Differentiation of Hematopoietic Stem Cells
Luena Papa, Mansour Djedaini, and Ronald Hoffman
Review Article (10 pages), Article ID 4067162, Volume 2019 (2019)

Oral Plaque from Type 2 Diabetic Patients Reduces the Clonogenic Capacity of Dental Pulp-Derived Mesenchymal Stem Cells
Antonella Bordin, Francesca Pagano, Eleonora Scaccia, Matteo Saccucci, Iole Vozza, Noemi Incerti, Antonella Polimeni, Elena Cavarretta, Isotta Chimenti, and Elena De Falco
Research Article (7 pages), Article ID 1516746, Volume 2019 (2019)

Hindawi
Stem Cells International
Volume 2019, Article ID 6865956, 2 pages
https://doi.org/10.1155/2019/6865956

Editorial

Metabolic Control of Stemness and Differentiation

Viviana Moresi,[1] **Athanassia Sotiropoulos**,[2] **Giuseppina Caretti**,[3] **and Alexandra Harvey**[4]

[1]*Department of Anatomy, Histology, Forensic Medicine & Orthopedics, Histology & Medical Embryology Section, Sapienza University of Rome and Interuniversity Institute of Myology, Italy*
[2]*Centre National de la Recherche Scientifique UMR 8104, Institut Cochin, Université Paris Descartes, Sorbonne-Paris-Cité, Paris, France*
[3]*Department of Biosciences, Università degli Studi Milano, Milan, Italy*
[4]*School of BioSciences, University of Melbourne, Parkville VIC, Australia*

Correspondence should be addressed to Viviana Moresi; viviana.moresi@uniroma1.it

Received 22 May 2019; Accepted 22 May 2019; Published 12 June 2019

Increasing evidence highlights a pivotal role for metabolism in stem cell physiology and lineage specification [1, 2]. Metabolism, indeed, is no longer considered merely an energy source nor an endpoint of gene regulation. Instead, metabolites and the nutrient environment are active players in determining intracellular signaling and enzymatic activities and consequently modulators of stem cell fate. Moreover, metabolic intermediates of cellular metabolism regulate epigenetic mechanisms, including histone modifications, DNA methylation, and noncoding RNAs, thereby modulating the global epigenome landscape and stemness [3].

This special issue brings together 9 papers to highlight recent developments in the field.

The most recent studies addressing the relevance of metabolism and nutrient availability in regulating stem cell biology are expertly reviewed. S. Wu et al. review the importance of one-carbon metabolism in mediating epigenetic modifications, i.e., DNA methylation, histone modification, and microRNAs, during embryonic development. Further, J. Spyrou et al. reviewed the critical role of the microenvironment in the retention of somatic cell memory by induced pluripotent stem cells, identifying previously poorly documented areas in this field. Lastly, C. Xie et al. review the emerging and debated role of mesenchymal stem cells in the vascular calcification process, reporting studies that support a role in facilitating vascular calcification, while others declare a protective role of mesenchymal stem cells in this process. Both these conflicting theories imply the modulations of cell-cell communications, paracrine signals, and exosomes and of the vascular microenvironment (vessel niche) that will impact cell fate.

In an extension of the role of metabolism in regulating stemness, W. Fu et al. and L. Papa et al. review the crucial role of mitochondrial dynamics in stem cell behavior and reprogramming. Changes in mitochondrial activity are no longer considered a passive consequence of metabolic reprogramming from glycolysis to oxidative phosphorylation during stem cell differentiation. Rather, the modulation of mitochondrial activity is critical for programming stem cell fate and differentiation potential [4, 5]. W. Fu et al. summarize the regulation of mitochondrial dynamics by intrinsic, extrinsic, and pharmacological factors and the impact of mitochondrial dynamics on stem cell fate, defining potential new applications in stem cell-based therapy. L. Papa et al. highlight recent advances in the emergent role of mitochondria in hematopoiesis, where the modulation of mitochondrial activity is critical for maintaining hematopoietic stem cell self-renewal potential and may be considered a tool to increase the *ex vivo* expansion of transplantable cells.

Given the strong link between metabolism and heritable changes to the epigenetic landscape, casting light on the mechanisms underlying the metabolic regulation of stem cell self-renewal and differentiation is important not only to understand tissue homeostasis in both physiological and pathological conditions but also to establish *in vitro* culture conditions which accurately replicate the physiological microenvironment to support normal cell physiology and function. To this end, J. G. Lees et al. elucidate the impact of physiological oxygen levels (5%) on human embryonic stem cells by integrating metabolic, transcriptomic, and epigenetic analyses. J. G. Lees et al. report that 5% oxygen increases glycolytic intermediates, glycogen, and the antioxidant response; reduces mitochondrial metabolism; and establishes a more permissive structure global epigenetic landscape in embryonic stem cells.

Nutrient availability also directly regulates the progression from a quiescent to an activated state of MuSC [6]. Muscle stem cells (MuSC) display low oxygen consumption and mitochondrial activity and are characterized by a specific fatty acid oxidation profile in their quiescent state. When activated, they increase glycolysis, fatty acid metabolism, and oxidative phosphorylation. Short-term caloric restriction has been shown to favor MuSC self-renewal, increasing oxidative activity and decreasing glycolysis [7]. In this special issue, T. Pavlidou et al. demonstrate that treatment with metformin, a calorie-restriction mimicking drug, *in vitro*, *ex vivo*, or *in vivo*, favors MuSC quiescence and a low metabolic state, delaying their activation and skeletal muscle regeneration.

Different metabolic features are often a signature of distinctive stem cell subpopulations. In this special issue, through high-resolution nuclear magnetic resonance metabolomic analyses of cell supernatants, C. Lefevre et al. define distinct metabolic signatures between visceral and subcutaneous adipose tissue stem cells, differentiated by their requirement for glutaminolysis and their ability to utilize pyruvate. These divergent metabolic profiles may contribute to the differing abilities of these populations to proliferate and to differentiate into adipocytes.

Alterations in metabolism have been associated with, and may contribute to, the onset or progression of numerous diseases. In support of this, A. Bordin et al. demonstrate a clear and biologically relevant effect of type 2 diabetes (T2D) patients' oral plaque in negatively regulating dental pulp stem cell clonogenicity. Their data suggest that there are key differences in plaque from T2D patients with periodontal disease (PD) relative to healthy individuals with PD which may be a result of underlying metabolic changes.

Collectively, the studies in this special issue provide insights into the metabolic control of stem cell maintenance, differentiation, and engraftment and also provide evidence for novel pharmacological interventions to manipulate stem cells. In addition, by elucidating the mechanisms underlying stem cell biology and highlighting the connections between cellular metabolism, mitochondria, and epigenetic regulation of stem cell fate, this special issue will have important implications for advances in stem cell research and reprogramming, particularly regarding novel approaches in regenerative medicine.

Conflicts of Interest

The authors declare that there is no conflict of interest regarding the publication of this editorial letter in this special issue.

Viviana Moresi
Athanassia Sotiropoulos
Giuseppina Caretti
Alexandra Harvey

References

[1] C. M. Metallo and M. G. Vander Heiden, "Understanding metabolic regulation and its influence on cell physiology," *Molecular Cell*, vol. 49, no. 3, pp. 388–398, 2013.

[2] K. Ito and K. Ito, "Metabolism and the control of cell fate decisions and stem cell renewal," *Annual Review of Cell and Developmental Biology*, vol. 32, no. 1, pp. 399–409, 2016.

[3] A. Brunet and T. A. Rando, "Interaction between epigenetic and metabolism in aging stem cells," *Current Opinion in Cell Biology*, vol. 45, pp. 1–7, 2017.

[4] D. H. Margineantu and D. M. Hockenbery, "Mitochondrial functions in stem cells," *Current Opinion in Genetics & Development*, vol. 38, pp. 110–117, 2016.

[5] C. D. Folmes, H. Ma, S. Mitalipov, and A. Terzic, "Mitochondria in pluripotent stem cells: stemness regulators and disease targets," *Current Opinion in Genetics & Development*, vol. 38, pp. 1–7, 2016.

[6] J. G. Ryall, "Metabolic reprogramming as a novel regulator of skeletal muscle development and regeneration," *FEBS Journal*, vol. 280, no. 17, pp. 4004–4013, 2013.

[7] M. Cerletti, Y. C. Jang, L. W. S. Finley, M. C. Haigis, and A. J. Wagers, "Short-term calorie restriction enhances skeletal muscle stem cell function," *Cell Stem Cell*, vol. 10, no. 5, pp. 515–519, 2012.

Hindawi
Stem Cells International
Volume 2019, Article ID 8195614, 17 pages
https://doi.org/10.1155/2019/8195614

Research Article

Oxygen Regulates Human Pluripotent Stem Cell Metabolic Flux

Jarmon G. Lees[1], **Timothy S. Cliff**[2,3], **Amanda Gammilonghi**[4], **James G. Ryall**[5], **Stephen Dalton**[2,3], **David K. Gardner**[1] and **Alexandra J. Harvey**[1]

[1]*School of BioSciences, The University of Melbourne, 11 Royal Parade, Parkville, 3010 VIC, Australia*
[2]*Department of Biochemistry and Molecular Biology, University of Georgia, 500 D.W. Brooks Drive, Athens, GA 30602, USA*
[3]*Centre for Molecular Medicine, University of Georgia, 500 D.W. Brooks Drive, Athens, GA 30602, USA*
[4]*Nanobiotechnology Research Laboratory, RMIT University, Melbourne, VIC 3010, Australia*
[5]*Centre for Muscle Research, Department of Physiology, The University of Melbourne, Melbourne, VIC 3010, Australia*

Correspondence should be addressed to David K. Gardner; david.gardner@unimelb.edu.au

Received 28 December 2018; Accepted 27 February 2019; Published 19 May 2019

Academic Editor: Antonio C. Campos de Carvalho

Metabolism has been shown to alter cell fate in human pluripotent stem cells (hPSC). However, current understanding is almost exclusively based on work performed at 20% oxygen (air), with very few studies reporting on hPSC at physiological oxygen (5%). In this study, we integrated metabolic, transcriptomic, and epigenetic data to elucidate the impact of oxygen on hPSC. Using ^{13}C-glucose labeling, we show that 5% oxygen increased the intracellular levels of glycolytic intermediates, glycogen, and the antioxidant response in hPSC. In contrast, 20% oxygen increased metabolite flux through the TCA cycle, activity of mitochondria, and ATP production. Acetylation of H3K9 and H3K27 was elevated at 5% oxygen while H3K27 trimethylation was decreased, conforming to a more open chromatin structure. RNA-seq analysis of 5% oxygen hPSC also indicated increases in glycolysis, lysine demethylases, and glucose-derived carbon metabolism, while increased methyltransferase and cell cycle activity was indicated at 20% oxygen. Our findings show that oxygen drives metabolite flux and specifies carbon fate in hPSC and, although the mechanism remains to be elucidated, oxygen was shown to alter methyltransferase and demethylase activity and the global epigenetic landscape.

1. Introduction

Oxygen is a critical, but often overlooked, metabolite within the stem cell niche. The mammalian reproductive tract, within which the preimplantation embryo develops, has been measured at 2-9% oxygen in the rat, rabbit, hamster, and rhesus monkey [1, 2]. The precise oxygen concentration experienced by the inner cell mass of the human blastocyst is unknown but likely approximates less than 5% [3–5]. In contrast, atmospheric (20%) oxygen remains the predominant concentration used for cell culture, including stem cells and human embryos, despite documented evidence of its detrimental impact [6], with limited adoption of more physiological oxygen concentrations [7].

PSC metabolism is characterized by a heavy dependenceon glycolysis, with ~50-70% of glucose being converted to lactate [8–11]. In contrast, mitochondrial oxidative phosphorylation (OXPHOS) occurs at relatively low levels in PSC compared to their differentiated counterparts [9, 12]. When cultured at 5% oxygen, hPSC increase the flux of glucose through glycolysis [11, 13, 14], increase glycolytic gene expression [11, 15], and decrease oxidative gene expression [14]. Oxygen has also been shown to regulate hPSC mitochondrial activity and biogenesis [14], as it occurs in somatic cells [16]. Physiological oxygen conditions therefore establish a PSC metabolic state characterized by increased glucose/lactate flux and suppressed mitochondrial biogenesis and activity relative to PSC developed in atmospheric oxygen. Glycolytic and mitochondrial flux in PSC also generates key epigenetic cofactors acetyl-CoA, alpha-ketoglutarate (αKG), NADH/NAD$^+$, and TCA intermediates including citrate and succinate, which maintain the highly acetylated euchromatic landscape characteristic of pluripotency, while in contrast, differentiated cell types are generally heterochromatic [17]. Currently, only

one study has looked at the impact of oxygen on hPSC epigenetic markers [18], in which 5% oxygen induced a euchromatic state in the chromatic configuration around the hypoxic response elements (HREs) of *OCT4*, *SOX2*, and *NANOG* pluripotency transcriptional promotors, leading to increased levels of H3K36me3, decreased H3K9me3, and a general increase in pluripotency markers, however none have integrated metabolic, epigenetic and transcriptomic data within a single culture system.

Oxygen is a key factor, not just in PSC culture, but in all cell, tissue, and organ cultures. However, our understanding of how oxygen acts as a nutrient and signaling molecule in PSC is limited. Because metabolism is inextricably linked to epigenetics [19–21] and, therefore, cell fate [17], it is important to define the role of oxygen in metabolic pathways. By using extracellular acidification rates (ECAR) and oxygen consumption rates (OCR) as measures of glycolysis and OXPHOS, respectively, we find that physiological (5%) oxygen levels decrease mitochondrial activity and increase glycolytic flux in hPSC. This was confirmed with heteronuclear single-quantum coherence (HSQC) nuclear magnetic resonance (NMR) spectroscopy of hPSC labeled with ^{13}C-glucose. Oxygen is therefore a key regulator of hPSC metabolism, directing the flux of glucose-derived carbon to lactate, alanine, glycogen, and glutathione at physiological oxygen and through the tricarboxylic acid (TCA) cycle to acetate at 20% oxygen. Coincident with altered intracellular metabolite flux, 5% oxygen increased acetylation and decreased methylation markers consistent with a more active gene regulatory network. RNA-seq analysis confirmed increases in transcription and glycolytic metabolism and confirmed the resulting epigenetic landscape at physiological oxygen levels. These findings show that 5% oxygen has a significant impact on intracellular metabolite fluxes in hPSC, metabolites which are known epigenetic cofactors, accompanied by increased H3K9/27ac and decreased H3K27me3. Although the mechanism remains to be elucidated, oxygen was shown to alter methyltransferase and demethylase activity influencing the global epigenetic landscape.

2. Results

2.1. Mitochondrial Activity Is Decreased at Physiological Oxygen. Mitochondrial metabolism is often considered negligible in hPSC [10, 22–24], as they are known to rely heavily on the glycolytic oxidation of glucose to lactate in the cytosol to meet their energy and biosynthetic needs [9, 19], and pluripotency is reportedly increased when the mitochondria are inhibited with antimycin A [22]. Paradoxically, attenuation of specific mitochondrial functions leads to apoptosis, tumourigenesis, or the loss of pluripotency. [25]. Significantly, the role of the hPSC mitochondria, the largest consumers of oxygen in the cell, has never been addressed under physiological oxygen conditions. Indeed, our current understanding of mitochondria, metabolism, and pluripotency is primarily based on work performed at 20% oxygen. To address this, we assessed the metabolic pathway activity of hPSC cultured under standard (20%) and physiological (5%) oxygen conditions using oxygen consumption and extracellular acidification rates.

Compared with hPSC cultured at 20% oxygen, those cultured at 5% had lower OCR signifying a lower resting mitochondrial activity (Figures 1(a) and 1(b)). Furthermore, cells cultured at 5% oxygen had reduced rates of oligomycin-sensitive oxygen consumption, consistent with a lower dependence on OXPHOS, and a lower rate of ATP production (Figure 1(c)). hPSC cultured at 5% oxygen were found to actively suppress mitochondrial activity (Figure 1(d)) but were able to match the maximum OCR of those grown at 20% oxygen when treated with the mitochondrial uncoupler FCCP (Figure 1(e)). hPSC at 20% oxygen moderated a higher basal OCR by increasing mitochondrial H^+ leak (Figure 1(f)), a strategy which limits not only ATP production but also ROS production [26]. Indeed, ROS production was not different under either oxygen condition (Figure 1(g)). Surprisingly, resting ECAR was not affected by 5% and 20% oxygen (Figure 1(i)); however, hPSC at 20% had almost four times the glycolytic reserve capacity of cells cultured at 5% (Figure 1(j)) indicating an active suppression of lactate flux at 20% oxygen. Taken together, the metabolic phenotype of hPSC grown at 5% oxygen is more glycolytic with active suppression of mitochondrial oxidative metabolism, while the metabolic phenotype at 20% oxygen makes more use of mitochondrial oxidation and has an active suppression of glycolytic metabolism (Figure 1(k)).

Clear differences in the metabolic profiles of hPSC due to oxygen in culture prompted the analysis of mitochondrial morphology by transmission electron microscopy (TEM), which has been related to mitochondrial function [9]. Irrespective of oxygen concentration, near-spherical mitochondria clustered perinuclearly and towards one pole of the nucleus with almost no evidence of elongation or reticulation (Figure 1(l)). Within the cytoplasm, the mitochondria were the most prominent organelles. At higher magnification, the hPSC mitochondrial crista structure was chaotic and disconnected lacking inner-membrane-to-outer-membrane organization, again with no apparent effect of oxygen (Figure 1(m)). This morphology is not surprising, given that the dominant mitochondrial morphology of the embryo's inner cell mass (ICM) cells is spherical, with clear matrices and few peripheral arched cristae [21, 27]. To characterize the pluripotency of the hPSC lines, we used an in vitro teratoma assay [28] to determine the germ layer differentiation potential. After 8 weeks in the presence of serum, both lines differentiated into teratomas with evidence of endoderm, mesoderm, and ectoderm tissues (Figure 1(n)). Standard pluripotency transcripts have been assessed previously and were not different due to oxygen [14]. Using ECAR, OCR, mitochondrial ROS levels, and mitochondrial morphology, we show that 5% oxygen decreases mitochondrial activity and increases flux from glucose to lactate in hPSC. These observations raised questions about the fate of glucose-derived carbon in hPSC cultured at physiological and nonphysiological oxygen.

2.2. Intracellular Metabolite Accumulation Is Regulated by Oxygen. Physiological (5%) and atmospheric (20%) oxygen results in distinct global metabolic profiles characterized by

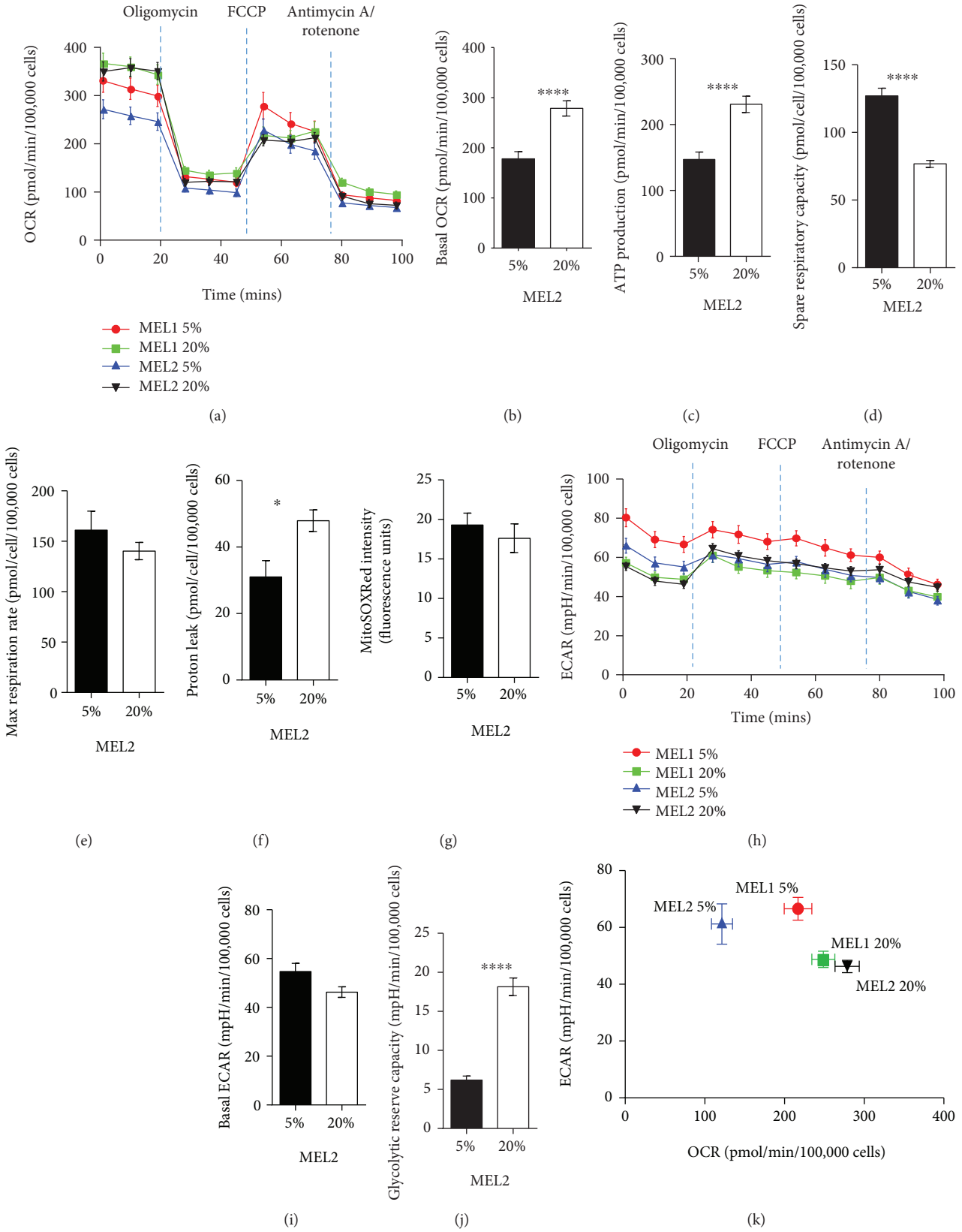

Figure 1: Continued.

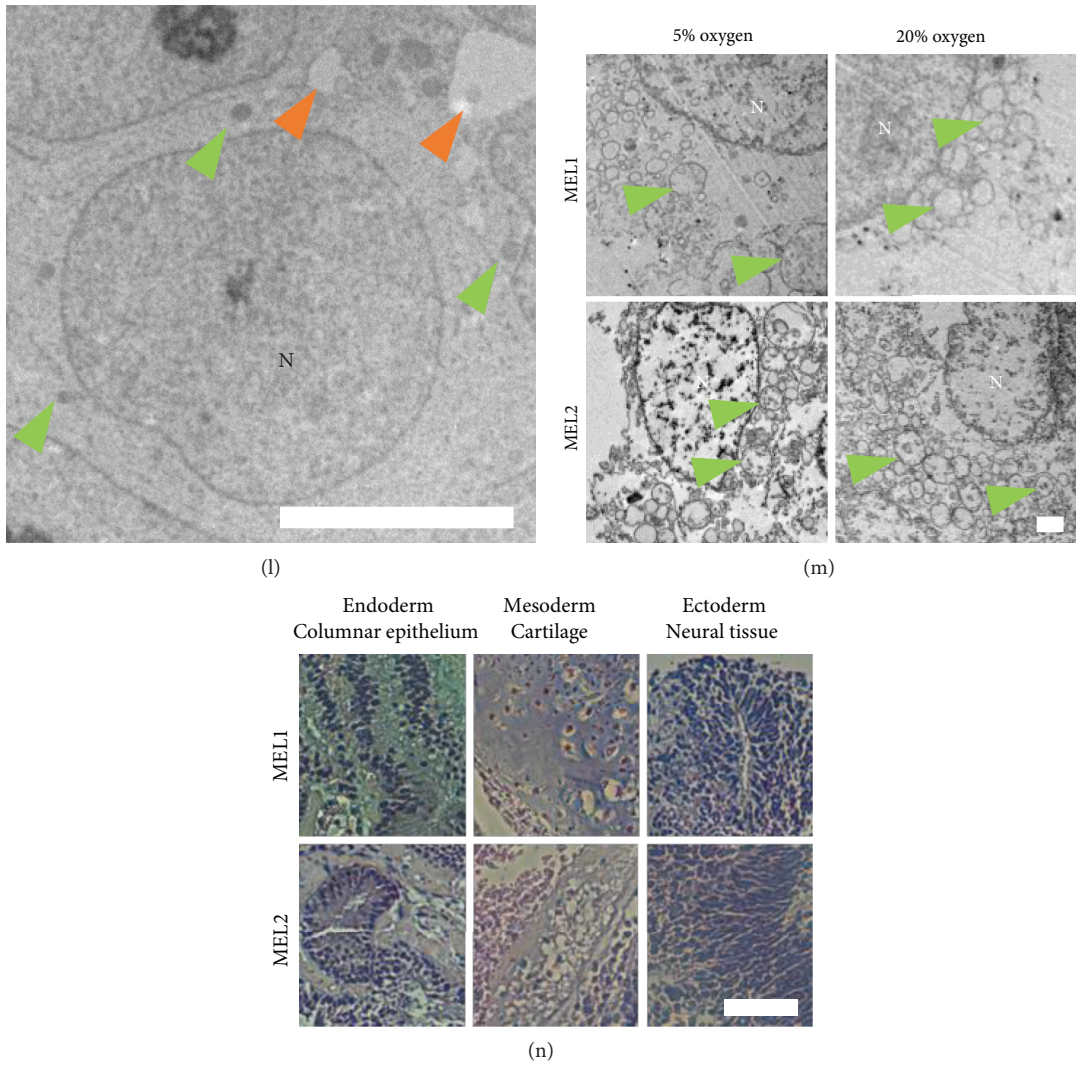

Figure 1: Physiological oxygen promotes a glycolytic metabolism in hPSC. (a) Oxygen consumption rate (OCR) analysis of MEL1 and MEL2 hPSC cultured under 5% and 20% oxygen conditions, assessed using oligomycin (1 μM), FCCP (0.3 μM), and antimycin A/rotenone (1 μM). (b–f) Basal OCR (b), ATP production (c), spare respiratory capacity (d), max respiration rate (e), and proton leak (f) as determined from OCR data. (g) Mitochondrial superoxide levels in MEL2 hPSC. (h) Extracellular acidification rate (ECAR) analysis of MEL1 and MEL2 hPSC cultured at 5% and 20% oxygen. (i–j) Basal ECAR (i) and glycolytic reserve capacity (j) determined from ECAR data. (k) Metabolic phenogram contrasting basal OCR and ECAR. (l) Transmission electron micrographs (TEM) of hPSC showing the nuclei (N), mitochondria (green arrows), and lipid droplets (orange arrows). (m) High magnification TEM of MEL1 and MEL2 hPSC identifying the mitochondria (green arrows) and their inner mitochondrial matrix development. (n) hPSC-derived in vitro teratomas showing ectoderm, mesoderm, and endoderm lineages. All assays performed in biological triplicate. Error bars represent the SEM. $^{****}p < 0.0001$, $^{***}p < 0.001$, $^{**}p < 0.01$, and $^{*}p < 0.05$ for 2-factor ANOVA flowed by simple main effects analyses. Scale bars: 5 μm (l), 2 μm (m), and 100 μm (n).

increased glycolytic and mitochondrial metabolism, respectively. To determine the underlying metabolite fluxes that contribute to these phenotypes, we performed metabolic labelling with uniformly labeled ^{13}C-glucose, followed by NMR-based fluxome analysis [29]. This methodology delivers a quantitative and temporal description of the metabolic landscape. Because we have demonstrated here, and previously by extracellular metabolite profiling [11, 14, 30], that oxygen impacts glycolytic flux, we focused primarily on this pathway for ^{13}C flux analysis. hPSC adapted to either 5% or 20% oxygen culture were labeled with ^{13}C-glucose over 0-4 h, and H,C-HSQC NMR spectroscopy was performed on polar and nonpolar cell fractions (Figure 2(a)). This time course allows us to track the fate of ^{13}C, the source of metabolites contributing to glycolytic fluxomes and pathway utilization, without the saturation problems associated with longer periods of metabolic labeling [19, 29], or the limitations of endpoint metabolic analyses as performed previously.. Representative spectra are shown in Figures 2(b) and 2(c). Following labeling with ^{13}C-glucose, we quantified the levels of ^{13}C-labeled metabolites (Figure 2(d)). The analysis included the quantitation of metabolites in the glycolytic pathway, tricarboxylic acid (TCA) cycle, transhydrogenase cycle, glutamate-glutamine cycle, and generation of

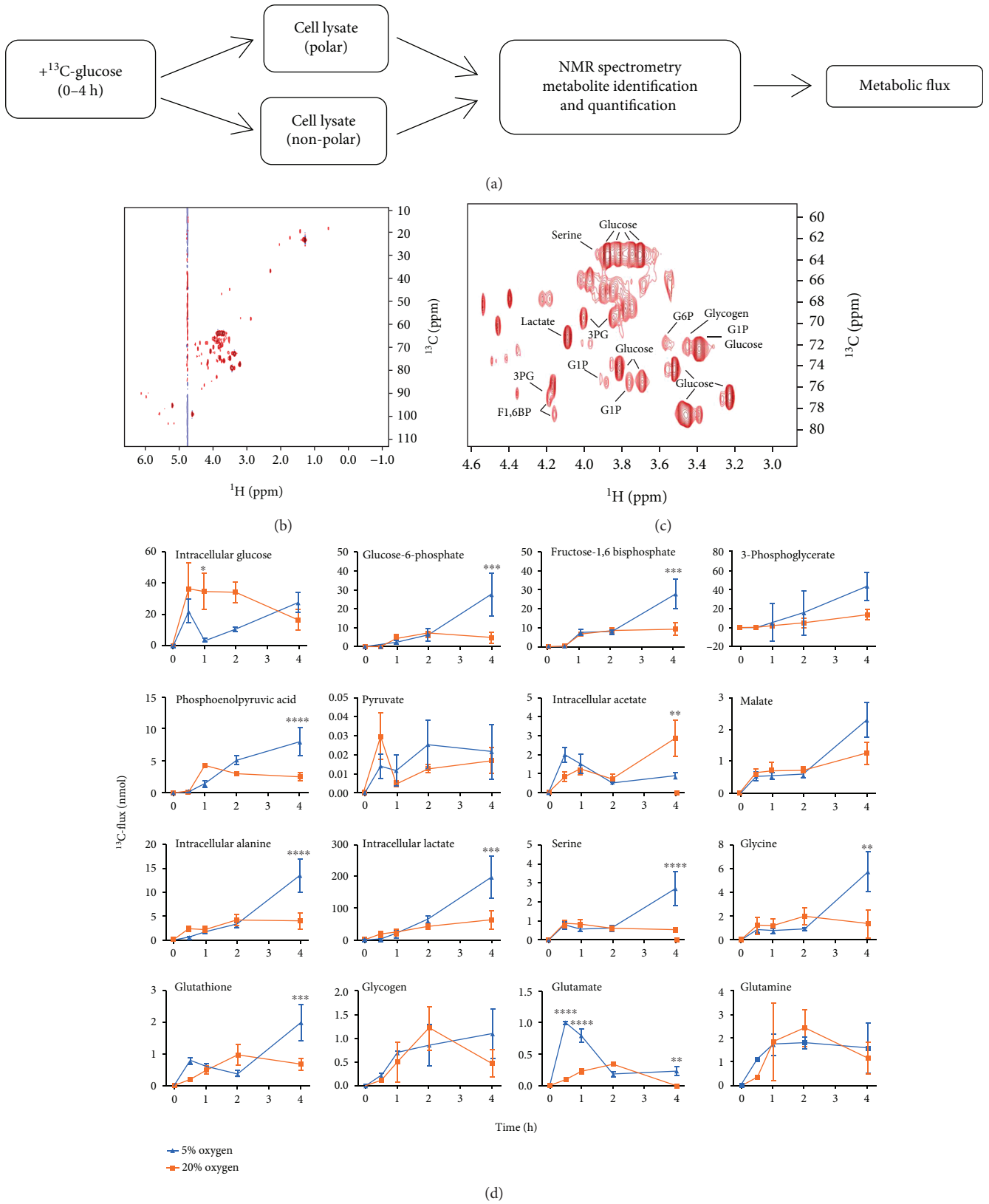

FIGURE 2: Intracellular glucose-derived metabolites accumulate more rapidly under physiological oxygen. (a) ^{13}C-glucose fluxomics workflow using NMR. (b–c) Representative 2D ^{1}H-^{13}C HSQC NMR spectra (b). Magnification of NMR spectrum showing representative metabolites (c). Each peak is a quantifiable carbon-hydrogen bond from a metabolite. (d) ^{13}C-flux analysis over 0–4 hours of MEL2 hPSC cultured under 5% or 20% oxygen. Measurements are of intracellular metabolite levels. All assays performed in biological triplicate. Error bars represent the SEM. $^{****}p < 0.0001$, $^{***}p < 0.001$, $^{**}p < 0.01$, and $^{*}p < 0.05$ for paired Student's t-test.

glutathione (GSH), acetate, glycogen, and amino acids. For example, we have previously measured the extracellular levels of alanine and lactate which were unchanged and increased, respectively, in response to 5% oxygen [14]. In the current study, we observed that intracellular accumulations of both alanine and lactate were unchanged by oxygen between 0 and 2 h but both increased 3-fold between 2 and 4 h (Figure 2(d)). Temporal fluxomics, therefore, is a powerful tool for identifying underlying metabolite fluxes prior to nutrient depletion over time. This analysis can also highlight key points of differential metabolic regulation due to oxygen. For example, our analysis suggests that hexokinase (HK) activity is saturated at 20% oxygen, indicated by the accumulation of intracellular glucose relative to glucose-6-phosphate (Figure 2(d)). This pattern is not observed at 5% oxygen, strongly suggesting that HK activity is oxygen regulated. This analysis shows that rates of metabolite accumulation associated with glycolysis are higher at 5% oxygen. Intracellular lactate and alanine showed a similar pattern (Figure 2(d)). Acetate and malate, TCA cycle metabolites, were also quantified (Figure 2(d)) where the only metabolite that accumulated more at 20% oxygen was acetate, indicating that flux through the TCA cycle may be elevated at 20% oxygen relative to 5% oxygen in hPSC. These data are consistent with ECAR and OCR analyses in Figure 1 showing elevated glycolysis at 5% oxygen and elevated mitochondrial oxidation at 20% oxygen.

2.3. Metabolic Flux Is Greater at Physiological Oxygen. Heatmaps of metabolite accumulation over time within oxygen treatments describe a rapid increase in all metabolic pathways at 5% oxygen, primarily between 2 and 4 h (Figure 3(a)), indicating hPSC have a faster metabolic rate under physiological oxygen conditions. At 20% oxygen, however, overall metabolite accumulation slowed, with only lactate and the TCA cycle metabolites malate and acetate increased between 2 and 4 h (Figure 3(a)) suggesting diversion of glucose products to alternative pathways. Contrasting oxygen conditions directly at each timepoint (Figure 3(b) and Supplementary Figure S1), glucose-derived intracellular metabolite levels were not significantly different between 0 and 2 h; however, at 5% oxygen, increased lactate, alanine, glycogen synthesis, and GSH production were observed by 4 h. These data clearly show that intracellular metabolites are oxygen regulated, plausibly by oxygen-sensitive metabolic enzymes. ROS production was not increased by low oxygen as has been suggested [21, 31], although levels of GSH and its precursors serine and glycine were higher, plausibly mitigating ROS levels. These findings confirm that oxygen, an easily controllable, physiologically relevant nutrient in cell culture, plays a leading role in defining the intracellular metabolite landscape in hPSC.

2.4. Physiological Oxygen Promotes H3K9/H3K27 Acetylation and Represses H3K27 Trimethylation. We have shown that oxygen controls the direction and magnitude of glucose-derived carbon flux within hPSC. Several metabolites which can be derived from glucose are epigenetic modifiers and cofactors which are required for the modulation of the epigenetic landscape [17, 32]. Global acetylation levels of H3K9 and H3K27 increased ~75% in hPSC cultured at 5% oxygen relative to those at 20% oxygen (Figure 4(a)). Global trimethylation of the transcriptional repressor H3K27 was 3-fold lower at 5% oxygen (Figure 4(a)). Taken together, this epigenetic profile is consistent with a more open chromatin structure at physiological oxygen [18]. RNA-seq of hPSC cultured long-term at 5% and 20% oxygen (Figure 4(b) and Supplementary Table 1) confirmed a more active transcriptome at 5% oxygen. Upregulated differentially expressed gene (DEG) counts were higher at 5% oxygen in the two hPSC lines assessed (Figure 4(c)). The cluster analysis of DEGs was consistent with ^{13}C flux analyses (Figure 4(d)), highlighting glycolysis as the most highly enriched functional cluster at 5% oxygen, followed by H3K27 demethylation. Glycolytic genes upregulated at 5% oxygen included *LDHA*, *PGK1*, and glucose transporters *SLC2A1* (*GLUT1*) and *SLC2A14* (*GLUT14*) (Figure 4(e)). Several of these transcripts have been independently validated by qPCR and microarray and confirmed to be oxygen-regulated in a consistent manner with the current findings [11, 15]. The RNA-seq data also confirms the increased carbon flux through glycolytic pathways (Figure 2(d)) and reduced H3K27me3 staining (Figure 4(a)) observed at 5% oxygen.

Further interrogation of RNA-seq data revealed the overall transcriptional response to oxygen conformed to a more open chromatin structure at 5% oxygen (Figures 4(e) and S2). In response to 5% oxygen, 46 and 47 DEGs were upregulated >2-fold in MEL2 and MEL1 hPSC lines, respectively. Transcripts upregulated at 5% oxygen in addition to the glycolytic genes mentioned previously include proteins that contribute to extracellular matrix organization (*PCDH10*, *FBN1*, *VCAN*, and *POSTN*), pro-apoptotic factors in response to mitochondrial damage (*BNIP3*), cell cycle (*BTG2*), early embryonic methylation patterning (*BORIS*), and signal transducers including hypoxia inducible factor-(HIF-) related genes (*ANXA3*, *GDF15*, *IFGBP2*, and *IFGBP5*). In response to culture at 20% oxygen, only 3 and 2 DEGs were upregulated >2-fold in the MEL2 and MEL1 hPSC lines, respectively. Of interest, follistatin (*FST*) which has a high affinity for activin A and leads to hPSC differentiation [33] was increased at 20% oxygen (Supplementary Figure S2). Consistent with previous reports [11, 14, 34–36], the remodeling of the metabolome did not coincide with a pronounced change in the majority of pluripotency markers. Pluripotency markers *OCT4*, *NANOG*, *MEIS1* *OTX2*, *SOX11*, *GDF3*, *REX1*, *FGF4*, *DPPA2*, *DPPA4*, and *hTERT* were unaltered due to oxygen (Supplementary Figure S3A). At 5% oxygen, the expression of the pluripotency marker *OCT6* (*POU3F1*) [37] was increased in both lines, while *SOX2* and *DNMT3B* were decreased in the MEL1 and both hPSC lines, respectively (Supplementary Figure S3). However, none of these genes reached the $\log_2(fc)=1$ threshold.

In order to understand more the transcriptional response to oxygen, we interrogated RNA-seq data to identify oxygen-regulated networks based on the identified DEGs. NetworkAnalyst [38] was used to generate zero-order protein-

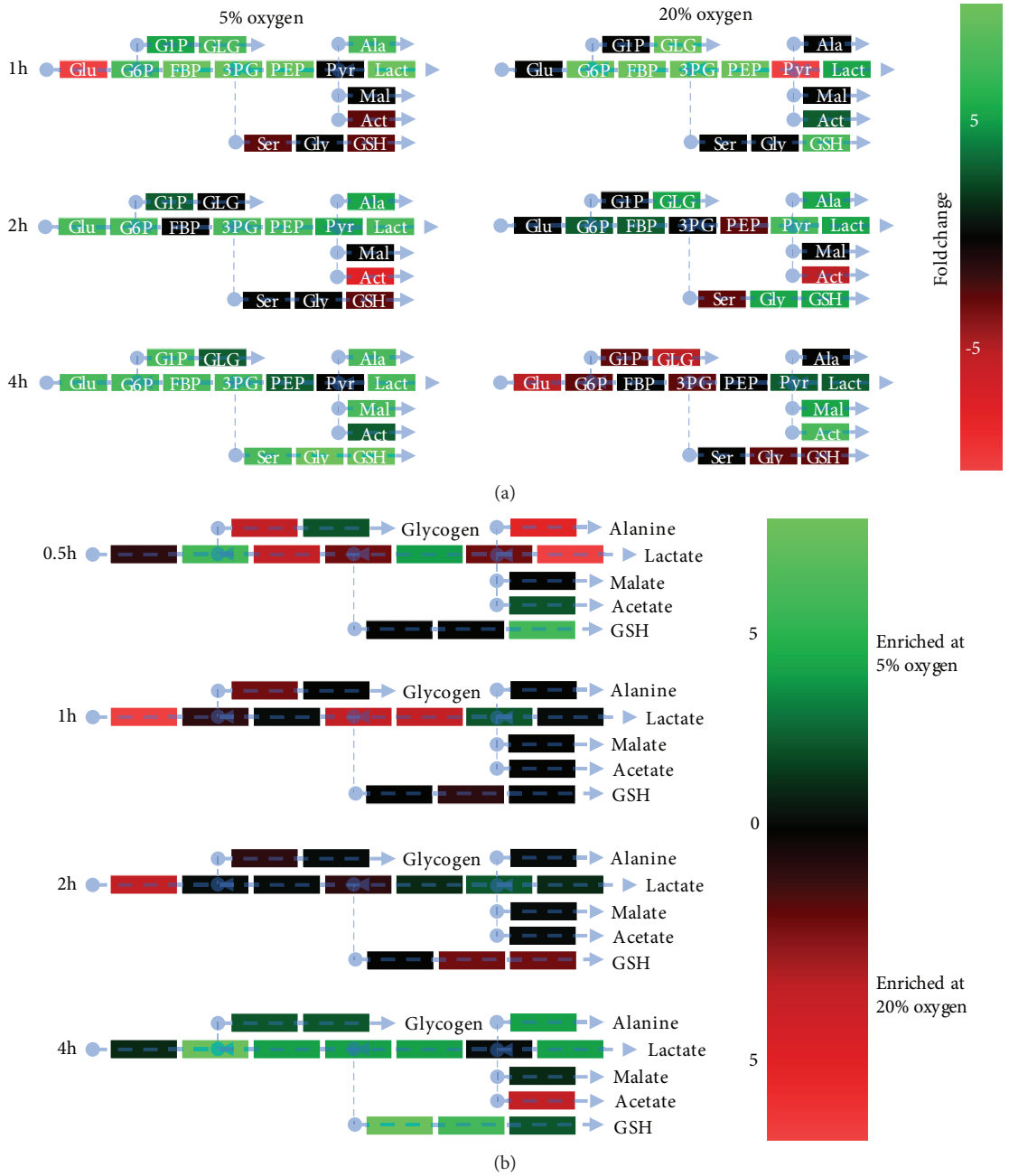

Figure 3: 5% oxygen stimulates glycolytic, glutathione, glycogen, and alanine accumulation in hPSC over time. (a) Heatmap comparing intracellular metabolite levels to those of the previous timepoint, organized into functional groups. Data are the fold change. Green indicates an increase from the previous timepoint. Red indicates a decrease from the previous timepoint. (b) Heatmap showing the enrichment of intracellular metabolites between hPSC cultured at 5% and 20% oxygen at each timepoint. Green indicates an enrichment at 5% relative to 20% oxygen. Red indicates an enrichment at 20% relative to 5% oxygen. All assays performed in biological triplicate.

protein networks based on known protein interactions of significant DEGs (Figures 5(a)–5(d)). Subsequent KEGG pathway analysis of hPSC networks upregulated at 5% oxygen highlighted glycolysis most prominently, followed by focal adhesion and pentose phosphate pathway activity (Figures 5(b) and 5(d)). In hPSC cultured at 20% oxygen, cell cycle was the most enriched pathway, followed by RNA transport and protein processing in the endoplasmic reticulum. These pathway enrichments based on known networked interactions were similar to GO and KEGG analyses performed using all DEGs, in which glycolysis, amino acid and carbon metabolism, and the HIF-1 hypoxic response were enriched at 5% oxygen (Supplementary Figures S3B and S4). As expected, *HIF-1α*, *HIF-1β*, and *HIF-2α* were not oxygen regulated at the mRNA level; however, HIF-1 target genes *ENO1*, *SERPINE1*, *ENO2*, *VEGFA*, *SLC2A1*, *EGLN1*, *PDK1*, *HK2*, *MAP2K1*, and *PFKFB3* were significantly increased at low oxygen (Supplementary Figure S3B). At

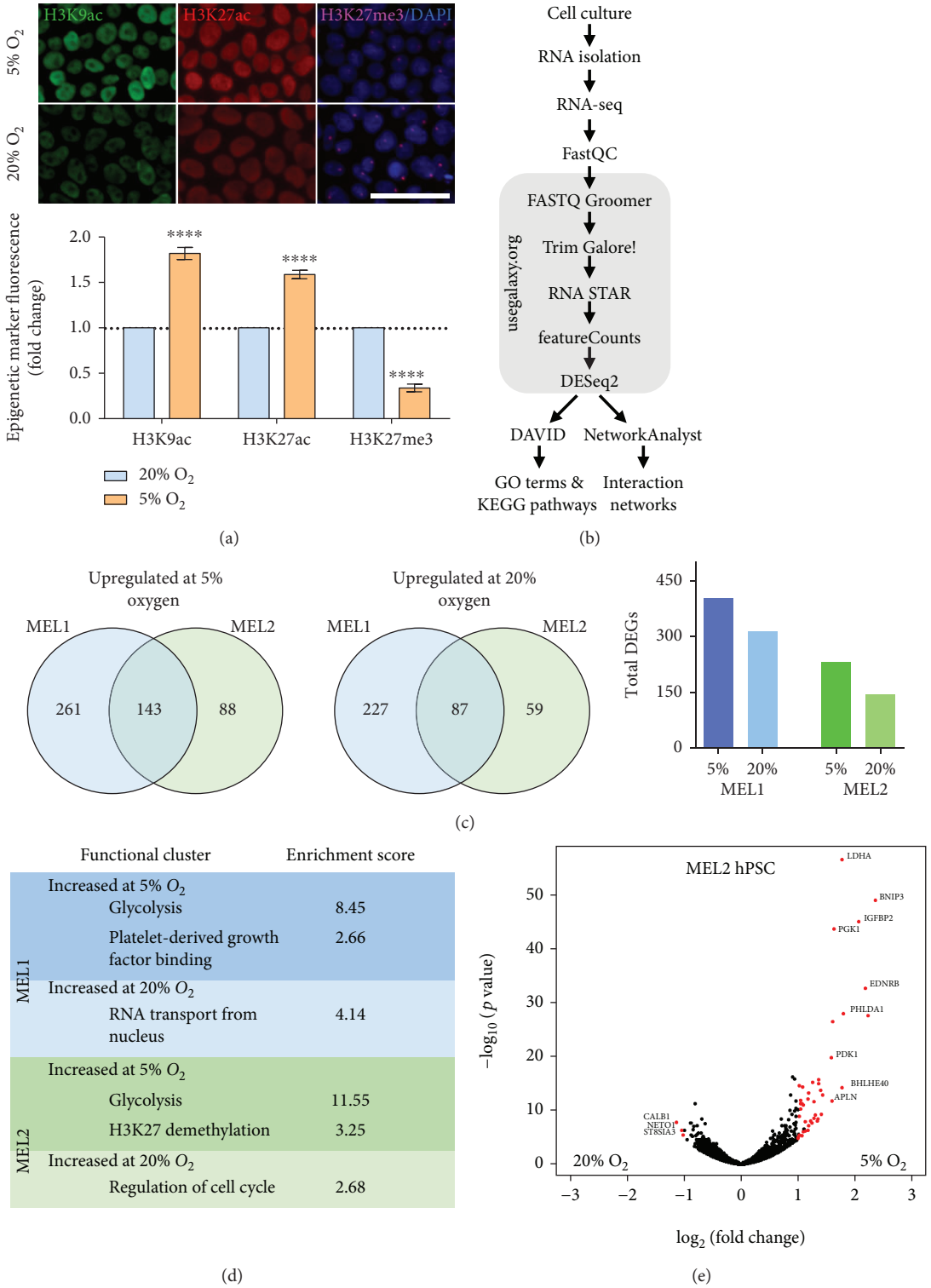

Figure 4: Global acetylation is increased, and methylation is decreased at 5% oxygen. (a) H3K9ac, H3K27ac, and K3K27me3 fold change of MEL2 hPSC at 5% relative to 20% oxygen. Scale is 50 μm. (b) Workflow for RNA-seq analysis using https://usegalaxy.org/, DAVID, and NetworkAnalayst. (c) Venn diagrams showing the overlap of genes upregulated in two hPSC lines at 5% oxygen and 20% oxygen and total DEG count. (d) Functional clusters with enrichment scores greater than 2 derived from *Biological Process* and *Molecular Function* GO terms. (e) Volcano plot of MEL2 hPSC transcriptional response to 5% and 20% oxygen. Red genes indicate a fold change value greater than 2 and an adjusted p value (Benjamini FDR) less than 0.05. All assays performed in biological triplicate. Error bars represent the SEM. $^{****}p < 0.0001$ for paired Student's t-test.

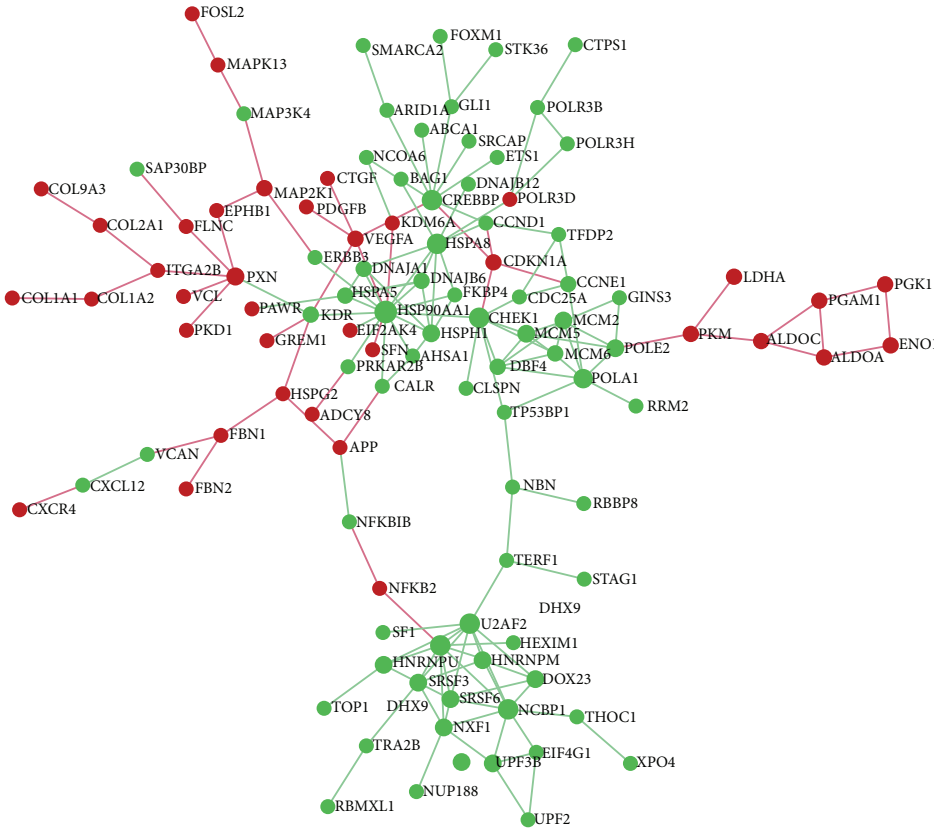

(a)

Upregulated at 5% oxygen

Pathway	Hits	*p* value
Glycolysis / gluconeogenesis	7	8.80E-08
Focal adhesion	10	1.60E-07
ECM-receptor interaction	5	0.00014
VEGF signaling pathway	4	0.00112
Osteoclast differentiation	4	0.00577
Renal cell carcinoma	3	0.00578
Glioma	3	0.00722
Pathways in cancer	6	0.0104
Pentose phosphate pathway	2	0.0118
Progesterone-mediated oocyte maturation	3	0.0128
Bladder cancer	2	0.0136
Prostate cancer	3	0.016
Gap junction	3	0.017
GnRH signaling pathway	3	0.0197
Fructose and mannose metabolism	2	0.0205
MAPK signaling pathway	5	0.0217
Regulation of actin cytoskeleton	4	0.0246
Pyruvate metabolism	2	0.0262

Upregulated at 20% oxygen

Pathway	Hits	*p* value
Cell cycle	11	4.67E-09
RNA transport	7	9.11E-05
Pyrimidine metabolism	6	0.000212
p53 signaling pathway	4	0.00276
mRNA surveillance pathway	4	0.00542
Prostate cancer	4	0.00668
Purine metabolism	5	0.0131
Pathways in cancer	7	0.0167
Protein processing in endoplasmic reticulum	4	0.0254

(b)

Figure 5: Continued.

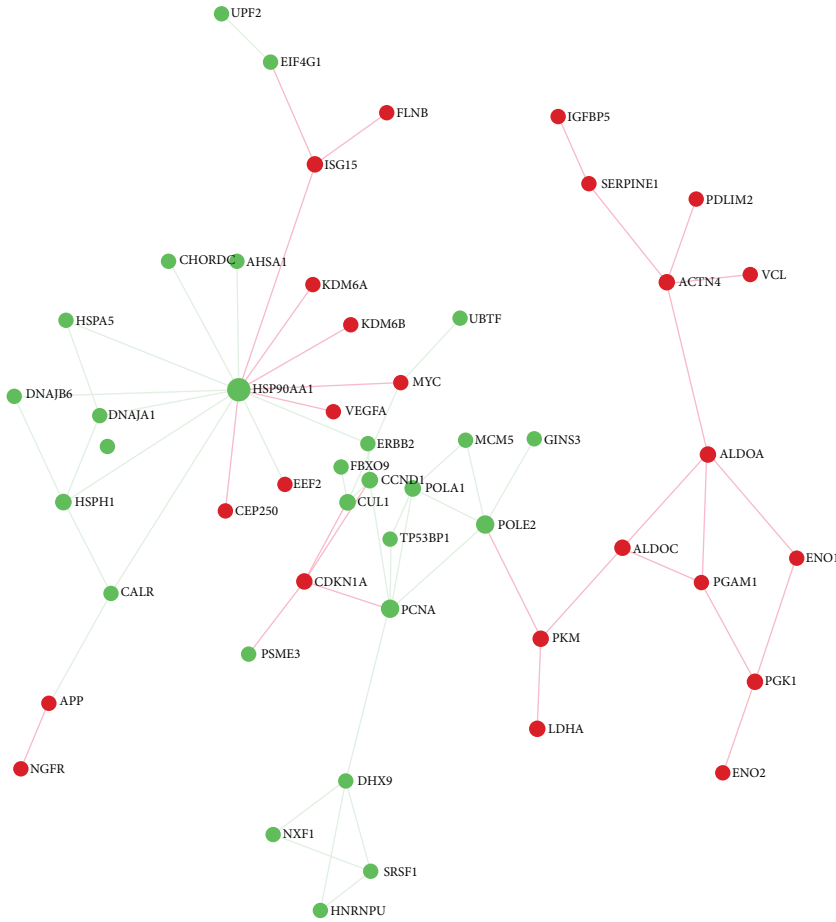

(c)

Upregulated at 5% oxygen

Pathway	Hits	*p* value
Glycolysis / gluconeogenesis	8	3.49E-11
Pentose phosphate pathway	2	0.00463
Focal adhesion	4	0.00618
Fructose and mannose metabolism	2	0.00815
Pyruvate metabolism	2	0.0105
p53 signaling pathway	2	0.0274
Adherens junction	2	0.0289
Chronic myeloid leukemia	2	0.0313
ErbB signaling pathway	2	0.0431

Upregulated at 20% oxygen

Pathway	Hits	*p* value
Cell cycle	4	0.000667
Prostate cancer	3	0.00292
HTLV-I infection	4	0.00386
Bladder cancer	2	0.00422
RNA transport	3	0.00826
Protein processing in endoplasmic reticulum	3	0.00881
Non-small cell lung cancer	2	0.0132
Pancreatic cancer	2	0.0225
mRNA surveillance pathway	2	0.031
Pyrimidine metabolism	2	0.0455

(d)

Figure 5: RNA-seq zero-order networks in hPSC due to 5% and 20% oxygen culture. (a) MEL1 hPSC differentially expressed genes due to oxygen were submitted to NetworkAnalyst and connected based on known protein:protein interactions. Red nodes are upregulated at 5% oxygen; green nodes are upregulated at 20% oxygen. Green/red intensity indicates the degree of fold change as indicated in the figure. (b) MEL1 hPSC KEGG pathways upregulated at 5% and 20% oxygen based on the zero-order network in Figure 5(a). (c) MEL2 hPSC zero-order and protein:protein interaction network. (d) MEL2 hPSC KEGG pathways upregulated at 5% and 20% oxygen based on the zero-order network in (c).

20% oxygen, terms related to cell cycle transitions were consistently enriched despite no evidence that oxygen affects the proliferative capacity of either of the hPSC lines used [14]. Under both oxygen conditions, chemokine signaling was decreased in the MEL1 line relative to that in the MEL2 line (Supplementary Figures S5A–S5D).

Together, these results demonstrate that a physiological oxygen concentration of 5% is able to globally increase acetylation and decrease methylation levels, plausibly responsible for the significant transcriptional response observed and consistent with a more open chromatin structure. This response not only includes the expected glycolytic and hypoxic response transcripts but is also enriched for genes in a range of metabolic pathways and those that contribute to the extracellular matrix. In contrast, an atmospheric oxygen concentration of 20% results in a repressed hPSC epigenetic profile as indicated by lower acetylation, higher methylation, and lower transcriptional activity. Overall, these results support a role for oxygen in determining the hPSC epigenetic landscape and implicate metabolites in this process, downstream of the change in oxygen.

2.5. Concurrent Methyltransferase and Demethylase Regulation by Oxygen. The results presented in the preceding paragraphs indicate that a change in oxygen is sufficient to alter hPSC histone methylation status. Next, we examined the transcript levels of methyl donors through the serine/glycine biosynthesis pathway and downstream methionine and folate cycles using RNA-seq data and qPCR (Supplementary Figure S6 and Supplementary Table 1). Glycolytic enzymes *LDHA*, which converts pyruvate to lactate, and *PGK1*, which catalyzes 1,3-bisphosphoglycerate metabolism to 3-phosphoglycerate (3PG), were also increased (Supplementary Figure S6A and Supplementary Table 1). 3PG marks the crossroads where carbon can either continue through glycolysis or be directed into the serine/glycine pathway. While intracellular levels of serine and glycine were increased at 5% oxygen, enzymes necessary for their synthesis were not regulated by oxygen (Supplementary Figure S6B). Plausibly, the mass effect of carbon flux through glycolysis is sufficient to increase serine/glycine production. Subsequent flux through the transsulphuration pathway to form cysteine and GSH is increased despite lower levels of *CBS* at 5% oxygen (Supplementary Figure S6C). Quantification by qPCR established that approximately half of the assessed enzyme transcript levels in the folate and methionine cycles were decreased at 5% oxygen, while the remaining genes were unaltered (Supplementary Figures S6D and S5E and Supplementary Table 1). From the RNA-seq analysis, folate cycle enzyme transcripts for *MTHFR* and *MTHFD1L* were downregulated at 5% oxygen, while *SHMT2* and *GLDC* were unaltered (Supplementary Figure S6D). In the methionine cycle, transcripts for *MAT2A*, *DNMT1*, and *DNMT3B* were downregulated, while those for *MAT2B*, *DNMT3A*, and *DNMT3L* remained unchanged (Supplementary Figure S6E). Consistent with a reduction in histone methylation, *MAT2A* was decreased at 5% oxygen. MAT2A interacts with the histone-lysine *N*-methyltransferase EZH2 [39], which also decreased at 5% oxygen (Supplementary Figure S6F), to specifically methylate H3K27 [40]. MAT2A is also responsible for the formation of the methyl donor S-adenosylmethionine (SAM) from methionine [32, 41], which donates a methyl group to histones or DNA. As*DNMT1* and *DNMT3B* were likewise downregulated at 5% oxygen, they may in part be responsible for reducing DNA methylation capacity although this was not assessed. Finally, in parallel with reduced histone methylation capacity through reduced *EZH2*, *MAT2A* expression and reduced global H3K27me3 (Figure 4(a)), RNA-seq analysis showed that lysine demethylases (KDMs) which remove methyl groups from histones were upregulated at 5% oxygen (Supplementary Figure S6F). *Lysine demethylase 7A* (*KDM7A*), *KDM6A*, *KDM4B*, and *KDM3A* were upregulated by more than 50%, while *KDM6B*, which specifically demethylates H3K27me3 [42, 43], was upregulated by 260% (Supplementary Table 1). Overall, these findings begin to show a link between a change in oxygen and the hPSC epigenetic landscape, suggesting a role for oxygen-regulated metabolites and enzymes in the process.

3. Discussion

Previous analyses of hPSC metabolism and its role in pluripotency have been described in cells cultured under 20% oxygen (5% CO2 in air; atmospheric). We have established that hPSC mitochondrial respiration is decreased at 5% oxygen, despite the absence of any apparent alterations to inner mitochondrial matrix organization. Beyond the production of ATP, mitochondrial respiration also generates ROS as H_2O_2 from complex III of the electron transport chain [44], which are thought to increase under conditions of low oxygen [31]. Compared with their better known role in DNA damage when in excess, ROS have been shown to directly alter the epigenetic landscape [45] by directly oxidising the methyl group of 5mC preventing methylation [46] and inducing DNA methylation at the promotor regions of acetyltransferases and methyltransferases [47]. Our study, however, reveals that a physiological concentration of oxygen did not elicit a change in steady-state ROS levels. Instead, intracellular glutathione production was doubled, plausibly mitigating any excess ROS production. The oxygen-regulated mechanisms driving hPSC acetylation and methylation may therefore be related to the altered metabolite fluxes we observed in this study.

A euchromatic state was established at 5% oxygen, consisting of increased global H3K9/27 acetylation and reduced H3K27 trimethylation. Metabolite levels and pathway fluxes alter the epigenetic landscape, potentially regulating global or localized patterns of genes to elicit cell fate [20, 21, 48, 49]. We show that 5% oxygen increases glucose-derived carbon flux, which feeds into serine/glycine biosynthesis, glycogen, lactate, alanine, and glutathione production. Despite elevated levels of serine, glycine, and glutathione at 5% oxygen, we observed depressed expression of enzymes throughout the folate and methionine cycles, which are necessary for the production of key methyltransferases such as SAM and EZH2 [40, 41]. *MAT2A*, but not *MAT2B* expression,

which together generate EZH2 and SAM from methionine, was also downregulated at 5% oxygen. In support of this, an identical *MAT2A*/*B* expression pattern is observed when methionine is removed from hPSC culture [32], leading to a reduction in SAM synthesis and a reduction in global methylation consistent with our findings. The repressed expression of key methyltransferase enzymes and the corresponding decrease in methylation at 5% oxygen is consistent with the profile of enhanced pluripotency [17]. Indeed, the acquisition of naïvety in mouse PSC is associated with demethylation events, specifically of H3K27me3 [19]. While oxygen did not generally affect pluripotency at a transcriptional level, consistent with several previous assessments [11, 14, 34–36], physiological oxygen was shown to promote a metabolome and epigenetic landscape characteristic of pluripotency. It is plausible that HIF signaling is partly responsible for the metabolic profile and therefore shift in physiology established at 5% oxygen, as over half of the upregulated HIF target genes function in glycolysis, consistent with the observed increases in glycolytic metabolism.

A question arising from our work is why 5% oxygen resulted in the lower accumulation of intracellular acetate coincident with higher global H3K9/27 acetylation. Of all assessed metabolites, only acetate, an essential metabolite for most cancers [50], was less present under 5% oxygen culture. Upon hPSC differentiation, global H3K9/27ac is lost; however, acetate supplementation is able to completely reverse this [17]. Notably, acetylation by acetate is achieved only after its conversion to acetyl-CoA, which is primarily formed through glycolytic-derived pyruvate. Pyruvate is metabolised to citrate in the mitochondria which is then exported to the cytosol where it is metabolised to acetyl-CoA [51], thus bypassing acetate. The lower accumulation of glucose-derived acetate at 5% oxygen may therefore signal a higher demand for acetyl-CoA for acetylation purposes.

Several key epigenetic cofactors can be derived from glucose metabolism and, thus, are potentially influenced by oxygen. The production of cytosolic acetyl-CoA requires glycolytic metabolism of citrate, while acetyl-CoA produced in the mitochondria from fatty acids is metabolised through the TCA cycle [51]. The current study cannot definitively conclude that the increased acetylation is glucose-derived; however, increased carbon flux through glycolysis such as that observed in this study at 5% oxygen has been shown to reduce deacetylase activity through reduced NAD^+ availability [52] and increase acetylation through glucose-derived acetyl-CoA [17]. Conversely, the observed reduction in histone methylation at 5% oxygen is likely due to the global increase in histone demethylases and general decrease in methyltransferase enzyme transcripts *MAT2A* and *EZH2* [53]. Furthermore, the downregulation of DNMTs at 5% oxygen is consistent with the global DNA methylation pattern seen in the 4-cell and blastocyst stage bovine embryo in response to oxygen [54], suggesting that the totipotent and pluripotent developmental stages represent heightened windows of sensitivity to oxygen concentration. Taken together, these data implicate the higher glycolytic flux generated at 5% oxygen in both the accumulation of acetylation and loss of methylation marks. These findings could be enhanced by tracing the origin of the acetyl groups on histone tails.

In this report, we show that physiological oxygen (5%) promotes a euchromatic state, increasing acetylation, activating demethylases, and deactivating methyltransferases, providing a basis for explaining how oxygen could influence hPSC by providing a more flexible transcriptional state. Moreover, this euchromatic state at 5% oxygen coincides with a wave of transcriptional activity and a time-dependent increase in the flux of glucose-derived carbon through multiple metabolic pathways. The requirement for pluripotent cells to maintain specific metabolic, epigenetic, and transcriptional profiles implicates oxygen as a key developmental regulator through its ability to influence metabolism. These findings have broad implications because the role of oxygen in metabolism, transcription, and epigenetics has obvious implications for all aspects of pluripotent cell culture, including differentiation assays, and disease modelling.

4. Materials and Methods

4.1. Cell Culture. hPSC MEL1 and MEL2 (Australian Stem Cell Centre) were cultured in mTeSR1™ medium (Stem Cell Technologies) on PSC qualified Matrigel™- (BD Biosciences) coated tissue culture plates (BD Biosciences). Cells were cultured in humidified CB 150 incubators (Binder Inc.) at 37°C with 5% CO_2 in air (20% oxygen), or 5% CO_2 and 5% O_2, and balanced with N_2. Cell passaging took place every 5 days using Dispase (Stem Cell Technologies), and the medium was refreshed every 24 h in a biosafety cabinet. To minimize exposure to 20% oxygen conditions during handling, the medium was preequilibrated under each respective oxygen condition. All cell cultures were acclimated to 5% or 20% oxygen conditions for a minimum of 2 passages before use.

4.2. Cellular Bioenergetics. hPSC were treated with Y-27632 (10 μM; AdipoGen) for 1 h prior to dissociation with TrypLE Select (Invitrogen) and seeded as single cells at a density of 40,000 cells/well in Seahorse XF24 assay microplates (In Vitro Technologies) and cultured at 5% or 20% oxygen. For cell number determination, a parallel seeding of 40,000 cells/well of a 96-well clear bottom plate (Falcon) in mTeSR1™ + Y-27632 was performed. After 24 h, the medium was refreshed with mTeSR1™, and after a further 24 h, cells in the assay plate were prepared for analysis. Cells were rinsed with 500 μL of warmed (37°C) Seahorse XF base medium (In Vitro Technologies) containing 13.7 mM glucose, 0.392 mM sodium pyruvate, and 2.94 mM L-glutamine (the levels found in mTeSR1™) at pH 7.4. A final volume of 630 μL was added to the assay plate before it was placed in a 1% CO_2 incubator for 1 h to stabilize the pH of the assay medium and the plate. A standard mitochondrial stress test assay (Seahorse Bioscience/In Vitro Technologies) was performed with an initial basal recording followed by sequential injections of oligomycin (1 μM final), carbonyl cyanide-p-trifluoromethoxyphenylhydrazone (FCCP; 50 nM final) and rotenone/antimycin A (1 μM final) every 24 minutes. Cells parallel seeded on clear 96-well plates were fixed in 70% ethanol and stained with DAPI. To determine the cell number, 5 representative images were taken of the cell

monolayer from each of 4 separate wells and analyzed using ImageJ, and the average cell number quantitated after adjusting for the well surface area. Assay results were normalized to the cell number, and metabolic parameters were determined using the publicly available Seahorse XF Cell Mito Stress Test Report Generator (Agilent Technologies).

4.3. Transmission Electron Microscopy. Approximately 4 million hPSC per treatment were processed for TEM using a protocol adapted from Underwood et al. [55]. hPSC were washed with 0.1M cacodylate buffer and then fixed for 30 min in cacodylate buffer containing 1% glutaraldehyde and 1% PFA at pH 7.4. Fixed cells were scraped and then centrifuged at 300g for 3 min and rinsed in cacodylate buffer 3 times. Pelleted cells were stained with 1% osmium tetroxide for 30 min, rinsed with cacodylate buffer, and then dehydrated through an ethanol gradient as follows: 50% ethanol for 10 min, 70% ethanol for 10 min, 90% ethanol for 10 min, 95% ethanol for 10 min, 100% ethanol for 15 min, and 100% electron microscopy grade ethanol for 30 min. Samples were then infiltrated with 200 μL resin (50% absolute acetone: 50% resin) in an open tube under agitation for 2 h. Resin was refreshed and infiltrated for 4 h under vacuum, then set in 100% resin at 80°C. Samples were sliced with a microtome, fixed to TEM grids, and imaged using a Jeol 2100F transmission electron microscope with an Oxford X-MaxN 80 T EDXS detector (Oxford Instruments), an EELS Spectrometer imaging filter (Gattan), and an Orius SC1000 CCD camera (Gattan). The microscope was operated at an accelerating voltage of 80 kV.

4.4. In Vitro Teratoma Assay. Methylcellulose (Sigma) was resuspended to make a 10% solution in knockout serum replacement (KOSR) medium consisting of DMEM/F12+L-glutamine (Thermo Fisher) with 20% (*v*/*v*) KOSR (Thermo Fisher), 0.1 mM NEAA (Thermo Fisher), and 10,000 U Pen-Strep (Thermo Fisher). hPSC cultured at 20% oxygen for over 5 passages were treated with Y-27632 (10 μM) for 1 h prior to dissociation with TrypLE Select. A 3 mm coat of methylcellulose was added to wells of a 24-well ultralow attachment plate (Corning) and incubated at 37°C for approximately 40 min until solidified. hPSC were harvested with 5 mL KOSR+20% FBS, then 6.25 million cells were centrifuged at 300 g and resuspended in 5 mL of KOSR+20% FBS +0.25 mL of undiluted Matrigel (Corning)+10 μM Y-27632. Approximately 5,000,000 cells (400 μL) were loaded into each well on top of the methylcellulose layer and the plates were centrifuged at 300g for 5 min until tight spheres of cells had formed; then, 200 μL of KOSR medium+10 μM Y-27632 was added and incubated overnight at 20% oxygen. After 24 h, following attachment of the spheres to the methylcellulose layer, the medium was aspirated and replaced with 400 μL/well of KOSR medium+20% FBS. After a further 24 h, the medium was completely aspirated and a second 3 mm layer of methylcellulose was added on top of the cell aggregate and placed in the incubator for ~40 min. Once solidified, 400 μL of KOSR medium+20% FBS was added on top of the methylcellulose layers. The medium was replaced every 48 h for 8 weeks. After 8 weeks of differentiation, *in vitro* teratomas were extracted, fixed, and stained with H&E for morphological analysis.

4.5. Fluxomics Using ^{13}C-glucose. To determine metabolite kinetics, uniformly labeled $^{13}C_6$ D-glucose (Sigma) was supplemented into glucose-free mTeSR1™ medium. Long-term 5% and 20% oxygen-adapted hPSC were treated with Y-27632 (10 μM) for 1 h, dissociated with TrypLE Select, and 4×10^6 cells were seeded as single cells in 100 mm dishes (Becton Dickinson) in glucose-free mTeSR1™ + $^{13}C_6$ D-glucose+Y-27632 and cultured at 5% or 20% oxygen. Upon reaching confluency, the medium was changed 4 h prior to labeling, with in-house glucose-free mTeSR1™ supplemented with D-glucose. After 4 h, custom mTeSR1™+$^{13}C_6$ D-glucose was added to timepoint dishes 1, 2, and 4 h, which were returned to their respective incubators for 1, 2, or 4 h, respectively. Timepoint 0 h was harvested immediately. For each collection, 10 mL of spent $^{13}C_6$ D-glucose medium was collected and stored at -80°C. Ice cold PBS was added to the cells prior to scraping, cell suspensions were centrifuged at 300g for 3 min, the supernatant was aspirated, and the pellets were snap frozen in liquid nitrogen before being stored at -80°C. A 1 cm^2 area of cells was left on each plate for cell number determination.

Sample preparation and NMR spectra acquisition were performed as previously described [29]. In detail, frozen cell pellets were lysed by cytolysis using molecular grade water on ice for 20 min. Cell lysates were separated into aqueous and organic phases using a 2 : 1 chloroform : methanol solution, followed by 1-part methanol and 1-part molecular grade water with vigorous vortexing between each step, and centrifuged at 3000 g at 4°C giving rise to a biphasic solution. The aqueous and organic phases were recovered and, together with the spent medium, were concentrated by lyophilization. The aqueous and media concentrates were reconstituted in deuterated water (D_2O; Cambridge Isotopes) with 1 mM DSS (Sigma). The organic concentrate was reconstituted in deuterated chloroform ($CDCl_3$; Cambridge Isotopes) and analyzed immediately. Samples were loaded into 3 mm glass tubes (Wilmad-LabGlass) and analyzed on a 63 mm bore 800 MHz spectrometer (Varian/Agilent Technologies) using VnmrJ software (Agilent Technologies) by collecting gradient-enhanced 1D-^{1}H and 2D-^{1}H,^{13}C-heteronuclear single-quantum coherence (cCHSQC) spectra. Acquisition and recycling time for aqueous, organic, and media samples were 6 h and 1.5 h, 4.5 h and 1.25 h, and 0.5 h and 0.125 h, respectively. Spectra were processed using Mnova (Mestrelab Research), by integrating peaks relative to DSS or $CDCl_3$. Chemical shift data from the Human Metabolome Database and Biological Magnetic Resonance Data Bank [56, 57] were used to identify metabolites, and integrals were transformed to mass quantities using standard curves. Mass quantities for each metabolite were standardized to 25 million cells and plotted as flux in nmol over time (h).

4.6. Immunofluorescence. For the quantification of histone acetylation and methylation markers, hPSC were fixed in PFA for 15 min, permeabilized using 1 M HCl for 20 min,

and blocked with 0.1% Triton X-100 and 5% species-specific serum in PBS for 1 h. Primary antibodies were incubated at 4°C for 24 h at the following concentrations: H3K9ac (Abcam) at 1 : 500, H3K27ac (Abcam) at 1 : 1000, and H3K27me3 (Abcam) at 1 : 250. Secondary antibodies Alexa Fluor 488 or 568 (Invitrogen) were used at 1 : 1000 and incubated at RT for 45 min. Nuclei were counterstained with 300 nM DAPI for 5 min at RT. For each marker of interest, exposure times for DAPI and primary were kept constant. Five representative colonies were imaged per treatment, and 10 cells were randomly selected per colony for fluorescence intensity analysis using ImageJ. Corrected total cell fluorescence (CTCF) was calculated using the following formula [58]: CTCF = integrated density − (area of nucleus × mean fluorescence of background readings). CTCF was then further normalized to the DAPI intensity for each selected nucleus.

4.7. Flow Cytometry. To determine mitochondrial ROS production, hPSC were dissociated using TrypLE Select, centrifuged at 300g, incubated in mTeSR1™ with the MitoSOX Red superoxide indicator (1 μM, Invitrogen) for 20 min at 37°C, counterstained with 300 nM DAPI, and washed twice with PBS. Cells were then run on a Beckman Coulter CyAn analyzer (Beckman Coulter), where a minimum of ten thousand live cell events were acquired using DAPI gating for each sample. Flow density plots were generated using Summit 4.3 software (Beckman Coulter). Mean $\log_{10}$ fluorescence data values were recorded and normalized for the statistical analysis.

4.8. qRT-PCR. Total RNA was isolated from hPSC using TRIzol (Invitrogen). RNA was isolated using a chloroform-induced triphasic solution before DNase treatment using DNase-I (Ambion). cDNA was synthesized from 1 μg of RNA using M-MLV Reverse Transcriptase (Promega). Triplicate reactions of each sample were run using EvaGreen Master Mix (Solis BioDyne) on a ViiA7™ thermocycler (Invitrogen). No-template control samples with nuclease-free water in place of cDNA were included for every primer set, and a –RT control was included to confirm appropriate cDNA synthesis. The relative abundance of each gene was normalized to that of *RPLP0* and analyzed using Q-Gene which is based on the ΔΔCt method. Standard curves were generated for each gene to control for primer-specific efficiencies. All PCR products were verified by sequencing. See Supplementary Table 2 for primers.

4.9. RNA-seq. RNA from MEL1 and MEL2 hPSC cultured at 5% and 20% oxygen was isolated using the RNeasy Plus Mini Kit (Qiagen). The RNA integrity numbers (RIN) of 10 for all samples were determined using the Agilent 2100 Bioanalyzer (Agilent Technologies). RNA was analyzed on the Illumina HiSeq 2500 Sequencing System (Illumina) at the Australian Genome Research Facility (AGRF) using 1 μg of total RNA as input. Sequencing was performed with 12 samples per lane, using 50 bp single-end reads. The quality of resultant raw FASTQ data files was assessed with FastQC. Data files were uploaded to the Galaxy platform [59] at https://usegalaxy.org/ and processed using the following pipeline: FASTQ Groomer to convert raw Illumina FASTQ files to Sanger Quality score format, Trim Galore! to trim the 13 bp of Illumina standard adapters, RNA STAR to align reads to the UCSC GRCh37/hg19 human reference genome, featureCounts to measure gene expression, and DESeq2 to identify DEGs. GO analysis of Biological Function terms and KEGG pathways were determined using DAVID. DEGs were submitted to NetworkAnalyst [38] to visualize zero-order protein-protein interaction (PPI) networks using the STRING interactome with a confidence score cut-off of 900.

4.10. Statistical Analyses. All data are presented as the mean ± SEM ($p < 0.05$). Statistical analyses were performed using Student's t-test to calculate differences between two groups, or following a two-factor ANOVA, significant main effects and interactions were further analyzed using simple main effects calculated using the MS residual from the initial ANOVA. All analyses were performed in Prism 7 (GraphPad) and unless otherwise stated $n = 3$, where n is the number of biological replicates.

Data Availability

The Gene Expression Omnibus accession number for the RNA-seq dataset reported in this paper is GSE117966.

Ethical Approval

All experimental procedures were carried out in accordance with and approved by the University of Melbourne Human Ethics Committee (approval number 0722502.1).

Conflicts of Interest

The authors declare no competing interests.

Authors' Contributions

J.G.L. performed all experiments, analyzed the data, designed the experiments, and prepared the manuscript. T.S.C. performed the ^{13}C-glucosemetabolic flux experiments. A.G. performed the TEM experiments. J.G.R. performed the Seahorse assays. J.G.R., S.D., D.K.G., and A.J.H. the designed experiments and edited the manuscript.

Acknowledgments

This work was supported by the Australian Research Council Special Research Initiative Stem Cells Australia (SR110001002), NIH grants to S.D. (P01 HL089471 and P01 GM75334), the Jasper Loftus-Hills Award (UTR7.116), the Alfred Nicholas Fellowship Award (UTR6.197), the FH Drummond Travel Award (UTR6.184), and the Science Abroad Travelling Scholarship (The University of Melbourne).

Supplementary Materials

Supplementary 1. Supplementary Figure 1: carbon tracing through metabolic pathways. Metabolite pathways organized into functional groups contributing to the production of

glycogen, glutathione, pyruvate, alanine, acetate, and lactate. Figures show the absolute levels of intracellular glucose derivatives in MEL2 hPSC at 0.5, 1, 2, and 4 hours when cultured under 5% and 20% oxygen. Lactate is plotted on the right y-axes. Supplementary Figure 2: RNA-seq volcano plots of the hPSC response to oxygen. Plots from left to right and top to bottom are the MEL1 hPSC transcriptional response to 5% and 20% oxygen and the transcriptional differences between hPSC lines at 5% oxygen, at 20% oxygen, and when the oxygen treatments are pooled. Red genes indicate a fold change value greater than 2 and an adjusted p value (Benjamini FDR) less than 0.05. Supplementary Figure 3: hPSC transcriptional response to 5% and 20% oxygen. (A) Pluripotency markers are generally not impacted by oxygen. (B) HIF-1 target genes show a strong transcriptional activation at 5% oxygen. Only statistics with a Benjamini score of <0.05 (p-adj) are shown. All assays performed in biological triplicate. $^{****}p < 0.0001$, $^{***}p < 0.001$, $^{**}p < 0.01$, and $^{*}p < 0.05$ for Benjamini scores. Supplementary Figure 4: Enriched GO and KEGG pathways due to oxygen. MEL1 and MEL2 hPSC GO and KEGG pathways upregulated after 5% and 20% oxygen culture. The contributing numbers of gene hits for each pathway are given with the ends of each bar. Only terms with a Benjamini score of <0.05 (p-adj) are shown. All assays performed in biological triplicate. $^{****}p < 0.0001$, $^{***}p < 0.001$, $^{**}p < 0.01$, and $^{*}p < 0.05$ for Benjamini scores. Supplementary Figure 5: RNA-seq minimum-order networks comparing hPSC lines. (A) Differentially expressed genes in hPSC lines (MEL1, MEL2) cultured at 5% oxygen were connected based on known protein:protein interactions (https://www.innatedb.ca/). Red nodes are upregulated in MEL1 hPSC; green nodes are upregulated in MEL2 hPSC. Grey nodes have known interactions with the seeds but were not regulated. Green/red intensity indicates the degree of fold change as indicated in the figure. (B) 5% oxygen cultured KEGG pathways upregulated in MEL1 and MEL2 hPSC based on the minimum-order network in Supplementary Figure 2A. (C) 20% oxygen minimum-order, protein:protein interaction network. (D) 20% oxygen KEGG pathways upregulated in MEL1 and MEL2 hPSC based on the minimum-order network in Supplementary Figure 2C. Supplementary Figure 6: methyltransferases and lysine demethylases synergistically reduce methylation at 5% oxygen. (A) Extracellular and intracellular levels of glycolytic metabolites and glycolytic enzymes in hPSC. (B) Intracellular levels of metabolites and enzymes in and related to the serine/glycine biosynthesis pathway. (C) Intercellular metabolite levels of transsulphuration pathway metabolites. (D) Expression of metabolites and transcripts for enzymes, in the folate cycle. (E) Expression of metabolites and transcripts for enzymes, in the methionine cycle. (F) Level of H3K27 trimethylation and transcripts for lysine demethylases and methyltransferases. All contributing assays performed in a minimum of biological triplicate. Bolded text indicates a significant increase (green) or decrease (red) in hPSC metabolite/transcript/-methylation level at 5% relative to 20% oxygen culture. Bolded black text indicates a nonsignificant result for an assessed parameter. Unbolded text indicates a parameter that was not assessed. Supplementary Table 2: related to experimental procedures. Human PCR primers for the serine/glycine biosynthesis pathway.

Supplementary 2. Supplementary Table 1: an attached excel file containing qPCR data relating to Supplementary Figure 5 and the 4 comparisons performed on RNA-seq data comparing MEL1 hPSC at 5% and 20% oxygen, MEL2 hPSC at 5% and 20% oxygen, MEL1 and MEL2 hPSC at 5% oxygen, and MEL1 and MEL2 hPSC at 20% oxygen.

References

[1] B. Fischer and B. D. Bavister, "Oxygen tension in the oviduct and uterus of rhesus monkeys, hamsters and rabbits," *Reproduction*, vol. 99, no. 2, pp. 673–679, 1993.

[2] J. A. Mitchell and J. M. Yochim, "Measurement of intrauterine oxygen tension in the rat and its regulation by ovarian steroid hormones," *Endocrinology*, vol. 83, no. 4, pp. 691–700, 1968.

[3] F. Rodesch, P. Simon, C. Donner, and E. Jauniaux, "Oxygen measurements in endometrial and trophoblastic tissues during early pregnancy," *Obstetrics & Gynecology*, vol. 80, no. 2, pp. 283–285, 1992.

[4] A. R. Clark, Y. M. Stokes, M. Lane, and J. G. Thompson, "Mathematical modelling of oxygen concentration in bovine and murine cumulus–oocyte complexes," *Reproduction*, vol. 131, no. 6, pp. 999–1006, 2006.

[5] A. J. Harvey, "The role of oxygen in ruminant preimplantation embryo development and metabolism," *Animal Reproduction Science*, vol. 98, no. 1-2, pp. 113–128, 2007.

[6] D. K. Gardner, "The impact of physiological oxygen during culture, and vitrification for cryopreservation, on the outcome of extended culture in human IVF," *Reproductive BioMedicine Online*, vol. 32, no. 2, pp. 137–141, 2016.

[7] M. S. Christianson, Y. Zhao, G. Shoham et al., "Embryo catheter loading and embryo culture techniques: results of a worldwide web-based survey," *Journal of Assisted Reproduction and Genetics*, vol. 31, no. 8, pp. 1029–1036, 2014.

[8] W. Zhou, M. Choi, D. Margineantu et al., "HIF1α induced switch from bivalent to exclusively glycolytic metabolism during ESC-to-EpiSC/hESC transition," *The EMBO Journal*, vol. 31, no. 9, pp. 2103–2116, 2012.

[9] S. Varum, A. S. Rodrigues, M. B. Moura et al., "Energy metabolism in human pluripotent stem cells and their differentiated counterparts," *PLoS One*, vol. 6, no. 6, article e20914, 2011.

[10] J. Zhang, I. Khvorostov, J. S. Hong et al., "UCP2 regulates energy metabolism and differentiation potential of human pluripotent stem cells," *The EMBO Journal*, vol. 30, no. 24, pp. 4860–4873, 2011.

[11] A. J. Harvey, J. Rathjen, L. J. Yu, and D. K. Gardner, "Oxygen modulates human embryonic stem cell metabolism in the absence of changes in self-renewal," *Reproduction, Fertility and Development*, vol. 28, no. 4, pp. 446–458, 2016.

[12] Y. M. Cho, S. Kwon, Y. K. Pak et al., "Dynamic changes in mitochondrial biogenesis and antioxidant enzymes during the spontaneous differentiation of human embryonic stem cells," *Biochemical and Biophysical Research Communications*, vol. 348, no. 4, pp. 1472–1478, 2006.

[13] C. E. Forristal, D. R. Christensen, F. E. Chinnery et al., "Environmental oxygen tension regulates the energy metabolism and self-renewal of human embryonic stem cells," *PLoS One*, vol. 8, no. 5, article e62507, 2013.

[14] J. G. Lees, J. Rathjen, J. R. Sheedy, D. K. Gardner, and A. J. Harvey, "Distinct profiles of human embryonic stem cell metabolism and mitochondria identified by oxygen," *Reproduction*, vol. 150, no. 4, pp. 367–382, 2015.

[15] S. D. Westfall, S. Sachdev, P. Das et al., "Identification of oxygen-sensitive transcriptional programs in human embryonic stem cells," *Stem Cells and Development*, vol. 17, no. 5, pp. 869–882, 2008.

[16] J. I. Piruat and J. Lopez-Barneo, "Oxygen tension regulates mitochondrial DNA-encoded complex I gene expression," *Journal of Biological Chemistry*, vol. 280, no. 52, pp. 42676–42684, 2005.

[17] A. Moussaieff, M. Rouleau, D. Kitsberg et al., "Glycolysis-mediated changes in acetyl-CoA and histone acetylation control the early differentiation of embryonic stem cells," *Cell Metabolism*, vol. 21, no. 3, pp. 392–402, 2015.

[18] R. Petruzzelli, D. R. Christensen, K. L. Parry, T. Sanchez-Elsner, and F. D. Houghton, "HIF-2α regulates NANOG expression in human embryonic stem cells following hypoxia and reoxygenation through the interaction with an Oct-Sox Cis regulatory element," *PLoS One*, vol. 9, no. 10, article e108309, 2014.

[19] B. W. Carey, L. W. S. Finley, J. R. Cross, C. D. Allis, and C. B. Thompson, "Intracellular α-ketoglutarate maintains the pluripotency of embryonic stem cells," *Nature*, vol. 518, no. 7539, pp. 413–416, 2015.

[20] A. J. Harvey, J. Rathjen, and D. K. Gardner, "Metaboloepigenetic regulation of pluripotent stem cells," *Stem Cells International*, vol. 2016, Article ID 1816525, 15 pages, 2016.

[21] J. G. Lees, D. K. Gardner, and A. J. Harvey, "Pluripotent stem cell metabolism and mitochondria: beyond ATP," *Stem Cells International*, vol. 2017, Article ID 2874283, 17 pages, 2017.

[22] S. Varum, O. Momčilović, C. Castro, A. Ben-Yehudah, J. Ramalho-Santos, and C. S. Navara, "Enhancement of human embryonic stem cell pluripotency through inhibition of the mitochondrial respiratory chain," *Stem Cell Research*, vol. 3, no. 2-3, pp. 142–156, 2009.

[23] W. Gu, X. Gaeta, A. Sahakyan et al., "Glycolytic metabolism plays a functional role in regulating human pluripotent stem cell state," *Cell Stem Cell*, vol. 19, no. 4, pp. 476–490, 2016.

[24] J. Zhang, E. Nuebel, G. Q. Daley, C. M. Koehler, and M. A. Teitell, "Metabolic regulation in pluripotent stem cells during reprogramming and self-renewal," *Cell Stem Cell*, vol. 11, no. 5, pp. 589–595, 2012.

[25] S. Mandal, A. G. Lindgren, A. S. Srivastava, A. T. Clark, and U. Banerjee, "Mitochondrial function controls proliferation and early differentiation potential of embryonic stem cells," *Stem Cells*, vol. 29, no. 3, pp. 486–495, 2011.

[26] A. J. Lambert and M. D. Brand, "Superoxide production by NADH: ubiquinone oxidoreductase (complex I) depends on the pH gradient across the mitochondrial inner membrane," *Biochemical Journal*, vol. 382, no. 2, pp. 511–517, 2004.

[27] A. H. Sathananthan and A. O. Trounson, "Mitochondrial morphology during preimplantational human embryogenesis," *Human Reproduction*, vol. 15, Supplement 2, pp. 148–159, 2000.

[28] D. J. Whitworth, J. E. Frith, T. J. R. Frith, D. A. Ovchinnikov, J. J. Cooper-White, and E. J. Wolvetang, "Derivation of mesenchymal stromal cells from canine induced pluripotent stem cells by inhibition of the TGFβ/activin signaling pathway," *Stem Cells and Development*, vol. 23, no. 24, pp. 3021–3033, 2014.

[29] T. S. Cliff, T. Wu, B. R. Boward et al., "MYC controls human pluripotent stem cell fate decisions through regulation of metabolic flux," *Cell Stem Cell*, vol. 21, no. 4, pp. 502–516.e9, 2017.

[30] J. G. Lees, D. K. Gardner, and A. J. Harvey, "Mitochondrial and glycolytic remodeling during nascent neural differentiation of human pluripotent stem cells," *Development*, vol. 145, no. 20, 2018.

[31] G. B. Waypa, J. D. Marks, R. Guzy et al., "Hypoxia triggers subcellular compartmental redox signaling in vascular smooth muscle cells," *Circulation Research*, vol. 106, no. 3, pp. 526–535, 2010.

[32] N. Shiraki, Y. Shiraki, T. Tsuyama et al., "Methionine metabolism regulates maintenance and differentiation of human pluripotent stem cells," *Cell Metabolism*, vol. 19, no. 5, pp. 780–794, 2014.

[33] L. Xiao, X. Yuan, and S. J. Sharkis, "Activin a maintains self-renewal and regulates fibroblast growth factor, Wnt, and bone morphogenic protein pathways in human embryonic stem cells," *Stem Cells*, vol. 24, no. 6, pp. 1476–1486, 2006.

[34] S. M. Prasad, M. Czepiel, C. Cetinkaya et al., "Continuous hypoxic culturing maintains activation of Notch and allows long-term propagation of human embryonic stem cells without spontaneous differentiation," *Cell Proliferation*, vol. 42, no. 1, pp. 63–74, 2009.

[35] N. R. Forsyth, A. Musio, P. Vezzoni, A. H. R. W. Simpson, B. S. Noble, and J. McWhir, "Physiologic oxygen enhances human embryonic stem cell clonal recovery and reduces chromosomal abnormalities," *Cloning and Stem Cells*, vol. 8, no. 1, pp. 16–23, 2006.

[36] T. Ezashi, P. Das, and R. M. Roberts, "Low O_2 tensions and the prevention of differentiation of hES cells," *Proceedings of the National Academy of Sciences of the United States of America*, vol. 102, no. 13, pp. 4783–4788, 2005.

[37] D. Acampora, D. Omodei, G. Petrosino et al., "Loss of the Otx2-binding site in the Nanog promoter affects the integrity of embryonic stem cell subtypes and specification of inner cell mass-derived epiblast," *Cell Reports*, vol. 15, no. 12, pp. 2651–2664, 2016.

[38] J. Xia, E. E. Gill, and R. E. W. Hancock, "NetworkAnalyst for statistical, visual and network-based meta-analysis of gene expression data," *Nature Protocols*, vol. 10, no. 6, pp. 823–844, 2015.

[39] A. H. Juan, S. Wang, K. D. Ko et al., "Roles of H3K27me2 and H3K27me3 examined during fate specification of embryonic stem cells," *Cell Reports*, vol. 17, no. 5, pp. 1369–1382, 2016.

[40] C. Zhao, H. Wu, N. Qimuge et al., "MAT2A promotes porcine adipogenesis by mediating H3K27me3 at Wnt10b locus and repressing Wnt/β-catenin signaling," *Biochimica et Biophysica Acta (BBA) - Molecular and Cell Biology of Lipids*, vol. 1863, no. 2, pp. 132–142, 2018.

[41] N. Shyh-Chang, J. W. Locasale, C. A. Lyssiotis et al., "Influence of threonine metabolism on S-adenosylmethionine and histone methylation," *Science*, vol. 339, no. 6116, pp. 222–226, 2013.

[42] H. Choudhry and A. L. Harris, "Advances in hypoxia-inducible factor biology," *Cell Metabolism*, vol. 27, no. 2, pp. 281–298, 2018.

[43] H.-Y. Lee, K. Choi, H. Oh, Y. K. Park, and H. Park, "HIF-1-dependent induction of Jumonji domain-containing protein

(JMJD) 3 under hypoxic conditions," *Molecules and Cells*, vol. 37, no. 1, pp. 43–50, 2014.

[44] E. L. Bell, T. A. Klimova, J. Eisenbart et al., "The Qo site of the mitochondrial complex III is required for the transduction of hypoxic signaling via reactive oxygen species production," *The Journal of Cell Biology*, vol. 177, no. 6, pp. 1029–1036, 2007.

[45] M. J. Hitchler and F. E. Domann, "Metabolic defects provide a spark for the epigenetic switch in cancer," *Free Radical Biology & Medicine*, vol. 47, no. 2, pp. 115–127, 2009.

[46] V. Valinluck and L. C. Sowers, "Endogenous cytosine damage products alter the site selectivity of human DNA maintenance methyltransferase DNMT1," *Cancer Research*, vol. 67, no. 3, pp. 946–950, 2007.

[47] S.-O. Lim, J. M. Gu, M. S. Kim et al., "Epigenetic changes induced by reactive oxygen species in hepatocellular carcinoma: methylation of the E-cadherin promoter," *Gastroenterology*, vol. 135, no. 6, pp. 2128–2140.e8, 2008.

[48] A. Moussaieff, N. M. Kogan, and D. Aberdam, "Concise review: energy metabolites: key mediators of the epigenetic state of pluripotency," *Stem Cells*, vol. 33, no. 8, pp. 2374–2380, 2015.

[49] D. R. Donohoe and S. J. Bultman, "Metaboloepigenetics: interrelationships between energy metabolism and epigenetic control of gene expression," *Journal of Cellular Physiology*, vol. 227, no. 9, pp. 3169–3177, 2012.

[50] S. A. Comerford, Z. Huang, X. du et al., "Acetate dependence of tumors," *Cell*, vol. 159, no. 7, pp. 1591–1602, 2014.

[51] K. E. Wellen, G. Hatzivassiliou, U. M. Sachdeva, T. V. Bui, J. R. Cross, and C. B. Thompson, "ATP-citrate lyase links cellular metabolism to histone acetylation," *Science*, vol. 324, no. 5930, pp. 1076–1080, 2009.

[52] J. G. Ryall, S. Dell'Orso, A. Derfoul et al., "The NAD+-dependent SIRT1 deacetylase translates a metabolic switch into regulatory epigenetics in skeletal muscle stem cells," *Cell Stem Cell*, vol. 16, no. 2, pp. 171–183, 2015.

[53] W. M. Skiles, A. Kester, J. H. Pryor, M. E. Westhusin, M. C. Golding, and C. R. Long, "Oxygen-induced alterations in the expression of chromatin modifying enzymes and the transcriptional regulation of imprinted genes," *Gene Expression Patterns*, vol. 28, pp. 1–11, 2018.

[54] W. Li, K. Goossens, M. van Poucke et al., "High oxygen tension increases global methylation in bovine 4-cell embryos and blastocysts but does not affect general retrotransposon expression," *Reproduction, Fertility and Development*, vol. 28, no. 7, pp. 948–959, 2016.

[55] J. M. Underwood, K. M. Imbalzano, V. M. Weaver, A. H. Fischer, A. N. Imbalzano, and J. A. Nickerson, "The ultrastructure of MCF-10A acini," *Journal of Cellular Physiology*, vol. 208, no. 1, pp. 141–148, 2006.

[56] E. L. Ulrich, H. Akutsu, J. F. Doreleijers et al., "BioMagResBank," *Nucleic Acids Research*, vol. 36, pp. D402–D408, 2007.

[57] D. S. Wishart, D. Tzur, C. Knox et al., "HMDB: the human metabolome database," *Nucleic Acids Research*, vol. 35, pp. D521–D526, 2007.

[58] R. A. McCloy, S. Rogers, C. E. Caldon, T. Lorca, A. Castro, and A. Burgess, "Partial inhibition of Cdk1 in G2 phase overrides the SAC and decouples mitotic events," *Cell Cycle*, vol. 13, no. 9, pp. 1400–1412, 2014.

[59] E. Afgan, D. Baker, M. van den Beek et al., "The galaxy platform for accessible, reproducible and collaborative biomedical analyses: 2016 update," *Nucleic Acids Research*, vol. 44, no. W1, pp. W3–W10, 2016.

Hindawi
Stem Cells International
Volume 2019, Article ID 9323864, 16 pages
https://doi.org/10.1155/2019/9323864

Research Article

Metabolic Phenotyping of Adipose-Derived Stem Cells Reveals a Unique Signature and Intrinsic Differences between Fat Pads

Camille Lefevre,[1,2] **Baptiste Panthu**,[1,2] **Danielle Naville**,[1,2] **Sylvie Guibert**,[3] **Claudie Pinteur**,[1,2] **Bénédicte Elena-Herrmann**,[3,4] **Hubert Vidal**,[1,2] **Gilles J. P. Rautureau**,[3] **and Anne Mey**[1,2]

[1]*Univ Lyon, CarMeN Laboratory, INSERM, INRA, INSA Lyon, Université Claude Bernard Lyon 1, 69921 Oullins Cedex, France*
[2]*Hospices Civils de Lyon, Faculté de Médecine, Hôpital Lyon Sud, 69921 Oullins Cedex, France*
[3]*Univ Lyon, CNRS, Université Claude Bernard Lyon 1, Ens de Lyon, Institut des Sciences Analytiques, UMR 5280, 5 rue de la Doua, F-69100 Villeurbanne, France*
[4]*Institute for Advanced Biosciences, CNRS UMR 5309, INSERM U1209, Université Grenoble Alpes, Grenoble, France*

Correspondence should be addressed to Anne Mey; anne.mey@inra.fr

Received 2 November 2018; Revised 11 January 2019; Accepted 3 February 2019; Published 14 May 2019

Academic Editor: Alexandra Harvey

White adipose tissues are functionally heterogeneous and differently manage the excess of energy supply. While the expansion of subcutaneous adipose tissues (SAT) is protective in obesity, that of visceral adipose tissues (VAT) correlates with the emergence of metabolic diseases. Maintained in fat pads throughout life, adipose stem cells (ASC) are mesenchymal-like stem cells with adipogenesis and multipotent differentiation potential. ASC from distinct fat pads have long been reported to present distinct proliferation and differentiation potentials that are maintained in culture, yet the origins of these intrinsic differences are still unknown. Metabolism is central to stem cell fate decision in line with environmental changes. In this study, we performed high-resolution nuclear magnetic resonance (NMR) metabolomic analyses of ASC culture supernatants in order to characterize their metabolic phenotype in culture. We identified and quantified 29 ASC exometabolites and evaluated their consumption or secretion over 72 h of cell culture. Both ASC used glycolysis and mitochondrial metabolism, as evidenced by the high secretions of lactate and citrate, respectively, but V-ASC mostly used glycolysis. By varying the composition of the cell culture medium, we showed that glutaminolysis, rather than glycolysis, supported the secretion of pyruvate, alanine, and citrate, evidencing a peculiar metabolism in ASC cells. The comparison of the two types of ASC in glutamine-free culture conditions also revealed the role of glutaminolysis in the limitation of pyruvate routing towards the lactate synthesis, in S-ASC but not in V-ASC. Altogether, our results suggest a difference between depots in the capacity of ASC mitochondria to assimilate pyruvate, with probable consequences on their differentiation potential in pathways requiring an increased mitochondrial activity. These results highlight a pivotal role of metabolic mechanisms in the discrimination between ASC and provide new perspectives in the understanding of their functional differences.

1. Introduction

White adipose tissue is an interesting source of multipotent stem cells sharing properties with mesenchymal stem cells and used for clinical applications. Indeed, in addition to their differentiation potential, adipose stem cells (ASC) display stromal functions (i) by supporting the growth of other stem cells [1], (ii) by controlling local inflammation through the secretion of cytokines or by the interaction with immune cells [2], and (iii) by controlling energy metabolism pathways by the secretion of hormones such as adiponectin [3]. For a long time, ASC properties have been used in regenerative medicine and for cell therapy [4] with an increasing interest for the use of their secretome [5]. However, their contribution to adipose tissue homeostasis and expansion in obesity is not clear, notably due to the functional heterogeneity of adipose fat pads.

White adipose tissue is split into different body regions with two main areas, the subcutaneous (SAT) and the visceral (VAT) white adipose depots that play distinct roles in the control of energy metabolism. Indeed, SAT expansion is protective in obesity while VAT expansion promotes the metabolic complications of obesity such as resistance to insulin and type 2 diabetes [6].

It has been reported that SAT and VAT have distinct functional properties regarding their capacity of fatty acid storage and the control of inflammation [7]. The metabolic protection by SAT is attributed to its ability to trap free fatty acids through triglyceride esterification (lipogenesis) protecting other organs from lipotoxicity [8] while the deleterious effect of expanding VAT is attributed to its higher lipolytic activity favoring the release of free fatty acids [6] and the delivery of proinflammatory cytokines such as IL6 [9]. It has been shown that VAT expansion occurs when the storage capacity of SAT is saturated [10], a process associated with stem cell proliferation and differentiation [11]. Whether this stem cell mobilization, to produce new adipocytes in obesity, is restricted to VAT remains controversial [12, 13], but it reveals distinct metabolic dialogs between stem cells and their environment.

Reinforcing the differences between adipose tissues, functional differences exist between ASC from distinct depots, with ASC from SAT (S-ASC) showing higher abilities to proliferate [14], to survive [7, 15], to accumulate lipids [7, 14], and to differentiate into adipocytes [16–18] than ASC from VAT (V-ASC). Interestingly, these differences observed with isolated ASC cultivated *in vitro* are thus intrinsic indicating distinct fate for ASC in distinct adipose depots [14].

Metabolic adaptation is central to the balance between proliferation and differentiation of stem cells that support tissue homeostasis and adaptation. It is assumed that proliferating stem cells exhibit a glycolytic metabolic program supporting cell synthesis [19] while the switch to mitochondrial activity and oxidative phosphorylation is required for differentiation [20]. In multipotent mesenchymal stem cells that can give rise to chondrocytes, osteoblasts, and adipocytes, the switch between glycolysis and oxidative phosphorylation further directs the lineage decision between osteogenesis and chondrogenesis according to the requirements of the mature cell phenotype for oxygen supply [21]. Similarly, ASC, which are intended to generate adipocytes in white adipose tissues, may preferentially depend on metabolic pathways related to fatty acid synthesis.

In this article, to further understand the intrinsic differences between ASC from distinct adipose depots, we addressed their metabolic features. To reach this goal, we have set up efficient isolation and culture conditions of ASC allowing the amplification of stem cells from SAT and from VAT collected from mice. The metabolic pathways involved in the maintenance of ASC were defined by using proton nuclear magnetic resonance (^{1}H-NMR). By quantifying the metabolites in the extracellular culture medium, we measured the consumption and secretion rates of a variety of metabolites to characterize and to compare the metabolic profiles during cell cultures of ASC from distinct adipose depot. Our results indicate that V- and S-ASC present significant metabolic differences among which the role of glutaminolysis is noticeable. Our data also shed new light on the balance between glycolysis and mitochondrial activity of ASC under the influence of the depot of origin.

2. Materials and Methods

2.1. Isolation and Culture of ASC. Mouse studies were performed with the approval of the Regional Committee of Ethics for Animal Experiments. After one week acclimatization, subcutaneous and epididymal adipose tissues were harvested from 10-12-week-old male C57BL/6J mice (Envigo, Gannat, France) killed by cervical dislocation. Adipose tissues were removed and left on ice in Hanks' balanced salt solution (Dutscher, Brumath, France) supplemented with 100 U/ml penicillin and 100 μg/ml streptomycin (Gibco, France) until isolation of adipose-derived stem cells. The adipose tissues were successively washed with Hanks solution and Dulbecco's phosphate balanced solution (PAA, France) before being torn into pieces. Pieces were incubated for 1 hour at 37°C in digestion buffer containing DPBS with calcium and magnesium supplemented with 2 mM glucose (Sigma-Aldrich, France), 1% bovine serum albumin (Dominique Dutscher), and 1 mg/ml collagenase (Sigma-Aldrich, France) and vortexed every 10 minutes. At the end of the process, digested adipose tissues were filtered on a 100 μm nylon filter (Dutscher) and suspended in culture medium containing Dulbecco's modified Eagle's medium-high glucose (DMEM-HG) supplemented with 2 mM L-glutamine-L-alanyl (stable glutamine), 1 mM pyruvate, 100 U/ml penicillin, 100 μg/ml streptomycin, 25 mM hepes, and 10% fetal calf serum from South America (all culture medium components were from Dominique Dutscher, France). The cells were centrifuged for 5 minutes at 600 g at room temperature. The pelleted stromal fractions were suspended in culture medium supplemented with 100 μM ascorbic acid (Sigma-Aldrich, France), 5 ng/ml human bFGF (eBioscience, France), and 5 U/ml heparin sodium (Sigma-Aldrich) and plated in 2 wells of 9.6 cm^2 (Dutscher). At confluency, cells were dissociated by trypsinization (0.05% trypsin-EDTA) and plated at a density of 1×10^4 cells by cm^2. This was the first passage. All the analyses were performed with cells collected after the 2nd passage. For cumulative growth curves, all the passages were performed like the first one.

Cells were cultured in a humidified 5% CO_2 atmosphere at 37°C, and medium was changed every two or three days except for metabolomic experiments.

2.2. Flow Cytometry. The cultured ASC were retrieved at passage 2 by trypsin digestion. After washing in PBS, cells were first incubated with the fixable viability dye eFluor 506 (Life Technologies SAS, France) in PBS. Cells were next suspended in fluorescence-activated cell sorting (FACS) buffer (10% BSA (fraction V, Euromedex), 0.1% NaN_3 in PBS) supplemented with the mixture of cell surface marker antibodies or their isotype controls. Antibodies used were CD45 APC-eFluor 780, CD31 PE-Cy7, CD90.2-FITC, and CD29-PE all from eBioscience (Thermo Fisher, France) and PdgfRα-

(CD140a-) BV421 and Sca-1 BUV395 from BD Biosciences (France). After 30-minute incubation on ice, cells were washed in FACS buffer and fixed in 3.7% formaldehyde. Acquisitions were performed using the facilities of the technical platform AniRA of the SFR Biosciences Gerland-Lyon Sud (US8/UMS3444) with an LSRII flow cytometer (BD Biosciences) equipped with 355, 488, and 633 nm lasers. Analyses were performed using the cloud-based platform Cytobank (http://www.cytobank.org).

2.3. Adipogenic Differentiation. For adipocyte differentiation, ASC were amplified until 80% of confluency was reached and culture medium replaced by differentiation medium containing Dulbecco's modified Eagle medium/Nutrient Mixture F12 (DMEM/F12; Dominique Dutscher, France), FBS 10% (Hyclone, France), 100 U/ml penicillin, 100 μg/ml streptomycin, 2 mM glutamine, 1 μg/ml insulin, 0.5 μM dexamethasone, 2 nM Triiodo-L-Thyronine 3 (T3), 0.5 μM 3-isobuthyl-1-methylxanthine (IBMX), 2 μM rosiglitazone, and 10 μg/ml transferrin, all from Sigma-Aldrich. After 7 days, adipocyte differentiation was measured by Oil red O staining of the neutral triglyceride and lipids. Cells were fixed in 10% formaldehyde (Carlo Erba, France) for 1 hour then washed with 60% isopropanol (Carlo Erba) twice, dried and colored by incubation for 10 minutes with 0.2% Oil red O (Sigma-Aldrich) in isopropanol. Brightfield images were taken with an optic microscope with a ×20 magnification. The expression of adipogenic genes (*Pparγ*, *Dgat2*, *and Hsl*) was measured by RT-qPCR.

2.4. Chondrogenic Differentiation. ASC were induced to differentiate into chondrocytes using the completed StemXVivo Chondrogenic differentiation medium (R&D Systems, France). Briefly, 2.5×10^5 cells were washed once in StemXVivo Chondrogenic base medium, resuspended in 0.5 ml of the StemXVivo Chondrogenic differentiation medium, and incubated in 15 ml falcon at 37°C and 5% CO_2. A pellet of 1-2 mm was formed. The chondrogenic differentiation medium was changed every 2-3 days. The pellet was harvested after 21 days of differentiation and fixed in 4% formaldehyde for 4 h at 4°C. The fixation was stopped with glycine 1 M (Sigma-Aldrich), and the pellet was washed with PBS before being incorporated in CryoFix Gel (BioGnost, France), frozen at -80°C, and then cut with a microtome (CryoStar NX50, Thermo Scientific). The pellet was stained for 30 minutes with alcian blue 8GX 1% (BioGnost) dye which colors glycosaminoglycans in cartilage. The nucleus was stained for 1 minute with a 0.1% fast red solution (Sigma-Aldrich), and the section was included in pertex. Images of 10 distinct fields by sample were obtained with an optic microscope (20x objective), and analysis was performed using the ImageJ software application Fiji to quantify the ratio of the alcian blue color surface to the total cell surface.

2.5. Osteogenic Differentiation. ASC were induced into osteocytes using the StemXVivo Mouse/Rat osteogenic/adipogenic supplement (R&D Systems). Briefly, 7.6×10^4 cells were suspended in 1.5 ml of complete medium and plated in a 24-well dish. After 1 day, cells were at 60-70% confluency. Cells were purged 3 h in StemXVivo osteogenic/adipogenic base media. Osteogenic differentiation was induced with 1 ml of StemXVivo Osteogenic differentiation media and was changed every 3-4 days. After 21 days, the cells were fixed for 15 minutes using 10% formaldehyde in PBS at room temperature. The osteogenic differentiation was revealed using 40 mM alizarin red dye (which stains calcium deposition) pH 4.3 (Sigma-Aldrich) for 20 minutes at room temperature. Brightfield images were taken with an optic microscope with a ×20 magnification. The expression of the osteocyte-specific genes *Dmp1* and *Gdf15* was measured by RT-qPCR.

2.6. Real-Time Quantitative PCR (RT-qPCR). The RNeasy Mini Kit (Qiagen, France) was used to extract RNA, following the provider instructions, from ASC that had been differentiated or not. The reverse transcription was performed using the Takara reverse transcriptase kit (Ozyme, France). RT-qPCR was performed using the TaqMan fast advanced master mix (Biosystems, France). Samples were run in duplicate. Gene expression levels were calculated using the Rotor-Gene Q series software and normalized using the mouse 40S ribosomal protein S17 (*Rs17*) as the housekeeping gene. The primers used are listed in Table 1.

2.7. Protein Analysis and Western Blot. ASC were cultivated until confluency and rinsed with PBS after removal of the culture supernatant. Whole cell lysates were prepared by adding per well of 9.6 cm^2, 300 μl of lysis buffer containing 1% IGPAL, 0.5% sodium deoxycholate, 0.1% sodium dodecyl sulfate (SDS), PBS without calcium without magnesium, 5 mM EDTA, 1 mM $NaVO_4$, 20 mM NAF, and 1 mM DL-dithiothreitol, and supplemented with a protease Inhibitor Cocktail (all reagents were obtained from Sigma, France). After incubation of 30 min on ice, cell lysates were centrifuged at 12,000 g for 20 min at 4°C to remove insoluble fragments. The total protein content in the supernatant was determined using the Pierce BCA Protein Assay Kit (Thermo Scientific, France) and BSA as the standard curve. For western blot analysis, proteins were denatured with loading buffer (25 mM Tris HCl, 6% glycerol, 0.5% SDS, 2% β-mercaptomethanol, 0.005% bromophenol blue) at 75°C for 10 min, and 20 μg protein per well was loaded. Proteins were separated on a 12% SDS-polyacrylamide gel and transferred on a PVDF membrane. The membranes were blocked in saturation buffer (0.3% Tween, 5% low-fat milk in TBS) for 2 h at room temperature and next incubated overnight at 4°C with the primary antibody diluted in saturation buffer. The following primary antibodies were used: rabbit anti-UCP2 (1/500, BioLegend, France) and mouse anti-α-tubulin (1/2000, Sigma, France). After washing three times with TBS-0.3% Tween, the membrane was incubated with the HRP-conjugated anti-rabbit antibody (Bio-Rad, France). After washing, peroxidase activity was detected by chemiluminescence using the Luminata Classico western HRP substrate (Millipore, France). Detection was made using the ChemiDoc XRS+ imaging system (Bio-Rad), and analysis

Table 1: Forward and reverse sequences of primers used in RT-qPCR.

Gene	Forward sequence ($5' \rightarrow 3'$)	Reverse sequence ($5' \rightarrow 3'$)
Housekeeping		
Rs17	AGCCCTAGATCAGGAGATCA	CTGGTGACCTGAAGGTTAG
Adipogenic		
Pparγ	TCTCTCCGTAATGGAAGACC	GCATTATGAGACATCCCCAC
Dgat2	TGGGTCCAGAAGAAGTTCCAGAAGTA	ACCTCAGTCTCTGGAAGGCCAAAT
Hsl	GTGTGTCAGTGCCTATTCAG	GTCAGCTTCTTCAAGGTATC
Osteogenic		
Dmp1	CCCACGAACAGTGAGTCATC	CATCTCCACTGTCGTCTTCA
Gdf15	CGGATACTCAGTCCAGAGGT	TCGGTGCACGCGGTAGGCTT
Other		
Ucp2	CCTGAAAGCCAACCTCATGAC	AGGATCCCAAGCGGAGAAAGG

was performed using the Quantity One software (Bio-Rad). Data were normalized relatively to α-tubulin.

2.8. Statistical Analysis. All results are expressed as means ± SEM. Student's t-test was used to evaluate the probability of significant differences between the ASC samples isolated from distinct fat pads. One-way ANOVA followed by Tukey's multiple comparison test was used when more than two conditions were compared. A p value < 0.05 was considered as significant. GraphPad Prism 5.0 software was used for all statistical analyses.

2.9. Metabolomic Analyses

2.9.1. Exometabolome Sample Preparation. Metabolite concentrations were measured in supernatants of ASC placed for the indicated time in culture medium composed of DMEM without glucose, without pyruvate, without glutamine, and without red phenol (PAN-Biotech, France) supplemented with 25 mM glucose, antibiotics, 20% FCS, 25 mM hepes, nonessential amino acid 1x (PAA, France), 4 mM L-glutamine (Corning, France), 1 mM pyruvate (Dutscher, France), 100 μM ascorbic acid, 5 ng/ml human bFGF, and 5 U/ml heparin sodium. This medium had the same nutrient composition as the growth culture medium and only differed by the absence of phenol red, the replacement of L-glutamine-L-alanyl (2 mM) by L-glutamine (4 mM). Cells were seeded at a density of 2×10^4 cells per cm^2 in a 12-well dish and cultured in 1.5 ml of culture medium. After 24 h, as the cells reached 70 to 80 percent of confluency, the medium was replaced by 500 μl of fresh culture medium, and the culture was maintained for 24, 48, or 72 h, as indicated in the figure legends. Culture medium in wells without cells was processed in the same ways to obtain the initial concentrations of metabolites in the medium (control). For studies examining the role of pyruvate, glucose, and glutamine supplies, cells were seeded as previously indicated and cultivated for 72 h. At confluency, culture medium was replaced by culture medium without pyruvate nor hepes and supplemented with the indicated concentrations of glucose and glutamine. The other components were at the concentrations indicated above. At the end of the culture, supernatants were collected and snap-frozen at -20°C for NMR analyses. For the preparation of exometabolome samples, 200 μl of centrifuged cell culture supernatant was supplemented with 400 μl of phosphate buffer pH 7.4 (160 mM Na_2HPO_4, 30 mM NaH_2PO_4, 1 mM TSP, and 3 mM NaN_3 in 100% D_2O) [22]. Samples were analyzed in 5 mm NMR tubes containing 550 μl of the sample mix. Control culture mediums were analyzed in parallel during each NMR session.

2.9.2. NMR Acquisition. All NMR experiments were acquired on a 600 MHz Bruker NMR spectrometer equipped with a 5 mm TCI cryoprobe at 30.0°C. A cooled SampleJet autosampler enabled high throughput data acquisition. A standard ^{1}H-1D NMR pulse sequence nuclear Overhauser effect spectroscopy (NOESY) with z-gradient and water presaturation (Bruker pulse program *noesygppr1d*) was recorded on each sample, with a total of 128 transient free induction decays (FID) and a spectral width of 20 ppm, and a relaxation delay was set to 4 seconds. The NOESY mixing time was set to 10 milliseconds, and the 90° pulse length was automatically determined for each sample (around 13 μs). The total acquisition time of each sample was 12 minutes and 15 seconds.

2.9.3. NMR Data Processing. All free induction decays (FIDs) were multiplied by an exponential function corresponding to a 0.3 Hz line-broadening factor prior to Fourier transform ^{1}H-NMR spectra which were manually phased and referenced to the glucose doublet at 5.23 ppm using TopSpin 2.2 (Bruker GmbH, Rheinstetten, Germany). TSP was not used for data processing in this study. For multivariate analyses, residual water signal (4.85–4.67 ppm) was excluded. Spectra were divided into 0.001 ppm-wide buckets over the chemical shift range (-0.2; 9.5 ppm) using the AMIX software (Bruker GmbH).

2.9.4. Spectra Analyses. Identification of the metabolites was carried out from the 1D NMR data using the software Chenomx NMR Suite 8.0 (Chenomx Inc., Edmonton, Canada) and confirmed from analysis of 2D ^{1}H-^{1}H TOCSY, ^{1}H-^{13}C HSQC, and ^{1}H J-Resolved NMR spectra recorded with standard parameters. The measured chemical shifts were compared to reference shifts of pure compounds using the

HMDB database [23]. Relative metabolite concentrations were determined using Chenomx software by manual fitting of the proton resonance lines for the compounds available in the database. The linewidth used in the reference database was adjusted to the width of one component of the alanine doublet. A pure standard lactate solution (1 g/l, Fisher) was used as an external concentration reference and exploited using the ERETIC2 utility from TopSpin (Bruker GmbH, Rheinstetten, Germany) to add a digitally synthesized peak to a spectrum [24]. Concentrations in the cell culture media are presented as absolute, not normalized data. They are apparent concentrations, as endogenous and FCS proteins were not removed from the NMR samples.

2.9.5. Multivariate Data Analyses. Multivariate analyses were performed on NMR spectra buckets in the absence of any normalization using SIMCA-P 13 (Umetrics, Umea, Sweden) with Pareto scaled variables. Principal component analysis (PCA) was used to derive the main sources of variance within the data set, assess sample homogeneity, and exclude biological or technical outliers. Orthogonal projection to latent structure discriminant analysis (O-PLS-DA) was used to build predictive sample classification models. Results were visualized on score plots, corresponding to sample projections onto the predictive axis and the first orthogonal component of the model, and the associated loading plot. The optimal number of orthogonal components was selected using a 7-fold cross-validation procedure. The R^2 and Q^2 parameters were computed to estimate the goodness of fit and prediction, i.e., the explained and predicted variances, respectively. The O-PLS-DA models were validated using permutations under the null hypothesis (1000 times); for each permutated classification labels, R^2 and Q^2 were recalculated and compared to the original ones, and their decrease indicates the good quality of the model [25]. Metabolites involved in class discrimination were highlighted with the statistical recoupling of variables (SRV) analysis [26]. SRV corresponds to an automatic binning scheme based on the relationship of correlation and covariance between consecutive variables, which is followed by a univariate unpaired two-tailed t-test calculated for each variable under the Benjamini–Hochberg correction to cope with multiple testing issues [27].

3. Results

3.1. Phenotypic Analysis and Stem Cell Properties of ASC Populations. S-ASC were isolated from subcutaneous and V-ASC from epididymal white adipose tissues in mice. ASC grew as monolayers in culture plates (Figure 1(a)). Starting from the stromal vascular fraction, our culture conditions led to the depletion in CD45+ and CD31+ cells representative of the hematopoietic and of the endothelial lineages, respectively, and to the enrichment into CD45- and CD31- cells at the end of the first passage. Analysis by flow cytometry showed that these cells were positive for mesenchymal stem cell markers (Sca1, CD29, and CD90) [28], and a fraction of them additionally expressed markers of the adipogenic potency (CD140a) (Figure 1(b)). However, these cells did not express CD24 (not shown) indicating that they were not committed to adipogenesis [29]. To confirm the mesenchymal stem cell identity of ASC, their multipotent differentiation potential was assessed [30]. Figure 2 shows that S- and V-ASC are able to differentiate into chondrocytes and into adipocytes, but only S-ASC can give rise to osteocytes, in accordance with a previous report [31]. Interestingly, both ASC had comparable efficiency to differentiate into chondrocytes, but V-ASC were less efficient than S-ASC to generate adipocytes. This was in accordance with the differences described between adipose depots regarding the fatty acid storage function. Altogether, these data confirm that our culture conditions are suitable to sustain the production of ASC from both SAT and VAT and to preserve their intrinsic functional differences.

3.2. Multivariate Statistical Analyses Discriminate S- and V-ASC and Highlight Differentially Secreted Metabolites. To define the best culture conditions to analyze the exometabolome (the ensemble of metabolites in the extracellular medium), we initially performed a comparison of the extracellular metabolite concentration variations over 24 to 72 h of culture (Figure S1). Culture supernatants of ASC cultivated during 72 h were analyzed by NMR spectrometry and delivered well-resolved ^{1}H-NMR metabolic profiles of the exometabolome. The ^{1}H-1D spectra presented typical sharp lines corresponding to small metabolites, overlaid with broad signals from lipids or larger proteins, which appeared negligible in the case of these culture supernatants (Figure 3). At 72 h, the steady state in metabolite changes was not reached even for the most proliferative population, S-ASC, except for essential amino acids which were still not depleted in the culture medium. The steady state in amino acid consumption reached after 48 h corresponded to growth arrest. These results show that medium replacement did not influence the linear consumption or secretion of metabolites analyzed from 24 to 72 h later and that cells analyzed in the conditions described in this study were still active for the glucose and the glutamine metabolisms.

As S- and V-ASC are known to functionally differ, we conducted multivariate data analyses of their exometabolome after 72 h of culture to identify the NMR spectra regions that correlate with cell types followed by peak identification. We also used univariate metabolite concentration comparisons to complement the analysis.

Multivariate data analyses were conducted on the NMR spectra bins (0.001 ppm; 9700 NMR spectral variables) to benefit from the full spectral dynamic range of information. To get a clear view on the metabolic differences between cell types, while avoiding the complexity induced by the production or consumption status of each metabolite, the analyses were performed on the absolute value of the NMR spectra variation to the original culture medium.

PCA unsupervised multivariate data analyses were first used to evaluate the dataset homogeneity and potential sample class discrimination. The dataset showed good homogeneity, though one sample from V-ASC appeared as a strong outlier on the PCA score plot and was subsequently removed from further analyses (this sample presented ethanol

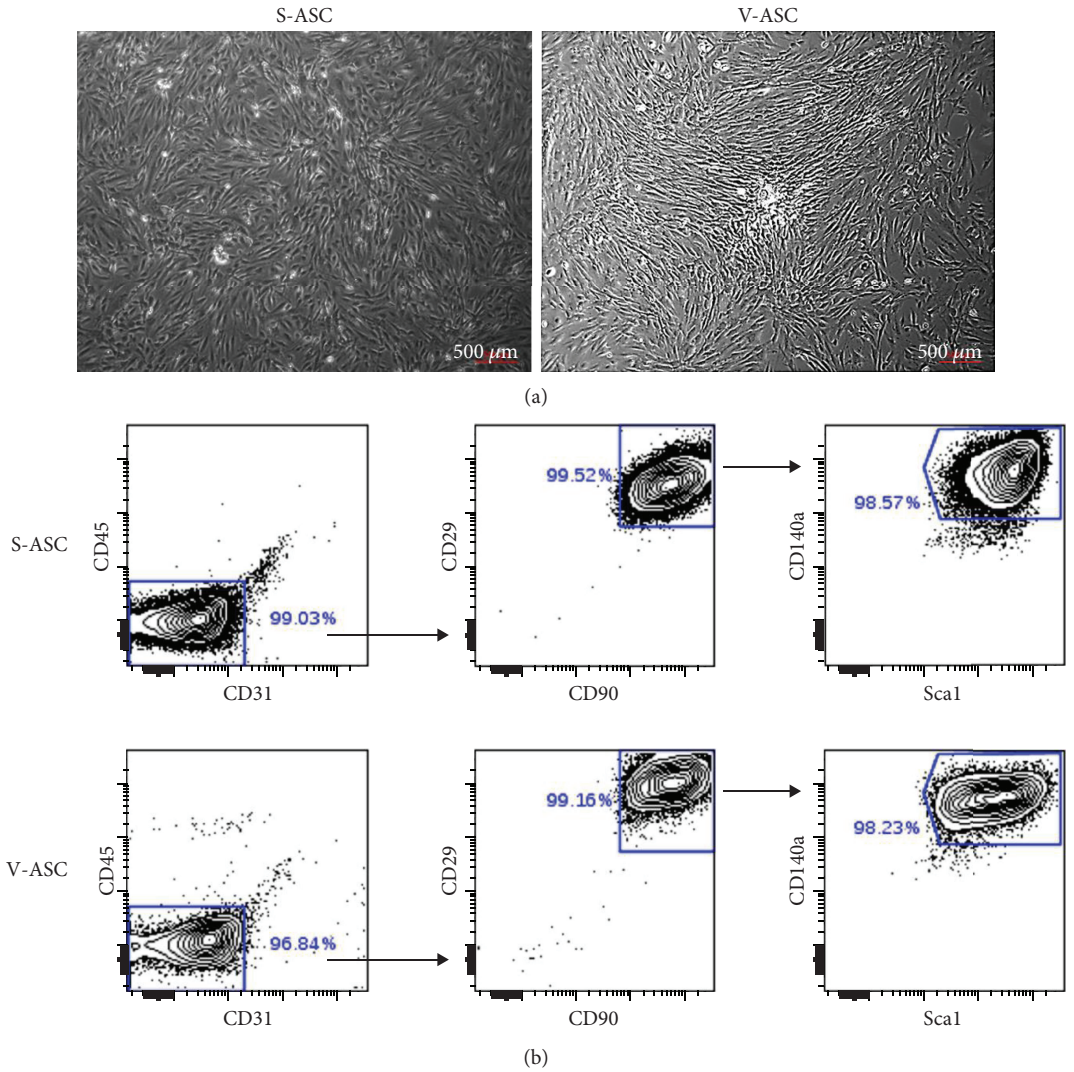

Figure 1: Characterization of ASC. S- and V-ASC were cultivated in ASC culture medium for 2 passages before analysis. (a) Feature of adipose-derived stem cells in culture: brightfield images of cells at confluency. (b) Membrane expression of markers of adipose stem cells CD29, CD90, Sca1, and CD140a analyzed by flow cytometry and represented as dot plot showing the percent of positive cells for the indicated markers.

contamination, data not shown). A straightforward discrimination between S-ASC and V-ASC was observed on the PCA unsupervised model (Figure 4(a)). Remarkably, the first principal component of this model could explain alone 68.4% of the variance within the dataset. Those untargeted results indicate significant differences of the metabolic profile between both cell types.

To specifically target the NMR regions discriminating S-ASC and V-ASC, a supervised analysis by O-PLS-DA [32, 33] was conducted on the 9700 NMR spectral variables. We obtained a strongly discriminating O-PLS-DA model (Figure 4(b)). The analysis of NMR regions presenting the most differentially expressed peaks pointed out 10 metabolites which concentration in the culture medium was the most influenced by the presence of the distinct ASC. Glucose, leucine, valine, glutamine, tyrosine, phenylalanine, lactate, and acetate appeared to vary more in V-ASC than in S-ASC culture supernatants, while citrate and alanine varied more in S-ASC than in V-ASC culture supernatants (Figure 4(c)). These results define distinct metabolic footprints of V- and S-ASC on their microenvironment and suggest metabolic differences between both cell types.

3.3. Depot-Specific Features of ASC Metabolic Signatures. Careful analysis of the ^{1}H-1D and 2D ^{1}H-^{1}H and ^{1}H-^{13}C NMR spectra provided the identification of 29 metabolites that were present in the S- and V-ASC supernatants after 72 h culture and that belong to a variety of biochemical classes (amino acids, sugars, and metabolic intermediates). We did not detect cell type-specific metabolites, but concentrations determined using the Chenomx software revealed quantitative differences (Table S1).

A scheme illustrating the main anabolic and catabolic pathways and key metabolites is presented in Figure 4(d). In this study, we analyzed changes at a given time in the composition of the cell culture supernatants in comparison

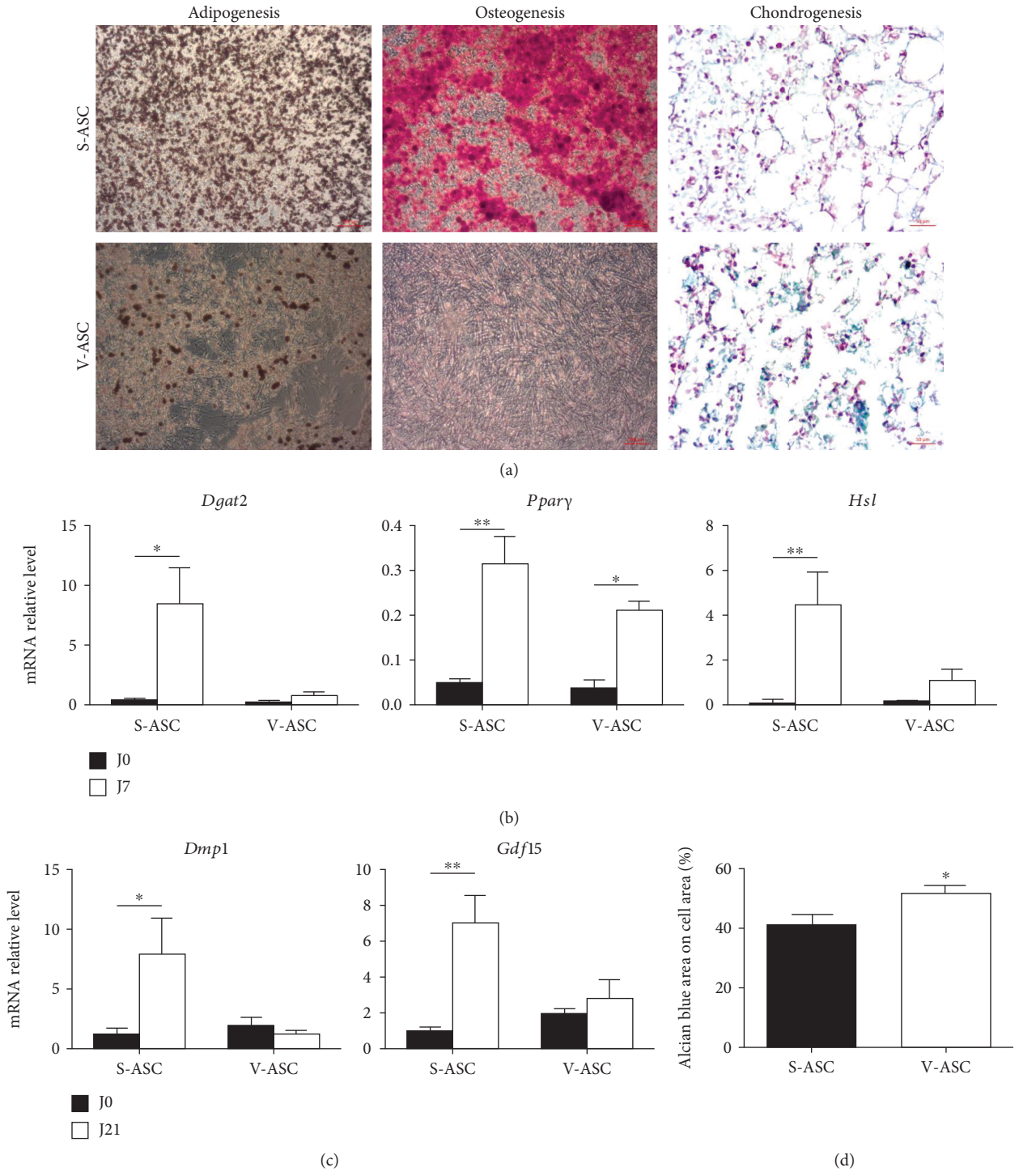

Figure 2: Differences between S- and V-ASC in their differentiation potential. S- and V-ASC were cultivated in ASC culture medium for 2 passages before (J0) the induction of differentiation into adipocytes for 7 days (J7) or into osteoblasts or chondrocytes for 21 (J21). (a) Brightfield images with a ×20 magnification represent adipocytes colored by Oil red O dye, osteoblasts colored with alizarin red dye, chondrocytes colored with alcian blue, and nucleus colored with fast red dye. (b) Quantification of adipogenic transcripts (*Dgat2*, *Pparγ*, and *Hsl*) by RT-qPCR analysis before and after induction of the adipogenic differentiation ($n = 3$). (c) Quantification of osteogenic genes *Dmp1* and *Gdf15*, which are, respectively, early and late markers of osteocytes, by RT-qPCR analysis before and after 21 days of osteogenic differentiation ($n = 3$). (d) Quantification of the chondrogenic differentiation by image analysis using the ImageJ software Fiji. Results present the ratio of the alcian blue-colored surface to the total cell surface and are representative of the proportion of chondrocyte-differentiated cells that are characterized by the expression of alcian blue-stained glycosaminoglycans. Analyzed pictures were from a ×20 magnification ($n = 4$). All results are mean ± SEM; statistics are from t-tests: $^{*}p < 0.05$ and $^{**}p < 0.01$.

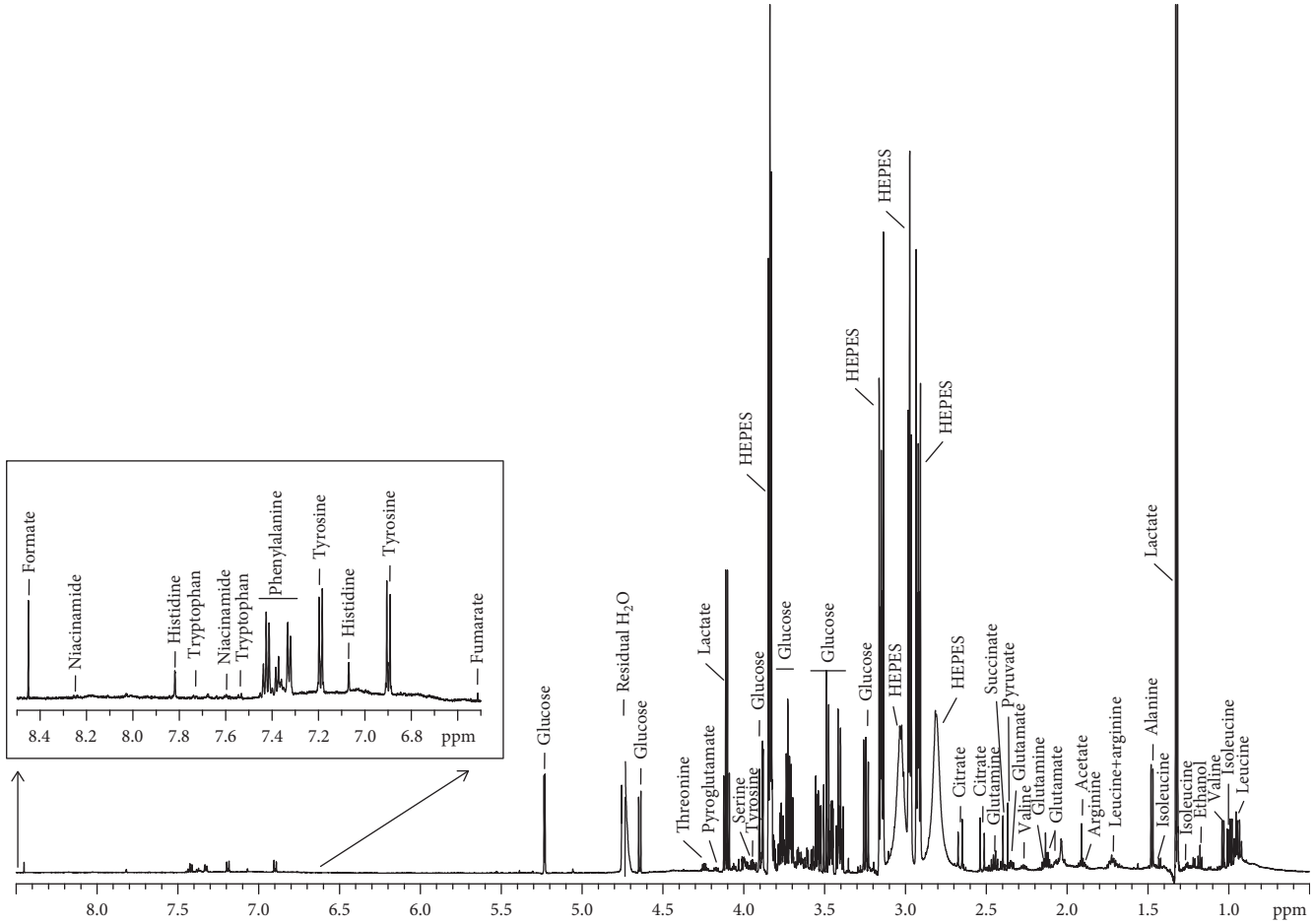

FIGURE 3: Typical ^{1}H-NMR spectrum of ASC supernatant (600 MHz, 30.0°C). Spectrum from 72 h culture of S-ASC supernatant is represented. Major metabolite peak assignments are indicated.

with the cell-free culture medium placed in the same conditions. Different from the intracellular compartment, the cell culture supernatant is not a homeostatic compartment. As a consequence, the exometabolome analyzed in this study does not reflect the status of the cells at a time but rather the addition of successive changes induced by the cellular activity during culture for a given period. Therefore, the correlation between the exometabolite concentrations in the cell culture supernatants and the number of cells at a given time is not linear. That is why all the results presented in the manuscript are metabolite concentrations in the culture supernatants without any normalization and for a given period of time. However, a major attention was paid to the number of cells to minimize the contribution of this parameter to the results.

Glucose and glutamine were the most consumed substrates, and their transformation products, lactate and glutamate, were among the most secreted metabolites, along with citrate and alanine (Figures 5(a), Figure S1). When considering glycolysis, the consumption of glucose mirrored the production of lactate indicating active glycolysis in ASC. The high level of lactate secretion demonstrates a high aerobic glycolytic activity in both S- and V-ASC. This singularity was previously described as the Warburg-like effect, a type of noncancer cell metabolism associated with self-renewing stem cells [34].

On the opposite, the consumption of glutamine generated few amounts of glutamate, indicating that the carbons generated from glutaminolysis were directed elsewhere, most probably towards the production of additional metabolites and cell growth, as suggested by the strong amino acid consumptions supporting the anabolism associated with protein synthesis (Table S1). Indeed, essential amino acids (EAAs), which cannot be synthetized in mammalian cells, such as phenylalanine, histidine, and threonine, branched chain essential amino acids (BCAAs: valine, leucine, and isoleucine), and even the semi-EAA tyrosine were similarly consumed by both ASC (Table S1). The consumption of EAA is essential and inherent to proliferating cells, but the secretion rather than incorporation of glutamate and alanine (Figures 5(a)) suggests an excess of these amino acid production regarding protein synthesis in the context of stem cells.

This ensemble of observations highlights a high glycolysis associated to a Warburg-like effect and glutaminolysis activity in ASC, typical of cells in active division as confirmed by the cell count along several passages (Figure 5(c)). However, interesting differences were observed between the two ASC

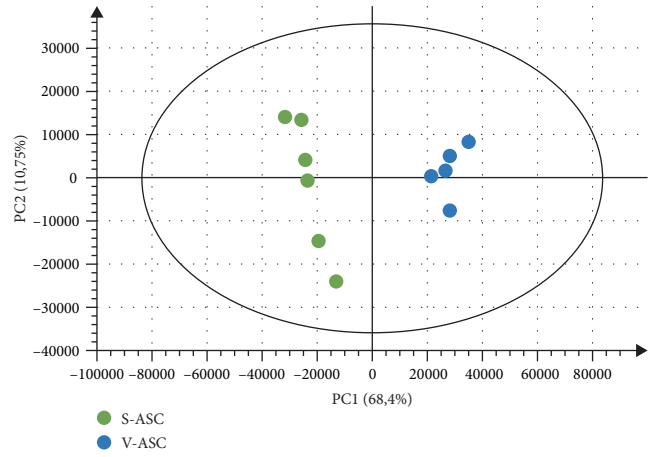

(a)

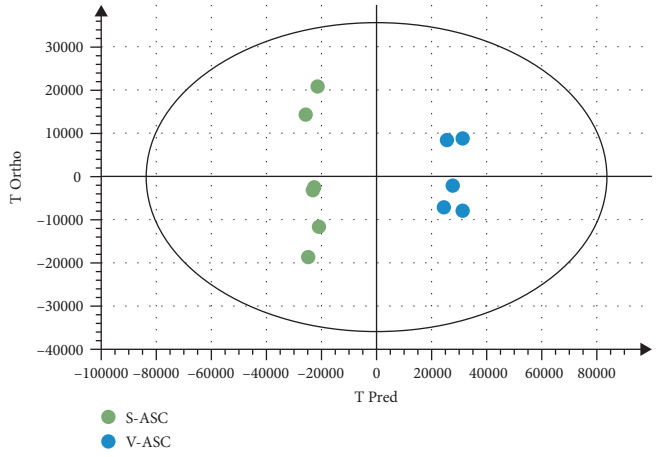

(b)

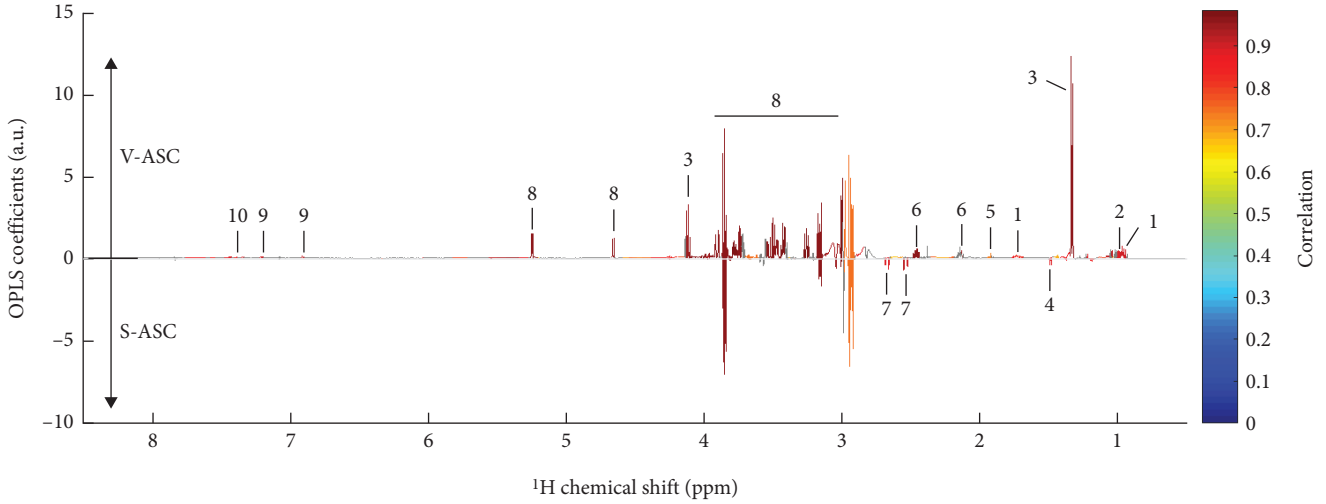

(c)

Figure 4: Continued.

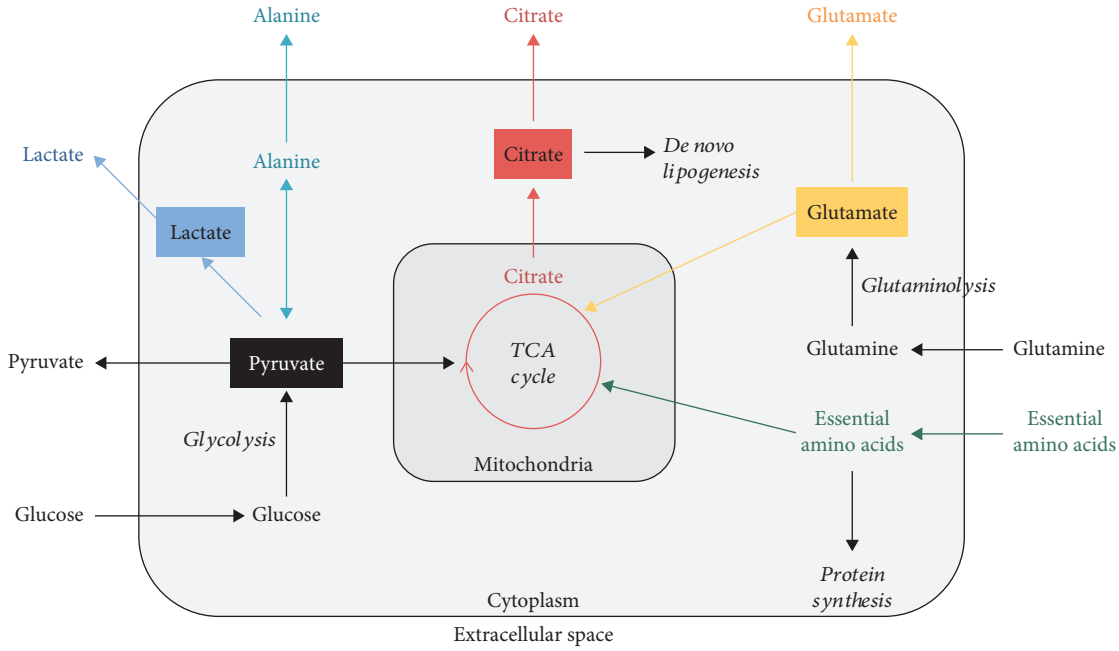

(d)

Figure 4: Multivariate statistical analyses of the differences between S- and V-ASC exometabolomes. High-resolution NMR multivariate data analyses unveil significant differences in extracellular metabolite variations between S-ASC and V-ASC at 75% confluency and cultivated for additional 72 h in media containing 25 mM glucose, 4 mM glutamine, 1 mM pyruvate, and nonessential amino acids as determined by NMR absolute spectra bins after subtraction of the culture medium signal analysis performed on NMR spectra buckets without normalization to the cell number. At the time of supernatant collection, cells were at confluency. (a) Untargeted principal component analysis (PCA) readily evidences the cell type as a major origin of the dataset variance. Score plot of the PCA model (PC1 and PC2) ($n = 11$, $R^2 = 0.962$, and $Q^2 = 0.843$ on 5 principal components). (b, c) Supervised multivariate data analysis (O-PLS-DA) optimizes the discrimination between both cell types after 72 h of culture. The strong discrimination of the multivariate model is shown by the high values of goodness-of-fit model parameters R^2 and Q^2 ($R^2(X) = 0.796$, $R^2(Y) = 0.991$, and $Q^2 = 0.969$). The discrimination robustness was validated by resampling 1000 times the model under the null hypothesis (data not shown), and the analysis of variance (CV-ANOVA) of the model led to a p value of 1.20×10^{-4}. (b) Score plot of the (1 + 1) O-PLS-DA model discriminating S-ASC (in green) and V-ASC (in blue). (c) O-PLS-DA loading plot after SRV analysis and Benjamini–Hochberg multiple testing correction. The O-PLS-DA loadings reveal the influential metabolite variations on the cell type discrimination (V-ASC upper panel and S-ASC lower panel). The loading plot was complemented by color-coded correlation [26] indicating statistically significant signals. Highlighted candidate biomarkers are (1) leucine, (2) valine, (3) lactate, (4) alanine, (5) acetate, (6) glutamine, (7) citrate, (8) glucose, (9) tyrosine, and (10) phenylalanine. (d) Simplified and nonquantitative representation of the main carbon metabolic pathways in actively dividing cells. Anabolic and catabolic pathways are represented in italics in relation to the metabolite secretome. Colors identify the metabolic pathways analyzed in this study. TCA: tricarboxylic acid cycle; EAA: essential amino acids.

populations. V-ASC secreted higher lactate concentrations and S-ASC higher citrate concentrations in culture supernatants (Figures 5(a)).

Illustrating the mitochondrial activity, citrate is a metabolite produced by the tricarboxylic acid (TCA) cycle. The citrate produced by the TCA pathway inside the mitochondria can be further processed as a substrate for ATP production or partly exported to the cytoplasm to fuel the de novo lipid biosynthesis pathway (Figure 3(d)), a feature required to the neosynthesis of membranes of highly proliferating cells [35]. These intracellular metabolite fluctuations are beyond the scope of this study.

Both lactate and citrate are features of highly proliferating stem cells and are, respectively, representative of the use of pyruvate in glycolysis and in the mitochondrial TCA cycle. A high level of glycolysis is the signature of undifferentiated cells [36] while citrate can be used for *de novo* lipogenesis to support the synthesis of new cell membranes [35]. The comparison of S- and V-ASC growth curves shows that V-ASC proliferated slower than S-ASC and generated at the third passage about 10-fold less cells (Figure 5(c)) despite a higher glycolytic activity. After the third passage, S-ASC entered the exponential growth phase while V-ASC proliferation started to decline (Figure 5(c)). In this study, cells were used at passage 2 where the cell number in both populations was still quite similar as shown in Figure 5(b) ruling out the influence of the number of cells in the lower citrate secretion by V-ASC. Therefore, the difference in the balance between lactate and citrate secretions is a key feature of the difference between S- and V-ASC that suggests distinct uses of pyruvate between the two populations.

Pyruvate diversion away from the mitochondria is an active process differentiating cancer and noncancer stem cells [37]. UCP2 has been evidenced as a gatekeeper of pyruvate entry into the mitochondria that limits mitochondrial catabolism of pyruvate [38] and promotes oxidation of

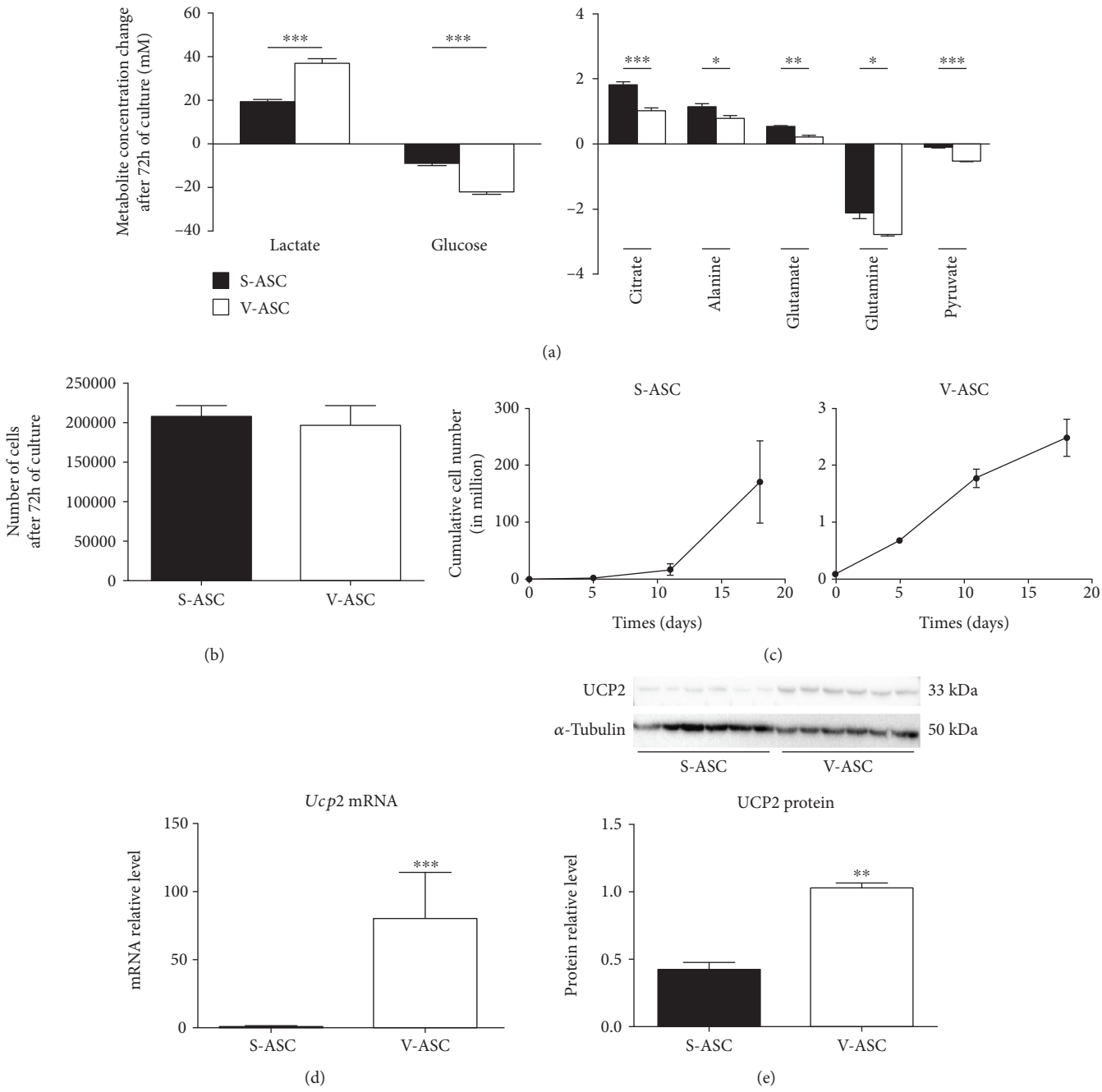

Figure 5: Quantitative comparison of S- and V-ASC secretomes: S- and V-ASC at 75% confluency were cultivated for 72 h in fresh culture medium containing pyruvate to reach confluency. Cells were counted as supernatants were collected for NMR analysis. Variations of the concentrations after deduction of the medium values are represented without normalization to the cell number. (a) Metabolites representing glycolysis (left panel) and other metabolites (right panel) showing significant differences between S- and V-ASC ($n = 6$). (b) Number of cells obtained after 72 h of culture with pyruvate. Cells were counted after collection of the culture supernatants ($n = 6$). (c) Cumulative growth curves: S- and V-ASC were cultivated in complete culture medium (see Materials and Methods) from the isolation to the 4th passage. The number of cells after each passage is represented ($n = 3$). (d) Comparison of *Ucp2* mRNA expression in S- and V-ASC. *Ucp2* mRNA levels were quantified by RT-qPCR in S- and V-ASC harvested at the second passage. Values are normalized on the expression of the housekeeping gene *RS17* ($n = 7$). (e) Comparison of UCP2 protein content in S- and V-ASC cell lysates by western blotting. Cell lysates were from S- and V-ASC harvested at the second passage. Images (top) were obtained with the ChemiDoc XRS+ imaging system (Bio-Rad) and were analyzed (bottom) with the Quantity One software (Bio-Rad). Values were normalized relatively to the α-tubulin protein expression ($n = 3$). All results are mean ± SEM; statistics are from t-tests: $^{*}p < 0.05$, $^{**}p < 0.01$, and $^{***}p < 0.001$.

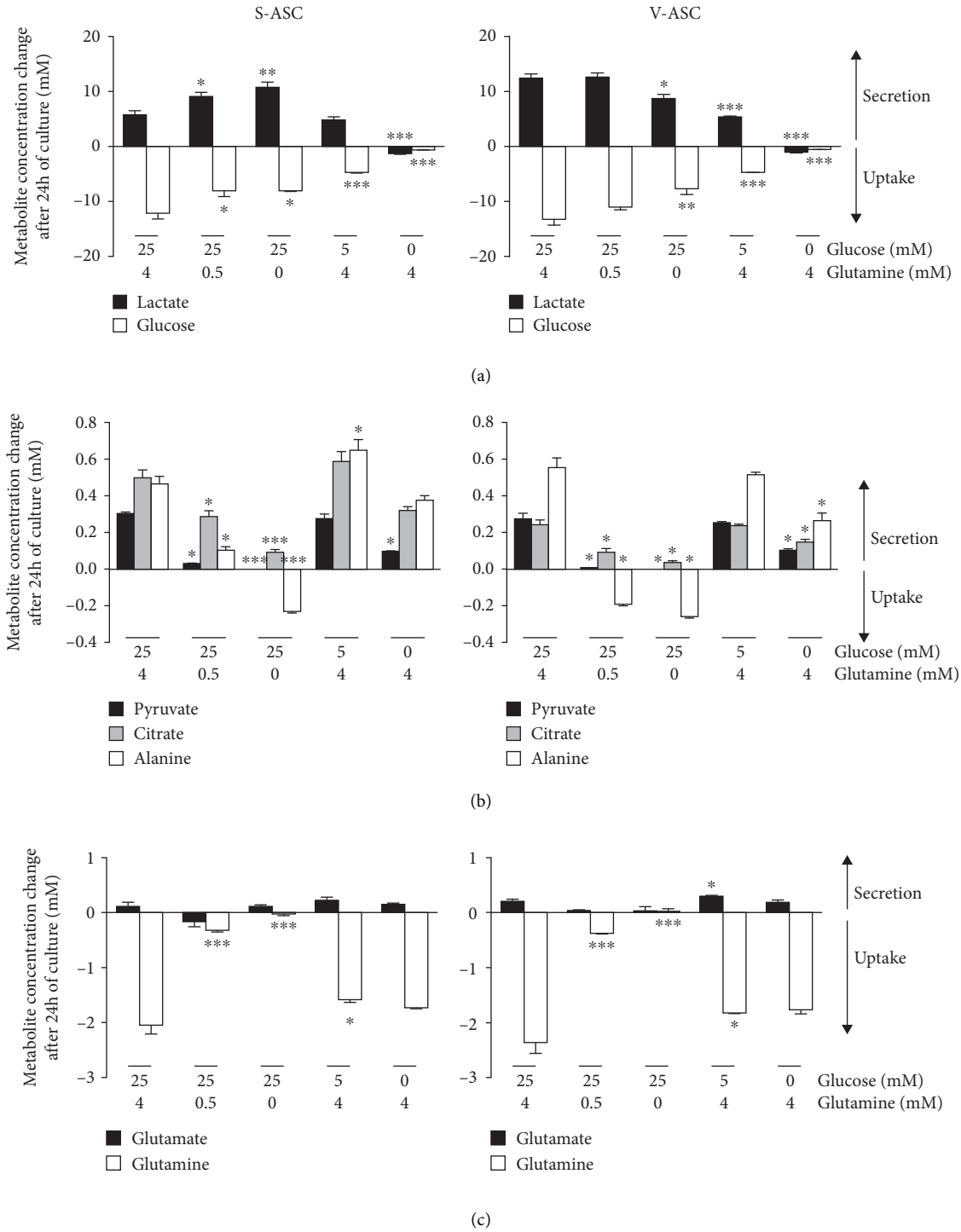

Figure 6: Role of glutamine and glucose in the secretome of ASC. ASC were cultivated for 72 h in fresh culture medium containing pyruvate to reach confluency. For additional 24 h of culture, the medium was replaced by pyruvate-free medium adapted to metabolomics analyses and supplemented with 0, 5, or 25 mM glucose in the presence of 0, 0.5, or 4 mM glutamine as indicated in the figure. Concentrations in culture supernatants were measured by ^{1}H-NMR. Results (mean ± SEM; $n = 3$) are the difference between concentrations in cell culture supernatants and the concentration in the initial medium placed in the same conditions (control). Values were not normalized to the cell number. Negative values represent metabolite consumptions and positive values the secretions at concentrations above the control. Results for S-ASC and V-ASC are represented back to back in the figures. (a) The glycolysis pathway is evidenced by monitoring glucose uptake and lactate secretion. (b) Pyruvate, citrate, and alanine secretions and uptakes. (c) The glutaminolysis pathway is evidenced by monitoring glutamine uptake and glutamate secretion. Statistics are from the one-way ANOVA test followed by Tukey's multiple comparison test: $^{*}p < 0.05$, $^{**}p < 0.01$, and $^{***}p < 0.001$ and comparison of the partially depleted medium conditions with the complete medium condition (25 mM glucose and 4 mM glutamine). In (b) and (c), values for pyruvate and glutamate concentrations in glutamine-free conditions are represented but too low to be visible at the scale of these figures.

alternative substrates such as glutamine and fatty acids [39]. Preventing OXPHOS activation, UCP2 expressed in embryonic stem cells favors their maintenance and is repressed as pluripotency is lost [40]. Measurements of *Ucp2* transcripts (Figure 5(d)) and UCP2 protein (Figures 5(d)) in ASC revealed the higher expression in V-ASC than in S-ASC, which is consistent in V-ASC cells with a reduced pyruvate routing into the mitochondria, an elevated lactate secretion, and a majored role of glycolysis for ATP production.

Altogether, ASC present the characteristics of proliferating stem cells, with a Warburg-like effect, associated with active amino acid consumption and a specific feature concerning both an elevated citrate secretion and a high glutamine consumption/low glutamate secretion.

However, compared with S-ASC, V-ASC metabolism supports a stronger Warburg-like effect and a lower TCA cycle activity. This imbalance may account for the lower ability of V-ASC to differentiate into adipocytes and their inability to give rise to osteoblasts compared with S-ASC (Figure 2). Indeed, both differentiation pathways require an increased mitochondrial activity [41] and, for osteogenesis and bone formation, the accumulation of citrate and the inhibition of glycolysis [21] [42]. On the contrary, chondrogenesis, which predominantly uses the glycolytic metabolism as a source of ATP [21], was obtained from both S- and V-ASC (Figure 2).

3.4. Glutamine Is a Key Player in the Control of Pyruvate Routing in ASC. To better characterize the S- and V-ASC metabolic differences, cells were cultivated in partially depleted culture media.

The Warburg-like effect and the citrate production involve, respectively, the glycolysis pathway and mitochondrial TCA cycle. To decipher the respective contributions of glucose and glutamine as sources of carbon in ASC, we performed end-point experiments with cells cultivated for 96 h, in culture media completely or partially depleted in glucose and/or glutamine during the last 24 h. The replacement of the medium and the measurement on a short period and on cells at confluency were chosen to avoid the influence of substrate depletion in other metabolites than glutamine and glucose. As expected, partial or total depletion of glutamine and/or glucose affected the final number of cells. We made the choice to present metabolite concentrations without normalization on cell number because they reflected the loss of cells and do not represent what happened before. Complete results are available in Table S2. Because pyruvate is the end product of glycolysis and a substrate for the TCA cycle, these experiments were performed in pyruvate-free medium to evaluate the respective contributions of glucose and glutamine to pyruvate secretions.

For both S- and V-ASC, the secretion of lactate was dependent on glucose availability (Figure 6(a) , left and right panels, respectively). Indeed, in the absence of glucose, no lactate was secreted in the culture supernatants. On the contrary, in the absence of glucose, cells consumed the little amount of lactate initially present in the medium. Importantly, glutamine privation completely switched the metabolism of S-ASC, but not V-ASC, towards lactate synthesis. Indeed, in glutamine-free medium, lactate secretion by S-ASC increased from 6.0 ± 0.7 mM to 11.0 ± 1 mM, but glucose uptake decreased from 12.1 ± 1.1 mM to 8.0 ± 0.15 mM (Figure 6(a). This could reflect a more efficient conversion of glucose into lactate by S-ASC in the absence of glutamine, probably at the expense of the alternative uses of glucose molecules, and indicated that glycolysis in S-ASC, but not in V-ASC, was sensitive to glutamine availability.

Modulating glutamine and/or glucose supply in the culture media without pyruvate revealed that the release of pyruvate, citrate, and alanine was dose-dependently correlated with glutamine concentration but not with glucose concentrations in S- and V-ASC. Only complete glucose deprivation decreased pyruvate secretion but to a lesser extent than in the absence of glutamine (Figure 6(b)). Pyruvate is an intermediate metabolite of many pathways. It is the end product of glycolysis that can be converted into alanine by transamination and into lactate through lactate synthesis or can enter the mitochondrial tricarboxylic acid cycle to produce citrate. The partial (V-ASC) or total (S-ASC) independence of citrate and alanine secretions regarding glycolysis (Figure 6(b)) further underlines the unexpected contribution of glutaminolysis for glucose consumption. The lack of pyruvate release in the absence of glutamine indicated an increase of pyruvate consumption by both ASC. Since citrate and alanine secretions were decreased in the absence of glutamine (Figure 6(b)), we can conclude that the consumed pyruvate was not used to feed the TCA cycle nor for alanine synthesis. Accordingly, in the case of S-ASC, pyruvate seemed to be redirected to lactate synthesis, raising the Warburg-like effect to levels comparable to those obtained with V-ASC in complete medium. We did not detect a clear dose response relationship between glutamate secretion and glutamine uptake, indicating that glutamate secretion in ASC is not exclusively linked to glutamine metabolism. Glucose depletion in the medium did not affect glutamate secretion nor glutamine consumption. This indicated that glycolysis was not involved in the control of glutaminolysis (Figure 6(c)).

These results indicate that glutaminolysis is central for the use of pyruvate in TCA cycle and in the synthesis of alanine in ASC. In S-ASC only, glutamine privation also leads to a drastic switch of pyruvate consumption towards lactate production, exacerbating the Warburg-like effect. Our results reveal that sensitivity to glutamine availability is a key feature discriminating both ASC populations and evidence a complex situation where glutamine could be used as an alternative source of carbon and/or where glutaminolysis could control the fate of glycolysis products. Further analyses involving fluxomics experiments and isotope labeling will be required to finely dissect the underlying mechanisms involved.

4. Conclusion

Altogether, our results show that ASC have a mixed metabolism based on both glycolysis and mitochondrial activity, similar to what was already reported for bone marrow mesenchymal stem cells [21]. Interestingly, we show that

glutaminolysis controls pyruvate consumption for use in TCA cycle and for alanine synthesis. Importantly, glutaminolysis also prevents the use of pyruvate for lactate production in S-ASC, but not in V-ASC. The apparent lack of this regulation level in V-ASC is compatible with the preferential use of pyruvate for lactate synthesis, probably at the expense of the mitochondrial activity, in these cells. As a consequence, S- and V-ASC can be discriminated by their relative secretion of lactate and citrate, lactate being more secreted by V-ASC and citrate by S-ASC.

To our knowledge, this study is the first one to describe at the metabolic level the differences between adipose-derived stem cells isolated from distinct adipose depots. Our results raise the possibility that mechanisms controlling the flux of pyruvate towards the synthesis of either lactate in the cytoplasm or citrate in the mitochondria could be related to the reported differences between S- and V-ASC in their proliferation and differentiation potentials. In the light of our results, the correlation between the emergence of pathologies related to the metabolic syndrome and the opposite changes affecting the expansion of the subcutaneous and the visceral adipose tissues may reflect a disruption of the metabolic program supporting ASC at the expense of their original functions.

Future challenge will be to characterize the mechanisms supporting the specific metabolism of ASC in each fat depot and the conditions leading to their breaking.

Data Availability

The data used to support the findings of this study are included within the article. For each metabolomic experiment presented in this article, the supplementary tables list the results obtained for all the metabolites identified by RMN analysis, even those that were not presented in the figures.

Conflicts of Interest

The authors declare that they have no conflict of interest.

Authors' Contributions

Camille Lefevre and Baptiste Panthu contributed equally to this work.

Acknowledgments

We thank Stéphanie Chanon from the CarMeN Laboratory, for her help in the ImageJ analysis of histological images. This study was supported by a grant from INRA (Institut National de la Recherche Agronomique) - CIRAD (Centre de Coopération Internationale en Recherche Agronomique pour le Développement): Glofoods programme and from recurrent funding from INSERM, Université Claude Bernard Lyon 1, and INRA to the CarMeN laboratory (INSERM U1060-INRA 1397). Camille Lefevre was supported by a PhD fellowship from the French Ministry of Higher Education and Scientific Research.

Supplementary Materials

Supplementary 1. Figure S1: kinetic study of the exometabolome of S-ASC. S-ASC were cultivated in medium containing pyruvate for 24 h to reach 70-80% confluency before replacement with medium of the same composition. Culture supernatants were collected after 24, 48, or 72 additional hours of culture without medium change. Cells were counted after collection of the supernatants. Concentrations have not been normalized to the cell number. (A) Kinetic of glutamine and glutamate variations. (B) Glycolysis kinetic. (C) Kinetic of citrate secretion. (D) Kinetic of the branched amino acid consumption. (E) Kinetic of alanine. ($n = 3$). (F) Cell count per well. All results are mean ± SEM.

Supplementary 2. Table S1: concentrations of metabolites measured by ^{1}H-NMR in S- and V-ASC supernatants after 72 h of culture in the conditions described in Figure 5. Metabolite concentrations in the medium placed in the same culture conditions but without cells have been deduced in the presented results. Data have not been normalized. The number of cells in each well is indicated. Concentrations in S- and in V-ASC were compared. Statistics are from t-tests; p value ≤ 0.05 is considered significant.

Supplementary 3. Table S2: concentrations of metabolites measured by ^{1}H-NMR in S- and V-ASC supernatants after 24 h of culture at confluency with variable concentrations of glutamine and glucose in the conditions described in Figure 6. Metabolite concentrations in the medium placed in the same culture conditions but without cells have been deduced in the presented results. Data have not been normalized. The number of cells in each well is indicated. Statistics are from one-way ANOVA followed by multiple comparison Tukey's tests. Comparisons are done relatively to the control medium culture condition (25 mM glucose and 4 mM glutamine). p value ≤ 0.05 is considered significant; ns: not significant.

References

[1] S. Méndez-Ferrer, T. V. Michurina, F. Ferraro et al., "Mesenchymal and haematopoietic stem cells form a unique bone marrow niche," *Nature*, vol. 466, no. 7308, pp. 829–834, 2010.

[2] M. Abumaree, M. Al Jumah, R. A. Pace, and B. Kalionis, "Immunosuppressive properties of mesenchymal stem cells," *Stem Cell Reviews*, vol. 8, no. 2, pp. 375–392, 2012.

[3] S. K. Kapur and A. J. Katz, "Review of the adipose derived stem cell secretome," *Biochimie*, vol. 95, no. 12, pp. 2222–2228, 2013.

[4] R. E. B. Fitzsimmons, M. S. Mazurek, A. Soos, and C. A. Simmons, "Mesenchymal stromal/stem cells in regenerative medicine and tissue engineering," *Stem Cells International*, vol. 2018, Article ID 8031718, 16 pages, 2018.

[5] F. Vizoso, N. Eiro, S. Cid, J. Schneider, and R. Perez-Fernandez, "Mesenchymal stem cell secretome: toward cell-free therapeutic strategies in regenerative medicine," *International Journal of Molecular Sciences*, vol. 18, no. 9, p. 1852, 2017.

[6] B. L. Wajchenberg, "Subcutaneous and visceral adipose tissue: their relation to the metabolic syndrome," *Endocrine Reviews*, vol. 21, no. 6, pp. 697–738, 2000.

[7] T. Tchkonia, Y. D. Tchoukalova, N. Giorgadze et al., "Abundance of two human preadipocyte subtypes with distinct capacities for replication, adipogenesis, and apoptosis varies among fat depots," *American Journal of Physiology. Endocrinology and Metabolism*, vol. 288, no. 1, pp. E267–E277, 2005.

[8] K. Frayn, "Adipose tissue as a buffer for daily lipid flux," *Diabetologia*, vol. 45, no. 9, pp. 1201–1210, 2002.

[9] L. Fontana, J. C. Eagon, M. E. Trujillo, P. E. Scherer, and S. Klein, "Visceral fat adipokine secretion is associated with systemic inflammation in obese humans," *Diabetes*, vol. 56, no. 4, pp. 1010–1013, 2007.

[10] M. Alligier, E. Meugnier, C. Debard et al., "Subcutaneous adipose tissue remodeling during the initial phase of weight gain induced by overfeeding in humans," *The Journal of Clinical Endocrinology and Metabolism*, vol. 97, no. 2, pp. E183–E192, 2012.

[11] E. Jeffery, C. D. Church, B. Holtrup, L. Colman, and M. S. Rodeheffer, "Rapid depot-specific activation of adipocyte precursor cells at the onset of obesity," *Nature Cell Biology*, vol. 17, no. 4, pp. 376–385, 2015.

[12] A. W. B. Joe, L. Yi, Y. Even, A. W. Vogl, and F. M. V. Rossi, "Depot-specific differences in adipogenic progenitor abundance and proliferative response to high-fat diet," *Stem Cells*, vol. 27, no. 10, pp. 2563–2570, 2009.

[13] R. Berry, E. Jeffery, and M. S. Rodeheffer, "Weighing in on adipocyte precursors," *Cell Metabolism*, vol. 19, no. 1, pp. 8–20, 2014.

[14] T. Tchkonia, N. Giorgadze, T. Pirtskhalava et al., "Fat depot–specific characteristics are retained in strains derived from single human preadipocytes," *Diabetes*, vol. 55, no. 9, pp. 2571–2578, 2006.

[15] C. U. Niesler, K. Siddle, and J. B. Prins, "Human preadipocytes display a depot-specific susceptibility to apoptosis," *Diabetes*, vol. 47, no. 8, pp. 1365–1368, 1998.

[16] P. Djian, A. K. Roncari, and C. H. Hollenberg, "Influence of anatomic site and age on the replication and differentiation of rat adipocyte precursors in culture," *The Journal of Clinical Investigation*, vol. 72, no. 4, pp. 1200–1208, 1983.

[17] M. Adams, C. T. Montague, J. B. Prins et al., "Activators of peroxisome proliferator-activated receptor gamma have depot-specific effects on human preadipocyte differentiation," *The Journal of Clinical Investigation*, vol. 100, no. 12, pp. 3149–3153, 1997.

[18] T. Tchkonia, N. Giorgadze, T. Pirtskhalava et al., "Fat depot origin affects adipogenesis in primary cultured and cloned human preadipocytes," *American Journal of Physiology. Regulatory, Integrative and Comparative Physiology*, vol. 282, no. 5, pp. R1286–R1296, 2002.

[19] K. Ito and T. Suda, "Metabolic requirements for the maintenance of self-renewing stem cells," *Nature Reviews. Molecular Cell Biology*, vol. 15, no. 4, pp. 243–256, 2014.

[20] A. Wanet, T. Arnould, M. Najimi, and P. Renard, "Connecting mitochondria, metabolism, and stem cell fate," *Stem Cells and Development*, vol. 24, no. 17, pp. 1957–1971, 2015.

[21] G. Pattappa, H. K. Heywood, J. D. de Bruijn, and D. A. Lee, "The metabolism of human mesenchymal stem cells during proliferation and differentiation," *Journal of Cellular Physiology*, vol. 226, no. 10, pp. 2562–2570, 2011.

[22] O. Beckonert, H. C. Keun, T. M. D. Ebbels et al., "Metabolic profiling, metabolomic and metabonomic procedures for NMR spectroscopy of urine, plasma, serum and tissue extracts," *Nature Protocols*, vol. 2, no. 11, pp. 2692–2703, 2007.

[23] D. S. Wishart, Y. D. Feunang, A. Marcu et al., "HMDB 4.0: the human metabolome database for 2018," *Nucleic Acids Research*, vol. 46, no. D1, pp. D608–D617, 2018.

[24] Y. S. Jung, J. S. Hyeon, and G. S. Hwang, "Software-assisted serum metabolite quantification using NMR," *Analytica Chimica Acta*, vol. 934, pp. 194–202, 2016.

[25] J. A. Westerhuis, H. C. J. Hoefsloot, S. Smit et al., "Assessment of PLSDA cross validation," *Metabolomics*, vol. 4, no. 1, pp. 81–89, 2008.

[26] V. Navratil, C. Pontoizeau, E. Billoir, and B. J. Blaise, "SRV: an open-source toolbox to accelerate the recovery of metabolic biomarkers and correlations from metabolic phenotyping datasets," *Bioinformatics*, vol. 29, no. 10, pp. 1348-1349, 2013.

[27] Y. Benjamini and Y. Hochberg, "Controlling the false discovery rate: a practical and powerful approach to multiple testing," *Journal of the Royal Statistical Society: Series B (Methodological)*, vol. 57, no. 1, pp. 289–300, 1995.

[28] W. P. Cawthorn, E. L. Scheller, and O. A. MacDougald, "Adipose tissue stem cells meet preadipocyte commitment: going back to the future," *Journal of Lipid Research*, vol. 53, no. 2, pp. 227–246, 2012.

[29] R. Berry and M. S. Rodeheffer, "Characterization of the adipocyte cellular lineage in vivo," *Nature Cell Biology*, vol. 15, no. 3, pp. 302–308, 2013.

[30] M. Dominici, K. Le Blanc, I. Mueller et al., "Minimal criteria for defining multipotent mesenchymal stromal cells. The International Society for Cellular Therapy position statement," *Cytotherapy*, vol. 8, no. 4, pp. 315–317, 2006.

[31] S. Baglioni, G. Cantini, G. Poli et al., "Functional differences in visceral and subcutaneous fat pads originate from differences in the adipose stem cell," *PLoS One*, vol. 7, no. 5, article e36569, 2012.

[32] J. M. Fonville, S. E. Richards, R. H. Barton et al., "The evolution of partial least squares models and related chemometric approaches in metabonomics and metabolic phenotyping," *Journal of Chemometrics*, vol. 24, no. 11-12, pp. 636–649, 2010.

[33] J. Trygg and S. Wold, "Orthogonal projections to latent structures (O-PLS)," *Journal of Chemometrics*, vol. 16, no. 3, pp. 119–128, 2002.

[34] T. Simsek, F. Kocabas, J. Zheng et al., "The distinct metabolic profile of hematopoietic stem cells reflects their location in a hypoxic niche," *Cell Stem Cell*, vol. 7, no. 3, pp. 380–390, 2010.

[35] L. C. Costello and R. B. Franklin, "A review of the important central role of altered citrate metabolism during the process of stem cell differentiation," *Journal of Regenerative Medicine and Tissue Engineering*, vol. 2, no. 1, p. 1, 2013.

[36] W.-M. Yu, X. Liu, J. Shen et al., "Metabolic regulation by the mitochondrial phosphatase PTPMT1 is required for hematopoietic stem cell differentiation," *Cell Stem Cell*, vol. 12, no. 1, pp. 62–74, 2013.

[37] E. Aguilar, I. Marin de Mas, E. Zodda et al., "Metabolic reprogramming and dependencies associated with epithelial cancer stem cells independent of the epithelial-mesenchymal transition program," *Stem Cells*, vol. 34, no. 5, pp. 1163–1176, 2016.

[38] C. Pecqueur, T. Bui, C. Gelly et al., "Uncoupling protein-2 controls proliferation by promoting fatty acid oxidation and limiting glycolysis-derived pyruvate utilization," *The FASEB Journal*, vol. 22, no. 1, pp. 9–18, 2008.

[39] A. Vozza, G. Parisi, F. De Leonardis et al., "UCP2 transports C4 metabolites out of mitochondria, regulating glucose and glutamine oxidation," *Proceedings of the National Academy of Sciences of the United States of America*, vol. 111, no. 3, pp. 960–965, 2014.

[40] J. Zhang, I. Khvorostov, J. S. Hong et al., "UCP2 regulates energy metabolism and differentiation potential of human pluripotent stem cells," *The EMBO Journal*, vol. 30, no. 24, pp. 4860–4873, 2011.

[41] Y. Zhang, G. Marsboom, P. T. Toth, and J. Rehman, "Mitochondrial respiration regulates adipogenic differentiation of human mesenchymal stem cells," *PLoS One*, vol. 8, no. 10, article e77077, 2013.

[42] L. C. Costello, R. B. Franklin, M. A. Reynolds, and M. Chellaiah, "The important role of osteoblasts and citrate production in bone formation: "osteoblast citration" as a new concept for an old relationship," *The Open Bone Journal*, vol. 4, no. 1, pp. 27–34, 2012.

Hindawi
Stem Cells International
Volume 2019, Article ID 7360121, 10 pages
https://doi.org/10.1155/2019/7360121

Review Article

Metabolism Is a Key Regulator of Induced Pluripotent Stem Cell Reprogramming

James Spyrou, David K. Gardner, and Alexandra J. Harvey

School of BioSciences, The University of Melbourne, Parkville, VIC 3010, Australia

Correspondence should be addressed to Alexandra J. Harvey; ajharvey@unimelb.edu.au

Received 28 December 2018; Revised 15 March 2019; Accepted 2 April 2019; Published 5 May 2019

Academic Editor: Oswaldo Keith Okamoto

Reprogramming to pluripotency involves drastic restructuring of both metabolism and the epigenome. However, induced pluripotent stem cells (iPSC) retain transcriptional memory, epigenetic memory, and metabolic memory from their somatic cells of origin and acquire aberrant characteristics distinct from either other pluripotent cells or parental cells, reflecting incomplete reprogramming. As a critical link between the microenvironment and regulation of the epigenome, nutrient availability likely plays a significant role in the retention of somatic cell memory by iPSC. Significantly, relative nutrient availability impacts iPSC reprogramming efficiency, epigenetic regulation and cell fate, and differentially alters their ability to respond to physiological stimuli. The significance of metabolites during the reprogramming process is central to further elucidating how iPSC retain somatic cell characteristics and optimising culture conditions to generate iPSC with physiological phenotypes to ensure their reliable use in basic research and clinical applications. This review serves to integrate studies on iPSC reprogramming, memory retention and metabolism, and identifies areas in which current knowledge is limited.

1. Introduction

The exogenous expression of the transcription factors OCT4, SOX2, KLF4, and c-MYC in both mouse and human somatic cells has enabled the derivation of cells with embryonic stem cell (ESC) -like properties, termed induced pluripotent stem cells (iPSC) [1, 2]. While these reprogrammed cells are capable of self-renewal, demonstrate *in vitro* differentiation potential equivalent to that of ESC and, in mice, are able to contribute to viable chimeras [3], several studies have raised concerns that iPSC retain somatic cell memory and acquire characteristics that may bias cell fate or impair cell function post-differentiation. As iPSC have the capacity to differentiate into cells of each of the three primary germ layers: endoderm, mesoderm, and ectoderm [4], they possess immense potential for clinical applications in disease modelling, drug discovery, and regenerative medicine. It is therefore of great importance for iPSC to be able to appropriately respond to their environment and acquire an ESC-like physiology to ensure that they can be safely and reliably used in the clinic and recapitulate the physiology of disease models in drug discovery and basic research.

Culture conditions and nutrient availability not only affect reprogramming itself but have a long-term impact on the resultant physiology of iPSC. This review therefore discusses recent advances in our understanding of factors that influence the efficiency of the reprogramming process, metabolic restructuring, and retention of somatic cell memory, as well as how it is essential to further elucidate how somatic cell memory is retained for the subsequent optimisation of the reprogramming process to generate iPSC with a physiological ESC-like phenotype and ensure long-term cellular health.

2. Reprogramming Necessitates Transcriptional, Epigenetic, and Metabolic Restructuring

In contrast to most somatic cells, which primarily utilise oxidative phosphorylation (OxPhos) for energy production [5], iPSC instead rely primarily on glycolysis [6–8]. This curious

metabolic phenotype resembles that of ESC [9] and recapitulates that of the inner cell mass (ICM) of the blastocyst, which is almost exclusively glycolytic [10, 11]. This metabolism is characterised by a high glucose to lactate flux even in the presence of adequate oxygen, a phenomenon known as aerobic glycolysis, first characterised by Warburg [12, 13]. While glycolysis is not as efficient as OxPhos in terms of the number of adenosine triphosphate (ATP) molecules produced per mol of glucose consumed, glycolysis can produce an equivalent amount of ATP in the same duration of time given a high glucose to lactate flux [14]. Glycolysis consequently plays a key role in the production of biosynthetic precursors, such as phospholipids and glycoproteins [15, 16], necessary to support proliferation and regulate cell function, and likely ensures protection of the genome from oxidative stress caused by excessive production of reactive oxygen species (ROS) [17].

Reprogramming to pluripotency involves a transition from a primarily oxidative to a primarily glycolytic metabolic phenotype [6, 9, 18], and this metabolic restructuring takes place in the initial phase of the reprogramming process. Oxygen consumption and ATP production, as well as gene expression levels of pathways such as glycolysis, the pentose phosphate pathway (PPP) and the tricarboxylic acid (TCA) cycle, are remodelled during reprogramming to levels similar to those found in ESC [9, 19, 20]. Following the restructuring of metabolism, the promoters of pluripotent genes undergo DNA demethylation, while those of somatic genes are methylated [21]. This results in the upregulation of endogenous NANOG, OCT4, and SOX2, activating the transcription factor network responsible for the establishment and maintenance of pluripotency [22]. The chromatin structure [23] and the epigenetic landscape [24] are remodelled to resemble those of ESC, to enable ongoing transcription of genes that underpin pluripotency. In addition, telomerase is upregulated [25], with a concomitant lengthening of telomeres to ESC-like lengths [26], providing improved genomic stability and protection against DNA damage. Significantly, as metabolic changes precede the upregulation of pluripotency markers [6], this illustrates that metabolic restructuring is a prerequisite for the successful establishment and maintenance of pluripotency, and that perturbations in this restructuring may have downstream effects on the subsequent stages of the reprogramming process, including remodelling of the epigenome and the successful establishment of a pluripotent state. Equally, altering relative metabolite availabilities during reprogramming, by modulating metabolism, will plausibly impact both metabolic and epigenetic remodelling and hence the acquisition of pluripotency. While the effects of some specific metabolites on improving or reducing reprogramming efficiency have been assessed, understanding how reprogramming under such conditions affects the restructuring of metabolism and the physiology and metabolic phenotype of resultant iPSC is limited.

3. Metabolism as a Driver of Reprogramming

A role for metabolism in regulating the acquisition of pluripotency has been demonstrated by studies investigating the effect of promoting glycolysis during the reprogramming process on reprogramming efficiency. Culturing adult human fibroblasts under physiological (5%) oxygen or supplementing culture medium during reprogramming with D-fructose-6-phosphate (F6P), a glycolytic stimulator and intermediate, significantly increases the number of derived iPSC colonies [7, 27]. As both physiological oxygen and F6P promote lactate production [10, 28, 29], they plausibly improve reprogramming efficiency by supporting and facilitating the transition to a primarily glycolytic metabolism. Similarly, upregulation of HIF1α, a transcription factor that upregulates glycolytic genes [30–33] and is stabilised by physiological oxygen [34, 35] and lactate [10], has been shown to significantly improve reprogramming efficiency [18]. In contrast, 2-deoxy-D-glucose (2-DG), a glycolytic inhibitor, reduces glucose to lactate flux, significantly reducing reprogramming efficiency [7, 36]. Combined, these studies highlight that the transition to a glycolytic metabolism is essential for reprogramming to take place.

In further support of the importance of glycolysis to reprogramming, different somatic cell types demonstrate different efficiencies of reprogramming to pluripotency, as well as different routes to pluripotency [37], and this has been attributed to the metabolic phenotype of the initial somatic cells. Somatic cell types that are metabolically more glycolytic and less oxidative, such as keratinocytes, reprogram to pluripotency with significantly greater efficiencies and more quickly than cell types that are less glycolytic and more oxidative, such as fibroblasts [7, 38]. In addition, progenitor and somatic stem cells, such as skeletal muscle stem cells [39] and hematopoietic stem cells [40], which exhibit a more glycolytic metabolism [41, 42], can be reprogrammed to pluripotency with a far greater efficiency than their terminally differentiated counterparts.

Reprogramming efficiency is also improved by modulating metabolism through transcription factor regulation. Takahashi and Yamanaka's original reprogramming method, employing retroviral-based expression of key transcription factors, resulted in relatively inefficient reprogramming, with only 0.02% of mouse somatic cells successfully acquiring a pluripotent ESC-like phenotype [1] and a similar reprogramming efficiency was observed for human fibroblasts [2]. The transcription factor c-MYC, one of the four factors used in the initial derivation of iPSC [1], is not essential for reprogramming, though its absence results in reprogramming that is slower and less efficient relative to when c-MYC is present [43]. c-MYC facilitates the upregulation of glycolytic genes [44], maintains a high glucose to lactate flux [45], promotes telomere elongation [46], and plays a critical role in regulating histone acetylation during reprogramming [47]. As such, it is likely that the impact of c-MYC on reprogramming is through its roles in regulating both metabolism and the epigenetic landscape, thereby promoting metabolic restructuring early in the reprogramming process. Similarly, LIN28a, which modulates both glycolysis and OxPhos by influencing mRNA translation [48], has been shown to improve reprogramming [49]. Hence, such data further illustrate a central role for metabolism in reprogramming, specifically

how modulation of metabolic pathways can impact the efficiency of iPSC derivation.

In addition to improving reprogramming efficiency with transcription factor-based methods, small molecules can also be used in place of transcription factors to reprogram somatic cells to pluripotency. These resultant cells are termed chemically induced pluripotent stem cells (ciPSC) and display similar morphological and physiological characteristics, differentiation potential, and global gene expression profiles, with traditional iPSC and ESC [50–52]. In a similar manner to the use of physiological oxygen and c-MYC, PS48, a small-molecule PDK1 activator, increases glycolytic gene expression with a corresponding increase in lactate production [36]. Significantly, PS48 can functionally replace SOX2, KLF4, and c-MYC in reprogramming keratinocytes when used alongside other small molecules such as sodium butyrate, a short-chain fatty acid, and A-83-01, a transforming growth factor beta (TGFβ) receptor inhibitor [36]. Upregulating glycolytic activity therefore not only improves reprogramming efficiency but can directly drive reprogramming itself, further supporting the central role of glycolysis in establishing pluripotency. However, beyond carbohydrate utilisation, the metabolic phenotypes of ciPSC and transcription factor-derived iPSC have not been compared and the downstream effects of chemical reprogramming on the physiology and differentiation potential of ciPSC have not been assessed.

Manipulating other culture conditions can likewise significantly impact reprogramming efficiency. In addition to the promotion of glycolytic metabolism, supplementing culture media during reprogramming with sodium butyrate facilitates the opening of chromatin and the activation of pluripotency genes and significantly improves the efficiency of reprogramming human fibroblasts to pluripotency [53]. The supplementation of sodium butyrate may reduce the retention of somatic cell epigenetic memory through DNA demethylation and the erasure of parental cell-specific epigenetic marks. Similarly, ascorbic acid (vitamin C) reduces histone H3 lysine 9 (H3K9) and H3K36 methylation, therefore promoting gene activation, through the regulation of histone demethylases JHDM1A and JHD1B [54], and improves the speed and efficiency of reprogramming somatic cells to pluripotency [54–56]. Vitamin C also reduces repressive DNA methylation by modulating the activity of ten-eleven translocation (TET) demethylases [57], converting 5-methylcytosine (5mC) to 5-hydroxymethylcytosine (5hmC). These results further highlight the importance of epigenetic remodelling in the reprogramming process, although to date, no studies have investigated how any of these methods may impact the metabolism and physiology of resultant iPSC. Further, as the reprogramming process involves a wide-scale resetting of histone and DNA methylation patterns [58], it is plausible that the epigenetic profiles of terminally differentiated cells serve as a barrier to reprogramming. Given that the epigenetic landscape is regulated by metabolite availability, as discussed below, the greater reprogramming efficiency observed in somatic stem cells may plausibly be a result of their metabolism. However, how the metabolic phenotypes of somatic stem cells relate to their efficiency in generating iPSC remains unexplored and developing interventions to alter the metabolic phenotype prior to reprogramming may therefore be of value.

Equally, culture conditions can drive reversion to different pluripotent states, accompanied by different metabolic states. Two distinct but stable pluripotent states, naïve and primed, have been reported, representing an early, more pluripotent developmental stage with higher developmental potential [59–61] and a later stage of development associated with differentiation bias [62], respectively. These differences are reflected by distinct epigenetic profiles, whereby naïve ESC are globally hypomethylated [63] and exhibit reduced histone methylation [64]. Both mouse and human naïve cells also differ from their primed counterparts in having a comparatively higher oxidative metabolism, inferred from a greater level of oxygen consumption and upregulation of enzymes involved in OxPhos [33, 64–68]. Indeed, the reduction in histone methylation is related to the oxidative metabolic phenotype of naïve mouse ESC, accompanied by decreased HIF pathway activity [64], illustrating the metabolic regulation of naïve and primed states, as well as the transitions between them. Further, Zhou and colleagues reported that the transition to a primarily glycolytic metabolism drives the conversion of both naïve mouse ESC to a primed state and that this transition is driven by HIF1α activity [33]. However, in addition to induction of naïvety through the provision of GSK3B and ERK inhibitors (2i), medium composition also differed, which may itself contribute to the metabolic shift. A number of human naïve states have been described, but no consensus exists on the factors required to establish naïvety in the human, and a spectrum of naïve characteristics is displayed [65]. Different protocols and media formulations for converting human pluripotent stem cells (PSC) to naïve cells may result in a diversity of metabolic states, each having different downstream effects on gene expression, the epigenetic landscape, and the regulation of pluripotency. However, metabolic characterisation of naïvety is limited to oxidative capacity and gene expression [38, 64–68]. Greater understanding of naïve metabolism, particularly in regard to carbohydrate and amino acid utilisation, may be pertinent for enhancing their derivation and maintenance, as optimising media, beyond the supplementation of inhibitors and growth factors, may be necessary to improve not only the conversion of primed to naïve iPSC but also the direct derivation of naïve iPSC from somatic cells.

Altered metabolism can have significant functional consequences on physiology, as highlighted by the current understanding of developmental origins of health and disease (DOHaD) [69, 70], whereby seemingly small changes in nutrient availability in utero can significantly impact subsequent adult health. Beyond the role of metabolism generating ATP, metabolic intermediates serve as cofactors for modifiers of the epigenetic landscape [17, 41, 71, 72]. Consequently, relative nutrient availability links the external microenvironment to regulation of the epigenome. Metabolites, including glucose-derived acetyl-CoA [73, 74], nicotinamide adenine dinucleotide (NAD^+) [75], S-adenosyl methionine (SAM)

[76, 77], L-proline [55, 78, 79], alpha-ketoglutarate (αKG) [80], and fatty acids [81], have been shown to modulate the epigenome, pluripotency, and cell fate [17, 71]. For example, αKG, derived from glucose and glutamine catabolism, modulates histone demethylation and TET-dependent DNA demethylation, regulating the expression of genes associated with pluripotency [80]. The intimate relationship between metabolism and epigenetics, termed metaboloepigenetics [71, 82, 83], highlights the importance of appropriately regulating metabolism and that perturbations in iPSC metabolite availability will have downstream effects on gene expression and cellular function and bias cell fate. Such effects will plausibly persist post-differentiation, thereby impacting applications of iPSC in regenerative medicine, disease modelling, and drug discovery.

4. Somatic Cell Memory and Incomplete Reprogramming

While iPSC display many hallmarks of pluripotency and similarities with ESC, iPSC from various somatic cell types retain transcriptional memory [84, 85], epigenetic memory [66, 86], and metabolic memory [87, 88] of their parental somatic cells and acquire genetic and epigenetic aberrations, including mtDNA mutations, distinct from either ESC or the parental somatic cells of origin [89, 90]. The retention of epigenetic memory, as well as transcriptional memory of somatic gene expression, illustrates that histone and DNA methylation profiles are not fully reset following reprogramming and, as this memory can bias the fate of iPSC towards their parental cell type [86], has downstream effects on iPSC gene expression and physiology. Demethylated regions (DMRs) in iPSC are retained from their somatic cell type of origin and can distinguish iPSC derived from different cell types, as well as iPSC from ESC [86]. Epigenetic memory has been shown to be progressively lost as iPSC undergo a greater number of passages [66]; however, it is not known whether somatic cell epigenetic marks are actually erased in iPSC post-reprogramming or whether there exists a selective pressure against iPSC that have retained epigenetic memory. This potential selection may in itself not result in iPSC with an ESC-like phenotype or epigenetic landscape, as the acquisition of aberrant epigenetic marks may provide a selective advantage over the retention of epigenetic memory.

The morphology of iPSC mitochondria resembles that of both ESC and somatic cells [9, 91, 92], highlighting that mitochondria are not fully restructured to an ESC-like state during reprogramming and that somatic mitochondrial physiology is likely partially retained in iPSC. Significantly, iPSC reprogrammed under physiological oxygen possess mitochondria that are less active and consume less oxygen, thereby more closely resembling the mitochondria of ESC [88]. Physiological oxygen, by modulating metabolism during reprogramming, therefore not only improves reprogramming efficiency but also promotes the acquisition of an ESC-like mitochondrial phenotype, reducing the retention of somatic cell metabolic memory. Furthermore, as the retention of somatic cell memory involves both epigenetic marks and metabolic pathway activity, this memory is plausibly related to the relative availabilities of metabolic intermediates that modulate the activity of epigenetic modifiers. Consequently, insufficient restructuring of metabolism can compromise the subsequent remodelling of the epigenetic landscape as a result of metaboloepigenetic regulation. While metabolism as a driver of reprogramming is well established, the precise role of metabolism in affecting epigenetic remodelling and the retention of epigenetic memory is unknown.

In addition to the retention of mitochondrial characteristics, iPSC have been shown to acquire and accumulate mitochondrial DNA (mtDNA) mutations [90], with the frequency of these defects increasing with somatic cell age [93]. These mutations have the potential to impair mitochondrial function and metabolism [94], which could also result in long-term changes to the epigenome through changes in the availability of acetyl-CoA and αKG. Though the downstream effects of mtDNA mutations on mitochondrial physiology and activity in iPSC are not fully understood, accumulation of these mutations in somatic cells can contribute to mitochondrial dysfunction, telomere shortening, senescence, and disease [95, 96], even at low frequencies [97]. Further, mtDNA mutations will be retained post-differentiation, compromising not only their safety in clinical applications but also their ability to recapitulate disease states, due to the confounding effects of cellular senescence and compromised metabolic function. Understanding the acquisition of mtDNA mutations by iPSC, their relationship with metabolic restructuring and how the accumulation of these mutations can be mitigated is essential to ensure that cell replacement strategies do not result in further functional deficits for the patient.

Panopoulos and colleagues [7] have also reported that levels of particular metabolites, such as polyunsaturated fatty acids (PUFAs), are significantly lower in human iPSC than in ESC, while other metabolites, including the methyl donor and cofactor for histone methyltransferases (HMT) SAM, were higher in iPSC. In addition, amino acid and lipid profiles, as well as metabolites involved in polyamine biosynthesis, differ between mouse iPSC and ESC [98]. These data reinforce the idea that while iPSC acquire a primarily glycolytic metabolism, they are not metabolically equivalent to ESC. This is pertinent given that PUFAs modulate oxidative metabolism by undergoing beta-oxidation to form acetyl-CoA, and elevated SAM levels result in increased histone methylation, highlighting that metabolic differences with ESC (Figure 1) will have long-term effects on both the metabolism and epigenome of iPSC and plausibly their differentiated derivatives [99]. PUFAs can be oxidised to produce eicosanoids, which can act as ligands to activate the nuclear receptor peroxisome proliferator-activated receptor gamma (PPARγ) [100, 101]. The activation of PPARγ has a wide variety of functions, such as mitigating oxidative stress caused by overproduction of ROS, which can have significant effects on reducing DNA and organelle damage and recruiting PPARγ coactivator 1-alpha (PGC-1α), a master regulator of mitochondrial biogenesis and metabolism [102]. Given that high levels of PUFAs are characteristic

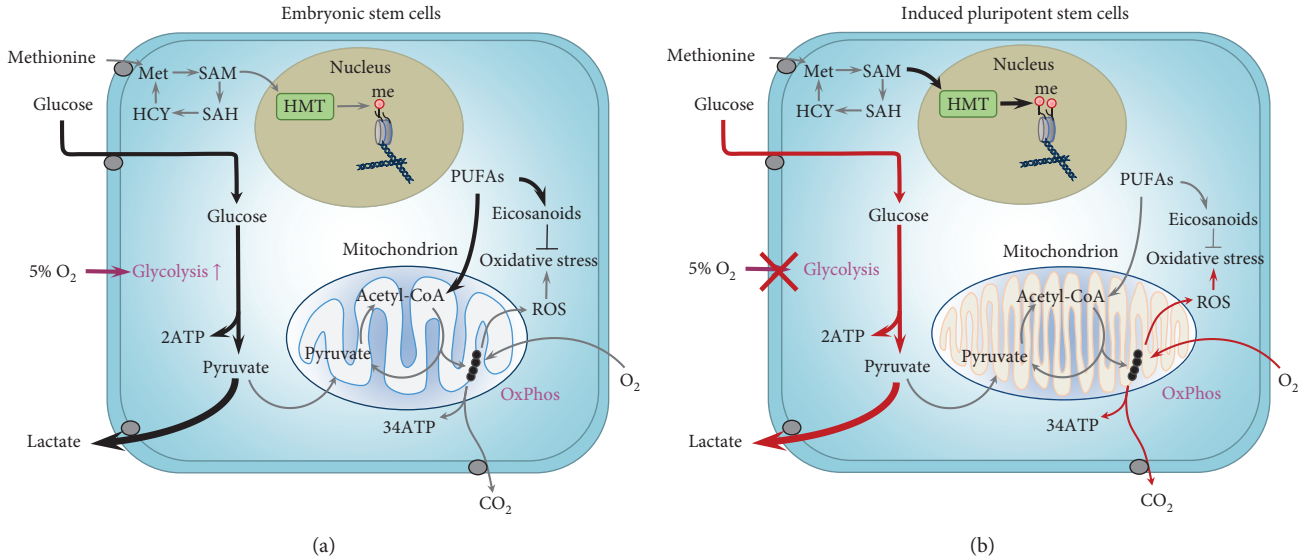

Figure 1: Metabolic differences between embryonic stem cells (ESC) (a) and induced pluripotent stem cells (iPSC) (b). Glycolytic rate, glucose consumption, and lactate production are altered in iPSC by both the retention of somatic cell metabolic memory and the acquisition of aberrant metabolic characteristics [87, 88]. Significantly, due to the retention of metabolic memory or the acquisition of metabolic aberrations, the capacity for iPSC to modulate glycolysis in response to changes in oxygen (O_2) is impaired. In contrast, this oxygen response, whereby glucose to lactate flux is significantly increased under physiological (5%) oxygen conditions relative to that under atmospheric (20%) oxygen, is well characterised in both ESC [28, 29] and the blastocyst [105]. Levels of polyunsaturated fatty acids (PUFAs), including arachidonic acid, linoleic acid, docosapentaenoic acid, and adrenic acid, are lower in iPSC than in ESC [7]. PUFAs regulate oxidative metabolism by undergoing beta-oxidation to produce acetyl-CoA and can be converted to eicosanoids, which can mitigate oxidative stress, caused by reactive oxygen species (ROS) as a result of oxidative phosphorylation (OxPhos), through the activation of peroxisome proliferator-activated receptor gamma (PPARγ) [100, 101]. Eicosanoids also plausibly regulate mitochondrial biogenesis and function though the action of PPARγ recruiting PPARγ coactivator 1-α (PGC-1α) [102]. Levels of the methyl donor and cofactor S-adenosyl methionine (SAM) are higher in iPSC than in ESC [7], resulting in a greater methylation (me) of histones in iPSC through the action of histone methyltransferases (HMT). SAM is produced from methionine (Met) and, when demethylated, results in S-adenosyl-L-homocysteine (SAH) which is hydrolysed to homocysteine (HCY) and converted into methionine. Mitochondria in iPSC morphologically resemble both those of ESC and somatic cells [9]. Mitochondrial activity in iPSC is affected by the culture conditions under which they are reprogrammed, whereby iPSC derived under physiological oxygen possess mitochondria that are less active and more ESC-like when compared to those of iPSC derived under atmospheric oxygen [88]. It has also been shown that iPSC acquire and accumulate mitochondrial DNA (mtDNA) mutations [90], with the frequency of these mutations increasing with parental somatic cell age [93]; however, the degree to which these mutations impact mitochondrial metabolism and activity in iPSC is unknown. However, in somatic cells, mtDNA mutations can contribute not only to mitochondrial dysfunction [95] but also to cellular senescence and telomere shortening [96]. Thick arrows indicate increased flux/activity. Red arrows indicate pathways affected by the retention of somatic cell memory or acquisition of metabolic aberrations in iPSC.

of ESC, the comparatively lower levels observed in iPSC likely reflect an aspect of metabolism that is insufficiently restructured during reprogramming. However, whether the levels of PUFAs and SAM in iPSC relate to those of their somatic cells of origin or if iPSC derived from different somatic cell types possess different levels of these metabolites remains unexplored. Plausibly, lower levels of PUFAs during early stages of reprogramming may impair mitochondrial remodelling due to insufficient activation of PPARγ and PGC-1α, contributing to the retention of metabolic memory. As such, supplementing culture conditions before and during reprogramming with PUFAs or eicosanoids may likely improve metabolic restructuring, reprogramming efficiency, and the physiology of resultant iPSC. Further, eicosanoids modulate both immune function and inflammation [103]. The likely lower levels of eicosanoids in iPSC may impact tolerance and responses to iPSC-derived cells following transplantation for uses in regenerative medicine.

Recently, it was demonstrated that iPSC derived from periodontal ligament (PDL) fibroblasts and neonatal human dermal fibroblasts (NHDF) were unable to regulate carbohydrate metabolism in response to physiological oxygen culture [87], a response that is characteristic of both human ESC (hESC) [28, 29, 104] and preimplantation embryos [105] and reflected a retention of somatic cell memory [87]. The inability of iPSC to respond appropriately to changing environments is concerning, as it will plausibly compromise their utility for clinical applications and may in part contribute to poor engraftment rates [106], although this is yet to be established. Further, reprogramming NHDF under physiological oxygen results in iPSC with greater transcriptional stability, longer telomeres, and fewer metabolic aberrations than those reprogrammed under atmospheric (20%) oxygen, although

irrespective of oxygen, iPSC retained metabolic memory from their somatic cells of origin [88], suggesting that the relative availabilities of other metabolites need to be altered.

Significantly, it is apparent from these studies that even cells from neonatal donors result in perturbed iPSC physiology. Parental cell age is negatively correlated with reprogramming efficiency [107], conceivably reflecting not only a more closed chromatin configuration but also changes in cell metabolism which accompany aging [108]. These changes, which include a reduction in ATP production [109] and the availability of metabolic intermediates such as NAD^+ [110, 111], have downstream effects on the epigenetic landscape of senescent cells. Significantly, iPSC derived from aged tissue have been found to be unable to suppress OxPhos, impacting their acquisition of a bona fide ESC-like metabolic phenotype. This lack of OxPhos suppression also had downstream effects on the epigenetic landscape of resultant iPSC by depleting citrate and thereby reducing histone acetylation [112]. Plausibly, irrespective of donor cell age, the culture conditions used to expand cells prior to reprogramming, as well as during, have a measurable effect on cell metabolism that results in the retention of epigenetic marks. Taken together, these data illustrate that the type and status of somatic cells have a significant impact on reprogramming, not only in regard to efficiency but also on the metabolic and epigenetic remodelling that takes place during the reprogramming process.

While different somatic cell types are known to display different reprogramming efficiencies, whether somatic cell types displaying distinct metabolomic profiles consequently establish different levels of metabolic restructuring has not been comprehensively assessed. Transcriptional, epigenetic, and metabolic differences between iPSC and ESC suggest that the reprogramming process is incomplete and that reprogramming itself leads to the acquisition of physiological defects in resultant iPSC. The potential ramifications of incomplete metabolic reprogramming on iPSC physiology have not been well explored. Equally, it remains to be elucidated whether somatic metabolic memory and the acquisition of aberrant metabolic profiles impact the transitions between pluripotent cell states. As epigenetic aberrations in iPSC have been shown to be retained through differentiation [99], suboptimal reprogramming conditions will plausibly have significant downstream consequences on the clinical applications of iPSC.

5. Conclusion

There are growing concerns over genetic, epigenetic and, more recently, metabolic stability in iPSC, which have the potential to compromise the reliability of iPSC for use in basic research or the safety and efficacy of their use in clinical applications. In particular, the retention of somatic cell metabolic memory and epigenetic memory will likely have downstream effects on iPSC physiology through metaboloepigenetic regulation of gene expression and cellular function. Metabolism has a profound effect on somatic cell reprogramming. Nutrient availability and metabolic pathway activity impact the efficiency and speed of reprogramming to pluripotency and, more recently, have been recognised to alter the physiology of resultant iPSC, as well as their capacity to regulate homeostasis in response to changes in their environment and plausibly facilitate reprogramming through regulation of the epigenome. This will have downstream consequences for all iPSC and their derivatives due to the heritable nature of epigenetic modifications. Reprogramming is not a single transition, but a dynamic multistage process; therefore, there may be state-specific requirements as both the metabolism and epigenome of somatic cells are restructured and a single-medium formulation may not be sufficient to promote optimal reprogramming. Consequently, multiple different aspects of iPSC physiology can be impacted by culture conditions during reprogramming. Hence, deriving iPSC under suboptimal conditions will plausibly have long-term repercussions on their integrity and physiology and compromise how they adapt and respond to their *in vivo* environment when employed in clinical applications. However, the physiology and functionality of cells differentiated from iPSC reprogrammed under different conditions have yet to be investigated, whereby the majority of studies that investigate iPSC differentiation do not extend beyond basic molecular characterisation. Different culture conditions or modulators of metabolism may be necessary during the reprogramming process and during iPSC maintenance to optimise the physiology, metabolism, and differentiation potential of iPSC and to ensure that differentiated cells are free from aberrations and respond appropriately to environmental stimuli.

To date, the significance of how culture conditions during reprogramming impact the physiology of resultant iPSC has not only been largely unexplored but ignored and underestimated. Observed perturbations in iPSC metabolism, epigenetics, and physiology likely underpin significantly compromised signalling pathways in multiple aspects of cell function, which will consequently impact their use in research, regenerative medicine, disease modelling, and drug discovery. Further investigation of how different culture conditions alter the metabolic and epigenetic remodelling that takes place during the reprogramming process, and how different metabolite availabilities may interact with the distinct metabolic and epigenetic status of various somatic cell types, is needed to develop reliable methods of generating iPSC with a bona fide ESC-like phenotype with no retention of somatic cell memory or acquisition of *de novo* aberrations.

Conflicts of Interest

The authors declare that there are no conflicts of interest regarding the publication of this paper.

References

[1] K. Takahashi and S. Yamanaka, "Induction of pluripotent stem cells from mouse embryonic and adult fibroblast cultures by defined factors," *Cell*, vol. 126, no. 4, pp. 663–676, 2006.

[2] K. Takahashi, K. Tanabe, M. Ohnuki et al., "Induction of pluripotent stem cells from adult human fibroblasts by defined factors," *Cell*, vol. 131, no. 5, pp. 861–872, 2007.

[3] K. Okita, T. Ichisaka, and S. Yamanaka, "Generation of germline-competent induced pluripotent stem cells," *Nature*, vol. 448, no. 7151, pp. 313–317, 2007.

[4] M. Stadtfeld and K. Hochedlinger, "Induced pluripotency: history, mechanisms, and applications," *Genes & Development*, vol. 24, no. 20, pp. 2239–2263, 2010.

[5] R. J. DeBerardinis, J. J. Lum, G. Hatzivassiliou, and C. B. Thompson, "The biology of cancer: metabolic reprogramming fuels cell growth and proliferation," *Cell Metabolism*, vol. 7, no. 1, pp. 11–120, 2008.

[6] C. D. L. Folmes, T. J. Nelson, A. Martinez-Fernandez et al., "Somatic oxidative bioenergetics transitions into pluripotency-dependent glycolysis to facilitate nuclear reprogramming," *Cell Metabolism*, vol. 14, no. 2, pp. 264–271, 2011.

[7] A. D. Panopoulos, O. Yanes, S. Ruiz et al., "The metabolome of induced pluripotent stem cells reveals metabolic changes occurring in somatic cell reprogramming," *Cell Research*, vol. 22, no. 1, pp. 168–177, 2012.

[8] A. J. Harvey, J. Rathjen, and D. K. Gardner, "The metabolic framework of pluripotent stem cells and potential mechanisms of regulation," in *Stem Cells in Reproductive Medicine: Basic Science and Therapeutic Potential*, C. Simón, A. Pellicer, and R. R. Pera, Eds., pp. 164–179, Cambridge University Press, New York, NY, USA, 2013.

[9] S. Varum, A. S. Rodrigues, M. B. Moura et al., "Energy metabolism in human pluripotent stem cells and their differentiated counterparts," *PLoS One*, vol. 6, no. 6, article e20914, 2011.

[10] D. K. Gardner, "Lactate production by the mammalian blastocyst: manipulating the microenvironment for uterine implantation and invasion?," *BioEssays*, vol. 37, no. 4, pp. 364–371, 2015.

[11] D. K. Gardner and A. J. Harvey, "Blastocyst metabolism," *Reproduction, Fertility, and Development*, vol. 27, no. 4, pp. 638–654, 2015.

[12] O. Warburg, "On respiratory impairment in cancer cells," *Science*, vol. 124, no. 3215, pp. 269-270, 1956.

[13] O. Warburg, F. Wind, and E. Negelein, "The metabolism of tumors in the body," *The Journal of General Physiology*, vol. 8, no. 6, pp. 519–530, 1927.

[14] T. Pfeiffer, S. Schuster, and S. Bonhoeffer, "Cooperation and competition in the evolution of ATP-producing pathways," *Science*, vol. 292, no. 5516, pp. 504–507, 2001.

[15] D. A. Hume and M. J. Weidemann, "Role and regulation of glucose metabolism in proliferating cells," *Journal of the National Cancer Institute*, vol. 62, no. 1, pp. 3–8, 1979.

[16] M. J. Morgan and P. Faik, "Carbohydrate metabolism in cultured animal cells," *Bioscience Reports*, vol. 1, no. 9, pp. 669–686, 1981.

[17] J. G. Lees, D. K. Gardner, and A. J. Harvey, "Pluripotent stem cell metabolism and mitochondria: beyond ATP," *Stem Cells International*, vol. 2017, Article ID 2874283, 17 pages, 2017.

[18] A. Prigione, N. Rohwer, S. Hoffmann et al., "HIF1α modulates cell fate reprogramming through early glycolytic shift and upregulation of PDK1-3 and PKM2," *Stem Cells*, vol. 32, no. 2, pp. 364–376, 2014.

[19] A. Prigione, B. Fauler, R. Lurz, H. Lehrach, and J. Adjaye, "The senescence-related mitochondrial/oxidative stress pathway is repressed in human induced pluripotent stem cells," *Stem Cells*, vol. 28, no. 4, pp. 721–733, 2010.

[20] C. D. Folmes, D. K. Arrell, J. Zlatkovic-Lindor et al., "Metabolome and metaboproteome remodeling in nuclear reprogramming," *Cell Cycle*, vol. 12, no. 15, pp. 2355–2365, 2014.

[21] R. Lister, M. Pelizzola, R. H. Dowen et al., "Human DNA methylomes at base resolution show widespread epigenomic differences," *Nature*, vol. 462, no. 7271, pp. 315–322, 2009.

[22] K. Lee, W. Wong, and B. Feng, "Decoding the pluripotency network: the emergence of new transcription factors," *Biomedicine*, vol. 1, no. 1, pp. 49–78, 2013.

[23] E. Apostolou and K. Hochedlinger, "Chromatin dynamics during cellular reprogramming," *Nature*, vol. 502, no. 7472, pp. 462–471, 2013.

[24] N. Maherali, R. Sridharan, W. Xie et al., "Directly reprogrammed fibroblasts show global epigenetic remodeling and widespread tissue contribution," *Cell Stem Cell*, vol. 1, no. 1, pp. 55–70, 2007.

[25] M. Stadtfeld, N. Maherali, D. T. Breault, and K. Hochedlinger, "Defining molecular cornerstones during fibroblast to iPS cell reprogramming in mouse," *Cell Stem Cell*, vol. 2, no. 3, pp. 230–240, 2008.

[26] R. M. Marion, K. Strati, H. Li et al., "Telomeres acquire embryonic stem cell characteristics in induced pluripotent stem cells," *Cell Stem Cell*, vol. 4, no. 2, pp. 141–154, 2009.

[27] Y. Yoshida, K. Takahashi, K. Okita, T. Ichisaka, and S. Yamanaka, "Hypoxia enhances the generation of induced pluripotent stem cells," *Cell Stem Cell*, vol. 5, no. 3, pp. 237–241, 2009.

[28] A. J. Harvey, J. Rathjen, L. J. Yu, and D. K. Gardner, "Oxygen modulates human embryonic stem cell metabolism in the absence of changes in self-renewal," *Reproduction, Fertility, and Development*, vol. 28, no. 4, pp. 446–458, 2016.

[29] J. G. Lees, J. Rathjen, J. R. Sheedy, D. K. Gardner, and A. J. Harvey, "Distinct profiles of human embryonic stem cell metabolism and mitochondria identified by oxygen," *Reproduction*, vol. 150, no. 4, pp. 367–382, 2015.

[30] J. W. Kim, I. Tchernyshyov, G. L. Semenza, and C. V. Dang, "HIF-1-mediated expression of pyruvate dehydrogenase kinase: a metabolic switch required for cellular adaptation to hypoxia," *Cell Metabolism*, vol. 3, no. 3, pp. 177–185, 2006.

[31] G. L. Semenza, "Hypoxia-inducible factor 1: master regulator of O_2 homeostasis," *Current Opinion in Genetics & Development*, vol. 8, no. 5, pp. 588–594, 1998.

[32] G. L. Semenza, P. H. Roth, H. M. Fang, and G. L. Wang, "Transcriptional regulation of genes encoding glycolytic enzymes by hypoxia-inducible factor 1," *The Journal of Biological Chemistry*, vol. 269, no. 38, pp. 23757–23763, 1994.

[33] W. Zhou, M. Choi, D. Margineantu et al., "HIF1α induced switch from bivalent to exclusively glycolytic metabolism during ESC-to-EpiSC/hESC transition," *The EMBO Journal*, vol. 31, no. 9, pp. 2103–2116, 2012.

[34] B. H. Jiang, G. L. Semenza, C. Bauer, and H. H. Marti, "Hypoxia-inducible factor 1 levels vary exponentially over a physiologically relevant range of O_2 tension," *American Journal of Physiology-Cell Physiology*, vol. 271, no. 4, pp. C1172–C1180, 1996.

[35] W. G. Kaelin Jr. and P. J. Ratcliffe, "Oxygen sensing by metazoans: the central role of the HIF hydroxylase pathway," *Molecular Cell*, vol. 30, no. 4, pp. 393–402, 2008.

[36] S. Zhu, W. Li, H. Zhou et al., "Reprogramming of human primary somatic cells by OCT4 and chemical compounds," *Cell Stem Cell*, vol. 7, no. 6, pp. 651–655, 2010.

[37] C. M. Nefzger, F. J. Rossello, J. Chen et al., "Cell type of origin dictates the route to pluripotency," *Cell Reports*, vol. 21, no. 10, pp. 2649–2660, 2017.

[38] T. Aasen, A. Raya, M. J. Barrero et al., "Efficient and rapid generation of induced pluripotent stem cells from human keratinocytes," *Nature Biotechnology*, vol. 26, no. 11, pp. 1276–1284, 2008.

[39] K. Y. Tan, S. Eminli, S. Hettmer, K. Hochedlinger, and A. J. Wagers, "Efficient generation of iPS cells from skeletal muscle stem cells," *PLoS One*, vol. 6, no. 10, article e26406, 2011.

[40] S. Eminli, A. Foudi, M. Stadtfeld et al., "Differentiation stage determines potential of hematopoietic cells for reprogramming into induced pluripotent stem cells," *Nature Genetics*, vol. 41, no. 9, pp. 968–976, 2009.

[41] J. G. Ryall, S. Dell'Orso, A. Derfoul et al., "The NAD^+-dependent SIRT1 deacetylase translates a metabolic switch into regulatory epigenetics in skeletal muscle stem cells," *Cell Stem Cell*, vol. 16, no. 2, pp. 171–183, 2015.

[42] T. Simsek, F. Kocabas, J. Zheng et al., "The distinct metabolic profile of hematopoietic stem cells reflects their location in a hypoxic niche," *Cell Stem Cell*, vol. 7, no. 3, pp. 380–390, 2010.

[43] M. Nakagawa, M. Koyanagi, K. Tanabe et al., "Generation of induced pluripotent stem cells without Myc from mouse and human fibroblasts," *Nature Biotechnology*, vol. 26, no. 1, pp. 101–106, 2008.

[44] C. V. Dang, "The interplay between MYC and HIF in the Warburg effect," *Oncogenes Meet Metabolism*, vol. 2007/4, pp. 35–53, 2008.

[45] T. S. Cliff, T. Wu, B. R. Boward et al., "MYC controls human pluripotent stem cell fate decisions through regulation of metabolic flux," *Cell Stem Cell*, vol. 21, no. 4, pp. 502–516.e9, 2017.

[46] M. L. De Bonis, S. Ortega, and M. A. Blasco, "SIRT1 is necessary for proficient telomere elongation and genomic stability of induced pluripotent stem cells," *Stem Cell Reports*, vol. 2, no. 5, pp. 690–706, 2014.

[47] R. Araki, Y. Hoki, M. Uda et al., "Crucial role of c-Myc in the generation of induced pluripotent stem cells," *Stem Cells*, vol. 29, no. 9, pp. 1362–1370, 2011.

[48] N. Shyh-Chang, H. Zhu, T. Yvanka de Soysa et al., "*Lin28* enhances tissue repair by reprogramming cellular metabolism," *Cell*, vol. 155, no. 4, pp. 778–792, 2013.

[49] J. Yu, M. A. Vodyanik, K. Smuga-Otto et al., "Induced pluripotent stem cell lines derived from human somatic cells," *Science*, vol. 318, no. 5858, pp. 1917–1920, 2007.

[50] P. Hou, Y. Li, X. Zhang et al., "Pluripotent stem cells induced from mouse somatic cells by small-molecule compounds," *Science*, vol. 341, no. 6146, pp. 651–654, 2013.

[51] D. Biswas and P. Jiang, "Chemically induced reprogramming of somatic cells to pluripotent stem cells and neural cells," *International Journal of Molecular Sciences*, vol. 17, no. 2, p. 226, 2016.

[52] A. L. Fritz, M. M. Adil, S. R. Mao, and D. V. Schaffer, "cAMP and EPAC signaling functionally replace OCT4 during induced pluripotent stem cell reprogramming," *Molecular Therapy*, vol. 23, no. 5, pp. 952–963, 2015.

[53] P. Mali, B. K. Chou, J. Yen et al., "Butyrate greatly enhances derivation of human induced pluripotent stem cells by promoting epigenetic remodeling and the expression of pluripotency-associated genes," *Stem Cells*, vol. 28, no. 4, pp. 713–720, 2010.

[54] T. Wang, K. Chen, X. Zeng et al., "The histone demethylases Jhdm1a/1b enhance somatic cell reprogramming in a vitamin-C-dependent manner," *Cell Stem Cell*, vol. 9, no. 6, pp. 575–587, 2011.

[55] S. Comes, M. Gagliardi, N. Laprano et al., "L-Proline induces a mesenchymal-like invasive program in embryonic stem cells by remodeling H3K9 and H3K36 methylation," *Stem Cell Reports*, vol. 1, no. 4, pp. 307–321, 2013.

[56] M. A. Esteban, T. Wang, B. Qin et al., "Vitamin C enhances the generation of mouse and human induced pluripotent stem cells," *Cell Stem Cell*, vol. 6, no. 1, pp. 71–79, 2010.

[57] E. A. Minor, B. L. Court, J. I. Young, and G. Wang, "Ascorbate induces ten-eleven translocation (Tet) methylcytosine dioxygenase-mediated generation of 5-hydroxymethylcytosine," *The Journal of Biological Chemistry*, vol. 288, no. 19, pp. 13669–13674, 2013.

[58] K. Hochedlinger and R. Jaenisch, "Induced pluripotency and epigenetic reprogramming," *Cold Spring Harbor Perspectives in Biology*, vol. 7, no. 12, 2015.

[59] B. T. Dodsworth, R. Flynn, and S. A. Cowley, "The current state of naïve human pluripotency," *Stem Cells*, vol. 33, no. 11, pp. 3181–3186, 2015.

[60] J. Nichols and A. Smith, "Naive and primed pluripotent states," *Cell Stem Cell*, vol. 4, no. 6, pp. 487–492, 2009.

[61] K. Osafune, L. Caron, M. Borowiak et al., "Marked differences in differentiation propensity among human embryonic stem cell lines," *Nature Biotechnology*, vol. 26, no. 3, pp. 313–315, 2008.

[62] G. Duggal, S. Warrier, S. Ghimire et al., "Alternative routes to induce naïve pluripotency in human embryonic stem cells," *Stem Cells*, vol. 33, no. 9, pp. 2686–2698, 2015.

[63] T. W. Theunissen, M. Friedli, Y. He et al., "Molecular criteria for defining the naive human pluripotent state," *Cell Stem Cell*, vol. 19, no. 4, pp. 502–515, 2016.

[64] H. Sperber, J. Mathieu, Y. Wang et al., "The metabolome regulates the epigenetic landscape during naive-to-primed human embryonic stem cell transition," *Nature Cell Biology*, vol. 17, no. 12, pp. 1523–1535, 2015.

[65] X. Liu, C. M. Nefzger, F. J. Rossello et al., "Comprehensive characterization of distinct states of human naive pluripotency generated by reprogramming," *Nature Methods*, vol. 14, no. 11, pp. 1055–1062, 2017.

[66] J. M. Polo, S. Liu, M. E. Figueroa et al., "Cell type of origin influences the molecular and functional properties of mouse induced pluripotent stem cells," *Nature Biotechnology*, vol. 28, no. 8, pp. 848–855, 2010.

[67] S. Warrier, M. van der Jeught, G. Duggal et al., "Direct comparison of distinct naive pluripotent states in human embryonic stem cells," *Nature Communications*, vol. 8, article 15055, 2017.

[68] C. B. Ware, A. M. Nelson, B. Mecham et al., "Derivation of naive human embryonic stem cells," *Proceedings of the National Academy of Sciences of the United States of America*, vol. 111, no. 12, pp. 4484–4489, 2014.

[69] T. Bianco-Miotto, J. M. Craig, Y. P. Gasser, S. J. van Dijk, and S. E. Ozanne, "Epigenetics and DOHaD: from basics to birth and beyond," *Journal of Developmental Origins of Health and Disease*, vol. 8, no. 05, pp. 513–519, 2017.

[70] L. C. Schulz, "The Dutch Hunger Winter and the developmental origins of health and disease," *Proceedings of the National Academy of Sciences of the United States of America*, vol. 107, no. 39, pp. 16757-16758, 2010.

[71] A. J. Harvey, J. Rathjen, and D. K. Gardner, "Metaboloepigenetic regulation of pluripotent stem cells," *Stem Cells International*, vol. 2016, Article ID 1816525, 15 pages, 2016.

[72] A. Nieborak and R. Schneider, "Metabolic intermediates - cellular messengers talking to chromatin modifiers," *Molecular Metabolism*, vol. 14, pp. 39–52, 2018.

[73] A. Moussaieff, M. Rouleau, D. Kitsberg et al., "Glycolysis-mediated changes in acetyl-CoA and histone acetylation control the early differentiation of embryonic stem cells," *Cell Metabolism*, vol. 21, no. 3, pp. 392–402, 2015.

[74] K. E. Wellen, G. Hatzivassiliou, U. M. Sachdeva, T. V. Bui, J. R. Cross, and C. B. Thompson, "ATP-citrate lyase links cellular metabolism to histone acetylation," *Science*, vol. 324, no. 5930, pp. 1076–1080, 2009.

[75] S. Imai, C. M. Armstrong, M. Kaeberlein, and L. Guarente, "Transcriptional silencing and longevity protein Sir2 is an NAD-dependent histone deacetylase," *Nature*, vol. 403, no. 6771, pp. 795–800, 2000.

[76] N. Shyh-Chang, J. W. Locasale, C. A. Lyssiotis et al., "Influence of threonine metabolism on S-adenosylmethionine and histone methylation," *Science*, vol. 339, no. 6116, pp. 222–226, 2013.

[77] N. Shiraki, Y. Shiraki, T. Tsuyama et al., "Methionine metabolism regulates maintenance and differentiation of human pluripotent stem cells," *Cell Metabolism*, vol. 19, no. 5, pp. 780–794, 2014.

[78] J. M. Washington, J. Rathjen, F. Felquer et al., "L-Proline induces differentiation of ES cells: a novel role for an amino acid in the regulation of pluripotent cells in culture," *American Journal of Physiology. Cell Physiology*, vol. 298, no. 5, pp. C982–C992, 2010.

[79] B. S. N. Tan, A. Lonic, M. B. Morris, P. D. Rathjen, and J. Rathjen, "The amino acid transporter SNAT2 mediates L-proline-induced differentiation of ES cells," *American Journal of Physiology. Cell Physiology*, vol. 300, no. 6, pp. C1270–C1279, 2011.

[80] B. W. Carey, L. W. S. Finley, J. R. Cross, C. D. Allis, and C. B. Thompson, "Intracellular α-ketoglutarate maintains the pluripotency of embryonic stem cells," *Nature*, vol. 518, no. 7539, pp. 413–416, 2015.

[81] L. Wang, T. Zhang, L. Wang et al., "Fatty acid synthesis is critical for stem cell pluripotency via promoting mitochondrial fission," *The EMBO Journal*, vol. 36, no. 10, pp. 1330–1347, 2017.

[82] D. R. Donohoe and S. J. Bultman, "Metaboloepigenetics: interrelationships between energy metabolism and epigenetic control of gene expression," *Journal of Cellular Physiology*, vol. 227, no. 9, pp. 3169–3177, 2012.

[83] W. G. Kaelin Jr. and S. L. McKnight, "Influence of metabolism on epigenetics and disease," *Cell*, vol. 153, no. 1, pp. 56–69, 2013.

[84] M. H. Chin, M. J. Mason, W. Xie et al., "Induced pluripotent stem cells and embryonic stem cells are distinguished by gene expression signatures," *Cell Stem Cell*, vol. 5, no. 1, pp. 111–123, 2009.

[85] Y. Ohi, H. Qin, C. Hong et al., "Incomplete DNA methylation underlies a transcriptional memory of somatic cells in human iPS cells," *Nature Cell Biology*, vol. 13, no. 5, pp. 541–549, 2011.

[86] K. Kim, A. Doi, B. Wen et al., "Epigenetic memory in induced pluripotent stem cells," *Nature*, vol. 467, no. 7313, pp. 285–290, 2010.

[87] A. J. Harvey, C. O'Brien, J. Lambshead et al., "Physiological oxygen culture reveals retention of metabolic memory in human induced pluripotent stem cells," *PLoS One*, vol. 13, no. 3, article e0193949, 2018.

[88] J. Spyrou, D. K. Gardner, and A. J. Harvey, "Metabolomic and transcriptional analyses reveal atmospheric oxygen during human induced pluripotent stem cell generation impairs metabolic reprogramming," *Stem Cells*, 2019.

[89] O. Kyriakides, J. A. Halliwell, and P. W. Andrews, "Acquired genetic and epigenetic variation in human pluripotent stem cells," *Engineering and Application of Pluripotent Stem Cells*, vol. 163, pp. 187–206, 2017.

[90] A. Prigione, B. Lichtner, H. Kuhl et al., "Human induced pluripotent stem cells harbor homoplasmic and heteroplasmic mitochondrial DNA mutations while maintaining human embryonic stem cell-like metabolic reprogramming," *Stem Cells*, vol. 29, no. 9, pp. 1338–1348, 2011.

[91] W. E. Lowry, L. Richter, R. Yachechko et al., "Generation of human induced pluripotent stem cells from dermal fibroblasts," *Proceedings of the National Academy of Sciences of the United States of America*, vol. 105, no. 8, pp. 2883–2888, 2008.

[92] S. T. Suhr, E. A. Chang, J. Tjong et al., "Mitochondrial rejuvenation after induced pluripotency," *PLoS One*, vol. 5, no. 11, article e14095, 2010.

[93] E. Kang, X. Wang, R. Tippner-Hedges et al., "Age-related accumulation of somatic mitochondrial DNA mutations in adult-derived human iPSCs," *Cell Stem Cell*, vol. 18, no. 5, pp. 625–636, 2016.

[94] Q. Chen, K. Kirk, Y. I. Shurubor et al., "Rewiring of glutamine metabolism is a bioenergetic adaptation of human cells with mitochondrial DNA mutations," *Cell Metabolism*, vol. 27, no. 5, pp. 1007–1025.e5, 2018.

[95] A. J. Dirks, T. Hofer, E. Marzetti, M. Pahor, and C. Leeuwenburgh, "Mitochondrial DNA mutations, energy metabolism and apoptosis in aging muscle," *Ageing Research Reviews*, vol. 5, no. 2, pp. 179–195, 2006.

[96] M. Picard and D. M. Turnbull, "Linking the metabolic state and mitochondrial DNA in chronic disease, health, and aging," *Diabetes*, vol. 62, no. 3, pp. 672–678, 2013.

[97] K. Khrapko and J. Vijg, "Mitochondrial DNA mutations and aging: devils in the details?," *Trends in Genetics*, vol. 25, no. 2, pp. 91–98, 2009.

[98] J. K. Meissen, B. T. K. Yuen, T. Kind et al., "Induced pluripotent stem cells show metabolomic differences to embryonic stem cells in polyunsaturated phosphatidylcholines and primary metabolism," *PLoS One*, vol. 7, no. 10, article e46770, 2012.

[99] R. Lister, M. Pelizzola, Y. S. Kida et al., "Hotspots of aberrant epigenomic reprogramming in human induced pluripotent stem cells," *Nature*, vol. 471, no. 7336, pp. 68–73, 2011.

[100] E. A. Ivanova, A. Parolari, V. Myasoedova, A. A. Melnichenko, Y. V. Bobryshev, and A. N. Orekhov, "Peroxisome proliferator-activated receptor (PPAR) gamma in cardiovascular disorders and cardiovascular surgery," *Journal of Cardiology*, vol. 66, no. 4, pp. 271–278, 2015.

[101] R. Marion-Letellier, G. Savoye, and S. Ghosh, "Fatty acids, eicosanoids and PPAR gamma," *European Journal of Pharmacology*, vol. 785, pp. 44–49, 2016.

[102] B. N. Finck and D. P. Kelly, "PGC-1 coactivators: inducible regulators of energy metabolism in health and disease," *The Journal of Clinical Investigation*, vol. 116, no. 3, pp. 615–622, 2006.

[103] A. C. Araújo, C. E. Wheelock, and J. Z. Haeggstrom, "The eicosanoids, redox-regulated lipid mediators in immunometabolic disorders," *Antioxidants & Redox Signaling*, vol. 29, no. 3, pp. 275–296, 2018.

[104] J. G. Lees, T. S. Cliff, A. Gammilonghi et al., "Oxygen regulates human pluripotent stem cell metabolic flux," *Stem Cells International*, vol. 2019, 2019.

[105] P. L. Wale and D. K. Gardner, "Oxygen regulates amino acid turnover and carbohydrate uptake during the preimplantation period of mouse embryo development," *Biology of Reproduction*, vol. 87, no. 1, pp. 1–8, 2012.

[106] A. D. Ebert, S. Diecke, I. Y. Chen, and J. C. Wu, "Reprogramming and transdifferentiation for cardiovascular development and regenerative medicine: where do we stand?," *EMBO Molecular Medicine*, vol. 7, no. 9, pp. 1090–1103, 2015.

[107] R. Trokovic, J. Weltner, P. Noisa, T. Raivio, and T. Otonkoski, "Combined negative effect of donor age and time in culture on the reprogramming efficiency into induced pluripotent stem cells," *Stem Cell Research*, vol. 15, no. 1, pp. 254–262, 2015.

[108] C. D. Wiley and J. Campisi, "From ancient pathways to aging cells-connecting metabolism and cellular senescence," *Cell Metabolism*, vol. 23, no. 6, pp. 1013–1021, 2016.

[109] K. R. Short, M. L. Bigelow, J. Kahl et al., "Decline in skeletal muscle mitochondrial function with aging in humans," *Proceedings of the National Academy of Sciences of the United States of America*, vol. 102, no. 15, pp. 5618–5623, 2005.

[110] A. P. Gomes, N. L. Price, A. J. Y. Ling et al., "Declining NAD^+ induces a pseudohypoxic state disrupting nuclear-mitochondrial communication during aging," *Cell*, vol. 155, no. 7, pp. 1624–1638, 2013.

[111] H. Massudi, R. Grant, N. Braidy, J. Guest, B. Farnsworth, and G. J. Guillemin, "Age-associated changes in oxidative stress and NAD^+ metabolism in human tissue," *PLoS One*, vol. 7, no. 7, article e42357, 2012.

[112] C. Zhang, M. Skamagki, Z. Liu et al., "Biological significance of the suppression of oxidative phosphorylation in induced pluripotent stem cells," *Cell Reports*, vol. 21, no. 8, pp. 2058–2065, 2017.

Hindawi
Stem Cells International
Volume 2019, Article ID 5980465, 19 pages
https://doi.org/10.1155/2019/5980465

Research Article

Metformin Delays Satellite Cell Activation and Maintains Quiescence

Theodora Pavlidou,[1] **Milica Marinkovic**,[1] **Marco Rosina**,[1] **Claudia Fuoco**,[1] **Simone Vumbaca**,[1] **Cesare Gargioli**,[1] **Luisa Castagnoli**,[1] **and Gianni Cesareni**[1,2]

[1]*Department of Biology, Tor Vergata University, 00133 Rome, Italy*
[2]*IRCCS, Fondazione Santa Lucia, Rome, Italy*

Correspondence should be addressed to Gianni Cesareni; cesareni@uniroma2.it

Received 6 July 2018; Revised 29 October 2018; Accepted 25 December 2018; Published 24 April 2019

Guest Editor: Viviana Moresi

The regeneration of the muscle tissue relies on the capacity of the satellite stem cell (SC) population to exit quiescence, divide asymmetrically, proliferate, and differentiate. In age-related muscle atrophy (sarcopenia) and several dystrophies, regeneration cannot compensate for the loss of muscle tissue. These disorders are associated with the depletion of the satellite cell pool or with the loss of satellite cell functionality. Recently, the establishment and maintenance of quiescence in satellite cells have been linked to their metabolic state. In this work, we aimed to modulate metabolism in order to preserve the satellite cell pool. We made use of metformin, a calorie restriction mimicking drug, to ask whether metformin has an effect on quiescence, proliferation, and differentiation of satellite cells. We report that satellite cells, when treated with metformin *in vitro*, ex vivo, *or in vivo*, delay activation, Pax7 downregulation, and terminal myogenic differentiation. We correlate the metformin-induced delay in satellite cell activation with the inhibition of the ribosome protein RPS6, one of the downstream effectors of the mTOR pathway. Moreover, *in vivo* administration of metformin induces a belated regeneration of cardiotoxin- (CTX-) damaged skeletal muscle. Interestingly, satellite cells treated with metformin immediately after isolation are smaller in size and exhibit reduced pyronin Y levels, which suggests that metformin-treated satellite cells are transcriptionally less active. Thus, our study suggests that metformin delays satellite cell activation and differentiation by favoring a quiescent, low metabolic state.

1. Introduction

Skeletal muscle regeneration relies on the dynamic interplay between satellite cells (SCs) and their environment, the stem cell niche [1]. In the adult muscle, under resting conditions, SCs are mitotically quiescent [2]. Following damage, they are activated and divide asymmetrically. One daughter cell returns to quiescence to reconstitute the stamina pool while the other one proliferates and differentiates to eventually form new myofibers [3]. In healthy conditions, SCs are only sporadically activated to counterbalance physiological tissue turnover. As a consequence, muscle mass loss is prevented. The stability of the SC pool and the integrity of the stem cell niche, however, are affected by aging or disease [4]. In pathological conditions, as in Duchenne muscular dystrophy (DMD), chronic inflammation stimulates SC proliferation and differentiation by sending sustained regeneration signals. This phenomenon contributes to the exhaustion of the SC pool and the ensuing decrease in the regeneration potential [5].

Metabolic flexibility controls the balance between stem cell fates, as unique bioenergetic demands underlie quiescence, stem cell proliferation, and lineage specification [6]. In several tissues, cellular quiescence is associated with low metabolic activity, little mitochondrial respiration, reduced translational rates, and activation of autophagy in order to provide nutrients for survival [7]. On the other hand, stem cell activation, including satellite cell activation, is characterized by elevated energy demands and is mediated by an oxidative respiration to glycolytic metabolism shift [8, 9]. Specifically, it has been demonstrated that different metabolic pathways take part in the establishment of the quiescent

state. SIRT1, a nutrient sensor, regulates the autophagic flux in SC progeny, and loss of SIRT1 leads to a delay in SC activation [10]. Rodgers et al. reported that mTOR activity, a known inhibitor of autophagy, is necessary for the transition of SCs and fibroadipogenic progenitors (FAP) from a G_0 phase to a G_{Alert} quiescent phase, where G_{Alert} stem cells have higher propensity to cycle, increased mitochondrial activity, and enhanced differentiation kinetics [11]. Furthermore, we have recently shown that AMPK activation by the antidiabetic drug metformin plays a negative role in C2C12 skeletal muscle differentiation and prevents permanent exit from the cell cycle, mimicking in this way the quiescent "reserve cell" phenotype [12].

Thus, perturbing stem cell metabolism may influence muscle regeneration. Cerletti et al. have demonstrated that short-term calorie restriction increases the percentage and the myogenic function of Pax-7-expressing cells in the muscles of young and old mice [13]. They associated this phenotype with an increased mitochondrial number in SCs derived from mice fed with a low-calorie diet and an enhanced transplantation potential. In accordance, chronic treatment with metabolic remodeling agents, such as AICAR and PPARδ agonist, favors oxidative metabolism in mdx mice [14, 15]. The natural phenol resveratrol is also reported to induce oxidative metabolism in mdx mice by increasing the levels and activity of SIRT1 [16] while favoring utrophin gene expression [17]. In order to further investigate the role of metabolic reprogramming in skeletal muscle stem cell fate, here we examine the effect of metformin on SC activation and differentiation *in vivo* and ex vivo.

Metformin (1,1-dimethylbiguanide hydrochloride) is a calorie restriction mimicking drug that is widely prescribed for the treatment of hyperglycemia in individuals with type II diabetes [18]. The main targets of metformin are hepatocyte mitochondria where it disrupts respiratory chain complex I leading to a decrease in the ATP/AMP ratio [19]. As a result of AMP accumulation, AMP-activated protein kinase (AMPK) is activated [20]. AMPK is a serine/threonine kinase which works as a sensor of changes in cellular energy levels and metabolic stress [21]. Different studies have described beneficial effects of metformin on the prevention and treatment of cancer as it exerts an antiproliferative effect by inhibiting mTOR. Specifically in MCF7 breast cancer cells, it has been shown that metformin inhibits cell growth through negative regulation of the mTOR pathway and 30% reduction in global protein synthesis [22]. The molecular mechanism underlying this antiproliferative effect has been characterized by revealing the proteomic profile of metformin-treated MCF7 cells [23].

In skeletal muscles, metformin has been demonstrated to protect mouse muscles from cardiotoxin-induced damage [24] and ameliorate the PGC1A and utrophin expression in dystrophic mice [25]. Notably, metformin is now tested in clinical trials for the improvement of muscle function in patients with Duchenne muscular dystrophy [26, 27].

Here, we focus on the effect of the drug on satellite cell activation and differentiation *in vivo* and ex vivo. Our results indicate that metformin delays the activation, Pax7 downregulation, and terminal myogenic differentiation of SCs. This belated SC activation is paralleled by a delayed regeneration of skeletal muscle injury, inhibition of mTOR, and reduced RPS6 phosphorylation that induce the low metabolic state associated with quiescence.

2. Materials and Methods

2.1. Animal Procedures. An equal number of 1.5-month-old C57BL/6 mice was used for control ($n = 12$) and metformin-treated ($n = 12$) experimental groups. Twelve C57BL/6 mice were pretreated with 300 mg/kg body weight of metformin (Sigma-Aldrich PHR1084) diluted in water for 21 days. Muscle crush injury was induced by cardiotoxin in already-anesthetized mice. Anesthesia was induced by an intramuscular injection of physiologic saline (10 ml/kg) containing ketamine (5 mg/ml) and xylazine (1 mg/ml). 10 $\mu\lambda$ of cardiotoxin isolated from *Naja pallida* (Latoxan L81-02) was intramuscularly administered into the tibialis anterior (TA), quadriceps, and gastrocnemius (GC) muscle, and after 4 and 7 days of treatment, control and metformin-treated mice were sacrificed. Metformin administration was maintained during the whole regeneration period. Isolated tibialis anterior (TA) muscles were snap frozen in OCT for cryosectioning with a Leica cryostat while the rest of the hind limb muscles were homogenized for cell isolation. Experiments on animals followed the rules of good animal experimentation of I.A.C.U.C. and obtained ethical approval released on 16/09/2011 from Italian Ministry of Health (protocol #163/2011-B).

2.2. SC Isolation. Hind limb muscles were gently isolated from mice, nonmuscle tissue was removed, and muscles were minced and subjected to enzymatic dissociation for 45 min at 37°C. The enzymatic mix was composed of 2 μg/ml collagenase A (Roche cat#10103586001), 2.4 U/ml dispase II (Roche cat#04942078001), and 0.01 mg/ml DNase I (Roche cat#04716728001) diluted in D-PBS with calcium (130 mg/l) and magnesium (200 mg/l). Enzymatic dissociation was stopped by the addition of Hank's balanced salt solution (HBSS), and the cell suspension was filtered progressively through a 100, 70, 40, and 30 μm cell strainer. Cells were incubated with the appropriate antibodies conjugated with magnetic microbeads and isolated using the MACS separation technology. Lineage negativity characterization was performed by using the antibodies CD45 (Miltenyi cat#130-052-301) and CD31 (Miltenyi cat#130-097-418). The $CD45^-/CD31^-$cells were further positively selected with an a7-integrin microbead antibody (Miltenyi cat#130-104-261). SCs were selected as $CD45^-/CD31^-/a7\text{-integrin}^+$ cells, and cell purity was confirmed by Pax7 expression.

2.3. Single-Fiber Isolation. To isolate single myofibers, EDL muscles were digested with 0.2 μg/μl collagenase A (Roche cat#10103586001) in Tyrode's medium (Sigma cat#T2145-10X1L) for 1 h at 37°C with gently shaking every 10 min. Muscles were dissociated by gentle triturating and were washed several times to eliminate cellular debris and contaminating cells. EDL myofibers were then

cultured in Tyrode's medium supplemented with 10% heat-inactivated fetal bovine serum and penicillin-streptomycin/antimycotic (100 U/100 g/ml).

2.4. Cell Cultures. SCs were cultured in a gelatin-coated dish with Dulbecco's modified Eagle's medium (DMEM) supplemented with 20% heat-inactivated fetal bovine serum, 10% heat-inactivated horse serum, 2% chicken embryo extract, penicillin-streptomycin (100 U/100 g/ml), 1 mM sodium pyruvate, and 10 mM HEPES. SCs spontaneously differentiate into multinucleated myotubes in culture medium. For cell proliferation and western blot experiments, SCs were expanded for four days in Cytogrow medium (Resnova) to allow a sufficient number of cells. SCs were then trypsinized and plated in culture medium. SCs were treated with 2 mM metformin every 48 h. The control samples were treated with an equal quantity of PBS.

2.5. Histological Analysis. Evaluation of the percentage of centronucleated myofibers was carried out by H&E staining. Centronucleated fibers were counted in 20 μm thick histological sections of skeletal muscle tissues, and a total number of at least 3000 fibers of the damaged area were counted for each mouse. The results were expressed as the percentage of centronucleated fibers to the total fiber number of the damaged area. Analysis was performed using ImageJ software.

2.6. Immunofluorescence. Fixation of cryosections was performed by incubation with 4% of paraformaldehyde (PFA) for 5 minutes, followed by rinsing with PBS containing 1% BSA and 0.1% Triton X-100 (5 min at RT), blocking with PBS containing 0.2% Triton X-100 and 20% goat serum (2 h at RT), and incubating with the primary antibody overnight at 4°C. Samples were then washed three times and incubated with the secondary antibody for 1 h at RT. Next, cryosections were washed three times and incubated with Hoechst (1 mg/ml, 5 min at RT), washed again, and mounted. SCs and single myofibers were fixed with 2% paraformaldehyde (PFA) for 15 minutes and permeabilized in 0.1% Triton X-100 for 5 min. Blocking was performed with 1% PBS containing 10% serum and 0.1% TritonX-100 for 1 h at RT. The cells were stained with the primary antibody for 1 h at RT, washed three times with PBS, and incubated with the secondary antibody for 30 min at RT.

Single myofibers were blocked with PBS containing 0.2% Triton X-100 and 20% goat serum for 2 h at RT and incubated with the primary antibody overnight. Single myofibers were washed three times and incubated with the secondary antibody for 1 h at RT. The fibers were finally washed three times, and nuclei were counterstained with Hoechst 33258 (1 mg/ml, 5 min at RT). The antibodies used were the following: rabbit anti-MyoD (1 : 20, Santa Cruz sc-760), mouse anti-MyHC (1 : 2, DSHB), rabbit anti-laminin (1 : 200, Sigma cat#L9393-.2ML), mouse anti-Pax7 (1 : 15, DSHB), mouse anti-myogenin (eBioscience cat#14-5643), rabbit anti-phospho RPS6 (Cell Signaling cat#3985), anti-rabbit secondary antibody conjugated with Alexa Fluor 555 (1 : 100, Life Technologies A-21428), and anti-mouse secondary antibody conjugated with Alexa Fluor 488 (1 : 100, Life Technologies A-11001).

2.7. Cell Proliferation Assay by BrdU/EdU. Cell proliferation was measured by BrdU (GE Healthcare) or EdU (Life Technologies Inc.). BrdU and EdU (5-ethynyl-2′-deoxyuridine) are nucleoside analogs of thymidine that are incorporated into DNA during active DNA synthesis. The cells were plated at the desired density and treated for 24 h with a 10 μM EdU solution prepared with culture media. The cells were fixed and permeabilized according to the manufacturer's protocol using 3.7% formaldehyde in PBS, followed by a 0.5% Triton® X-100 permeabilization step. After that, cells were incubated with the Click-iT EdU reaction mix (1X Click-iT® reaction buffer CuSO, Alexa Fluor® azide, and reaction buffer additive) for 30 min at room temperature protected from light. Finally, the samples were washed twice with 3% BSA in PBS and stained for nuclei. Images were acquired with a Leica fluorescent microscope (DMI6000B).

2.8. Cell Growth Curve. Proliferation of *in vitro* metformin-treated and control SCs was monitored by counting the total cell nuclei per image field after 2 and 4 days of treatment. The monitoring of SC cell growth was performed according to our previous report [12]. Briefly, the cells were plated in the same initial number in all conditions, and at each time point, cells were fixed with 2% paraformaldehyde solution in 1X PBS for 10 minutes at room temperature (RT). Following staining with 2 μg/ml Hoechst 33342 (Thermo Fisher Scientific) in 0.1% Triton X-100 (*v*/*v*) in 1X PBS for 5 minutes, acquisition of images was carried out by a Leica DM6000B (Leica Microsystems) automated fluorescence microscope. In total, 25 fields/wells were acquired by a 5×5 matrix covering the whole surface of the sample. Counting of the nuclei was performed by using the CellProfiler software, and the data were represented as mean of four independent cell isolations and biological replicates. Doubling time analysis was performed by using the nonlinear regression/exponential growth equation tool in GraphPad Prism. All replicates were analyzed separately. Doubling time is reported as hours ± SEM.

2.9. Immunoblotting. Protein extraction and western blot analysis were performed as reported from our previous publication [12]. The antibodies used were as follows: mouse anti-Pax7 (1 : 500, DSHB AB_528428), rabbit anti-MyoD (1 : 500, Santa Cruz sc-760), mouse anti-MyHC (1 : 500, DSHB MF20), rabbit anti-Tom20 (1 : 1000, Cell Signaling 42406), mouse anti-Sirt1 (1 : 1000, Cell Signaling 8469), rabbit anti-acH3 (1 : 1000, Cell Signaling 9649), rabbit anti-phospho AMPK (Thr172) antibody (1 : 1000, Cell Signaling 2535), rabbit anti-AMPK (1 : 1000, Cell Signaling 2603), rabbit anti-phospho P70S6K (Thr421/Ser424) (1 : 1000, Cell Signaling 9204), rabbit anti-P70S6K (1 : 1000, Cell Signaling 9202), rabbit anti-phospho RPS6 (Ser240/244) antibody (1 : 1000, Cell Signaling 2215), rabbit anti-RPS6 (1 : 1000, Cell Signaling 2217), and rabbit anti-tubulin antibody (1 : 500, Santa Cruz sc-9104). Densitometric analysis was performed using ImageQuant.

Normalization of phosphorylated and total proteins was performed by using tubulin or vinculin. Finally, the ratio between the phosphorylated and total protein was indicated.

2.10. Mito Stress Analysis. Cells were plated at a density of 3000 cells/well on Seahorse XF96 Cell Culture Microplates (Agilent) in Cytogrow medium overnight.

Cells were treated in SC culture medium with 2 mM metformin or PBS as a control for 24 h.

The Mito Stress Test was performed according to Agilent's recommendations, stimulating the mitochondrial respiratory chain with 1 μM oligomycin, 1.5 μM FCCP, and 1 μM rotenone/antimycin.

For normalization, immediately after the assay completion, cells were fixed with 2% PFA for 20 minutes at RT and washed 3 times with 1X PBS. Nuclei were stained with Hoechst 33342 (1 : 5000) in 0.1% Triton X-100 for 5 minutes at RT and washed 3 times with 1X PBS. The central 10x field of each well was acquired, and counting of nuclei was performed with the CellProfiler software. The total number of nuclei per well was estimated calculating the field-to-well ratio. OCR values were reported as pmol O_2/min/1000 cells.

2.11. Apoptosis Detection. For apoptosis detection by annexin V/PI, cells were analyzed by flow cytometry after staining with annexin V/PI following protocol instructions (Cell Signaling Technology). After treatment, adherent and floating cells were collected, washed twice with ice-cold PBS, and suspended in annexin V binding buffer. 1 μl of annexin V-FITC conjugate and 12.5 μl of PI were added to each sample, and samples were incubated for 10 minutes on ice protected from light. Stained cells were diluted in ice-cold buffer and directly analyzed by a BD FACSCalibur flow cytometer. This double staining allows highlighting four distinct cell populations: alive cells (annexin V negative, PI negative), early apoptotic cells (annexin V positive, PI negative), late apoptotic cells (annexin V positive, PI positive), and necrotic cells (annexin V negative, PI positive). Cell percentage for each population was determined using the FlowJo software (FlowJo, LLC, USA).

2.12. RNA Level Detection by Pyronin Y Staining. Cells were resuspended in Hank's solution, washed two times, and fixed in cold methanol : acetone (4 : 1) for 30 min at 4°C. The samples were then washed twice and incubated with 0.5 μg/ml pyronin Y for 30 min at 37°C. Before analysis by the BD FACSCalibur flow cytometer, cells were transferred into ice for at least 10 min. Pyronin Y is excited at 488 nm, emits at 575 nm, and analyzed in a linear scale.

2.13. Statistical Analysis. All the data presented are mean values ± SEM of at least three experiments. Student's t-test or ANOVA statistical analysis was used to estimate the significance of the observed differences in the means in all experiments. The differences were considered significant at $p < 0.05$.

3. Results

3.1. Metformin Delays Pax7 Downregulation. Quiescent SCs express the transcription factor Pax7 [28]. After activation, each SC divides asymmetrically, producing one myoblast $Pax7^+$, $MyoD^+$, that amplifies and differentiates and one quiescent stem cell. When myoblasts commit to skeletal muscle differentiation, the expression of Pax7 is downregulated and they stop proliferating and express the myogenic factor myogenin [3]. In order to understand the role of metformin in SC proliferation, we isolated SCs from C57BL/6 mice by microbead technology as $CD45^-$, $CD31^-$, and $a7\text{-integrin}^+$ cells and treated them with 2 mM metformin for 2, 4, and 8 days in DMEM-supplemented medium. Four days after plating, most SCs already express MyoD irrespective of metformin treatment. We observed, however, that the downregulation in the expression of Pax7 is delayed in metformin-treated SCs (Figures 1(a) and 1(b)). The percentage of SCs that remains positive for both Pax7 and MyoD is significantly higher after 4 days of metformin treatment when compared to the control, while the fraction of SCs committed to myogenic differentiation ($Pax7^-/MyoD^+$) remains significantly lower in the treated sample. After 8 days, the fraction of cells that do not express Pax7 ($Pax7^-/MyoD^+$) is similar in both the metformin-treated and untreated cultures.

We further monitored the expression of Pax7 and MyoD by western blot analysis. This analysis, however, (Figure S1) did not reveal significant differences in the kinetic of expression of the two myogenic markers suggesting that the differences observed at the level of single-cell analysis are blurred in the bulk analysis.

We also investigated SC proliferation by monitoring the number of SCs that incorporate BrdU and noticed that it is significantly higher in the metformin-treated sample at day 4 of treatment (Figures 2(a) and 2(b)), a result that is in accordance with the belated Pax7 downregulation. In spite of the higher number of metformin-treated cells still actively incorporating BrdU at day 4, the total number of cells is lower in the treated sample than in control as indicated by the exponential growth curve (Figure 2(c)). In addition, by calculating the doubling time, we observed that metformin-treated SCs are characterized by a longer doubling time compared to the control. These differences, however, are not statistically significant (Figure 2(d)). These observations are consistent with the conclusion that metformin holds the SCs for a longer time in a predifferentiation stage where they express both Pax7 and MyoD and are still actively replicating.

3.2. Metformin Delays SC Differentiation. Given that metformin treatment delays the downregulation of Pax7 expression in SCs, we further asked whether metformin also affects SC terminal differentiation. As shown in Figure 3, metformin significantly defers the expression of the early differentiation marker myogenin after 2 days of treatment (Figures 3(a) and 3(b)), while it reduces the expression of myosin heavy chain (MyHC) (Figures 3(c) and 3(d)) and affects the formation of multinucleated myotubes (Figure 3(e)). The above results were confirmed by western blot analysis for the expression

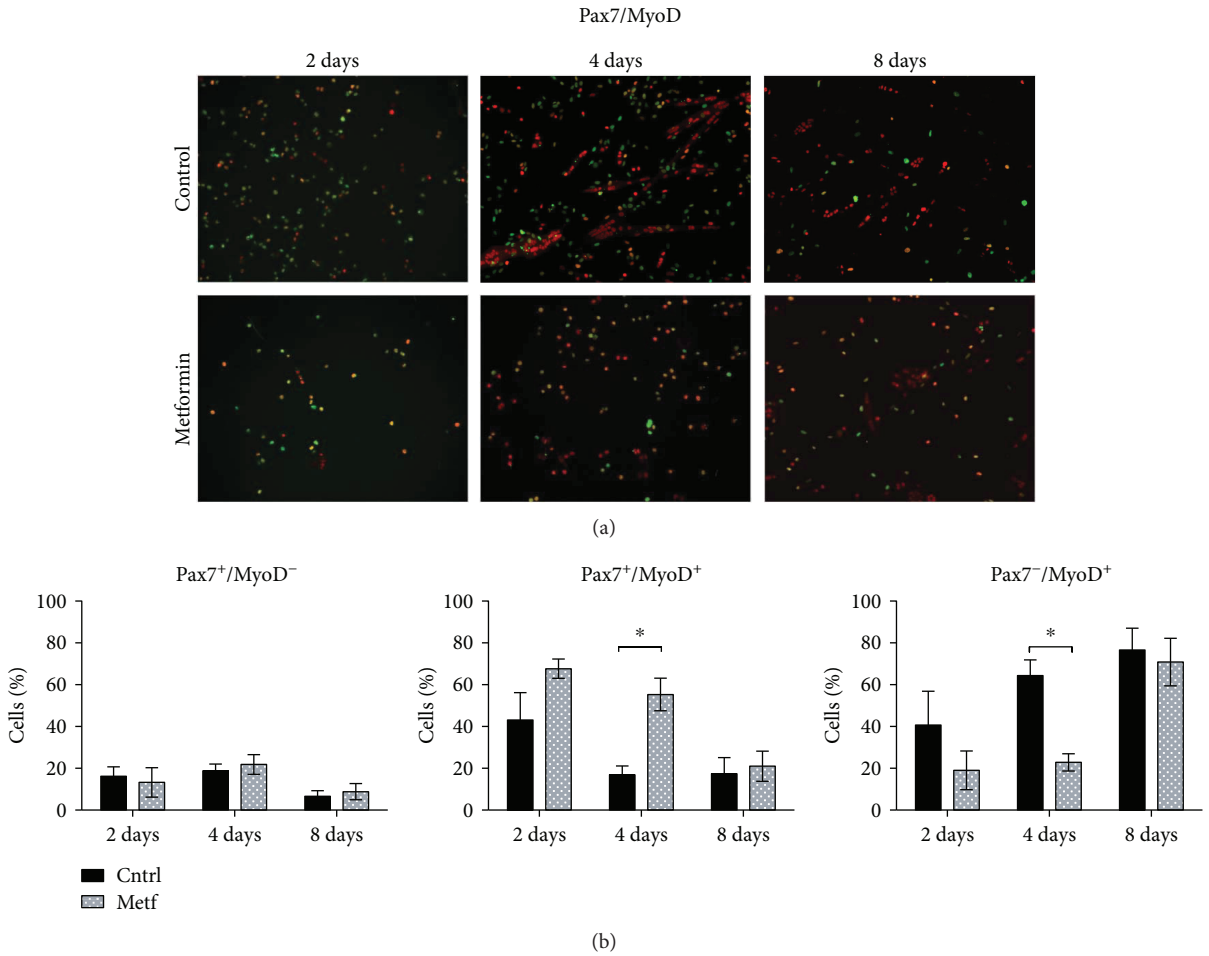

Figure 1: Metformin delays Pax7 downregulation. (a) SCs were isolated from C57BL/6 mice, attached onto plastic plates, and treated with 2 mM metformin for 2, 4, and 8 days. SCs were further analyzed by immunofluorescence microscopy for the expression of Pax7 and MyoD. (b) The percentage of cells expressing $Pax7^+/MyoD^-$, $Pax7^+/MyoD^+$, and $Pax7^-/MyoD^+$ after 2, 4, and 8 days of treatment with metformin was calculated in three independent cell isolations and experimental replicates ($n = 3$). Statistical significance was evaluated by the ANOVA test ($^*p < 0.05$).

of MyHC protein levels in control and metformin-treated SCs. As shown in Figures 3(f) and 3(g), protein levels of MyHC are significantly lower in the metformin samples at all time points analyzed (2, 4, 6, and 8 days of treatment).

3.3. Metformin Delays the Activation and Proliferation of Myofiber-Associated SCs. In order to study the effect of metformin on the transition from quiescence to the proliferative state, we isolated single myofibers from the extensor digitorum longus (EDL) muscle of C57BL/6 mice and treated them with 2 mM metformin for 24 h and 48 h. The propensity of the SC to cycle was evaluated by measuring the incorporation of EdU (5-ethynyl-2′-deoxyuridine), a thymidine analog (Figure 4). After 24 hours, fewer SCs incorporate EdU when compared to the control sample (Figure 4(b)). During the following 24 hours, the percentage of SCs incorporating EdU increases in the metformin sample while still remaining significantly lower compared to controls. These results suggest that metformin delays the transition of the fiber-associated SCs from quiescence to the active, proliferative state.

3.4. Metformin Downregulates RPS6 in Myofiber-Associated SCs. Activation of AMPK [20] and the ensuing inactivation of mTOR signaling [22] are two readouts of metformin treatment. Thus, we investigated the activation of the downstream mTOR effector RPS6 in SCs associated with single myofibers.

Isolated myofibers were treated *in vitro* with 2 mM metformin for 24 h and 48 h, and the phosphorylation of RPS6 was examined by immunofluorescence (Figure 5(a)). The levels of phosphorylated RPS6 (ph-RPS6) after 24 h and 48 h of treatment are lower in the metformin-treated myofibers compared to the untreated control (Figure 5(b)). The activation of RPS6 was also monitored in lysates of isolated SCs treated *in vitro* with 2 mM metformin for 4 days. After 4 days of metformin treatment, the fraction of RPS6 protein that is phosphorylated is lower (Figures 5(c) and 5(d)). The inhibition of RPS6 was accompanied by a significant activation of the AMPK, the main molecular target of metformin. As shown in Figures 5(e) and 5(f), the ratio of phosphorylated AMPK to total AMPK is significantly higher upon metformin treatment.

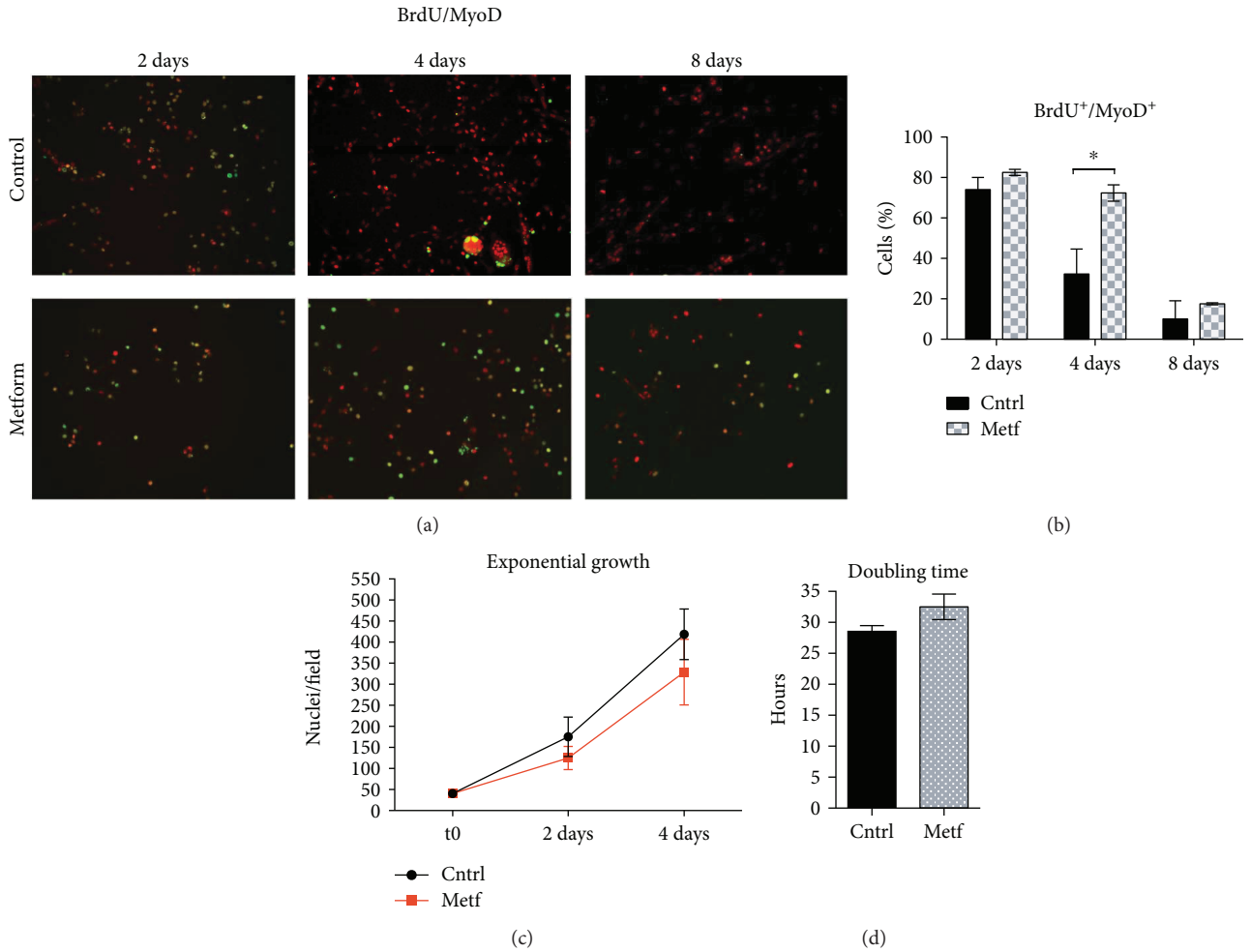

Figure 2: Metformin delays SC cycle exit. (a) SCs were treated upon attachment for 2, 4, and 8 days with 2 mM metformin. 24 h before fixation, a BrdU labeling reagent was added to the culture medium and cells were further analyzed by fluorescence microscopy for the incorporation of BrdU and the expression of MyoD. (b) The percentage of cells expressing $BrdU^+/MyoD^+$ after 2, 4, and 8 days of treatment with metformin was calculated after three independent cell isolations and experimental replicates ($n = 3$). Statistical significance was evaluated by the ANOVA test ($^*p < 0.05$). (c) Growth curve of control and metformin-treated SCs. SCs were treated with 2 mM metformin *in vitro* for 2 and 4 days, and the number of nuclei per field was counted by immunofluorescence microscopy. The initial number of plated cells was the same in each condition. The growth curves are derived from four independent biological replicates ($n = 4$). Statistical significance was evaluated by the ANOVA test ($^*p < 0.05$). (d) Doubling time analysis of control and metformin-treated cells. The analysis was performed using the nonlinear regression/exponential growth equation tool in GraphPad Prism. The bar graph represents the average of four independent biological replicates ($n = 4$). Statistical significance was evaluated by Student's t-test ($^*p < 0.05$).

Given that RPS6 phosphorylation correlates with global protein synthesis, this result suggests that metformin negatively modulates protein synthesis of SCs when they are cultivated both *in vitro* after purification and in a condition in isolated myofibers that is more similar to their natural in vivo niche.

3.5. Metformin Delays Skeletal Muscle Regeneration In Vivo. Next, we investigated the effect of metformin treatment on the activation of SCs *in vivo* during skeletal muscle damage and regeneration. C57BL/6 mice were pretreated with metformin for 21 days by administration in drinking water as shown in the experimental design (Figure 6(a)). Injection of cardiotoxin into the tibialis anterior (TA) was used to induce muscle damage. Regeneration was monitored at 4 and 7 days postinjury (DPI) while metformin treatment was maintained until the sacrifice of the animals. Newly formed myofibers can be readily distinguished in muscle cross sections for their small caliber and for the presence of centrally located myonuclei [1]. To evaluate the regeneration kinetics, we measured the number of centronucleated fibers in metformin-treated and untreated mice. As shown in Figures 6(b) and 6(c), the percentage of centrally nucleated myofibers at 4 DPI is significantly lower in the metformin-treated muscles compared to the control. On the contrary, at 7 DPI, the percentage of newly formed myofibers in the control sample decreases, while it increases in the metformin sample, even though this difference is not statistically significant (p value = 0.5030). This observation is compatible with the hypothesis that the muscles of the metformin-conditioned mice have a delay in the onset of the regeneration process and are still

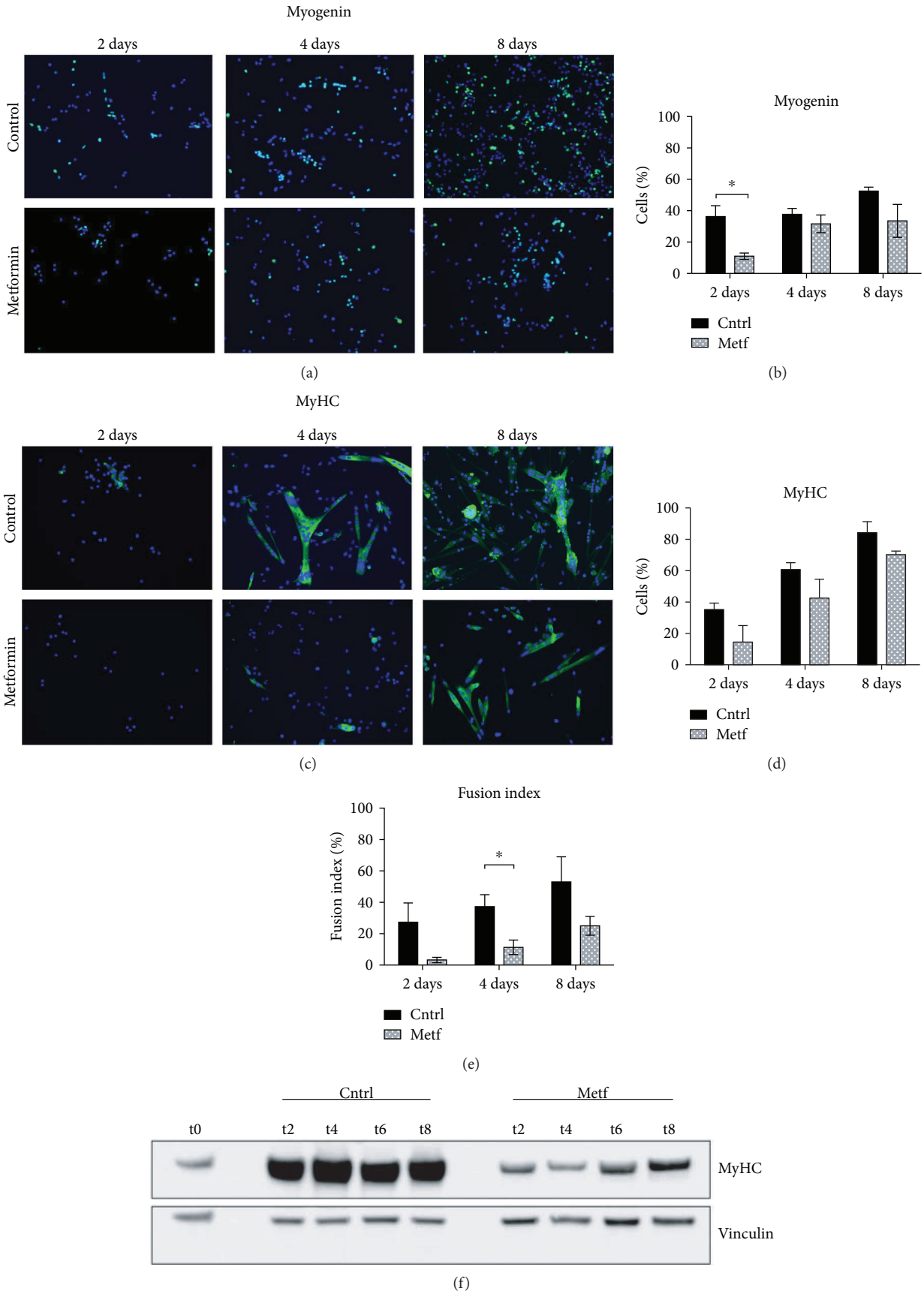

Figure 3: Continued.

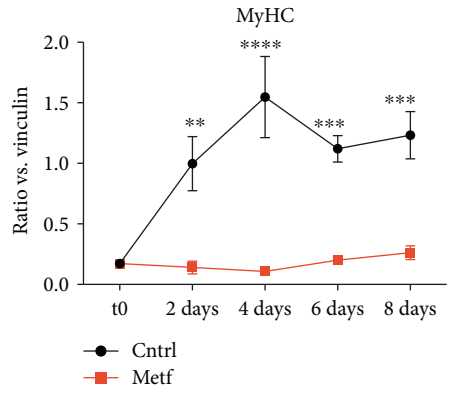

(g)

Figure 3: Metformin delays SC differentiation. (a) SCs were isolated from C57BL/6 mice, attached to a plastic dish, and treated with 2 mM metformin for 2, 4, and 8 days. The SCs were analyzed by immunofluorescence microscopy for the expression of the early myogenic marker myogenin. (b) The percentage of cells expressing myogenin after 2, 4, and 8 days of treatment with metformin was averaged from the results of three independent cell isolations and experimental replicates ($n = 3$). Statistical significance was evaluated by the ANOVA test ($^{*}p < 0.05$). (c) SCs were treated upon attachment for 2, 4, and 8 days with 2 mM metformin and analyzed by fluorescence microscopy for the expression of the myosin heavy chain (MyHC). (d) The percentage of cells expressing MyHC after 2, 4, and 8 days of treatment with metformin was analyzed after three independent cell isolations and experimental replicates ($n = 3$). Statistical significance was evaluated by the ANOVA test ($^{*}p < 0.05$). (e) The fusion index was calculated as the % of nuclei inside myotubes over the total number of *nuclei*. A myotube is defined as a cell expressing MyHC and containing at least three *nuclei* inside a continuous cell membrane. Statistical significance was evaluated by the ANOVA test ($^{*}p < 0.05$) after three independent cell isolations and experimental replicates ($n = 3$). (f) Western blot analysis for the expression of MyHC of control and metformin-treated SCs after 2, 4, 6, and 8 days of treatment (t2, t4, t6, and t8, respectively). Vinculin was used as a loading control. (g) Quantitation graph of MyHC protein levels monitored by western blot in four independent cell isolations and biological replicates ($n = 4$). Statistical significance was evaluated by the ANOVA test ($^{****}p < 0.0001$).

fully regenerating at 7 DPI. In agreement with this hypothesis, at 4 DPI, significantly smaller fibers (fiber group with size 0-250 μM^2) are observed in the muscles of the control mice (Figure 6(d)), while at 7 DPI, the number of myofibers with a smaller cross-sectional area is significantly higher in the metformin-treated regenerating muscles than in the control (Figure 6(e)), consistent with a delay in the completion of the regeneration process. In order to further investigate the role of metformin in skeletal muscle regeneration, we isolated SCs from the cardiotoxin-injured mice at days 1, 2, 4, and 7 postinjury and cultured them *in vitro*. Upon attachment, the expression of myogenic markers and terminal differentiation were monitored by immunofluorescence. SCs derived from mice that had received metformin exhibited delayed myotube formation *in vitro*, as shown by staining with myosin heavy chain (MyHC) antibodies. Control SCs differentiate readily *in vitro* already from the first day after injury, while the metformin-treated SCs achieve the same level of differentiation when they are purified from mice four days after injury (Figure S2). We conclude that metformin delays SC-dependent muscle regeneration.

3.6. The Activation and Proliferation of Myofiber-Associated SCs Are Delayed after In Vivo Administration of Metformin. We further evaluated the perturbation of SC activation induced by in vivo metformin administration. C57BL/6 mice received metformin in water for 21 days, and individual myofibers were isolated and cultured *in vitro* for 24 h and 48 h. The propensity of SCs to proliferate was monitored by measuring EdU incorporation in $Pax7^{+}$ cells while metabolic activation was assessed by looking at the phosphorylation of RPS6. In metformin-treated mice, 24 hours after myofiber isolation, fewer than 10% SCs are observed to incorporate EdU. After 48 hours, this percentage almost doubles but it is still significantly lower than the 80% EdU-positive SCs in the untreated controls (Figures 7(a) and 7(b)). Moreover, the SCs in myofibers from metformin-treated mice exhibit a significantly reduced phosphorylation of RPS6 (Figures 7(c) and 7(d)). In conclusion, exposure of SCs to metformin either *in vivo* or ex vivo delays their activation.

3.7. Sirt-1 Activity in SCs Is Not Affected by Metformin Treatment. Given that metformin mimics glucose restriction and affects SC metabolism by activating AMPK and by inhibiting the downstream marker mTOR, we asked whether these effects are mediated by Sirt1 activation. To this end, we analyzed the protein levels of Sirt1 and acetylated H3 (acH3) by western blot in SCs treated with 2 mM metformin *in vitro* for 2, 4, 6, and 8 days (Figure 8(a)). As shown in Figure 8, metformin does not affect Sirt1 levels (Figure 8(b)) while acetylation of H3 is increased upon 4 days of metformin treatment (Figure 8(c)). From the above results, we can conclude that metformin's effect on SC activation and differentiation is not mediated by Sirt1 activation.

3.8. Metformin Induces a Mitochondrial Stress in SCs In Vitro. Since metformin is known to target the mitochondrial respiratory complex, we next asked whether the observed effect of metformin on satellite cell differentiation was accompanied by a perturbation of metabolism. In order to assess the effect of metformin on SC mitochondrial function,

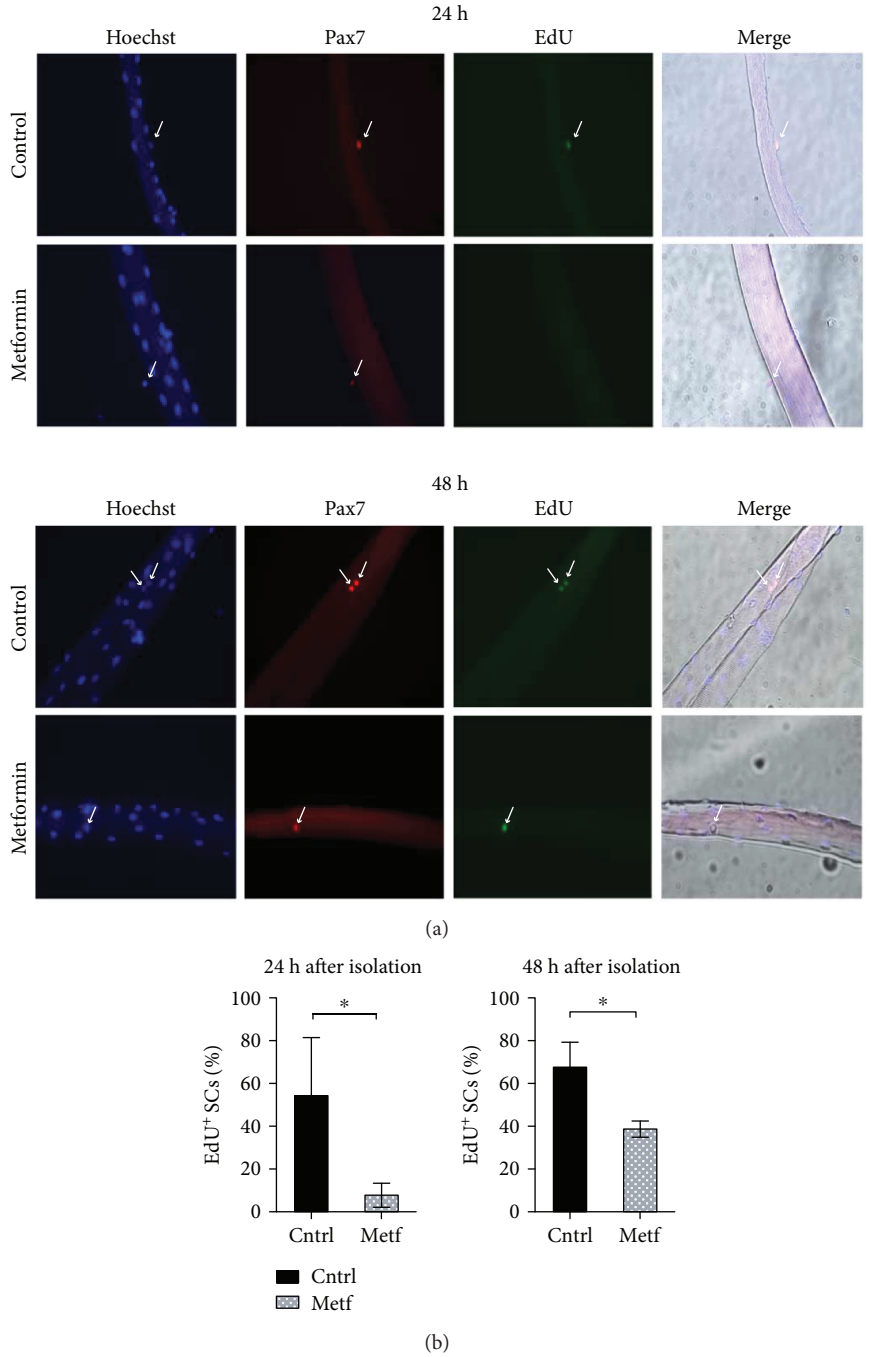

Figure 4: Metformin delays SC activation. (a) Myofibers were isolated from C57BL/6 mice and treated *in vitro* with 2 mM metformin in Tyrode's medium containing an EdU labeling agent. The SCs associated with the myofibers were analyzed by immunofluorescence microscopy for the expression of Pax7 and the incorporation of EdU after 24 h and 48 h of culture. (b) The percentage of SCs that have incorporated EdU after 24 h and 48 h in culture was calculated after three independent single-fiber isolations and experimental replicates. Statistical significance was evaluated by Student's *t*-test ($^*p < 0.05$) (n 24 h control = 56 SCs, n 24 h metf = 54 SCs, n 48 h control = 68 SCs, and n 48 h metf = 52 SCs).

we isolated SCs and treated them *in vitro* for 24 h with 2 mM metformin. Following treatment, oxygen consumption was measured with a Seahorse instrument after sequential drug treatment. As shown in Figure 9(a), metformin negatively affects the SC mitochondrial respiratory flux and decreases both basal respiration (Figure 9(b)) and maximal respiration (Figure 9(c)).

A decrease in basal respiration could be caused either by a reduction in the number of mitochondria or by a decline in the activity of the respiratory chain. To distinguish between the two alternatives, we measured the levels of the mitochondrial structural protein Tom20. As shown in Figure 9(f), the levels of Tom20 do not significantly decrease after metformin treatment, confirming that

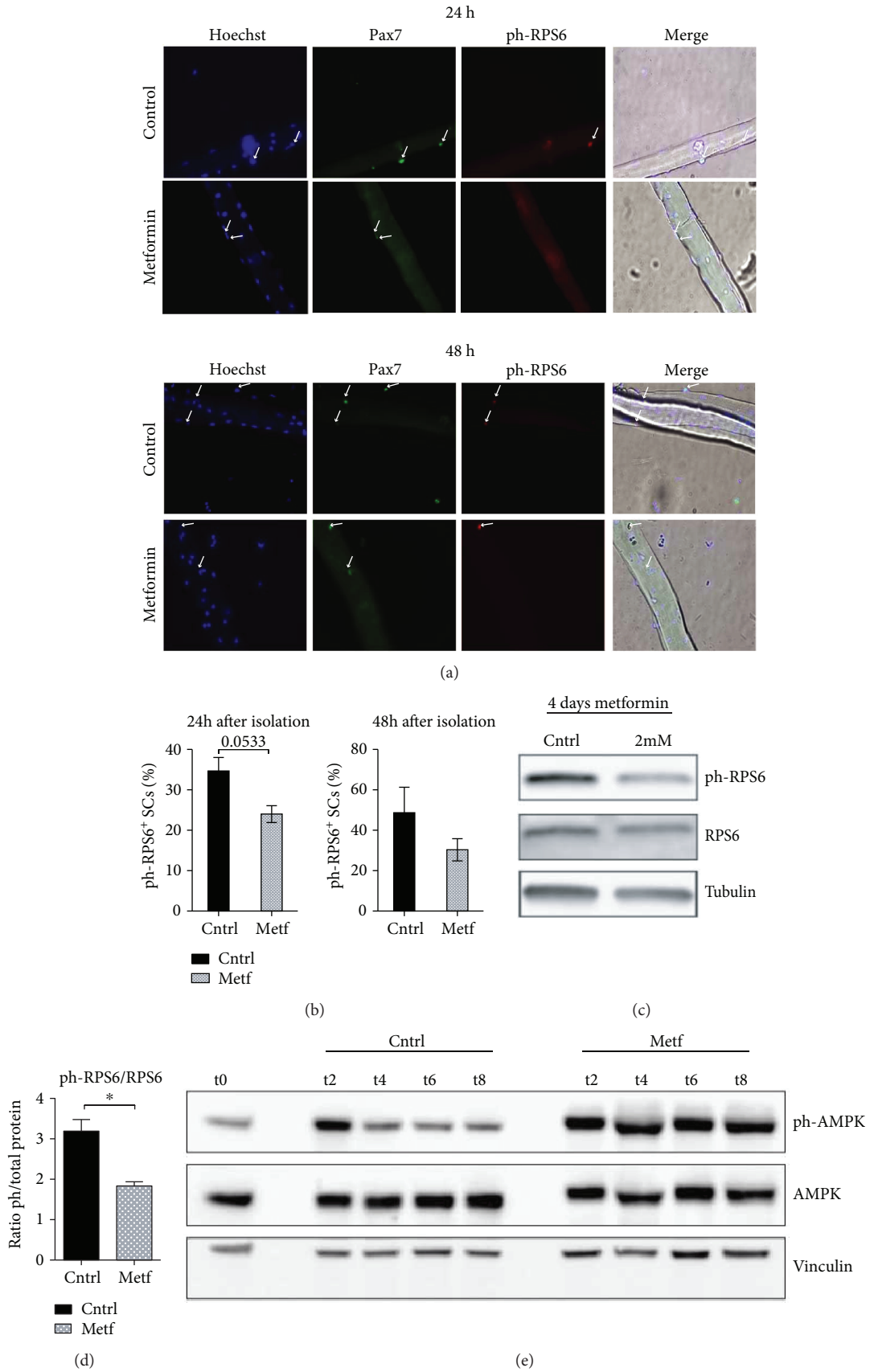

Figure 5: Continued.

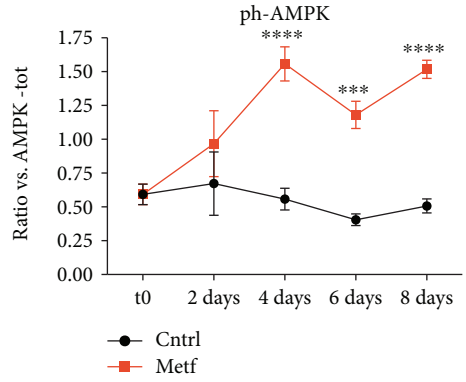

(f)

Figure 5: Metformin negatively modulates the phosphorylation of RPS6 in SCs. (a) Single myofibers were isolated from C57BL/6 mice and treated *in vitro* with 2 mM metformin. The SCs associated with the myofibers were analyzed by immunofluorescence microscopy for the expression of Pax7 and p-RPS6 after 24 h and 48 h of culture. (b) The percentage of SCs that are positive for p-RPS6 after 24 h and 48 h in culture was calculated after three independent single-fiber isolations and experimental replicates. Statistical significance was evaluated by Student's t-test ($^{*}p < 0.05$) (number of counted SCs in each sample: 24 h control = 86, 24 h metf = 82, 48 h control = 72, and 48 h metf = 69). (c) Isolated SCs were treated *in vitro* for 4 days with 2 mM metformin, and protein extracts were analyzed by SDS-PAGE for the expression of ph-RPS6 and total RPS6 protein. Tubulin was used as a loading control. (d) Quantitation graph of ph-RPS6 to total RPS6 protein levels monitored by western blot in three independent cell isolations and biological replicates ($n = 3$). Statistical significance was evaluated by Student's t-test ($^{*}p < 0.05$). (e) Western blot analysis for the expression of ph-AMPK and total AMPK protein of control and metformin-treated SCs after 2, 4, 6, and 8 days of treatment (t2, t4, t6, and t8, respectively). Vinculin was used as a loading control. (f) Quantitation graph of ratio ph-AMPK/total AMPK monitored by western blot in four independent cell isolations and biological replicates ($n = 4$). Statistical significance was evaluated by the ANOVA test ($^{****}p < 0.0001$).

metformin affects the efficiency of the respiratory chain. On the contrary, at day 8, the protein levels of Tom20 significantly increase in the metformin-treated samples, which is in accord with the belated differentiation of metformin-treated SCs since it is known that myogenic differentiation is followed by a switch to oxidative phosphorylation metabolism [29, 30].

3.9. Metformin-Treated SCs Are Transcriptionally Quieter and Smaller in Size. We finally asked whether metformin treatment affects the proliferation potential and metabolic activation of isolated SCs. SCs, isolated from C57BL/6 mice and treated *in vitro* with 2 mM metformin immediately after isolation, fail to attach to the gelatin-coated culture dish even after 4 days, whereas most control SCs adhere to the plastic dish and start proliferating (Figure S3). Analysis of apoptosis with annexin V/propidium iodide (PI) double staining revealed a small, nonsignificant increase of early apoptotic cells in these SCs treated with metformin (Figures 10(a) and 10(b)). In addition, SCs treated with metformin immediately upon isolation for 48 h are smaller in size compared to the untreated control (Figure 10(c)) and display reduced levels of pyronin Y staining (Figure 10(d)). Pyronin Y is an RNA intercalator and is used here as a measure of RNA content. This staining protocol allows distinguishing quiescent cells (with low RNA levels) from activated cells in G1 which are characterized by higher RNA levels [31].

The above results show that metformin-treated SCs are small quiescent cells characterized by a reduced transcriptional activity and a limited potential to grow as adherent cells compared to the untreated counterparts. These observations are consistent with a model implying a delay in SC exit from quiescence following treatment with metformin.

4. Discussion

In the unperturbed adult muscle, SCs are mitotically quiescent. Maintenance of quiescence and the ability to regain quiescence after activation are essential for the long-term homeostasis of the stem cell pool [32, 33]. The balance between cell quiescence, differentiation, and renewal is one of the most important factors for efficient regeneration after tissue damage and aging or in disease.

Aged SCs fail to maintain quiescence, and once activated, commitment to the myogenic lineage is favored at the expense of self-renewal [34]. Along the same lines, one of the pathological features of Duchenne muscular dystrophy is the depletion of the SC pool induced by repeated cycles of degeneration-regeneration [35–37]. Understanding and learning to control the mechanisms involved in the establishment and maintenance of SC quiescence remain an issue of interest. The SC state is influenced by a variety of intrinsic and extrinsic factors, with the microenvironment and the stem cell niche having unique and indispensable roles.

Recent studies have highlighted the role of metabolism in SC activation and function. SC number, differentiation potential, and functional engraftment efficiency are increased following calorie restriction in either the donor or the recipient mice [13]. Furthermore, SCs derived from mTOR-knockout mice exhibit defective proliferation and differentiation kinetics and express lower levels of Pax7, Myf5, MyoD, and myogenin [38]. Recently, Haller et al.

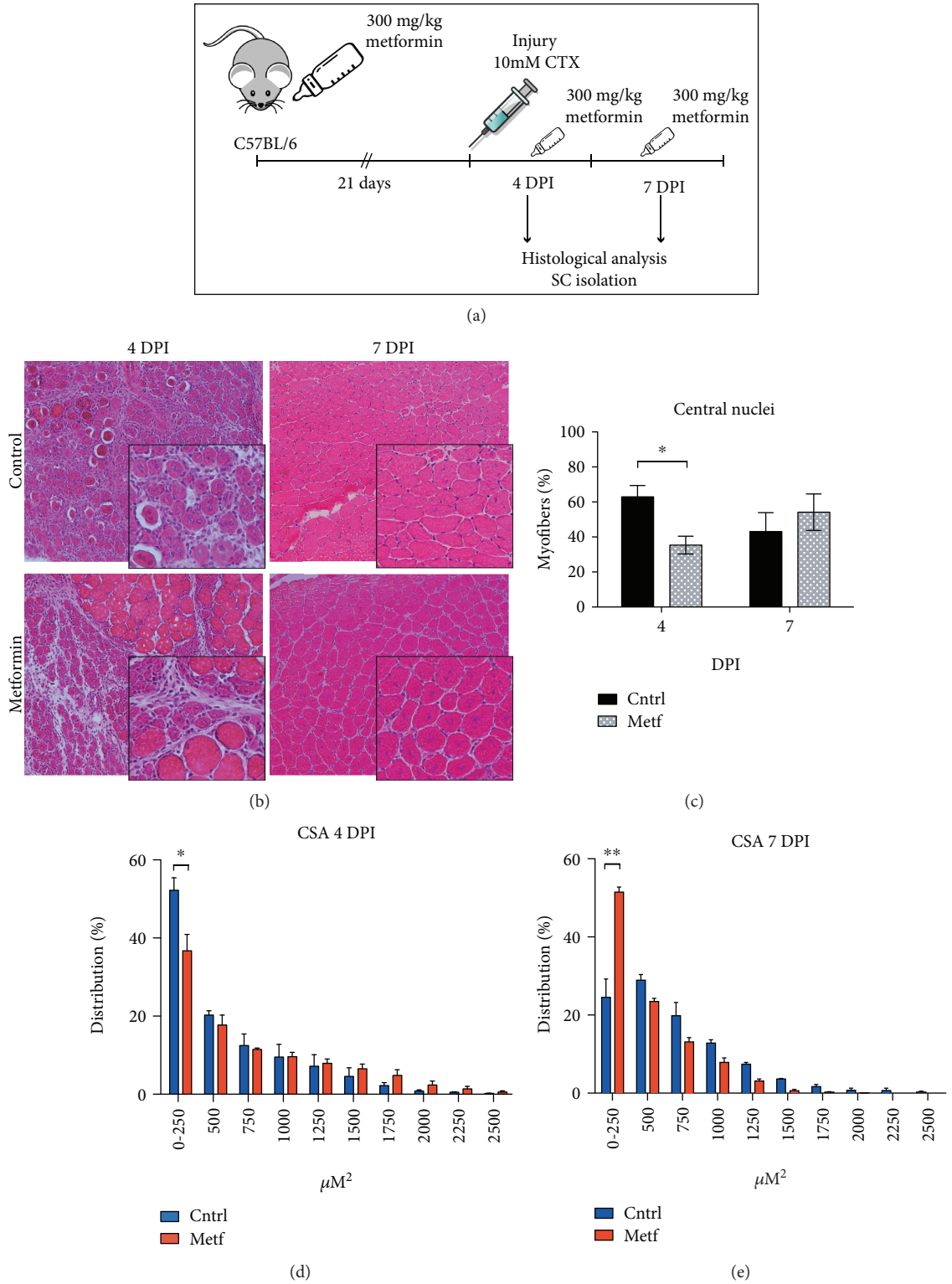

Figure 6: Metformin delays skeletal muscle regeneration *in vivo*. (a) Experimental design of the in vivo administration of metformin to cardiotoxin- (CTX-) injured C57BL/6 mice. (b) Representative images of H&E staining on TA muscle sections of control and metformin-treated mice at 4 and 7 days of post-cardiotoxin (CTX) injury (DPI). (c) Quantitation of the centrally located myonuclei was performed on TA muscle sections upon H&E staining of control and metformin samples. The percentage of centronucleated myofibers is reported as the total number of centronucleated myofibers to the total number of myofibers in the damaged muscle area. Statistical significance was evaluated by the ANOVA test ($^{*}p < 0.05$) (n control = 3 mice, n metformin = 3 mice). (d) Cross-sectional area (CSA) distribution of myofibers in the control and metformin-treated mice 4 days after CTX injury (n control = 3 mice, ($^{*}p < 0.05$). (e) Cross-sectional area (CSA) distribution of myofibers in the control and metformin-treated mice 7 days after CTX injury (n metformin = 3 mice, $^{**}p < 0.01$).

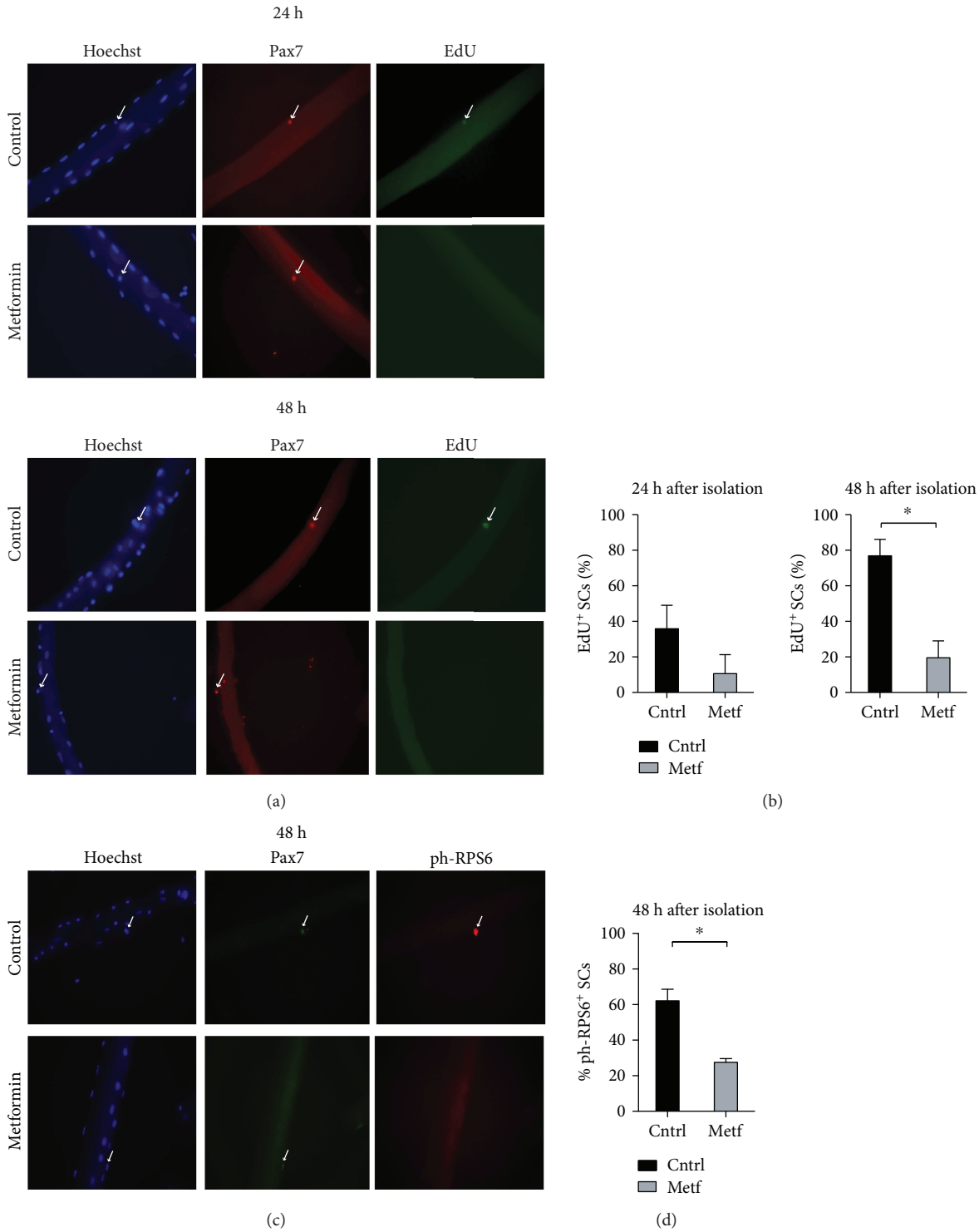

Figure 7: Metformin delays SC activation upon administration *in vivo*. (a) Single myofibers were isolated from control and metformin-treated C57BL/6 mice and cultured *in vitro* in Tyrode's medium containing an EdU labeling agent. The SCs associated with the myofibers were analyzed by immunofluorescence microscopy for the expression of Pax7 and the incorporation of EdU after 24 h and 48 h of culture. (b) Percentage of EdU-positive SCs associated with single myofibers isolated from control and metformin-treated C57BL/6 mice. The SCs associated with the myofibers were analyzed by immunofluorescence microscopy for the expression of Pax7 and the incorporation of EdU after 24 h and 48 h of culture (n24h cntrl = 48 SCs, n24h metf = 40 SCs, n48h cntrl = 40 SCs, and n48h metf = 36 SCs). (c) Single myofibers were isolated from control and metformin-treated C57BL/6 mice and cultured *in vitro*. The SCs associated with the myofibers were analyzed by immunofluorescence microscopy for the expression of Pax7 and ph-RPS6 after 48 h of culture. (d) Quantitation of the percentage of myofibers associated SCs positive for ph-RPS6 after 48 h in culture. Myofibers were isolated from control and metformin-conditioned C57BL/6 mice (n48h cntrl = 42 SCs, n48h metf = 40 SCs).

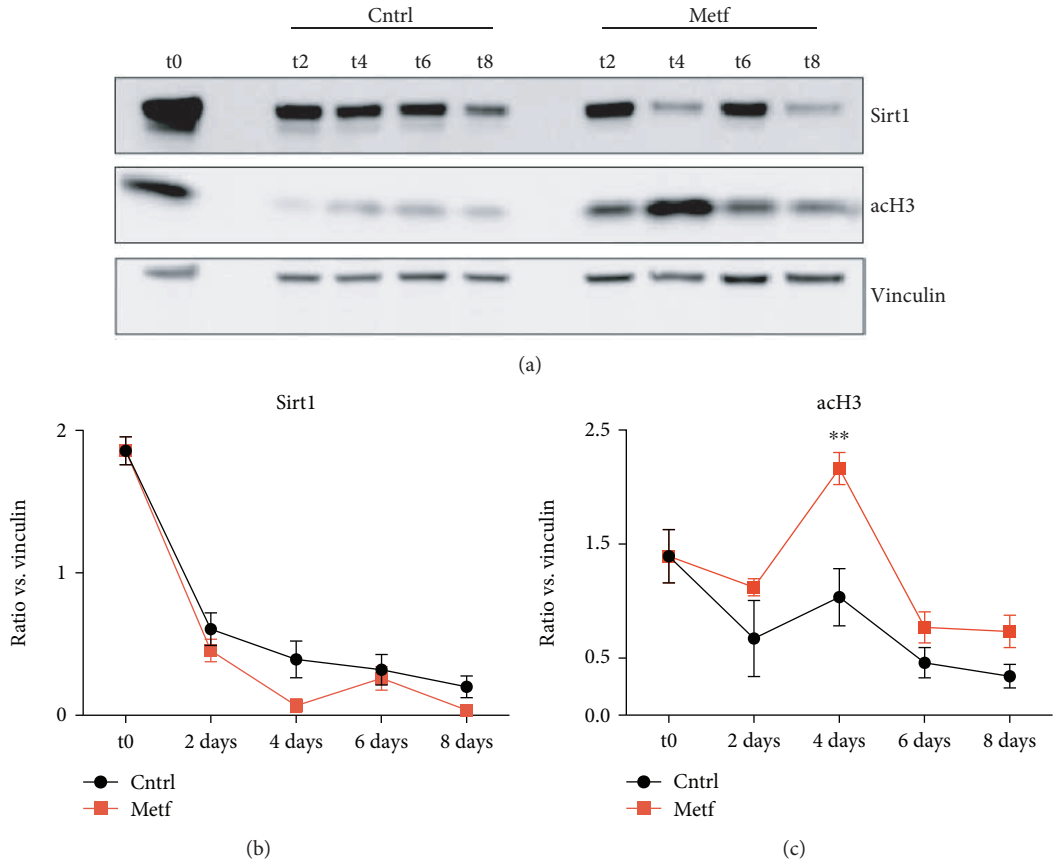

FIGURE 8: Sirt1 levels in metformin-treated SCs. (a) Western blot analysis for the expression of Sirt1 and acH3 in control and metformin-treated SCs after 2, 4, 6, and 8 days of treatment (t2, t4, t6, and t8, respectively). Vinculin was used as a loading control. (b) Quantitation graph of Sirt1 protein levels monitored by western blot in four independent cell isolations and biological replicates ($n = 4$). Statistical significance was evaluated by the ANOVA test ($^*p < 0.05$). (c) Quantitation graph of acH3 protein levels monitored by western blot in four independent cell isolations and biological replicates ($n = 4$). Statistical significance was evaluated by the ANOVA test ($^*p < 0.05$).

have reported the transient activation of mTOR signaling in different cell types during tissue regeneration [39]. However, after repeated regeneration cycles, mTOR signaling has an inhibitory role on stem cell maintenance. It was proposed that pharmacological inhibition of mTOR by rapamycin is sufficient for stem cell pool maintenance in different tissues, including muscle stem cells.

Building on these studies, we investigated the effect of metformin, a calorie restriction mimicking drug that inhibits the mTOR pathway, on the activation, proliferation, and differentiation of SCs. In the previous study, we have demonstrated that metformin inhibits C2C12 myogenic differentiation, by preventing irreversible cell cycle exit and reducing MyoD and p21cip1 levels [12]. Our current study extends the effect of the drug on primary SCs *in vitro*, ex vivo, and *in vivo*. In particular, our results show that isolated SCs, treated *in vitro* with 2 mM metformin, retain the expression of Pax7 for a longer time compared to controls. The expression of Pax7 is accompanied by a prolonged phase of BrdU incorporation, which indicates that metformin belates the final differentiation.

The delayed Pax7 downregulation is accompanied by a belated expression of myogenic differentiation markers (myogenin and MyHC) and by a reduced fusion index. However, myogenin levels were significantly lower only at day 2 in the metformin-treated samples.

Since Pax7 promotes progenitor commitment to the muscle lineage, we hypothesized that metformin delays the process of SC progenitor activation and entry into the cell cycle. In order to gain further insight into the molecular underpinnings of the role of metformin in SC activation, we isolated individual myofibers from C57BL/6 mice and treated them *ex vivo* with 2 mM metformin. The SCs associated with metformin-treated myofibers exhibit reduced EdU incorporation after 24 h and 48 h of culture when compared to controls. This low propensity to proliferate is matched by a decreased ribosome protein S6 (RPS6) phosphorylation. Likewise, the reduction in the level of phospho-RPS6 is observed also in isolated SCs that were cultured and treated with 2 mM metformin for 4 days *in vitro*. RPS6 is a downstream target of mTOR, which is inhibited by the metformin-activated AMPK. Thus, metformin hinders translation by inhibiting the mTOR/P70S6K, RPS6, and 4E-BP1 axis.

We extended these observations *in vivo*, by studying the regeneration of skeletal muscle and the activation of

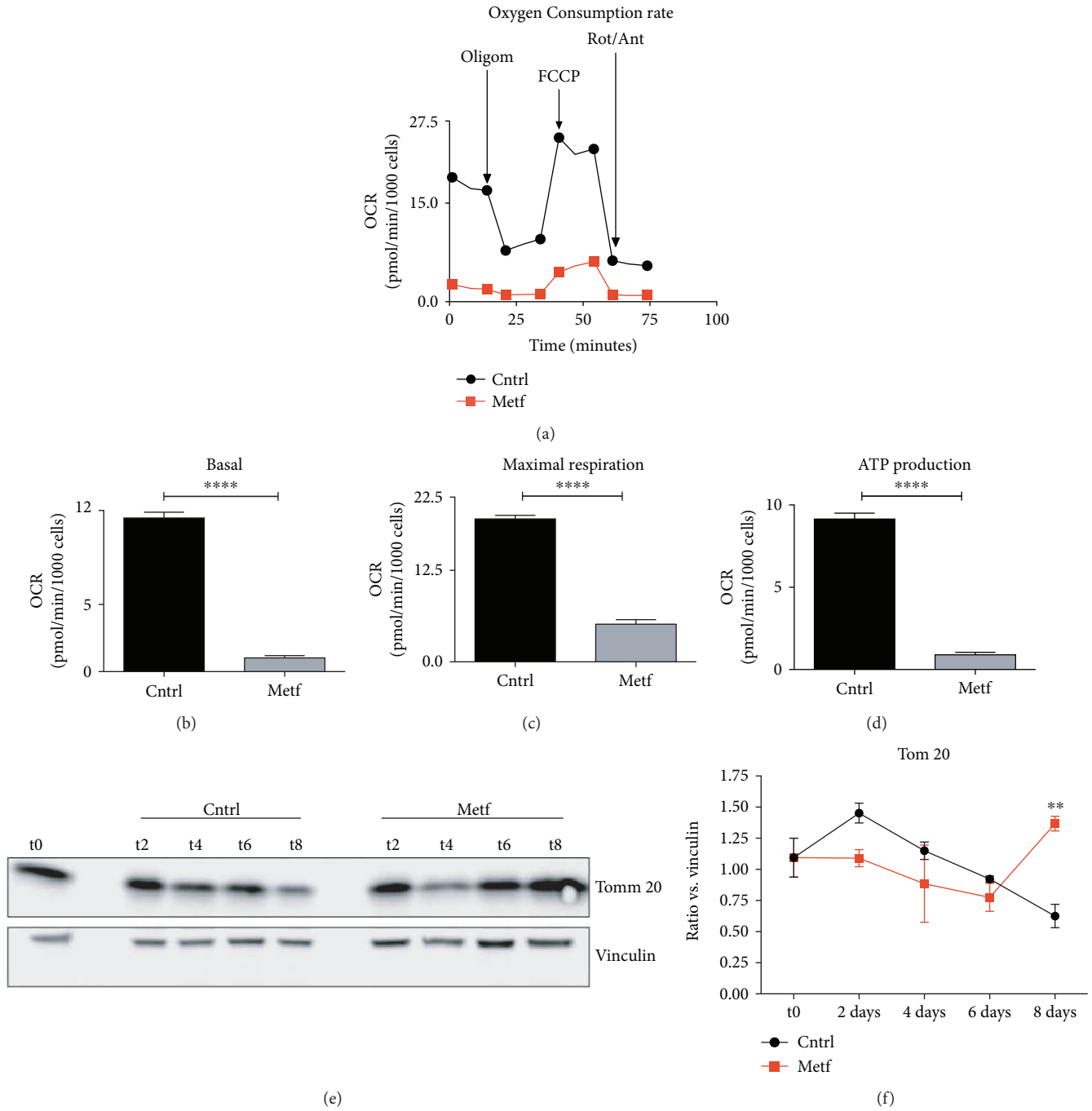

FIGURE 9: Metformin inhibits mitochondrial respiration in SCs. (a) Oxygen consumption rate (OCR) of the Mito Stress Test conducted with a Seahorse Extracellular Flux Analyzer. OCR is expressed in pmol of O_2 consumed per minute, normalized over the number of cells in the assay well. Oligomycin (Oligom.), FCCP, and rotenone/antimycin (Rot/Ant) were sequentially added to the well to perturb the electron transport chain machinery. (b–d) Bar plot graphs of mitochondrial functional parameters: (b) basal respiration is the delta between the basal OCR and the lowest plateau reached upon Rot/Ant injection, (c) maximal respiration is inferred as the delta between Rot/Ant and FCCP maximal plateau, and (d) ATP production is referred to as the delta between the basal and the oligomycin injection. Statistical analysis was performed through Student's t-test ($^{****}p < 0.0001$, $n = 4$). (e) Western blot analysis of Tom20 protein levels in control and metformin-treated SCs after 2, 4, 6, and 8 days of treatment (t2, t4, t6, and t8, respectively). Vinculin was used as a loading control. (f) Quantitation graph of Tom20 protein levels monitored by western blot in four independent cell isolations and biological replicates ($n = 4$). Statistical significance was evaluated by the ANOVA test ($^{**}p < 0.01$).

SCs upon muscle injury. After metformin administration, mice were subjected to muscle damage by CTX and the regeneration process was monitored by measuring the number of centronucleated myofibers and myofiber cross-sectional area (CSA) at 4 and 7 days of postinjury. The percentage of centronucleated myofibers in the

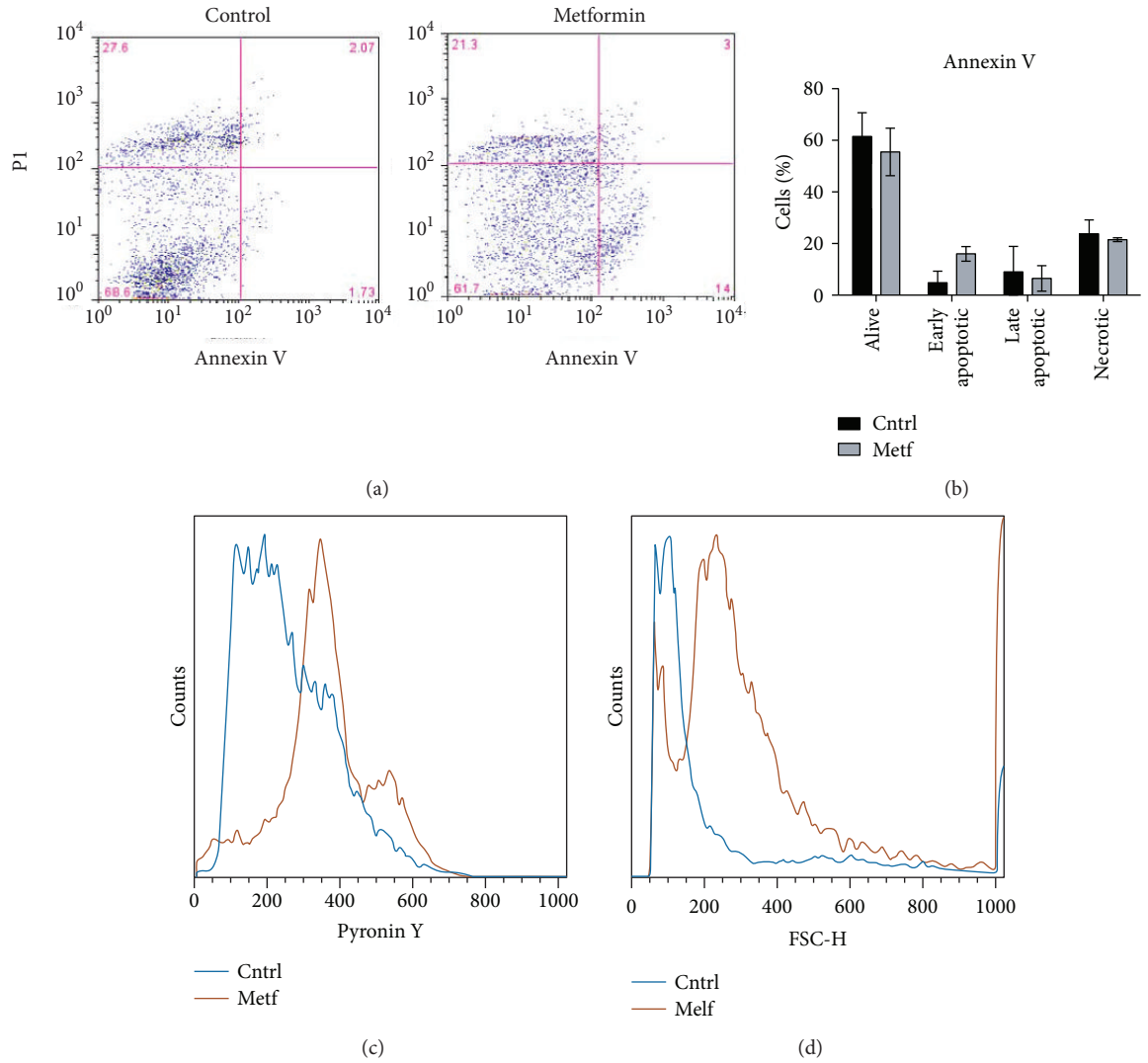

Figure 10: *In vitro* metformin-treated SCs retain stem cell characteristics. (a) Dot plot of flow cytometric analysis of apoptotic cells after metformin treatment *in vitro*. Cell populations: alive cells (annexin V negative, PI negative), early apoptotic cells (annexin V positive, PI negative), late apoptotic cells (annexin V positive, PI positive), and necrotic cells (annexin V negative, PI positive). The position of the quadrant lines was stabilized based on the distinguishing cell populations. (b) Quantitation of the percentages of alive, early apoptotic, late apoptotic, and necrotic cells (n experimental replicates = 2). (c) Representative histogram of the forward scattering (FSC) parameter by FACS analysis in control and metformin-treated SCs. (d) Representative histogram of pyronin Y FACS analysis in control and metformin-treated SCs.

metformin-treated mice is lower than that in the control at 4 days after injury. Moreover, at 7 days of postinjury, control myofibers show a larger cross-sectional area (500 ha^2) than the metformin-conditioned mice that still retain more myofibers with a CSA around 250 co^2. These data suggest that metformin-treated mice are still fully regenerating 7 days after injury. Furthermore, SCs isolated from metformin-conditioned mice differentiate and fuse into myotubes later compared to controls *in vitro*. This is consistent with the hypothesis that metformin delays skeletal muscle regeneration *in vivo*.

We additionally isolated individual myofibers from C57BL/6 mice treated with metformin for 21 days and cultured them *in vitro*, in EdU-containing medium. We observed a reduced percentage of proliferating SCs (i.e., positive for EdU). A similar result was also obtained when myofibers were treated with metformin *in vitro*. Notably, this nonproliferating phenotype is accompanied by a reduction in the percentage of ph-RPS6-positive SCs.

To further gain an insight into the mechanisms by which metformin disturbs SC metabolism, resulting in their activation and proliferation, we focused on the expression of Sirt1. Sirt1 is one of the most important class III histone deacetylases that has been proposed to play a crucial role as a metabolic regulator in different cell types. Specifically in muscle, Ryall et al. have demonstrated that upon activation SC switch to glycolysis, intracellular NAD^+ levels are decreased and subsequently the activity of Sirt1 is inhibited [40]. As a result, H4K16 acetylation increases and the transcription of the myogenic genes begins. On the other hand, Tang and Rando

proposed that SC exit from quiescence necessitates an increase in autophagic flux which is mediated by Sirt1 [10]. In our conditions, we observed that Sirt1 levels remain unaffected upon metformin treatment and this result allows us to conclude that metformin's effects on SCs are not mediated by Sirt1.

On the other hand, after analysis of the SC mitochondrial respiration, we noted a significant impairment of oxidative phosphorylation in the metformin-treated samples. By further analyzing the levels of Tom20 protein, a mitochondrial structure marker, we observed that metformin does not significantly impact Tom20 levels, suggesting that the drug affects the efficiency of the respiratory chain. However, Tom20 levels significantly increase at day 8 in the metformin-treated SCs, which is in accordance with the fact that metformin delays SC differentiation.

Ultralow attachment culture dishes allow formation of myospheres [41] from muscle-derived cells by providing a niche-like environment and by helping maintain a more primitive cell state [42]. Given that metformin delays the activation of SCs associated with individual myofibers, we extended our observations by treating SCs with metformin immediately after isolation in order to check their stem cell characteristics. Interestingly, different from control cells, metformin-treated cells do not attach to the gelatin-coated cultured dishes and remain alive in suspension. The nonadherent metformin-treated SCs do not show significant signs of apoptosis and appear to be smaller and transcriptionally quieter than the control.

Our results suggest that metformin delays SC activation by preserving them in a less active metabolic state. As a result, metformin-treated SCs are delayed in their differentiation *in vitro*. Consistently, the process of muscle regeneration after cardiotoxin injury *in vivo* is also delayed.

The importance of nutrient availability and metabolism in the process of differentiation has been highlighted by different studies. Our data are in accordance with the work of Rodgers et al. [11] which reports that mTOR activity is necessary and sufficient for the transition of SCs from a quiescent G_0 phase into a quiescent, more stress responsive, G_{Alert} phase. This intermediate G_{Alert} state allows SCs to perform their first division faster than SCs in the G_0 state. G_{Alert} is associated with activated mTOR and RPS6 signaling, which are negatively modulated by metformin. In addition, our results strengthen the notion that quiescent SCs have a low metabolic rate and support the view that their activation and entry into the cell cycle can be manipulated by interfering with their metabolism [43]. Finally, our results are in accord with mTOR being responsible for the activation of different somatic stem cell populations and support the exploration of its pharmacological perturbation as a useful tool for stem cell maintenance [39].

One of the current goals in the field of skeletal muscle biology is to understand the etiology of SC exhaustion during aging and improve muscle function by targeting the rejuvenation of the old SC population. Both intrinsic and extrinsic factors of the SC environment seem to be involved in aged SC loss of function, such as increased DNA damage, epigenetic modifications, or altered metabolic signaling [44]. In 2013, Sandri et al. [45] demonstrated an increased phosphorylation of RPS6 and activation of mTOR signaling in aged mice, in accord with the findings of Cerletti et al. [13] that AMPK activation by a low-calorie diet improves the activity of SCs in the muscles of old mice. Other studies have focused on the pharmacological inhibition of p38 MAPK [46], silencing of the p16 cell cycle regulator [47], or augmentation of the autophagic flux [48] as different approaches for the rejuvenation of the geriatric muscle. In this context, our study suggests that the metabolic perturbation induced by metformin, by forcing SCs into a low metabolic state, sustains their persistence in a quiescent state. These findings highlight a possible use of metformin as a pharmacological intervention for muscle stem cell maintenance during the repeated regeneration cycles in disease [49, 50] or in aging, when chronic activation of mTOR signaling occurs [51, 52].

Data Availability

The data used to support the findings of this study are available from the corresponding author upon request.

Conflicts of Interest

The authors have no conflict of interest to declare.

Acknowledgments

This work was supported by the DEPTH project of the European Research Council (grant agreement 322749) to GC.

Supplementary Materials

Supplementary 1. Figure S1: Pax7 and MyoD protein levels, monitored by western blot, are not affected by metformin. (a) SCs treated upon attachment with 2 mM metformin were analyzed for the expression of Pax7 and MyoD by western blot after 2, 4, 6, and 8 days of treatment (t2, t4, t6, and t8, respectively). Vinculin was used as a loading control. (b) Quantitation graphs of Pax7 and MyoD protein levels monitored by western blot in four independent cell isolations and biological replicates ($n = 4$). Statistical significance was evaluated by the ANOVA test ($^*p < 0.05$).

Supplementary 2. Figure S2: metformin delays SC differentiation in mice after CTX muscle injury. (a) SCs isolated from control and metformin-treated mice 1, 2, 4, and 7 days after CTX treatment were cultured *in vitro* and examined for their myogenic differentiation potential 2 days after attachment by immunofluorescence analysis. The expression of MyHC was used as a differentiation marker. (b) The fusion index was calculated as the % ratio of the nuclei inside the myotubes to the total number of *nuclei*. Statistical significance was evaluated by Student's t-test ($^*p < 0.05$).

Supplementary 3. Figure S3: metformin-treated SCs do not attach on gelatin-coated plates. (a) Representative bright-field images of SCs treated with 2 mM metformin immediately after isolation. SCs were isolated from C57BL/6 mice and incubated on a gelatin-coated culture dish for 4 days.

References

[1] H. Yin, F. Price, and M. A. Rudnicki, "Satellite cells and the muscle stem cell niche," *Physiological Reviews*, vol. 93, no. 1, pp. 23–67, 2013.

[2] A. MAURO, "Satellite cell of skeletal muscle fibers," *The Journal of Biophysical and Biochemical Cytology*, vol. 9, no. 2, pp. 493–495, 1961.

[3] Y. X. Wang and M. A. Rudnicki, "Satellite cells, the engines of muscle repair," *Nature Reviews Molecular Cell Biology*, vol. 13, no. 2, pp. 127–133, 2012.

[4] J. V. Chakkalakal, K. M. Jones, M. A. Basson, and A. S. Brack, "The aged niche disrupts muscle stem cell quiescence," *Nature*, vol. 490, no. 7420, pp. 355–360, 2012.

[5] F. Rahimov and L. M. Kunkel, "The cell biology of disease: cellular and molecular mechanisms underlying muscular dystrophy," *The Journal of Cell Biology*, vol. 201, no. 4, pp. 499–510, 2013.

[6] C. D. L. Folmes, P. P. Dzeja, T. J. Nelson, and A. Terzic, "Metabolic plasticity in stem cell homeostasis and differentiation," *Cell Stem Cell*, vol. 11, no. 5, pp. 596–606, 2012.

[7] J. R. Valcourt, J. M. S. Lemons, E. M. Haley, M. Kojima, O. O. Demuren, and H. A. Coller, "Staying alive: metabolic adaptations to quiescence," *Cell Cycle*, vol. 11, no. 9, pp. 1680–1696, 2012.

[8] P. Hsu and C.-K. Qu, "Metabolic plasticity and hematopoietic stem cell biology," *Current Opinion in Hematology*, vol. 20, no. 4, pp. 289–294, 2013.

[9] S. Y. Lunt and M. G. Vander Heiden, "Aerobic glycolysis: meeting the metabolic requirements of cell proliferation," *Annual Review of Cell and Developmental Biology*, vol. 27, no. 1, pp. 441–464, 2011.

[10] A. H. Tang and T. A. Rando, "Induction of autophagy supports the bioenergetic demands of quiescent muscle stem cell activation," *The EMBO Journal*, vol. 33, no. 23, pp. 2782–2797, 2014.

[11] J. T. Rodgers, K. Y. King, J. O. Brett et al., "mTORC1 controls the adaptive transition of quiescent stem cells from G_0 to G_{Alert}," *Nature*, vol. 510, no. 7505, pp. 393–396, 2014.

[12] T. Pavlidou, M. Rosina, C. Fuoco et al., "Regulation of myoblast differentiation by metabolic perturbations induced by metformin," *PLoS One*, vol. 12, no. 8, article e0182475, 2017.

[13] M. Cerletti, Y. C. Jang, L. W. S. Finley, M. C. Haigis, and A. J. Wagers, "Short-term calorie restriction enhances skeletal muscle stem cell function," *Cell Stem Cell*, vol. 10, no. 5, pp. 515–519, 2012.

[14] V. Ljubicic, S. Khogali, J.-M. Renaud, and B. J. Jasmin, "Chronic AMPK stimulation attenuates adaptive signaling in dystrophic skeletal muscle," *American Journal of Physiology-Cell Physiology*, vol. 302, no. 1, pp. C110–C121, 2012.

[15] V. E. Jahnke, J. H. van der Meulen, H. K. Johnston et al., "Metabolic remodeling agents show beneficial effects in the dystrophin-deficient mdx mouse model," *Skeletal Muscle*, vol. 2, no. 1, p. 16, 2012.

[16] V. Ljubicic, M. Burt, J. A. Lunde, and B. J. Jasmin, "Resveratrol induces expression of the slow, oxidative phenotype in mdx mouse muscle together with enhanced activity of the SIRT1-PGC-1α axis," *American Journal of Physiology-Cell Physiology*, vol. 307, no. 1, pp. C66–C82, 2014.

[17] B. S. Gordon, D. C. Delgado Díaz, and M. C. Kostek, "Resveratrol decreases inflammation and increases utrophin gene expression in the mdx mouse model of Duchenne muscular dystrophy," *Clinical Nutrition*, vol. 32, no. 1, pp. 104–111, 2013.

[18] B. Viollet, B. Guigas, N. S. Garcia, J. Leclerc, M. Foretz, and F. Andreelli, "Cellular and molecular mechanisms of metformin: an overview," *Clinical Science*, vol. 122, no. 6, pp. 253–270, 2012.

[19] M. R. Owen, E. Doran, and A. P. Halestrap, "Evidence that metformin exerts its anti-diabetic effects through inhibition of complex 1 of the mitochondrial respiratory chain," *The Biochemical Journal*, vol. 348, no. 3, pp. 607–614, 2000.

[20] G. Zhou, R. Myers, Y. Li et al., "Role of AMP-activated protein kinase in mechanism of metformin action," *The Journal of Clinical Investigation*, vol. 108, no. 8, pp. 1167–1174, 2001.

[21] D. G. Hardie, "AMP-activated protein kinase: an energy sensor that regulates all aspects of cell function," *Genes & Development*, vol. 25, no. 18, pp. 1895–1908, 2011.

[22] R. J. O. Dowling, M. Zakikhani, I. G. Fantus, M. Pollak, and N. Sonenberg, "Metformin inhibits mammalian target of rapamycin-dependent translation initiation in breast cancer cells," *Cancer Research*, vol. 67, no. 22, pp. 10804–10812, 2007.

[23] F. Sacco, A. Silvestri, D. Posca et al., "Deep proteomics of breast cancer cells reveals that metformin rewires signaling networks away from a pro-growth state," *Cell Systems*, vol. 2, no. 3, pp. 159–171, 2016.

[24] F. Langone, S. Cannata, C. Fuoco et al., "Metformin protects skeletal muscle from cardiotoxin induced degeneration," *PLoS One*, vol. 9, no. 12, article e114018, 2014.

[25] V. Ljubicic and B. J. Jasmin, "Metformin increases peroxisome proliferator-activated receptor γ co-activator-1α and utrophin A expression in dystrophic skeletal muscle," *Muscle & Nerve*, vol. 52, no. 1, pp. 139–142, 2015.

[26] P. Hafner, U. Bonati, D. Rubino et al., "Treatment with L-citrulline and metformin in Duchenne muscular dystrophy: study protocol for a single-centre, randomised, placebo-controlled trial," *Trials*, vol. 17, no. 1, 2016.

[27] P. Hafner, U. Bonati, B. Erne et al., "Improved muscle function in Duchenne muscular dystrophy through L-arginine and metformin: an investigator-initiated, open-label, single-center, proof-of-concept-study," *PLoS One*, vol. 11, no. 1, article e0147634, 2016.

[28] D. D. W. Cornelison and B. J. Wold, "Single-cell analysis of regulatory gene expression in quiescent and activated mouse skeletal muscle satellite cells," *Developmental Biology*, vol. 191, no. 2, pp. 270–283, 1997.

[29] A. Wagatsuma and K. Sakuma, "Mitochondria as a potential regulator of myogenesis," *The Scientific World Journal*, vol. 2013, Article ID 593267, 9 pages, 2013.

[30] C. N. Lyons, S. C. Leary, and C. D. Moyes, "Bioenergetic remodeling during cellular differentiation: changes in cytochrome c oxidase regulation do not affect the metabolic phenotype," *Biochemistry and Cell Biology*, vol. 82, no. 3, pp. 391–399, 2004.

[31] Z. Darzynkiewicz, G. Juan, and E. F. Srour, "Differential staining of DNA and RNA," *Current Protocols in Cytometry*, vol. 30, 2004.

[32] C. R. R. Bjornson, T. H. Cheung, L. Liu, P. V. Tripathi, K. M. Steeper, and T. A. Rando, "Notch signaling is necessary to

maintain quiescence in adult muscle stem cells," *Stem Cells*, vol. 30, no. 2, pp. 232–242, 2012.

[33] P. Mourikis, R. Sambasivan, D. Castel, P. Rocheteau, V. Bizzarro, and S. Tajbakhsh, "A critical requirement for notch signaling in maintenance of the quiescent skeletal muscle stem cell state," *Stem Cells*, vol. 30, no. 2, pp. 243–252, 2012.

[34] A. Bigot, W. J. Duddy, Z. G. Ouandaogo et al., "Age-associated methylation suppresses SPRY1, leading to a failure of re-quiescence and loss of the reserve stem cell pool in elderly muscle," *Cell Reports*, vol. 13, no. 6, pp. 1172–1182, 2015.

[35] H. M. Blau, C. Webster, and G. K. Pavlath, "Defective myoblasts identified in Duchenne muscular dystrophy," *Proceedings of the National Academy of Sciences of the United States of America*, vol. 80, no. 15, pp. 4856–4860, 1983.

[36] H. M. Blau, C. Webster, G. K. Pavlath, and C. P. Chiu, "Evidence for defective myoblasts in Duchenne muscular dystrophy," in *Gene Expression in Muscle*, R. C. Strohman and S. Wolf, Eds., vol. 182 of Advances in Experimental Medicine and Biology, pp. 85–110, 1985.

[37] L. Heslop, J. E. Morgan, and T. A. Partridge, "Evidence for a myogenic stem cell that is exhausted in dystrophic muscle," *Journal of Cell Science*, vol. 113, Part 12, pp. 2299–2308, 2000.

[38] P. Zhang, X. Liang, T. Shan et al., "mTOR is necessary for proper satellite cell activity and skeletal muscle regeneration," *Biochemical and Biophysical Research Communications*, vol. 463, no. 1-2, pp. 102–108, 2015.

[39] S. Haller, S. Kapuria, R. R. Riley et al., "mTORC1 activation during repeated regeneration impairs somatic stem cell maintenance," *Cell Stem Cell*, vol. 21, no. 6, pp. 806–818.e5, 2017.

[40] J. G. Ryall, S. Dell'Orso, A. Derfoul et al., "The NAD^+-dependent SIRT1 deacetylase translates a metabolic switch into regulatory epigenetics in skeletal muscle stem cells," *Cell Stem Cell*, vol. 16, no. 2, pp. 171–183, 2015.

[41] K. A. Westerman, A. Penvose, Z. Yang, P. D. Allen, and C. A. Vacanti, "Adult muscle 'stem' cells can be sustained in culture as free-floating myospheres," *Experimental Cell Research*, vol. 316, no. 12, pp. 1966–1976, 2010.

[42] H. Obokata, K. Kojima, K. Westerman et al., "The potential of stem cells in adult tissues representative of the three germ layers," *Tissue Engineering. Part A*, vol. 17, no. 5-6, pp. 607–615, 2011.

[43] D. Montarras, A. L'honoré, and M. Buckingham, "Lying low but ready for action: the quiescent muscle satellite cell," *The FEBS Journal*, vol. 280, no. 17, pp. 4036–4050, 2013.

[44] E. Bengal, E. Perdiguero, A. L. Serrano, and P. Muñoz-Cánoves, "Rejuvenating stem cells to restore muscle regeneration in aging," *F1000Res*, vol. 6, p. 76, 2017.

[45] M. Sandri, L. Barberi, A. Y. Bijlsma et al., "Signalling pathways regulating muscle mass in ageing skeletal muscle: the role of the IGF1-Akt-mTOR-FoxO pathway," *Biogerontology*, vol. 14, no. 3, pp. 303–323, 2013.

[46] B. D. Cosgrove, P. M. Gilbert, E. Porpiglia et al., "Rejuvenation of the muscle stem cell population restores strength to injured aged muscles," *Nature Medicine*, vol. 20, no. 3, pp. 255–264, 2014.

[47] P. Sousa-Victor, S. Gutarra, L. García-Prat et al., "Geriatric muscle stem cells switch reversible quiescence into senescence," *Nature*, vol. 506, no. 7488, pp. 316–321, 2014.

[48] L. García-Prat, M. Martínez-Vicente, E. Perdiguero et al., "Autophagy maintains stemness by preventing senescence," *Nature*, vol. 529, no. 7584, pp. 37–42, 2016.

[49] C. Webster and H. M. Blau, "Accelerated age-related decline in replicative life-span of Duchenne muscular dystrophy myoblasts: implications for cell and gene therapy," *Somatic Cell and Molecular Genetics*, vol. 16, no. 6, pp. 557–565, 1990.

[50] A. Sacco, F. Mourkioti, R. Tran et al., "Short telomeres and stem cell exhaustion model Duchenne muscular dystrophy in mdx/mTR mice," *Cell*, vol. 143, no. 7, pp. 1059–1071, 2010.

[51] T. Nacarelli, A. Azar, and C. Sell, "Aberrant mTOR activation in senescence and aging: a mitochondrial stress response?," *Experimental Gerontology*, vol. 68, pp. 66–70, 2015.

[52] S. C. Johnson, P. S. Rabinovitch, and M. Kaeberlein, "mTOR is a key modulator of ageing and age-related disease," *Nature*, vol. 493, no. 7432, pp. 338–345, 2013.

Hindawi
Stem Cells International
Volume 2019, Article ID 9757201, 15 pages
https://doi.org/10.1155/2019/9757201

Review Article

Mitochondrial Dynamics: Biogenesis, Fission, Fusion, and Mitophagy in the Regulation of Stem Cell Behaviors

Wenyan Fu,[1,2] Yang Liu,[1,2] and Hang Yin[1,2]

[1]*Center for Molecular Medicine, The University of Georgia, GA 30602, USA*
[2]*Department of Biochemistry and Molecular Biology, The University of Georgia, GA 30602, USA*

Correspondence should be addressed to Hang Yin; hyin@uga.edu

Received 29 December 2018; Accepted 5 March 2019; Published 7 April 2019

Guest Editor: Viviana Moresi

Stem cells have the unique capacity to differentiate into many cell types during embryonic development and postnatal growth. Through coordinated cellular behaviors (self-renewal, proliferation, and differentiation), stem cells are also pivotal to the homeostasis, repair, and regeneration of many adult tissues/organs and thus of great importance in regenerative medicine. Emerging evidence indicates that mitochondria are actively involved in the regulation of stem cell behaviors. Mitochondria undergo specific dynamics (biogenesis, fission, fusion, and mitophagy) during stem cell self-renewal, proliferation, and differentiation. The alteration of mitochondrial dynamics, fine-tuned by stem cell niche factors and stress signaling, has considerable impacts on stem cell behaviors. Here, we summarize the recent research progress on (1) how mitochondrial dynamics controls stem cell behaviors, (2) intrinsic and extrinsic factors that regulate mitochondrial dynamics, and (3) pharmacological regulators of mitochondrial dynamics and their therapeutic potential. This review emphasizes the metabolic control of stemness and differentiation and may shed light on potential new applications in stem cell-based therapy.

1. Introduction

Embryonic stem cells (ESCs) have the pluripotent potential to generate all adult cell types. Adult stem cells instead are multipotent or unipotent and only give rise to limited numbers of cell types. By definition, stem cells must reproduce themselves, a process called self-renewal. Stem cell self-renewal is of great importance to the long-term maintenance of stem cell populations and the transient expansion of stem cells during development and tissue regeneration. Stem cell can self-renew through asymmetrical or symmetrical cell divisions. Through asymmetric cell division, a stem cell gives rise to a daughter stem cell and a daughter progenitor cell. The latter usually has limited lineage potential or progresses closer to the terminal differentiation. Progenitor cells can further differentiate into mature cell types, but by definition, progenitor cells lose their long-term self-renewing potential. Under the homeostatic condition, stem cells keep a delicate balance between self-renewal and differentiation through various intrinsic and extrinsic mechanisms [1]. Defects in stem cell self-renewal lead to their depletion and senescence, eventually result in developmental defects, failed tissue homeostasis, impaired tissue regeneration, and cancer [2, 3].

Differentiated somatic cells can be reprogrammed to induced pluripotent stem cells (iPSCs) by modulating specific transcription factors and/or signaling pathways. The ability to reprogram patient-specific cells into iPSCs offers therapeutic strategies in regenerative medicine for many congenital and acquired human diseases. iPSCs possess many characteristics similar to ESCs and adult stem cells, indicative of conserved mechanisms in regulating stem cell behaviors. Elucidating mechanisms that control stem cell behaviors have great significance in adult stem cell/iPSC-based regenerative medicine.

Mitochondria are the powerhouse of cells. Besides energy generation, mitochondria also participate in calcium signaling, redox homeostasis, differentiation, proliferation, and apoptosis. Mitochondria are quite dynamic organelles—they continuously undergo biogenesis, fission, fusion, mitophagy, and motility. Mitochondrial dynamics differs in different types of cells and meets the specific functional needs of the

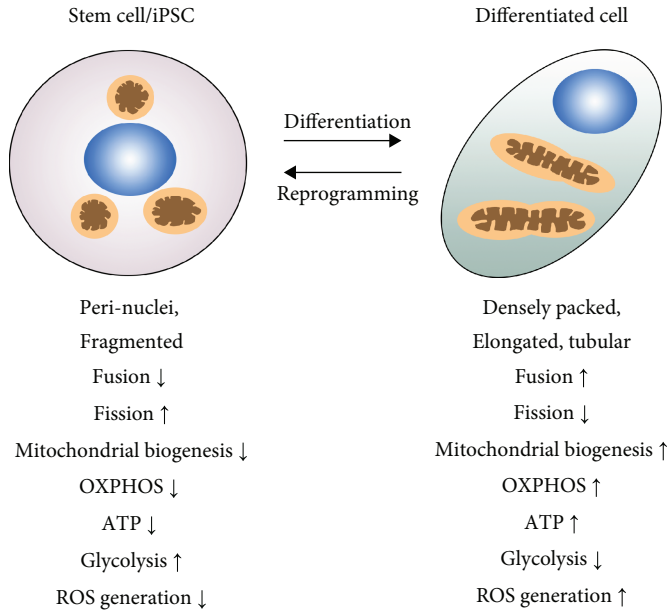

Figure 1: A simplified common scheme of mitochondrial dynamics in stem cells and differentiated cells. In most types of stem cells and reprogrammed iPSCs, mitochondria are usually localized in the nuclear periphery and characterized by sphere, fragmented, and punctate morphologies with fewer cristae (immature morphology). Correspondingly, mito-fission is high whereas mitochondrial biogenesis is low, which maintains low mitochondrial mass. Stem cells generally rely on glycolysis as the major energy source and have low levels of ATP, OXPHOS, and ROS levels. In differentiated cells, mitochondria change to more enlarged and elongated tubular morphology. Correspondingly, mito-fusion and biogenesis increase with the accumulation of mitochondria. Comparably, differentiated cells have higher ATP, ROS, and OXPHOS levels.

cell. Mitochondrial fission (mito-fission) allocates mitochondrial contents during cell division, generates heterogeneity, and aids in eradicating damaged mitochondria. Mitochondrial fusion (mito-fusion) enables mitochondrial content exchange and calcium and ROS buffering, promoting overall mitochondrial function. Coordinated biogenesis and mitophagy ensure sustainable mitochondrial functions. Overall, mitochondrial dynamics assists cells in meeting the needs for cellular energy during proliferation, differentiation, and apoptosis. In stem cells, the dynamics of mitochondria tightly connects to stem cell behaviors. Disrupting or modulating mitochondrial dynamics can have profound impacts on stem cell behaviors. Addressing how stem cell behaviors interplay with mitochondrial dynamics sheds light on the fascinating stem cell biology and also holds a promise to improve clinical applications of stem cells for regenerative medicine.

2. Mitochondrial Dynamics in Stem Cells and Differentiated Cells

Mitochondrial dynamics differs between stem cells and differentiated cells (Figure 1). In stem cells, mitochondria are generally characterized as perinuclear-localized, in sphere, fragmented, and punctate shapes, and with fewer cristae. It is generally believed that mitochondria in stem cells are in an immature state, in which OXPHOS, ATP, and ROS levels are low. This state of mitochondria matches the overall function of stem cells—in a simplified point of view, stem cells serve to preserve the nuclear genome, epigenome, and mitochondrial genomes for differentiated cells. Thus, an immature state of mitochondria helps stem cells protect against ROS-induced genotoxicity, which would lead to more widespread and disastrous consequences in stem cells than in differentiated cells. Upon differentiation to terminal cell types, mitochondrial content increases, which is concomitant with the change of mitochondrial morphology—the appearance of enlarged, elongated, and tubular shapes. In differentiated cells, mitochondria are densely packed, and some are highly branched and distributed throughout the cytoplasm. Along with the maturation, mitochondrial ATP, OXPHOS, and ROS levels also increase in differentiated cells. The switch of cellular metabolism from glycolytic to oxidative types has been observed in the differentiation processes of many stem cell populations [4–7].

Stem cells and terminally differentiated cells also possess different mitochondrial dynamics, which is associated with the changes in morphology and metabolism during differentiation. At the transcriptional level, elevated mRNA of mito-fission gene *Drp1* is detected in ESCs and iPSCs comparing to differentiated cells. DRP1 protein and its active form phosphorylated DRP1 (p-DRP1 Ser 616) accumulate more in ESCs or iPSCs than in differentiated cells [8–11]. On the other hand, differentiated cells have increased abundance of mito-fusion genes *Mfn1* and *Mfn2* mRNAs [10] as well as elevated protein levels of MFN1, MFN2, and OPA1 in differentiated cells [9, 12]. The above correlations indicate that the differentiation processes of ESCs/iPSCs are concomitant with a shift from mito-fission in ESCs and iPSCs to mito-fusion in differentiated cells.

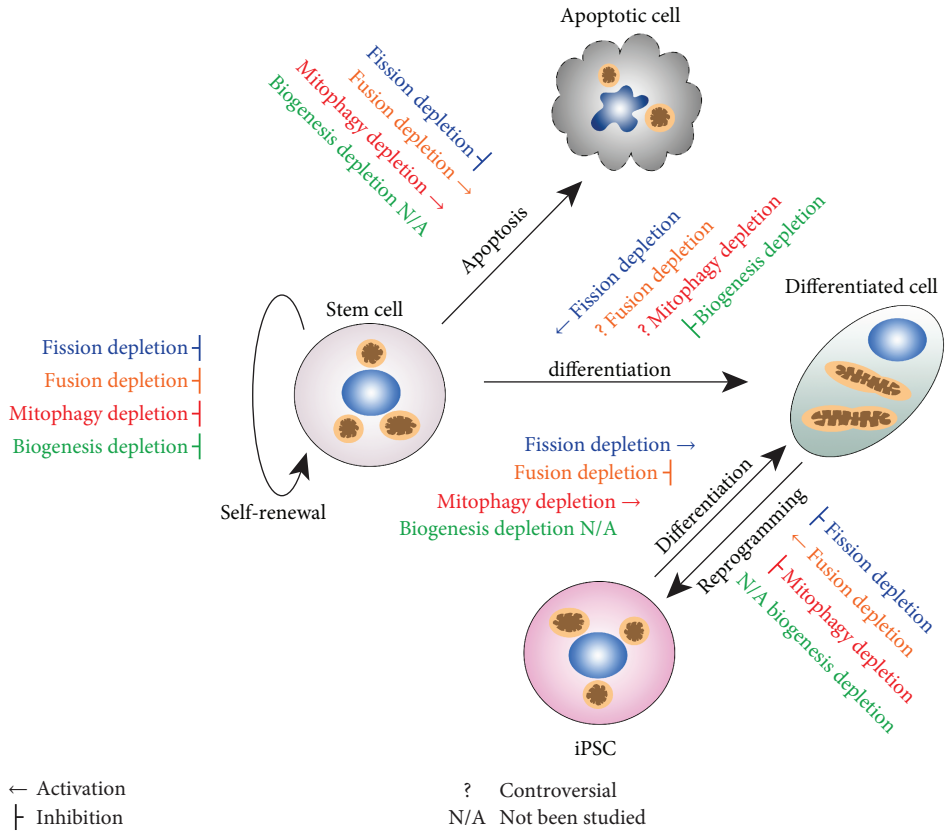

Figure 2: Modulating mitochondrial dynamics impacts on stem cell behaviors. Blockades of mitochondrial dynamics, fission (blue), fusion (orange), mitophagy (red), and biogenesis (green), affect stem cell differentiation, self-renewal, apoptosis, differentiation, and reprogramming. Downregulation of mito-fission usually leads to impaired self-renewal and the loss of stemness in stem cells, while increasing differentiation. Stem cells are often protected from apoptosis. Fission blockade also decreases the reprogramming efficiency. Downregulation of mito-fusion impairs stem cell self-renewal and may have diverse effects on stem cell differentiation. In general, mito-fusion protects stem cells from apoptosis, and the mito-fusion blockade often results in increased vulnerability to stress. Downregulation of mito-fusion improves the reprogramming efficiency. The blockade of mitophagy also impairs stem cell self-renewal as well as decreases reprogramming efficiency. The function of mitophagy in stem cell differentiation has not been understood clearly enough and may be stem cell type-specific and lineage-specific. Mitochondrial biogenesis is generally pivotal for stem cell maintenance. Downregulation of biogenesis impairs stem cell self-renewal and differentiation. More detailed information on stem cell behaviors and their regulation by mitochondrial dynamics are listed in Table 1.

Besides mitochondrial fission and fusion, the expression levels of genes that are crucial for mitochondrial biogenesis (e.g., PGC-1α, PGC-1β, TFAM, and NRF1) also increase during the early differentiation of stem cells. This is accompanied with increased mitochondrial proteins and elevated mitochondrial mass [13–15]. Thus, the differentiation process is also associated with increased mitochondrial biogenesis.

3. Mitochondrial Dynamics Controls Stem Cell Behaviors

3.1. Mito-Fission. Mitochondrial dynamics not only indicates undifferentiated vs. differentiated states of stem cells but also, reversely, modulates stem cell behaviors (Figure 2 and Table 1). The fragmented morphology of mitochondria in stem cells leads to an intriguing question—is mito-fission essential for the stemness? As Drp1 plays a critical role in mito-fission, some recent studies sought to answer the question by genetically knocking out or knocking down Drp1 or pharmacologically inhibiting Drp1 with its specific inhibitor, mitochondrial division inhibitor 1 (mDivi-1). In human iPSCs (hiPSCs), both Drp1 knockout and Drp1 inhibitor mDivi-1 treatment promote hiPSCs to differentiate into cardiomyocytes with augmented cardiac-specific gene expression. In addition, Drp1 downregulation in hiPSCs also elicits the metabolic switch from glycolysis (featured in stem cells) to OXPHOS (features in differentiated cells) [10]. iPSCs treated with mDivi-1 lose their typical morphology and adopt shapes resembling differentiated cells instead. mDivi-1-treated iPSCs also have reduced alkaline phosphatase (AP) staining [16], in line with the loss of stemness upon Drp1 downregulation. A similar effect of mito-fission on stemness is also observed in the cancer stem cells. In nasopharyngeal carcinoma cells (NPC), stem cell markers Oct4 and ABCG2 diminish when Drp1 activation (p-Drp1 Ser 616) is downregulated by Cox2 blockade, indicating the loss of stemness [17].

Table 1: A summary of the effects on stem cell behaviors upon modulating key factors in mitochondrial dynamics.

Dynamics	Key factors	Modulation	Effect on stem cell or iPSC behavior	References
Mito-fission	Drp1, Fis1	Downregulation of Drp1	Promote stem cell differentiation	[10, 16, 17]
			Lose stemness	[17, 18]
			Decrease reprogramming efficiency to iPSCs	[11, 19]
		Downregulation of Drp1/Fis1	Block apoptosis	[38–41]
		Upregulation of Drp1	Improve reprogramming efficiency to iPSCs	[20]
			Lose stemness	[21, 22]
Mito-fission	OPA1, Mfn 1/2	Downregulation of OPA1/Mfn1/2	Impair stem cell differentiation	[12, 42, 45]
			Promote neuron stem cell differentiation	[30]
			Impair iPSC differentiation	[44]
			Impair self-renewal	[30, 47]
			Improve reprogramming efficiency	[9]
		Upregulation of Mfn 2	Promote stem cell differentiation	[43]
			Induce iPSC differentiation	[44]
			Protect cell from apoptosis	[48, 49]
Mitophagy	Pink1, Parkin, Atg12, Atg3, Bnip3	Downregulation of Atg12/Atg3/Fis1/Pink1/Parkin	Impair self-renewal	[50–53]
			Decrease reprogramming efficiency to iPSCs	[51, 54]
		Downregulation of Atg12/Pink1	Promote stem cell differentiation	[50, 54]
		Downregulation of Atg3	Display abnormal differentiation	[51]
		Downregulation of Pink1	Impair neuron stem cell differentiation	[57]
		Downregulation of Pink1/Parkin/Bnip3	Lose the function of protecting the cell from apoptosis	[59–61]
Mito-biogenesis	PGC1α	Inhibition of biogenesis	Inhibit differentiation	[62]
		Inhibition or activation of biogenesis	Lose stemness	[64, 65]
		Inhibition of biogenesis	Cause cell death	[66]
		Activation of biogenesis	Promote stem cell differentiation	[63]

This table includes most key factors that are directly involved in mito-fission, mito-fusion, mitophagy, and mitochondrial biogenesis that are mentioned in this review. The effects of these key factors on stem cell behaviors are listed with the numbers of the references.

Drp1-dependent mito-fission is also associated with stem cell asymmetric division. Katajisto et al. reported that mitochondria are asymmetrically divided into daughter cells during stem cell division—the daughter cell that receives more young mitochondria becomes the self-renewed stem cell [18]. The asymmetric division of young and old mitochondria depends on Drp1-mediated mito-fission. Interestingly, Drp1 inhibition by mDivi-1 results in the random allocation of young and old mitochondria during stem cell division and impaired self-renewal and stemness [18].

Besides the maintenance of stemness, mito-fission also has a critical function in the progress of reprogramming—the *de novo* establishment of stemness. Knocking down mito-fission mediators, Drp1, Mid51, and Gdap1, markedly decreases the reprogramming efficiency as evidenced by a fewer number of alkaline phosphatase- (AP-) positive adherent colonies during reprogramming [11, 19].

Reprogramming is a stepwise process. Differentiated cells must overcome several barriers to obtain pluripotency. As stem cells and differentiated cells have distinct mitochondrial characteristics, the remodeling of mitochondria is conceivably one of the obstacles for reprogramming. It is generally accepted that mito-fission is induced during reprogramming [8, 11]. However, whether increasing mito-fission can increase reprogramming efficiency remains controversial. A possible explanation for the conflicting observations may lie in side effects (e.g., ROS production, apoptosis, and mitochondria integrity impairment) caused by excessive fission. Many pathways and factors have been implicated in activating mito-fission. Of note, fatty acid synthesis promotes mito-fission and also improves the reprogramming into hiPSCs [20]. In this scenario, fatty acid synthesis seemingly promotes fission in a mild and healthy level, at which mitochondria remain in a good condition for reprogramming. In contrast, excessive fission apparently impairs stemness of embryonic stem cells (ESCs) [21]. Excessive fission increases intracellular Ca^{2+} level and CaMKII activity, leading to the degradation of β-catenin, a critical factor for pluripotency maintenance [21]. Growth factor erv1-like (Gfer) represses Drp1 expression and mito-fission. Gfer downregulation in ESCs augments Drp1-dependent mito-fission yet results in the loss of stemness [22]. In this scenario, the loss of stemness seems to attribute to apoptosis, supporting the above notion that only an appropriate level of mito-fission promotes the establishment of stemness in reprogramming. Besides apoptosis, excessive mito-fission also leads to the abnormal accumulation of ROS [23–26] and causes the loss of self-renewal capacity in some stem cell populations [27–30]. It

is noteworthy that a moderate level of ROS is necessary for the maintenance of self-renewal in some types of stem cells [31, 32]. Thus, balancing the impacts of mito-fission on mitochondrial functions (e.g., bioenergetics, ROS generation, and apoptosis) is pivotal for the maintenance and establishment of stemness.

Notably, mito-fission is elevated under stress conditions [33–35]. This is mostly studied in nonstem cells. In physiological conditions with mild stress, mito-fission is associated with prosurvival mitophagy to clear defective mitochondria [36, 37]. However, under extreme stress conditions, the mitochondrial network is fragmented due to extensive mito-fission. Drp1- and Fis1-mediated mito-fission contributes to apoptosis [38–40]. Inhibiting Drp1 activity prevents the loss of mitochondrial membrane potential and the release of cytochrome *c* in Hela and COS7 cells and hence protects against apoptosis [39, 40]. Drp1 activity is controlled by its phosphorylation at serine 656 residue (p-Drp1 Ser 656). Sympathetic activity activates cAMP-dependent protein kinase (PKA), which phosphorylates Drp1 at serine 656 and consequently inhibits Drp1 activity in PC12 cells. Reversely, calcium mobilization and the activation of calcineurin phosphatase lead to dephosphorylation of this site on Drp1 and hence apoptosis [38]. In Hela cells, the downregulation of mitochondrial fission 1 (Fis1) robustly inhibits cell death [40]. Back to the stem cell context, Drp1 inhibitor mDivi-1 blocks Drp1 translocation from the cytosol to mitochondria and protects rat hippocampal neural stem cells from palmitate-induced apoptosis and cell death [41]. Thus, inhibiting mito-fission may hold potential in protecting stem cells from apoptosis under pathological stress conditions.

3.2. Mito-Fusion. Mito-fusion enables content exchange between individual mitochondrion as well as between mitochondria and nucleus. Mito-fusion requires the coordination of multiple interacting factors. The fusion of mitochondrial outer membrane is mediated by Mfn1 and Mfn2. Inner membrane fusion requires long-form OPA1. All the mediators are associated with fusion-mediated regulation of stem cell behaviors (Figure 2 and Table 1).

Mito-fusion is necessary for stem cell differentiation. In most differentiated somatic cells, mitochondria are in tubular and network structure. In *Drosophila* intestinal stem cells (ISCs), defective mito-fusion due to OPA1 knockdown impairs stem cell differentiation [42]. Under a prodifferentiation condition, OPA1-/- ISCs do not express differentiation-specific markers but instead show the characteristics of stem cells [42]. The gene trapping of mito-fusion protein Mfn2 or OPA1 in ESCs exhibits the same phenotype—the differentiation of ESCs to cardiomyocytes is blunted [12]. Factors regulating mito-fusion are also involved in the fate determination of stem cells. Mitochondrial carrier homolog 2 (MTCH2) is a regulator of mito-fusion, metabolism, and apoptosis. In MTCH2-/- ESCs, mitochondria fail to elongate and the stem cells have a delay in exiting the naïve pluripotency stage upon differentiation stimulation. Interestingly, Mfn2 overexpression or a dominant negative form of Drp1 rescues mito-fusion in MTCH2-/- ESCs and drives the stem cells to exit the naïve state and enter the prime state [43].

Mito-fusion is apparently essential for iPSC differentiation as well. In neurogenic differentiation of hiPSCs, Mfn2 knockdown results in deficits in neurogenesis and synapse formation [44]. In contrast, overexpression of Mfn2 in hiPSCs can promote the differentiation and maturation of neurons [44].

Although plenty of evidence indicates that the blockade of mito-fusion impedes stem cell differentiation, this notion cannot be generalized to all types of stem cells or all cell fate lineages. For example, in neural stem cells (NSCs), mitochondria are in the tubular structure instead of fragmented [30]. It would be expected that mito-fusion may differently impact on NSC differentiation. Indeed, the knockout of mito-fusion genes reduces the self-renewing capacity of neural stem cells due to ROS accumulation and NRF-2-mediated retrograde signaling [30]. Murine mesenchymal stem cells (MSCs) represent another example for differential requirements of mito-fusion in lineage differentiation. MSCs are multipotent stem cells that can differentiate into adipocytes, osteocytes, and chondrocytes. During adipogenic and osteogenic differentiation, the expression of mito-fusion factors increases and mitochondria fuse and elongate. However, chondrogenic differentiation is accompanied with fragmented mitochondria and increased expression of mito-fission factors [45]. With Mfn2 downregulation in MSCs, the differentiation into adipogenic and osteogenic lineages fails, whereas chondrogenesis is abolished only when Drp1 is downregulated [45]. Intracellular ROS levels may contribute to the diverse effects of mito-fusion on stem cell differentiation. It has been observed that mitochondria adopt a fragmented structure and produce more ROS in fusion-deficient stem cells [30, 42]. ROS apparently have different effects on stem cell differentiation. For example, in mesenchymal stem cell (MSC) differentiation, a high level of ROS favors adipogenesis whereas a low ROS level prefers osteogenesis [46]. Multiple REDOX sensors (e.g., p38-MAPK, ERK1/2, and JNK) may mediate the diverse effects of ROS on stem cell differentiation. Cleary, our knowledge in the interplay between mito-fusion and stem cell differentiation is far from complete.

Only a limited number of studies have reported the interaction between mito-fusion and stem cell self-renewal. In NSCs, dampening mito-fusion by deleting OPA1 or Mfn1/2 impairs the self-renewing capacity, suggesting that mito-fusion is necessary for self-renewal [30]. On the other hand, mito-fusion seemingly facilitates stem cell self-renewal. Wu et al. reported that the epithelial-mesenchymal transition (EMT) of mammary stem cells induces mito-fusion through miR200c-PGC1α-Mfn1 pathway [47]. Mfn1 is required for PKCζ-mediated NUMB phosphorylation and hence directs asymmetry division and self-renewal [47]. As to reprogramming, it has been reported that Mfn1/2 depletion promotes reprogramming and the maintenance of pluripotency. The downregulation of Mfn1/2 activates Ras-Raf and HIF-1α and facilitates the transition to glycolytic metabolism [9].

Opposite to mito-fission, which induces apoptosis and cell death, mito-fusion protects cells from apoptosis. COS7 cells with activated Mfn2 have an increase of the nucleotide exchange rate, and the cells are protected against free

radical-induced depolarization. The underlying mechanism is shown—the activated Mfn2 interferes with BAX activation and cytochrome *c* release [48]. With the overexpression of rat Fzo1 (a counterpart of human Mfn proteins), Hela cells adopt an elongated mitochondrial structure and become protected from etoposide-induced cell death. Reversely, gene silencing of Fzo1 causes an increase of susceptibility to radical-induced cell death [49].

3.3. Mitophagy. Mitochondrial quality and integrity are essential for normal functions of mitochondria. Defective mitochondria can be cleared by mitophagy, which plays critical roles in stem cell maintenance (Figure 2 and Table 1). Multiple studies indicated that stem cell self-renewal relies on mitophagy. In hematopoietic stem cells (HSCs), Atg12 knockout blockades mitophagy and results in aberrant accumulation of mitochondria. The self-renewal and differentiation potential of HSCs are impaired by Atg12 knockout, which exacerbates during aging [50]. In Atg3 knockout ESCs, the accumulation of defective mitochondria is accompanied by elevated ROS production, leading to the impairment of self-renewal [51]. In human leukemia stem cells (LSCs), Fis1 (mitochondrial fission 1) depletion attenuates mitophagy, leading to cell cycle arrest and impaired self-renewal. It has been shown that AMPK activates Fis1-dependent mitophagy, and AMPK inhibition mimics the Fis1 depletion-induced mitophagy defect [52]. In $Tie2^+$ HSCs, mitophagy is essential for self-renewing expansion [53]. It was shown that the activation of PPAR-fatty acid oxidation pathway promotes HSC self-renewing expansion by recruiting Parkin to mitochondria. Silencing Pink1 or Parkin not only abrogates the self-renewal but also inhibits the maintenance of $Tie2^+$ HSCs [53].

Likewise, mitophagy is necessary for reprogramming. Loss of Pink1-dependent mitophagy dampens reprogramming efficiency [54]. Similar negative effect on reprogramming was also observed in response to Atg3 knockout-induced mitophagy defect [51].

Both stem cell self-renewal and iPSC reprogramming require mitochondria in high quality and a low level of ROS. Excessive ROS have been detected in mitophagy-defective stem cells [51, 55, 56]. Given the detrimental effects of ROS on stem cell self-renewal, it is reasonable to conceive that mitophagy has a pivotal role in protecting stem cells from the loss of self-renewal and maintenance.

The function of mitophagy in stem cell differentiation may vary in different types of stem cells and differ at stages in the differentiation process. Mitophagy defect in Atg12 knockout HSCs leads to differentiation [50]. Atg12-/- HSCs express higher levels of premyeloid markers and form unipotent mature colonies. Although Atg12-/- HSCs have elevated ROS levels, the prodifferentiation effect is likely not driven by ROS accumulation because a ROS scavenger NAC does not abolish the differentiation [50]. Similarly, mitophagy deficiency induced by Pink1 knockout in iPSCs promotes differentiation. Pink1-/- iPSCs have strong tendency to spontaneously differentiate into heterogeneous cell types [54]. However, it should be kept in mind that abnormal differentiation could occur under mitophagy deficiency, as exampled by delayed expression of certain endoderm and mesoderm markers during the differentiation of Atg3-/- ESCs [51]. On the other hand, mitophagy deficiency may impede stem cell differentiation in some types of stem cells. For example, the loss of Pink1 in NSCs leads to retarded differentiation towards mature neurons with an unknown mechanism [57]. During C2C12 myoblast differentiation, mitophagy is induced in the early stage of myogenesis to clear preexisting mitochondria and make way for newly generated OXPHOS-competent mitochondria from a burst of mitochondrial biogenesis [58]. In this scenario, mitophagy blockade impairs myogenic differentiation.

As a mitochondrial quality control, mitophagy acts to protect cells from apoptosis. In chlorpyrifos-induced apoptosis of SH-SY5Y cells, Pink1/Parkin-mediated mitophagy is increased and Parkin knockdown drastically increases apoptosis. On the other hand, Parkin overexpression alleviates apoptosis [59]. Similarly, mitophagy protects human vascular smooth muscle cells from atherogenic lipid-induced apoptosis as evidenced by extensive apoptosis upon Pink1/Parkin silencing [60]. Bnip3 is another mitophagy-related protein that protects against apoptosis. The phosphorylation of Bnip3 drives prosurvival mitophagy to protect HL-1 cardiac cells from apoptosis [61]. The phosphorylation of serine residues 17 and 24 flanking Bnip3 LIR (LC3 binding region) promotes its binding to LC3B, which signals mitochondria for lysosomal degradation prior to cytochrome *c* release-induced apoptosis [61]. In NSCs, Pink1 knockout leads to an increase of apoptosis in the absence of stress [57].

3.4. Mitochondrial Biogenesis. In both ESCs and iPSCs, mitochondrial biogenesis is concomitant with differentiation (Figure 2 and Table 1) [13, 14]. Peroxisome proliferator-activated receptor gamma coactivators (PGC-1) play pivotal roles in mitochondrial biogenesis. The genetic deletion of both PGC-1α and PGC-1β in brown adipocyte progenitors drastically abolishes the differentiation into brown adipocytes [62]. On the other hand, the upregulation of mitochondrial biogenesis also facilitates differentiation [63]. It has been reported that Wnt signaling promotes osteoblastic differentiation of murine mesenchymal C3H10T1/2 cells in a mitochondrial biogenesis-dependent manner. Wnt activation induces biogenesis and augments mitochondrial ATP and ROS production. The suppression of mitochondrial biogenesis with AZT abrogates the differentiation upon Wnt activation. Consistent with the observation, stimulating mitochondrial biogenesis with TFAM further increases the differentiation.

Whether mitochondrial biogenesis directly impacts on stemness remains largely elusive. It is generally accepted that mitochondrial biogenesis maintains at a low level in stem cells, resulting in few mitochondria and a low level of ROS. The low level of mitochondrial biogenesis seems to be necessary for the stemness and quiescence. First, this note is supported by observations from HSCs in SDF-1/CXCL12 transgene mice with constitutive active CXCR4 pathway [64]. In these mice, mitochondrial biogenesis in HSCs is upregulated and the HSCs express increased

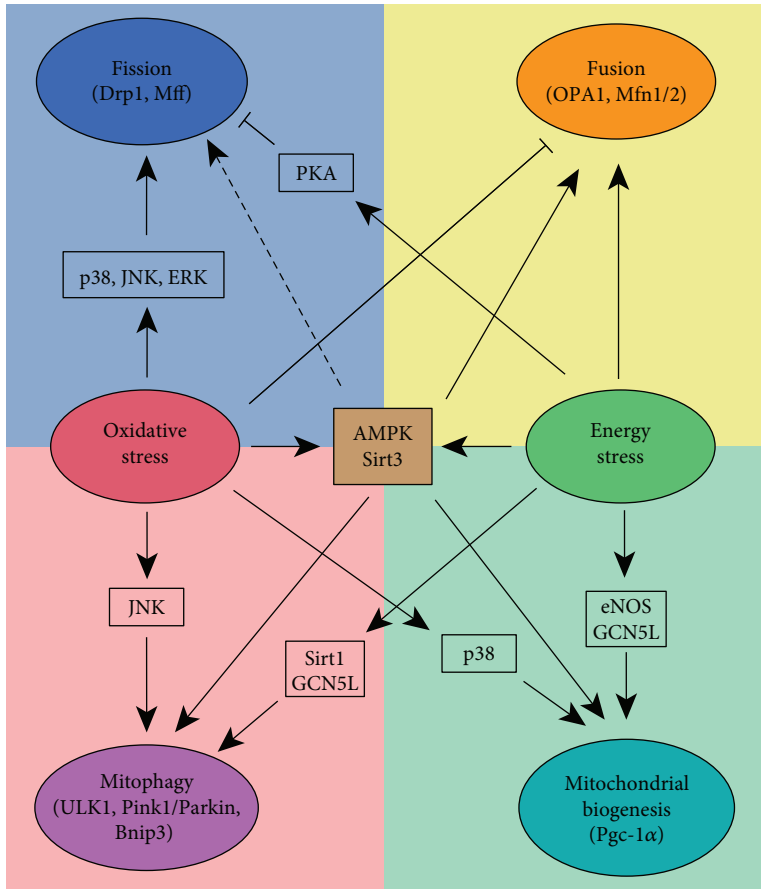

Figure 3: Mitochondrial dynamics is regulated through multiple pathways. Oxidative stress and energy stress have distinct impacts on mito-fission (blue), mito-fusion (orange), mitophagy (pink), and mito-biogenesis (green) via distinct signaling pathways. The dash line denotes that the results from multiple studies are conflicting.

CD34, indicative of a loss of Lin(-)/Sca1(+)/c-Kit(+) primitive state and long-term repopulating potential. In another study, mTOR activation, as a result of Tuberous Sclerosis Complex (TSC) knockout, increases mitochondrial biogenesis and ROS production in HSCs [65]. The quiescence in these HSCs is disrupted, which can be rescued by a ROS scavenger NAC. Although both studies reveal an intriguing correlation between an increase of mitochondrial biogenesis and the loss of stemness and stem cell quiescence, it remains unclear whether mitochondrial biogenesis is the direct cause of the above effects.

Downregulation of mitochondrial biogenesis via genetic approaches is not easy since such manipulations are always associated with cell death. Pharmacological inhibition of mitochondrial biogenesis may also affect cell survival. For example, XCT790 is a specific inhibitor of ERRα-PGC-1 signaling pathway and acts to inhibit mitochondrial biogenesis [66]. Treating cancer stem-like cells with XCT790 lowers cell viability and suppresses Wnt, STAT3, and TGF-β prosurvival pathways. The cell death may be due to low-energy stress caused by reduced mitochondrial mass and function, as a supplement of acetyl-L-carnitine can rescue cell death.

4. Mitochondrial Dynamics Is Regulated under Stress

Many (but not all) types of adult stem cells with long-term self-renewing capabilities exist in a quiescent or slow-proliferating state. Stem cells in this state are often exposed to relatively low levels of oxygen and growth factors from their niches. As discussed before, mitochondrial dynamics has profound impacts on stem cell behaviors. Here, we review some recent findings on stress-induced alterations of mitochondrial dynamics, which conceivably also affect stem cell behaviors (Figure 3).

4.1. Oxidative Stress. ETC activities in mitochondria is a major source of intracellular ROS. ROS is neutralized by various antioxidant defense systems. Oxidative stress occurs when an excessive amount of ROS accumulates. Accumulating evidence suggests that ROS regulate mitochondrial dynamics.

In stem cells and progenitor cells, oxidative stress promotes mito-fission. Oxidative stress induced directly by hydrogen peroxide (H_2O_2) treatment results in mitochondrial fragmentation in myoblasts. Drp1-specific inhibitor,

mDivi1, attenuates mitochondrial fragmentation, indicating the fragmentation is Drp1-dependent [33]. Hypoxia promotes mito-fission in stem cells [34, 67, 68]. In periodontal ligament stem cells, $CoCl_2$ treatment, a condition mimicking hypoxia (pseudohypoxia), results in ROS-mediated mito-fission and apoptosis, which can be rescued by NAC [67]. Energy overloading can also induce oxidative stress and promote mito-fission [20, 69]. Prolonged exposure to saturated free fatty acids (e.g., palmitate) is cytotoxic to neural stem cells, which can be prevented by the Drp1 inhibitor mDivi-1 [41].

Intriguingly, ROS can function as signaling molecules to regulate stem cell behaviors via REDOX sensors. It is well known that ROS can activate many MAPKs, including p38, ERK1/2, and JNK [70]. These MAPKs, functioning as REDOX sensors, have diverse functions in stem cells [11, 28, 71, 72]. One particular function is to regulate oxidative stress-induced mito-fission. The activation of ERK1/2 further phosphorylates Drp1 to promote mito-fission, which results in stem cell proliferation or reprogramming [11, 73]. Succinate induces ROS and promotes human mesenchymal stem cell (hMSC) migration. The activation of PKC upon succinate treatment activates p38 MAPK, which leads to Drp1 translocation onto the mitochondrial outer membrane for fission.

ROS have opposite effects on mito-fusion. Oxidative stress disrupts mito-fusion and leads to fragmented mitochondrial morphology. In osteosarcoma and cardiomyoblasts, oxidative stress (induced by H_2O_2 exposure) decreases the active OPA1 isoform [74]. Consistently, in fibroblasts, H_2O_2 treatment results in polyubiquitination-mediated Mfn1/2 degradation [75].

ROS-induced mito-fission is vital for mitophagy. Aberrant ROS accumulation in mitochondria causes mitochondrial dysfunction and the defective mitochondria need to be cleared by mitophagy. Pink1 and Parkin promote Mfn1/2 ubiquitination and increase mito-fission-dependent mitophagy to clear ROS-overloaded mitochondria [75]. Moreover, many studies have demonstrated that augmented ROS is a trigger for mitophagy [76–79]. REDOX sensor JNK participates in ROS-induced mitophagy via mitophagy-related protein Bnip3 [80]. It is found that Bnip3 expression in cardiomyocytes is correlated to JNK activity. Prolonged JNK activation overrides the inhibitory effect of AKT on FOXO3, resulting in elevated FOXO3 activity and the expression of its target Bnip3. In this scenario, mitophagy is induced by JNK activation [80].

ROS also promote mitochondrial biogenesis. ROS are found to upregulate PGC-1α activity in various cellular contexts [81–84]. Many signaling pathways have been shown to regulate PGC-1α in response to oxidative stress. One of these pathways is p38 MAPK signaling, which activates PGC-1α [85, 86]. In C2C12 myoblasts, p38 MAPK phosphorylates PGC-1α (at residues threonine 262, serine 265, and threonine 298) and stabilizes PGC-1α protein [86]. Another example is the induction of Sirt3, a deacetylase enriched in mitochondria, by oxidative stress. Sirt3 overexpression in neurons protects against oxidative stress-induced neuronal injury via orchestrating Ca^{2+} homeostasis and mitochondria biogenesis [87]. In human umbilical endothelial cells, H_2O_2 activates Sirt3 to deacetylate FOXO3, thus increasing PGC-1α and TFAM expression [88].

4.2. Energy Stress. Mitochondria elongate upon energy deprivation, which is mediated by the downregulation of active Drp1 (p-Drp1 Ser 616) and redirection of Drp1 from mitochondria [89]. cAMP-dependent protein kinase (PKA) signaling pathway controls cell growth in response to nutrient deprivation [38, 90]. PKA is activated upon energy depletion. Active PKA phosphorylates Drp1 (p-Drp1 Ser 637) and inactivates Drp1, which inhibits mito-fission in Hela cells [90]. It remains unknown whether PKA is responsible for p-Drp1 Ser 616 increase under starvation [91]. AMPK, another sensor of energy stress, is induced by both energy deprivation and ROS [70, 92–94]. Numerous studies have established tight connections between AMPK and mitochondrial dynamics. In endothelial cells, pharmacological activation of AMPK with AICAR prevents mito-fission by inactivating Drp1 [95]. On the other hand, the activation of AMPK with AICAR in U2OS cells is sufficient to promote mito-fission in the absence of mitochondrial stress [35]. It has been reported that active AMPK phosphorylates Mff at Ser 155 and Ser 172 residues, which is required for Drp1 recruitment to mitochondria during fission [35]. The function of AMPK on mitochondrial fission may depend on the cellular need. Upon extreme stress conditions, AMPK-mediated fission might be a dominant effect to facilitate mitochondria clearance. When damaged mitochondria are eliminated and stress is reduced, AMPK may help cells restore mitochondrial function by promoting fusion instead of fission.

In contrast to mito-fission, starvation induces mito-fusion via upregulating Mfn1 [89]. It has been postulated that the tubular mitochondrial structure in mouse embryonic fibroblasts under energy stress prevents mitochondria from autophagy-induced mitophagy. Maintaining mitochondrial mass or even increasing mitochondrial mass upon starvation permits mitochondria to maximize the energy supply for the whole cell [89]. AMPK is also a key regulator for mito-fusion at least in the aging context. In *C. elegans*, APMK and dietary restriction protect body-wall muscle cells from aging by maintaining mitochondria in a fusion state [96]. In addition, the activation of AMPK with its activator AICAR can induce fusion in rat hepatocyte and protect the cells from drug-induced apoptosis [97]. Sirt3 also promotes mito-fusion. Sirt3 deacetylates OPA1 and increases its GTPase activity for mitochondrial fusion [98]. The Sirt3-dependent activation of OPA1 preserves the mitochondrial network and protects cardiomyocytes from doxorubicin-mediated cell death [98]. Mito-fusion conceivably can buffer stress conditions in mitochondria. The regulation of mito-fusion by Sirt3 echoes this function of mito-fusion as demonstrated by responses to calcium and ROS in neurons [87].

Energy stress increases NAD^+/NADH ratio, which activates sirtuin family. Sirt1 has received much attention on its antiaging effects, which may be attributed to its indispensable role in maintaining mitochondria homeostasis. Sirt1 acts mainly in mitochondrial mitophagy [99–102].

Table 2: A summary of pharmacological tools for mito-fission, mito-fusion, and mitochondrial biogenesis modulation and their reported effects.

Name	Function and mechanism	Physiological effect in nonstem cell	Physiological effect in stem cell
mDivi-1	Fission inhibitor: inhibit assembly of Drp1 and its GTPase activity	Prevent cell death	Prevent stem cell death; promote hiPSC differentiation
P110	Fission inhibitor: block Drp1/Fis1 interaction	Prevent stress- or injury-induced cell death	N/A
Dynasore	Fission inhibitor: noncompetitively inhibit the Drp1 GTPase activity	Protect cardiomyocyte from ischemia/reperfusion injury	N/A
M1	Fusion activator	Reduce cytochrome *c* release and protect rotenone-induced cell death	N/A
Leflunomide	Fusion activator: promote fusion by inhibition of pyrimidine synthesis	Protect cells from apoptosis	N/A
XCT790	Biogenesis inhibitor: inhibit ERRα-PGC-1 signaling pathway	N/A	Induce cancer stem cell death; induce cell cycle arrest
Azithromycin or doxycycline	Biogenesis inhibitor: inhibit mitochondrial protein translation	N/A	Induce cancer stem cell death

This table lists the reported effects of mito-fission inhibitors, mito-fusion activators, and mitochondrial biogenesis inhibitors in nonstem cells and stem cells. N/A denotes no study has been conducted.

The Sirt1-specific activator SRT1720 and NAM (promoting Sirt1 activity via increasing NAD^+) decrease mitochondria content by facilitating mitophagy in human fibroblasts [99]. In line with this, Sirt1 inhibition is underlying impaired mitophagy in disease models. In DNA repair-deficient XPA mouse models, PARP1 activation blunts mitophagy through Sirt1 inhibition and causes mitochondrial dysfunction [100]. Sirt1 deacetylates autophagy-related proteins (LC3, Atg5, and Atg7), leading to phagophore maturation and mitophagy in mouse embryonic fibroblasts (MEF), HEK293, and Hela cells [101, 102]. Besides Sirt1, GCN5L and Sirt3, which specifically function as deacetylase in mitochondria, are also involved in mitophagy induced under energy deprivation. In MEF and HepG2 cells, long-term genetic depletion of GCN5L reduces mitochondrial mass via autophagy-induced mitophagy [103, 104], which is also reported to be Sirt3-dependent [104]. In MEF cells, GCN5L knockout has a positive effect on the expression and activity of transcriptional factor EB (TFEB), a master regulator of autophagy and its downstream targets [103]. Instead, Sirt3 deacetylates FOXO3 to increase the expression of mitophagy mediators (such as Bnip3, NIX, and LC3) [88]. AMPK also participates in mitophagy regulation under energy stress. As an energy sensor, AMPK phosphorylates ULK1 and hence connects energy sensing to mitophagy in MEFs [105] and exercise-induced mitophagy in mice [106]. As mentioned before, AMPK activates Fis1 in human leukemia stem cells (LSCs) to promote mitophagy and LSC stemness maintenance [52].

Mitochondrial biogenesis is often coincident with mitophagy. In GCN5L knockout MEFs, TFEB and PGC-1α are induced to promote mitochondrial biogenesis. The concurrent induction of mitophagy and biogenesis increases the mitochondrial turnover rate and ensures mitochondrial homeostasis [103]. Endothelial nitric oxide synthase (eNOS) is another factor that mediates energy deficiency-induced mitochondrial biogenesis. eNOS increases under caloric restriction and has an essential function in caloric restriction-induced mitochondrial biogenesis [107]. In the skeletal muscle, AMPK activation is also associated with mitochondrial biogenesis. In response to chronic energy deprivation, mitochondria undergo AMPK-dependent adaptive biogenesis [108, 109]. The treatment of β-GPA (mimicking chronic energy deprivation) activates AMPK and consequently results in mitochondria biogenesis in the muscle [110]. Mechanistically, AMPK may promote mitochondrial biogenesis by activating the nuclear respiratory factor-1 (NRF-1)/mTFA axis [111] or PGC-1α [110, 112]. By far, there is no direct evidence showing that the AMPK activator can induce mitochondrial biogenesis in stem cells.

5. Pharmacological Regulators of Mitochondrial Dynamics and the Potential Applications

5.1. Mito-Fission Inhibitors. As discussed above, inhibitors of mito-fission may protect stem cells from apoptosis and promote iPSC differentiation (Table 2). mDivi-1 is a widely used fission inhibitor, which inhibits the assembly of Drp1, and its GTPase activity meanwhile does not interfere with mito-fusion [113]. Several studies have reported that mDivi-1 protects stem cells from cell death. In type 2 diabetes, mDivi-1 treatment protects hippocampal neural stem cells from palmitate-induced apoptosis [41]. It has been discussed in this review that fission blockade promotes iPSC differentiation, which may have clinical potential in cardiac regeneration. In this regard, pharmacological inhibition of Drp1 with mDivi-1 increases mitochondrial respiration and promotes human iPSC differentiation into cardiac lineage-committed cells [10].

P110 is another mito-fission inhibitor, acting by blocking Drp1/Fis1 interaction [23]. P110 was first used as a protector for neuronal cells. In cultured neurons, P110 treatment prevents mitochondrial fragment and excessive

ROS production, improves mitochondrial integrity and membrane potential, and protects the cells from stress-induced death [23]. Other studies have utilized P110 to inhibit mitochondrial fission for protecting the cell from stress- or injury-induced death, especially on cardiac disease models. In both *in vitro* and *in vivo* studies, P110 treatment improves acute infarction-induced cell death and prevents cardiac dysfunction [114].

Dynasore is a cell-permeable inhibitor of dynamin. Dynasore functions to noncompetitively inhibit the GTPase activity of Dynamin1, Dynamin2, and Drp1 and hence is used as a mito-fission inhibitor [115]. Similar to the other two inhibitors, dynasore protects the cardiomyocyte from ischemia/reperfusion injury *in vivo* [116]. Comparing to the other two inhibitors, dynasore has less specificity towards mito-fission inhibition.

In summary, although it has not been tested extensively, mito-fission inhibitors may have potential in stem cell-based regenerative medicine. Extra care should be taken to prevent the loss of stemness and stem cell homeostasis upon mito-fission inhibition.

5.2. Mito-Fusion Activators. Only limited numbers of mito-fusion regulators are currently available. One activator is fusion promotor M1, which was introduced in 2012. Mitochondrial fragmentation is prominent in 1-methyl-4-phenyl-pyridinium- (MPP+-) treated SH-SY5Y cells, which model the neuron cell death in Parkinson disease. In this model, mito-fusion promotor M1 treatment reduces cytochrome *c* release and protects cells from cell death [117]. Similarly, mito-fusion promotor M1 is also protective for in vitro Parkinson disease model induced by rotenone [118].

The other mito-fusion activator is leflunomide, a new chemical introduced in 2018. This activator was identified in a small-molecule compound screening for MFN1/MFN2-dependent mitochondrial elongation. Hela cells treated with leflunomide show elongated mitochondrial network and increased Mfn1/2 expression. Mechanistically, leflunomide seems to be effective via the inhibition of pyrimidine synthesis. Leflunomide can reduce doxorubicin-induced PARP and cleaved-caspase 3 activity in MEF cells and protect PC12 cells from apoptosis [119].

Although it has not been used in a study with stem cells, mito-fusion promotor M1 and leflunomide may have therapeutic potential in inducing stem cell/iPSC differentiation in clinical settings (Table 2).

5.3. Biogenesis Inhibitors. Pharmacological inhibition of mitochondria biogenesis causes cell death. However, it may serve as targeted mitochondrial therapies for cancer (Table 2). Some studies have tested mitochondrial biogenesis inhibitors on cancer stem cells, which tend to be chemoresistant. A characteristic of cancer stem cells is the high mitochondria content, which may allow therapeutic strategies to eradicate these cells by mitochondrial biogenesis inhibition [120]. XCT790 is a specific inhibitor of ERRα-PGC-1 signaling pathway and inhibits mitochondrial biogenesis. Treating cancer stem cells with XCT790 suppresses cell viability by reducing prosurvival pathways [66]. Human non-small-cell lung cancer cells treated with XCT790 display reduced mitochondrial mass as well as increased ROS level, which modulates p53 and Rb signaling pathway for cell cycle arrest [121]. However, the effect of CXT790 on normal cell has not been evaluated.

Azithromycin and doxycycline are FDA-approved antibiotics that inhibit mitochondrial biogenesis via inhibiting mitochondrial protein translation. These antibiotics inhibit tumor sphere formation in eight different types of cancer stem cells (breast, DCIS, ovarian, prostate, lung, pancreatic, melanoma, and glioblastoma) [122]. Of the two, doxycycline has lower toxicity to normal cells [123] and may also have a favorable anti-inflammatory effect [124].

6. Perspective

Accumulating evidence shows that mitochondrial dynamics delicately interplays with stem cell behaviors. Stem cell behaviors (self-renewal, maintenance, proliferation, cell fate determination, and differentiation) can be altered by modulating mitochondrial fission, fusion, mitophagy, and biogenesis. As an emerging field, there are many questions awaiting to be answered related to stem cells and mitochondrial dynamics. The recent advance in inhibitors and activators of mito-fission and mito-fusion may allow the modulation of mitochondrial dynamics in various stem cell models. Moreover, pathways that participate in stress-induced mitochondrial dynamics regulation and responsive to mitochondrial dynamics should be examined in stem cell populations.

Disclosure

The content is solely the responsibility of the authors and does not necessarily represent the official views of the National Institutes of Health or American Heart Association.

Conflicts of Interest

The authors declare no competing interests.

Acknowledgments

Research reported in this publication was supported by the National Institute of Arthritis and Musculoskeletal and Skin Diseases of the National Institutes of Health under Award number 1R01AR070178 and the American Heart Association Grant-in-Aid 17GRNT33700260 to H. Yin.

References

[1] L. I. Zon, "Intrinsic and extrinsic control of haematopoietic stem-cell self-renewal," *Nature*, vol. 453, no. 7193, pp. 306–313, 2008.

[2] S. J. Morrison and J. Kimble, "Asymmetric and symmetric stem-cell divisions in development and cancer," *Nature*, vol. 441, no. 7097, pp. 1068–1074, 2006.

[3] S. K. Pazhanisamy, "Stem cells, DNA damage, ageing and cancer," *Hematology/Oncology and Stem Cell Therapy*, vol. 2, no. 3, pp. 375–384, 2009.

[4] M. Noguchi and A. Kasahara, "Mitochondrial dynamics coordinate cell differentiation," *Biochemical and Biophysical Research Communications*, vol. 500, no. 1, pp. 59–64, 2018.

[5] T. Wai and T. Langer, "Mitochondrial dynamics and metabolic regulation," *Trends in Endocrinology and Metabolism*, vol. 27, no. 2, pp. 105–117, 2016.

[6] X. Xu, S. Duan, F. Yi, A. Ocampo, G. H. Liu, and J. C. Izpisua Belmonte, "Mitochondrial regulation in pluripotent stem cells," *Cell Metabolism*, vol. 18, no. 3, pp. 325–332, 2013.

[7] H. Chen and D. C. Chan, "Mitochondrial dynamics in regulating the unique phenotypes of cancer and stem cells," *Cell Metabolism*, vol. 26, no. 1, pp. 39–48, 2017.

[8] L. Wang, X. Ye, Q. Zhao et al., "Drp1 is dispensable for mitochondria biogenesis in induction to pluripotency but required for differentiation of embryonic stem cells," *Stem Cells and Development*, vol. 23, no. 20, pp. 2422–2434, 2014.

[9] M. J. Son, Y. Kwon, M. Y. Son et al., "Mitofusins deficiency elicits mitochondrial metabolic reprogramming to pluripotency," *Cell Death and Differentiation*, vol. 22, no. 12, pp. 1957–1969, 2015.

[10] A. Hoque, P. Sivakumaran, S. T. Bond et al., "Mitochondrial fission protein Drp1 inhibition promotes cardiac mesodermal differentiation of human pluripotent stem cells," *Cell Death Discovery*, vol. 4, no. 1, p. 39, 2018.

[11] J. Prieto, M. Leon, X. Ponsoda et al., "Early ERK1/2 activation promotes DRP1-dependent mitochondrial fission necessary for cell reprogramming," *Nature Communications*, vol. 7, no. 1, article 11124, 2016.

[12] A. Kasahara, S. Cipolat, Y. Chen, G. W. Dorn, and L. Scorrano, "Mitochondrial fusion directs cardiomyocyte differentiation via calcineurin and notch signaling," *Science*, vol. 342, no. 6159, pp. 734–737, 2013.

[13] C. T. Chen, Y. R. V. Shih, T. K. Kuo, O. K. Lee, and Y. H. Wei, "Coordinated changes of mitochondrial biogenesis and antioxidant enzymes during osteogenic differentiation of human mesenchymal stem cells," *Stem Cells*, vol. 26, no. 4, pp. 960–968, 2008.

[14] Y. M. Cho, S. Kwon, Y. K. Pak et al., "Dynamic changes in mitochondrial biogenesis and antioxidant enzymes during the spontaneous differentiation of human embryonic stem cells," *Biochemical and Biophysical Research Communications*, vol. 348, no. 4, pp. 1472–1478, 2006.

[15] A. Prigione and J. Adjaye, "Modulation of mitochondrial biogenesis and bioenergetic metabolism upon in vitro and in vivo differentiation of human ES and iPS cells," *The International Journal of Developmental Biology*, vol. 54, no. 11-12, pp. 1729–1741, 2010.

[16] A. Vazquez-Martin, S. Cufi, B. Corominas-Faja, C. Oliveras-Ferraros, L. Vellon, and J. A. Menendez, "Mitochondrial fusion by pharmacological manipulation impedes somatic cell reprogramming to pluripotency: new insight into the role of mitophagy in cell stemness," *Aging*, vol. 4, no. 6, pp. 393–401, 2012.

[17] T. J. Zhou, S. L. Zhang, C. Y. He et al., "Downregulation of mitochondrial cyclooxygenase-2 inhibits the stemness of nasopharyngeal carcinoma by decreasing the activity of dynamin-related protein 1," *Theranostics*, vol. 7, no. 5, pp. 1389–1406, 2017.

[18] P. Katajisto, J. Dohla, C. L. Chaffer et al., "Asymmetric apportioning of aged mitochondria between daughter cells is required for stemness," *Science*, vol. 348, no. 6232, pp. 340–343, 2015.

[19] J. Prieto, M. Leon, X. Ponsoda et al., "Dysfunctional mitochondrial fission impairs cell reprogramming," *Cell Cycle*, vol. 15, no. 23, pp. 3240–3250, 2016.

[20] L. Wang, T. Zhang, L. Wang et al., "Fatty acid synthesis is critical for stem cell pluripotency via promoting mitochondrial fission," *The EMBO Journal*, vol. 36, no. 10, pp. 1330–1347, 2017.

[21] X. Zhong, P. Cui, Y. Cai et al., "Mitochondrial dynamics is critical for the full pluripotency and embryonic developmental potential of pluripotent stem cells," *Cell Metabolism*, 2018.

[22] L. R. Todd, M. N. Damin, R. Gomathinayagam, S. R. Horn, A. R. Means, and U. Sankar, "Growth factor erv1-like modulates Drp1 to preserve mitochondrial dynamics and function in mouse embryonic stem cells," *Molecular Biology of the Cell*, vol. 21, no. 7, pp. 1225–1236, 2010.

[23] X. Qi, N. Qvit, Y. C. Su, and D. Mochly-Rosen, "A novel Drp1 inhibitor diminishes aberrant mitochondrial fission and neurotoxicity," *Journal of Cell Science*, vol. 126, no. 3, pp. 789–802, 2013.

[24] T. Yu, S. S. Sheu, J. L. Robotham, and Y. Yoon, "Mitochondrial fission mediates high glucose-induced cell death through elevated production of reactive oxygen species," *Cardiovascular Research*, vol. 79, no. 2, pp. 341–351, 2008.

[25] G. Liot, B. Bossy, S. Lubitz, Y. Kushnareva, N. Sejbuk, and E. Bossy-Wetzel, "Complex II inhibition by 3-NP causes mitochondrial fragmentation and neuronal cell death via an NMDA- and ROS-dependent pathway," *Cell Death and Differentiation*, vol. 16, no. 6, pp. 899–909, 2009.

[26] T. Yu, J. L. Robotham, and Y. Yoon, "Increased production of reactive oxygen species in hyperglycemic conditions requires dynamic change of mitochondrial morphology," *Proceedings of the National Academy of Sciences of the United States of America*, vol. 103, no. 8, pp. 2653–2658, 2006.

[27] K. Ito, A. Hirao, F. Arai et al., "Regulation of oxidative stress by ATM is required for self-renewal of haematopoietic stem cells," *Nature*, vol. 431, no. 7011, pp. 997–1002, 2004.

[28] K. Ito, A. Hirao, F. Arai et al., "Reactive oxygen species act through p38 MAPK to limit the lifespan of hematopoietic stem cells," *Nature Medicine*, vol. 12, no. 4, pp. 446–451, 2006.

[29] C. L. Bigarella, R. Liang, and S. Ghaffari, "Stem cells and the impact of ROS signaling," *Development*, vol. 141, no. 22, pp. 4206–4218, 2014.

[30] M. Khacho, A. Clark, D. S. Svoboda et al., "Mitochondrial dynamics impacts stem cell identity and fate decisions by regulating a nuclear transcriptional program," *Cell Stem Cell*, vol. 19, no. 2, pp. 232–247, 2016.

[31] H. Morimoto, K. Iwata, N. Ogonuki et al., "ROS are required for mouse spermatogonial stem cell self-renewal," *Cell Stem Cell*, vol. 12, no. 6, pp. 774–786, 2013.

[32] M. K. Paul, B. Bisht, D. O. Darmawan et al., "Dynamic changes in intracellular ROS levels regulate airway basal stem cell homeostasis through Nrf2-dependent notch signaling," *Cell Stem Cell*, vol. 15, no. 2, pp. 199–214, 2014.

[33] S. Iqbal and D. A. Hood, "Oxidative stress-induced mitochondrial fragmentation and movement in skeletal muscle myoblasts," *American Journal of Physiology. Cell Physiology*, vol. 306, no. 12, pp. C1176–C1183, 2014.

[34] D. Y. Kim, S. Y. Jung, Y. J. Kim et al., "Hypoxia-dependent mitochondrial fission regulates endothelial progenitor cell migration, invasion, and tube formation," *The Korean Journal of Physiology & Pharmacology*, vol. 22, no. 2, pp. 203–213, 2018.

[35] E. Q. Toyama, S. Herzig, J. Courchet et al., "AMP-activated protein kinase mediates mitochondrial fission in response to energy stress," *Science*, vol. 351, no. 6270, pp. 275–281, 2016.

[36] Y. Lee, H. Y. Lee, R. A. Hanna, and A. B. Gustafsson, "Mitochondrial autophagy by Bnip3 involves Drp1-mediated mitochondrial fission and recruitment of Parkin in cardiac myocytes," *American Journal of Physiology-Heart and Circulatory Physiology*, vol. 301, no. 5, pp. H1924–H1931, 2011.

[37] K. Mao, K. Wang, X. Liu, and D. J. Klionsky, "The scaffold protein Atg11 recruits fission machinery to drive selective mitochondria degradation by autophagy," *Developmental Cell*, vol. 26, no. 1, pp. 9–18, 2013.

[38] J. T. Cribbs and S. Strack, "Reversible phosphorylation of Drp1 by cyclic AMP-dependent protein kinase and calcineurin regulates mitochondrial fission and cell death," *EMBO Reports*, vol. 8, no. 10, pp. 939–944, 2007.

[39] S. Frank, B. Gaume, E. S. Bergmann-Leitner et al., "The role of dynamin-related protein 1, a mediator of mitochondrial fission, in apoptosis," *Developmental Cell*, vol. 1, no. 4, pp. 515–525, 2001.

[40] Y. J. Lee, S. Y. Jeong, M. Karbowski, C. L. Smith, and R. J. Youle, "Roles of the mammalian mitochondrial fission and fusion mediators Fis1, Drp1, and Opa1 in apoptosis," *Molecular Biology of the Cell*, vol. 15, no. 11, pp. 5001–5011, 2004.

[41] S. Kim, C. Kim, and S. Park, "Mdivi-1 protects adult rat hippocampal neural stem cells against palmitate-induced oxidative stress and apoptosis," *International Journal of Molecular Sciences*, vol. 18, no. 9, 2017.

[42] H. Deng, S. Takashima, M. Paul, M. Guo, and V. Hartenstein, "Mitochondrial dynamics regulates Drosophila intestinal stem cell differentiation," *Cell Death Discovery*, vol. 4, no. 1, 2018.

[43] A. Bahat, A. Goldman, Y. Zaltsman et al., "MTCH2-mediated mitochondrial fusion drives exit from naïve pluripotency in embryonic stem cells," *Nature Communications*, vol. 9, no. 1, p. 5132, 2018.

[44] D. Fang, S. Yan, Q. Yu, D. Chen, and S. S. Yan, "Mfn2 is required for mitochondrial development and synapse formation in human induced pluripotent stem cells/hiPSC derived cortical neurons," *Scientific Reports*, vol. 6, no. 1, article 31462, 2016.

[45] M. F. Forni, J. Peloggia, K. Trudeau, O. Shirihai, and A. J. Kowaltowski, "Murine mesenchymal stem cell commitment to differentiation is regulated by mitochondrial dynamics," *Stem Cells*, vol. 34, no. 3, pp. 743–755, 2016.

[46] F. Atashi, A. Modarressi, and M. S. Pepper, "The role of reactive oxygen species in mesenchymal stem cell adipogenic and osteogenic differentiation: a review," *Stem Cells and Development*, vol. 24, no. 10, pp. 1150–1163, 2015.

[47] M. J. Wu, Y. S. Chen, M. R. Kim et al., "Epithelial-mesenchymal transition directs stem cell polarity via regulation of mitofusin," *Cell Metabolism*, 2018.

[48] M. Neuspiel, R. Zunino, S. Gangaraju, P. Rippstein, and H. McBride, "Activated mitofusin 2 signals mitochondrial fusion, interferes with Bax activation, and reduces susceptibility to radical induced depolarization," *Journal of Biological Chemistry*, vol. 280, no. 26, pp. 25060–25070, 2005.

[49] R. Sugioka, S. Shimizu, and Y. Tsujimoto, "Fzo1, a protein involved in mitochondrial fusion, inhibits apoptosis," *The Journal of Biological Chemistry*, vol. 279, no. 50, pp. 52726–52734, 2004.

[50] T. T. Ho, M. R. Warr, E. R. Adelman et al., "Autophagy maintains the metabolism and function of young and old stem cells," *Nature*, vol. 543, no. 7644, pp. 205–210, 2017.

[51] K. Liu, Q. Zhao, P. Liu et al., "ATG3-dependent autophagy mediates mitochondrial homeostasis in pluripotency acquirement and maintenance," *Autophagy*, vol. 12, no. 11, pp. 2000–2008, 2016.

[52] S. Pei, M. Minhajuddin, B. Adane et al., "AMPK/FIS1-mediated mitophagy is required for self-renewal of human AML stem cells," *Cell Stem Cell*, vol. 23, no. 1, pp. 86–100.e6, 2018.

[53] K. Ito, R. Turcotte, J. Cui et al., "Self-renewal of a purified *Tie2*$^{+}$ hematopoietic stem cell population relies on mitochondrial clearance," *Science*, vol. 354, no. 6316, pp. 1156–1160, 2016.

[54] A. Vazquez-Martin, C. den Haute, S. Cufí et al., "Mitophagy-driven mitochondrial rejuvenation regulates stem cell fate," *Aging*, vol. 8, no. 7, pp. 1330–1352, 2016.

[55] M. A. Bin-Umer, J. E. McLaughlin, M. S. Butterly, S. McCormick, and N. E. Tumer, "Elimination of damaged mitochondria through mitophagy reduces mitochondrial oxidative stress and increases tolerance to trichothecenes," *Proceedings of the National Academy of Sciences of the United States of America*, vol. 111, no. 32, pp. 11798–11803, 2014.

[56] W. Wu, H. Xu, Z. Wang et al., "PINK1-Parkin-mediated mitophagy protects mitochondrial integrity and prevents metabolic stress-induced endothelial injury," *PLoS One*, vol. 10, no. 7, article e0132499, 2015.

[57] S. K. Agnihotri, R. Shen, J. Li, X. Gao, and H. Bueler, "Loss of PINK1 leads to metabolic deficits in adult neural stem cells and impedes differentiation of newborn neurons in the mouse hippocampus," *The FASEB Journal*, vol. 31, no. 7, pp. 2839–2853, 2017.

[58] J. Sin, A. M. Andres, D. J. R. Taylor et al., "Mitophagy is required for mitochondrial biogenesis and myogenic differentiation of C2C12 myoblasts," *Autophagy*, vol. 12, no. 2, pp. 369–380, 2015.

[59] H. Dai, Y. Deng, J. Zhang et al., "PINK1/Parkin-mediated mitophagy alleviates chlorpyrifos-induced apoptosis in SH-SY5Y cells," *Toxicology*, vol. 334, pp. 72–80, 2015.

[60] A. Swiader, H. Nahapetyan, J. Faccini et al., "Mitophagy acts as a safeguard mechanism against human vascular smooth muscle cell apoptosis induced by atherogenic lipids," *Oncotarget*, vol. 7, no. 20, pp. 28821–28835, 2016.

[61] Y. Zhu, S. Massen, M. Terenzio et al., "Modulation of serines 17 and 24 in the LC3-interacting region of Bnip3 determines pro-survival mitophagy versus apoptosis," *The Journal of Biological Chemistry*, vol. 288, no. 2, pp. 1099–1113, 2013.

[62] M. Uldry, W. Yang, J. St-Pierre, J. Lin, P. Seale, and B. M. Spiegelman, "Complementary action of the PGC-1 coactivators in mitochondrial biogenesis and brown fat differentiation," *Cell Metabolism*, vol. 3, no. 5, pp. 333–341, 2006.

[63] J. H. An, J. Y. Yang, B. Y. Ahn et al., "Enhanced mitochondrial biogenesis contributes to Wnt induced osteoblastic differentiation of C3H10T1/2 cells," *Bone*, vol. 47, no. 1, pp. 140–150, 2010.

[64] C. Mantel, S. Messina-Graham, and H. E. Broxmeyer, "Upregulation of nascent mitochondrial biogenesis in mouse hematopoietic stem cells parallels upregulation of CD34 and loss of pluripotency: a potential strategy for reducing oxidative risk in stem cells," *Cell Cycle*, vol. 9, no. 10, pp. 2008–2017, 2014.

[65] C. Chen, Y. Liu, R. Liu et al., "TSC-mTOR maintains quiescence and function of hematopoietic stem cells by repressing mitochondrial biogenesis and reactive oxygen species," *The Journal of Experimental Medicine*, vol. 205, no. 10, pp. 2397–2408, 2008.

[66] A. De Luca, M. Fiorillo, M. Peiris-Pages et al., "Mitochondrial biogenesis is required for the anchorage-independent survival and propagation of stem-like cancer cells," *Oncotarget*, vol. 6, no. 17, pp. 14777–14795, 2015.

[67] Y. He, X. Gan, L. Zhang et al., "$CoCl_2$ induces apoptosis via a ROS-dependent pathway and Drp1-mediated mitochondria fission in periodontal ligament stem cells," *American Journal of Physiology. Cell Physiology*, vol. 315, no. 3, pp. C389–C397, 2018.

[68] G. Santilli, G. Lamorte, L. Carlessi et al., "Mild hypoxia enhances proliferation and multipotency of human neural stem cells," *PLoS One*, vol. 5, no. 1, article e8575, 2010.

[69] S. G. Canfield, I. Zaja, B. Godshaw, D. Twaroski, X. Bai, and Z. J. Bosnjak, "High glucose attenuates anesthetic cardioprotection in stem-cell-derived cardiomyocytes: the role of reactive oxygen species and mitochondrial fission," *Anesthesia and Analgesia*, vol. 122, no. 5, pp. 1269–1279, 2016.

[70] J. A. McCubrey, M. M. Lahair, and R. A. Franklin, "Reactive oxygen species-induced activation of the MAP kinase signaling pathways," *Antioxidants & Redox Signaling*, vol. 8, no. 9-10, pp. 1775–1789, 2006.

[71] N. Gaiano and G. Fishell, "The role of notch in promoting glial and neural stem cell fates," *Annual Review of Neuroscience*, vol. 25, no. 1, pp. 471–490, 2002.

[72] Q. Jin, R. Li, N. Hu et al., "DUSP1 alleviates cardiac ischemia/reperfusion injury by suppressing the Mff-required mitochondrial fission and Bnip3-related mitophagy via the JNK pathways," *Redox Biology*, vol. 14, pp. 576–587, 2018.

[73] J. A. Kashatus, A. Nascimento, L. J. Myers et al., "Erk2 phosphorylation of Drp1 promotes mitochondrial fission and MAPK-driven tumor growth," *Molecular Cell*, vol. 57, no. 3, pp. 537–551, 2015.

[74] I. Garcia, W. Innis-Whitehouse, A. Lopez, M. Keniry, and R. Gilkerson, "Oxidative insults disrupt OPA1-mediated mitochondrial dynamics in cultured mammalian cells," *Redox Report*, vol. 23, no. 1, pp. 160–167, 2018.

[75] A. Rakovic, A. Grunewald, J. Kottwitz et al., "Mutations in PINK1 and Parkin impair ubiquitination of mitofusins in human fibroblasts," *PLoS One*, vol. 6, no. 3, article e16746, 2011.

[76] M. Frank, S. Duvezin-Caubet, S. Koob et al., "Mitophagy is triggered by mild oxidative stress in a mitochondrial fission dependent manner," *Biochimica et Biophysica Acta (BBA) - Molecular Cell Research*, vol. 1823, no. 12, pp. 2297–2310, 2012.

[77] I. Kim, S. Rodriguez-Enriquez, and J. J. Lemasters, "Selective degradation of mitochondria by mitophagy," *Archives of Biochemistry and Biophysics*, vol. 462, no. 2, pp. 245–253, 2007.

[78] Y. Kurihara, T. Kanki, Y. Aoki et al., "Mitophagy plays an essential role in reducing mitochondrial production of reactive oxygen species and mutation of mitochondrial DNA by maintaining mitochondrial quantity and quality in yeast," *The Journal of Biological Chemistry*, vol. 287, no. 5, pp. 3265–3272, 2012.

[79] Y. Wang, Y. Nartiss, B. Steipe, G. A. McQuibban, and P. K. Kim, "ROS-induced mitochondrial depolarization initiates PARK2/PARKIN-dependent mitochondrial degradation by autophagy," *Autophagy*, vol. 8, no. 10, pp. 1462–1476, 2014.

[80] A. H. Chaanine, D. Jeong, L. Liang et al., "JNK modulates FOXO3a for the expression of the mitochondrial death and mitophagy marker BNIP3 in pathological hypertrophy and in heart failure," *Cell Death & Disease*, vol. 3, no. 2, p. 265, 2012.

[81] S. D. Chen, D. I. Yang, T. K. Lin, F. Z. Shaw, C. W. Liou, and Y. C. Chuang, "Roles of oxidative stress, apoptosis, PGC-1α and mitochondrial biogenesis in cerebral ischemia," *International Journal of Molecular Sciences*, vol. 12, no. 10, pp. 7199–7215, 2011.

[82] I. Irrcher, V. Ljubicic, and D. A. Hood, "Interactions between ROS and AMP kinase activity in the regulation of PGC-1α transcription in skeletal muscle cells," *American Journal of Physiology. Cell Physiology*, vol. 296, no. 1, pp. C116–C123, 2009.

[83] K. Palikaras and N. Tavernarakis, "Mitochondrial homeostasis: the interplay between mitophagy and mitochondrial biogenesis," *Experimental Gerontology*, vol. 56, pp. 182–188, 2014.

[84] T. Wenz, "Regulation of mitochondrial biogenesis and PGC-1α under cellular stress," *Mitochondrion*, vol. 13, no. 2, pp. 134–142, 2013.

[85] W. Cao, K. W. Daniel, J. Robidoux et al., "p38 mitogen-activated protein kinase is the central regulator of cyclic AMP-dependent transcription of the brown fat uncoupling protein 1 gene," *Molecular and Cellular Biology*, vol. 24, no. 7, pp. 3057–3067, 2004.

[86] P. Puigserver, J. Rhee, J. Lin et al., "Cytokine stimulation of energy expenditure through p38 MAP kinase activation of PPARγ coactivator-1," *Molecular Cell*, vol. 8, no. 5, pp. 971–982, 2001.

[87] S. H. Dai, T. Chen, Y. H. Wang et al., "Sirt3 protects cortical neurons against oxidative stress via regulating mitochondrial Ca^{2+} and mitochondrial biogenesis," *International Journal of Molecular Sciences*, vol. 15, no. 8, pp. 14591–14609, 2014.

[88] A. H. H. Tseng, S.-S. Shieh, and D. L. Wang, "SIRT3 deacetylates FOXO3 to protect mitochondria against oxidative damage," *Free Radical Biology & Medicine*, vol. 63, pp. 222–234, 2013.

[89] A. S. Rambold, B. Kostelecky, N. Elia, and J. Lippincott-Schwartz, "Tubular network formation protects mitochondria from autophagosomal degradation during nutrient starvation," *Proceedings of the National Academy of Sciences of the United States of America*, vol. 108, no. 25, pp. 10190–10195, 2011.

[90] C. R. Chang and C. Blackstone, "Cyclic AMP-dependent protein kinase phosphorylation of Drp1 regulates its GTPase activity and mitochondrial morphology," *The Journal of Biological Chemistry*, vol. 282, no. 30, pp. 21583–21587, 2007.

[91] S. H. Ko, G. E. Choi, J. Y. Oh et al., "Succinate promotes stem cell migration through the GPR91-dependent regulation of DRP1-mediated mitochondrial fission," *Scientific Reports*, vol. 7, no. 1, p. 12582, 2017.

[92] E. C. Hinchy, A. V. Gruszczyk, R. Willows et al., "Mitochondria-derived ROS activate AMP-activated protein kinase (AMPK) indirectly," *The Journal of Biological Chemistry*, vol. 293, no. 44, pp. 17208–17217, 2018.

[93] P. T. Mungai, G. B. Waypa, A. Jairaman et al., "Hypoxia triggers AMPK activation through reactive oxygen species-mediated activation of calcium release-activated calcium channels," *Molecular and Cellular Biology*, vol. 31, no. 17, pp. 3531–3545, 2011.

[94] R. C. Rabinovitch, B. Samborska, B. Faubert et al., "AMPK maintains cellular metabolic homeostasis through regulation of mitochondrial reactive oxygen species," *Cell Reports*, vol. 21, no. 1, pp. 1–9, 2017.

[95] J. Li, Y. Wang, Y. Wang et al., "Pharmacological activation of AMPK prevents Drp1-mediated mitochondrial fission and alleviates endoplasmic reticulum stress-associated endothelial dysfunction," *Journal of Molecular and Cellular Cardiology*, vol. 86, pp. 62–74, 2015.

[96] H. J. Weir, P. Yao, F. K. Huynh et al., "Dietary restriction and AMPK increase lifespan via mitochondrial network and peroxisome remodeling," *Cell Metabolism*, vol. 26, no. 6, article e885, pp. 884–896.e5, 2017.

[97] S. W. S. Kang, G. Haydar, C. Taniane et al., "AMPK activation prevents and reverses drug-induced mitochondrial and hepatocyte injury by promoting mitochondrial fusion and function," *PLoS One*, vol. 11, no. 10, article e0165638, 2016.

[98] S. A. Samant, H. J. Zhang, Z. Hong et al., "SIRT3 deacetylates and activates OPA1 to regulate mitochondrial dynamics during stress," *Molecular and Cellular Biology*, vol. 34, no. 5, pp. 807–819, 2014.

[99] S. Y. Jang, H. T. Kang, and E. S. Hwang, "Nicotinamide-induced mitophagy: event mediated by high NAD^+/NADH ratio and SIRT1 protein activation," *The Journal of Biological Chemistry*, vol. 287, no. 23, pp. 19304–19314, 2012.

[100] E. F. Fang, M. Scheibye-Knudsen, L. E. Brace et al., "Defective mitophagy in XPA via PARP-1 hyperactivation and NAD^+/SIRT1 reduction," *Cell*, vol. 157, no. 4, pp. 882–896, 2014.

[101] R. Huang, Y. Xu, W. Wan et al., "Deacetylation of nuclear LC3 drives autophagy initiation under starvation," *Molecular Cell*, vol. 57, no. 3, pp. 456–466, 2015.

[102] I. H. Lee, L. Cao, R. Mostoslavsky et al., "A role for the NAD-dependent deacetylase Sirt1 in the regulation of autophagy," *Proceedings of the National Academy of Sciences of the United States of America*, vol. 105, no. 9, pp. 3374–3379, 2008.

[103] I. Scott, B. R. Webster, C. K. Chan, J. U. Okonkwo, K. Han, and M. N. Sack, "GCN5-like protein 1 (GCN5L1) controls mitochondrial content through coordinated regulation of mitochondrial biogenesis and mitophagy," *The Journal of Biological Chemistry*, vol. 289, no. 5, pp. 2864–2872, 2014.

[104] B. R. Webster, I. Scott, K. Han et al., "Restricted mitochondrial protein acetylation initiates mitochondrial autophagy," *Journal of Cell Science*, vol. 126, no. 21, pp. 4843–4849, 2013.

[105] D. F. Egan, D. B. Shackelford, M. M. Mihaylova et al., "Phosphorylation of ULK1 (hATG1) by AMP-activated protein kinase connects energy sensing to mitophagy," *Science*, vol. 331, no. 6016, pp. 456–461, 2011.

[106] R. C. Laker, J. C. Drake, R. J. Wilson et al., "Ampk phosphorylation of Ulk1 is required for targeting of mitochondria to lysosomes in exercise-induced mitophagy," *Nature Communications*, vol. 8, no. 1, p. 548, 2017.

[107] E. Nisoli, C. Tonello, A. Cardile et al., "Calorie restriction promotes mitochondrial biogenesis by inducing the expression of eNOS," *Science*, vol. 310, no. 5746, pp. 314–317, 2005.

[108] A. E. Civitarese, S. Carling, L. K. Heilbronn et al., "Calorie restriction increases muscle mitochondrial biogenesis in healthy humans," *PLoS Medicine*, vol. 4, no. 3, article e76, 2007.

[109] G. López-Lluch, N. Hunt, B. Jones et al., "Calorie restriction induces mitochondrial biogenesis and bioenergetic efficiency," *Proceedings of the National Academy of Sciences of the United States of America*, vol. 103, no. 6, pp. 1768–1773, 2006.

[110] H. Zong, J. M. Ren, L. H. Young et al., "AMP kinase is required for mitochondrial biogenesis in skeletal muscle in response to chronic energy deprivation," *Proceedings of the National Academy of Sciences of the United States of America*, vol. 99, no. 25, pp. 15983–15987, 2002.

[111] R. Bergeron, J. M. Ren, K. S. Cadman et al., "Chronic activation of AMP kinase results in NRF-1 activation and mitochondrial biogenesis," *American Journal of Physiology. Endocrinology and Metabolism*, vol. 281, no. 6, pp. E1340–E1346, 2001.

[112] S. Jager, C. Handschin, J. St.-Pierre, and B. M. Spiegelman, "AMP-activated protein kinase (AMPK) action in skeletal muscle via direct phosphorylation of PGC-1α," *Proceedings of the National Academy of Sciences of the United States of America*, vol. 104, no. 29, pp. 12017–12022, 2007.

[113] A. Cassidy-Stone, J. E. Chipuk, E. Ingerman et al., "Chemical inhibition of the mitochondrial division dynamin reveals its role in Bax/Bak-dependent mitochondrial outer membrane permeabilization," *Developmental Cell*, vol. 14, no. 2, pp. 193–204, 2008.

[114] M.-H. Disatnik, J. C. B. Ferreira, J. C. Campos et al., "Acute inhibition of excessive mitochondrial fission after myocardial infarction prevents long-term cardiac dysfunction," *Journal of the American Heart Association*, vol. 2, no. 5, article e000461, 2013.

[115] E. Macia, M. Ehrlich, R. Massol, E. Boucrot, C. Brunner, and T. Kirchhausen, "Dynasore, a cell-permeable inhibitor of dynamin," *Developmental Cell*, vol. 10, no. 6, pp. 839–850, 2006.

[116] D. Gao, L. Zhang, R. Dhillon, T. T. Hong, R. M. Shaw, and J. Zhu, "Dynasore protects mitochondria and improves cardiac lusitropy in Langendorff perfused mouse heart," *PLoS One*, vol. 8, no. 4, article e60967, 2013.

[117] D. Wang, J. Wang, G. M. C. Bonamy et al., "A small molecule promotes mitochondrial fusion in mammalian cells," *Angewandte Chemie*, vol. 51, no. 37, pp. 9302–9305, 2012.

[118] K. Peng, L. Yang, J. Wang et al., "The interaction of mitochondrial biogenesis and fission/fusion mediated by PGC-1α regulates rotenone-induced dopaminergic neurotoxicity," *Molecular Neurobiology*, vol. 54, no. 5, pp. 3783–3797, 2017.

[119] L. Miret-Casals, D. Sebastian, J. Brea et al., "Identification of new activators of mitochondrial fusion reveals a link between

mitochondrial morphology and pyrimidine metabolism," *Cell Chemical Biology*, vol. 25, no. 3, article e264, pp. 268–278.e4, 2018.

[120] G. Farnie, F. Sotgia, and M. P. Lisanti, "High mitochondrial mass identifies a sub-population of stem-like cancer cells that are chemo-resistant," *Oncotarget*, vol. 6, no. 31, pp. 30472–30486, 2015.

[121] J. Wang, Y. Wang, and C. Wong, "Oestrogen-related receptor alpha inverse agonist XCT-790 arrests A549 lung cancer cell population growth by inducing mitochondrial reactive oxygen species production," *Cell Proliferation*, vol. 43, no. 2, pp. 103–113, 2010.

[122] R. Lamb, B. Ozsvari, C. L. Lisanti et al., "Antibiotics that target mitochondria effectively eradicate cancer stem cells, across multiple tumor types: treating cancer like an infectious disease," *Oncotarget*, vol. 6, no. 7, pp. 4569–4584, 2015.

[123] M. Y. Chang, Y. H. Rhee, S. H. Yi et al., "Doxycycline enhances survival and self-renewal of human pluripotent stem cells," *Stem Cell Reports*, vol. 3, no. 2, pp. 353–364, 2014.

[124] T. Krakauer and M. Buckley, "Doxycycline is anti-inflammatory and inhibits staphylococcal exotoxin-induced cytokines and chemokines," *Antimicrobial Agents and Chemotherapy*, vol. 47, no. 11, pp. 3630–3633, 2003.

Hindawi
Stem Cells International
Volume 2019, Article ID 2875189, 11 pages
https://doi.org/10.1155/2019/2875189

Review Article

The Emerging Role of Mesenchymal Stem Cells in Vascular Calcification

Changming Xie[1,2] **Liu Ouyang**[2] **Jie Chen**[3] **Huanji Zhang**[1] **Pei Luo**[4] **Jingfeng Wang**[2] **and Hui Huang**[1,2]

[1]*Department of Cardiology, The Eighth Affiliated Hospital, Sun Yat-sen University, Shenzhen 518000, China*
[2]*Guangdong Provincial Key Laboratory of Malignant Tumor Epigenetics and Gene Regulation, Department of Cardiology, Sun Yat-sen Memorial Hospital, Sun Yat-sen University, Guangzhou 510120, China*
[3]*Department of Radiation Oncology, Sun Yat-sen Memorial Hospital, Sun Yat-sen University, Guangzhou 510120, China*
[4]*State Key Laboratory for Quality Research of Chinese Medicines, Macau University of Science and Technology, Taipa 999078, Macau*

Correspondence should be addressed to Hui Huang; huanghui765@hotmail.com

Received 16 October 2018; Revised 12 January 2019; Accepted 11 February 2019; Published 1 April 2019

Guest Editor: Athanassia Sotiropoulos

Vascular calcification (VC), characterized by hydroxyapatite crystal depositing in the vessel wall, is a common pathological condition shared by many chronic diseases and an independent risk factor for cardiovascular events. Recently, VC is regarded as an active, dynamic cell-mediated process, during which calcifying cell transition is critical. Mesenchymal stem cells (MSCs), with a multidirectional differentiation ability and great potential for clinical application, play a duplex role in the VC process. MSCs facilitate VC mainly through osteogenic transformation and apoptosis. Meanwhile, several studies have reported the protective role of MSCs. Anti-inflammation, blockade of the BMP2 signal, downregulation of the Wnt signal, and antiapoptosis through paracrine signaling are possible mechanisms. This review displays the evidence both on the facilitating role and on the protective role of MSCs, then discusses the key factors determining this divergence.

1. Introduction

Vascular calcification (VC) is a pathological accumulation of calcium phosphate crystal depositing in the medial and intimal layers of the vessel wall. This common pathologic hallmark is shared by multiple chronic diseases. For example, atherosclerosis and its comorbidities, such as diabetes and chronic kidney disease (CKD), display this feature. Calcification is a major risk factor for cardiovascular mobility and mortality [1]. However, the exact mechanisms underlying VC are poorly characterized. Reliable clinical therapies are in high demand. However, there are no effective treatments currently able to reverse calcium deposition. Recently, VC is considered an active process regulated by cellular pathways resembling those participating in bone morphogenesis. Some cell types consisting of the arterial wall would reprogram their genetic expression patterns, transform into osteoblast-like cells, and initiate the mineralization of the extracellular matrix (ECM) in response to multiple stimulations, involving cyclic strain overload [2], inflammation [3], and metabolic disorder [4, 5]. The interaction between the bone and cardiovascular system gives rise to tremendous interest among researchers. For example, Cianciolo et al. and Fadini et al. found that bone marrow-derived cells could immigrate from circulation into vessels, transform into osteogenic cells, and then facilitate VC [6, 7]. One subpopulation of those bone marrow-derived cells is CD34+ (marker of hematopoietic stem cells) cells including endothelial precursor cells (EPCs) and calcifying myeloid cells. While the other is CD34- mesenchymal stem cells (MSCs) [6, 8].

Mesenchymal stem cells, also known as marrow stromal cells, bone marrow fibroblasts, or skeletal stem cells, are typically defined as follows: (1) MSCs must be plastic-adherent when maintained in standard culture conditions, (2) MSCs

must express CD105, CD73, and CD90 and lack the expression of CD45, CD34, CD14 or CD11b, CD79α or CD19, and HLA-DR surface molecules, and (3) MSCs must differentiate into osteoblasts, adipocytes, and chondroblasts in vitro [9]. Based on their source and location, they could be classified as bone marrow- (BM-) MSCs, peripheral blood-MSCs, or pericytes [10]. As has been observed previously, MSCs are well demonstrated to exhibit remarkable immune regulation and anti-inflammation capacities such as angiogenesis in regenerative medicine [11]. Therefore, it is likely that MSCs are candidates to contribute to the alleviation of VC. According to Zhu et al., coculture of vascular smooth muscle cells (VSMCs) with BM-MSCs could inhibit vascular calcification via the Wnt signaling pathway [12]. However, Cho et al. calculated the calcium accumulation level of arteries in an atherosclerosis model and found it to be increased significantly after injecting MSCs [13].

For now, the role of MSCs in the VC process still remains unclear and controversial. Whether MSCs facilitate or inhibit VC is a pending question yet to be identified.

This review begins with a brief description of the physiological functions of MSCs and definition of VC, followed by a discussion of recent studies of MSCs in VC and their underlying pleiotropic mechanism.

2. Physiological Roles of MSCs in the Vascular System

Blood vessels are the most widely distributed tissue in the human body and are vital for the development, normal physiology, and most, if not all, human diseases. As one type of vascular progenitor cells, MSCs serve as essential participants in the formation, repair, and remodeling of arterial vessels [14]. It is widely accepted that MSCs could differentiate into endothelial cells, VSMCs, or pericytes [15–17]. Besides, MSCs have the capacity to promote angiogenesis by secreting proangiogenic factors or producing extracellular vesicles in a paracrine-dependent manner [18]. In addition, studies proved that MSCs are able to govern immunity and restrain inflammation. BM-MSCs could suppress T cell proliferation by secreting soluble factors with immunosuppressive activity, including indoleamine 2,3-dioxygenase (IDO), prostaglandin E2 (PGE2), interleukin 10 (IL-10), IL-6, and IL-17 [19]. All of these promising effects make them a potential therapy required for vascular repair and regeneration.

3. Characters of Vascular Calcification

VC refers to ectopic deposits of hydroxyapatite with a high degree of crystallization in the wall of vessels. VC frequently occurs in atherosclerosis, hypertension, diabetes, CKD, and aging [20]. Morphologically, VC can be divided into intimal and medial calcification. Calcification of the intimal layer usually occurs in large- and medium-sized elastic arteries [21]. It was considered a feature of advanced atherosclerosis and may be responsible for coronary ischemic events. However, some other research reported that most calcified plaques may be more stable and that the plaques that are most vulnerable to rupture may be those which have a mixed composition of calcified and noncalcified tissue [22]. Intimal VC is more relevant to vascular senescence and chronic inflammation [23]. Medial calcification, with pathological characteristics of nonocclusive and preferential development along elastic fibers, is dramatically increased in chronic kidney disease-mineral and bone disorder (CKD-MBD) [24]. Disturbances of calcium and phosphate metabolism, a perturbation of the bone vascular axis, and reduction of calcification inhibitors are all considered potential mechanisms.

Cells from all layers of the vessel wall could transform into osteoblast-like cells. Taking calcified VSMCs for example, they lost parts of their contractile phenotype, which is supported by downregulation of α-smooth muscle actin (α-SMA) and SM-22. Meanwhile, they are featured by abnormal increasing expression of the osteogenesis gene, for instance, Runt-related transcription factor 2 (Runx2), osterix, osteopontin (OPN), and osteocalcin (OCN) [3].

VC was initiated by matrix vesicles (MVs), which are produced by osteoblast-like cells and act as sites for hydroxyapatite crystal precipitation. Meanwhile, elastin is degraded due to the overexpression of matrix metalloproteinase by calcified cells, which in turn promotes VSMCs losing their contractile markers. Taken together, phenotypic transition is the driving factor during the calcification process.

4. Evidence of the Facilitating Role of MSCs in VC

As discussed above, osteoblast-like cells are the key contributor of VC. Owning the potential of osteogenic differentiation and recruitment to injury vessels, MSCs play a critical role in the "circulating calcifying cell theory"; in other words, they may act as a source of osteoblast-like cells.

Several in vitro studies provided direct evidences on the ability of MSCs to differentiate into osteoblast-like cells in VC cultured osteogenic media. When treated with dexamethasone, β-glycerophosphate (β-GP), and L-ascorbic acid, murine MSCs can be induced to osteoblast-like cells that have strong expression of type I collagen and bone morphogenetic protein-2 (BMP2) and are positive in von Kossa staining [25]. Uremic serum can induce a calcific phenotype in human MSCs in a BMP2/4-dependent manner, accompanied by matrix remodeling and calcification [26], which may serve as a mechanism underlining CKD-related bone disorder. Moreover, MSCs isolated from ApoE-/- mice showed a significant increase in in vitro osteogenesis and chondrogenesis in a cartilage intermediate, which indicates that MSCs may contribute to the ectopic calcification of atherosclerotic plaque [27].

Circulating MSCs can migrate through the blood stream and reach the site of injury in the vessel wall. VC often emerges as a secondary alteration of vessel damage, where a similar recruitment process can be found. Several chemokines have been reported to be involved in the MSC recruitment process of VC: the accelerating effect of transforming growth factor (TGF-β) in VC has been widely accepted [28–30]. Intravenous injection of recombinant active TGF-β1 in uninjured mice rapidly mobilized MSCs into circulation with an amplification effect by the cascade

expression of monocyte chemotactic protein-1 (MCP-1) [31, 32]. In a model of crossing LDLR-/- mice with transgenic mice, fed with high-fat western diets, in which all the MSC-derived cells were fluorescently labeled, Wang et al. reported that both active TGF-β1 mouse levels and MSCs in circulating blood were upregulated at the same time points when these cells appeared at the aortic tissue and lately VC appeared severely. Immunohistochemistry staining showed that the increased active TGF-β1 level was seen throughout the whole wall of the aorta. [30]. As a potent mitogen and chemoattractant, a platelet-derived growth factor (PDGF) has been found to disturb the vascular homeostasis by inflammation, oxidative stress, and phenotype transition, all of which accelerate the process of VC [8]. PDGF-BB was found to be most effective in stimulating MSC migration among other PDGF isoforms and even TGF-β, BMP2, and SDF-α [33]. Interestingly, in Fiedler et al.'s research about vascular calcifying progenitor cells, the chemotactic effect of PDGF-AB exceeds that of PDGF-BB in the case of primary osteoblasts, which reveals a subtype specificity. Under some pathological conditions such as renal ischemia-reperfusion injury and inflammatory cardiomyopathy, stromal cell-derived factor 1 (SDF-1) promotes homing of MSCs to injury sites and enhances the retention of infused cells [34–37]. Wu et al. demonstrated that sympathetic denervation could increase bone formation in distraction osteogenesis. Norepinephrine promotes in local vessels the secretion of SDF-1, which attracts MSCs staying in vessels instead of migrating to the lesioned bone [38]. Parathyroid hormone (PTH), which is unregulated pathologically in CKD, induces an increased expression of SDF-1 through the downregulation of dipeptidylpeptidase IV [39]. Here, we summarize the potential chemokines of MSCs in Table 1.

More directly, Cho et al. calculated the calcium accumulation level of arteries in an atherosclerosis model and found it to be increased significantly after injecting calcifying progenitor cells [13]. Transplantation of BM-MSCs induced vascular remodeling and calcification after balloon angioplasty in hyperlipidemia rats [40]. Another previous study showed increased intramyocardial calcification that resulted from MSC homing after direct transplantation of unselected BM cells [41]. In heterotypical transplantation of MSCs with an established three-dimensional collagen-based skeleton to rat models of CKD, aortas and MSC-containing collagen gels showed distinct similarities in the calcification and upregulation of the osteolytic markers and ECM remodeling with increased expression of osteopontin, collagen I/III/IV, fibronectin, and laminin [42]. To assess the intrinsic calcification capacity of MSCs and the effect of the atherosclerotic environment, a similar experiment where MSCs loaded on collagen-glycosaminoglycan scaffolds were implanted subcutaneously to ApoE-/- was conducted [27]. From above, it is disappointing to find that VC can be a potential side effect of MSC therapy. However, more frustratingly, MSCs are also reported to be involved in VC under many pathological stages in vivo. A research described the biological behavior of adventitial Gli1+ MSCs in ApoE-/- mice with CKD: MSCs migrated into the media in both CKD and sham groups. During 16 weeks after nephrectomy, where severe calcification occurred, they differentiate into VSMCs firstly but eventually lost the expression of VSMC markers and turn to osteoblast-like cells that have strong costaining for Runx2 and are located within calcium tracer-positive areas. This research proposed that MSCs are a major source of osteoblast-like cells during VC [43]. Chlamydia pneumoniae infection may promote VC by indirectly stimulating the phenotypic conversion of MSCs [44].

5. Evidence of the Protective Role of MSCs in VC

MSCs have been identified as an effective agent for application in various diseases/complications including VC. Wang et al. have proved that the bioactive substance secreted by MSCs could retard murine VSMC calcification induced by β-GP with conditioned medium from MSCs (MSC-CM) [45, 46]. Consistent with the above study, Zhu and her colleagues established the indirect coculture system of VSMCs and MSCs with Transwell. Calcification of VSMCs in the lower layer with osteogenic medium was significantly decreased [12].

According to previous evidence, there are four potential pathways involved in MSCs protection of VC.

5.1. Inhibition of Inflammation. The MSC-CM is well known to be a rich source of autologous cytokines, based on which cell-free stem treatment was developed. Various factors derived from MSC-CM such as IL-4, IL-6, and IL-1RA are capable of expressing an anti-inflammatory effect [47, 48], which have been proven to play a role in lung injury, myocardial infarction, and corneal wound [46]. For myocardial infarction, a novel research reports that MSC-derived exosomes can improve the microenvironment contributing to angiogenesis and anti-inflammation [49]. The close association of VC with inflammation has been summarized by many excellent papers [50–52]. Directly, TNF-α, IL-1β, and IL-6, which play crucial roles in the initiation and progression of VC, were found to be suppressed when treated with MSC-CM [45]. NF-κB is a crucial pathway in vascular inflammation [53]. It was downregulated when MSCs' paracrine function was enhanced in lipopolysaccharide-induced inflammation.

5.2. Blockade of the BMP2-Smad1/5/8 Signaling Pathway. Wang et al. firstly demonstrated that MSC-CM suppression of calcification may be mediated by the expression of bone morphogenetic protein-2 (BMP2) and the BMP2 receptor-Smad1/5/8 signaling pathway [46]. BMPs are a superfamily of transforming growth factor-beta (TGF-β) and secretory growth factor, which play a role in bone formation. As described above, BMPs are reported to be expressed strongly in VC and accelerated atherosclerotic intimal calcification in BMP2 transgenic/ApoE-knockout mice [25, 26, 54]. Unfortunately, how MSCs suppress the BMP2 signal is still unclear.

5.3. Downregulation of the Canonical Wnt Signaling Pathways. Three Wnt pathways have been described: the Wnt/β-catenin (canonical pathway) [55], the Wnt/Ca2+ noncanonical pathway, and the noncanonical planar cell polarity pathway (PCP), all of which have been implicated in human cardiovascular diseases [56]. The crucial role of

Table 1: Chemokines of MSCs.

Factors	Main characters	Reference
TGF-β	(1) TGF-β can be released by the damaged vessel cells and lesioned artery and involved in vascular regeneration and VC (2) TGF-β couples bone resorption with formation by inducing MSC migration and participates in bone and cartilage metabolism. Subchondral bone MSCs activated by TGF-β seem to initiate osteoarthritis (3) TGF-β promotes homing of BM-MSC in a tissue lesion, for example, renal ischemia-reperfusion injury (4) TGF-β may regulate the SDF-1/CXCR4 axis and MCP-1 to induce MSC homing	[30–32, 36, 82–87]
PDGF-BB	(1) PDGF has the highest effect among other cytokines (SDF-1a, CXCL16, MIP, etc.), and PDGF-BB is the most strong one among PDGF isoforms in vitro (2) PDGF-BB has been proven to be involved in myocardial and lung functional tissue regeneration, angiogenesis, and VC by recruiting MSCs (3) PDGF-BB has been applied for bone regeneration and proven to recruit MSCs to the scaffolds	[13, 33, 82, 88–92]
PDGF-AA	(1) PDGF-AA's chemotaxis effect is lower than that of PDGF-BB, but stronger in recruiting osteogenic differentiated progenitor cells (2) PDGF-AA can promote MSC proliferation and differentiation (3) The effect of PDGF-AA can be blocked by TGF-β	[82, 93–95]
SDF-1	(1) SDF-1 can be released by the endothelium and ischemic myocardium in myocardial infarction, inflammatory cardiomyopathy, and vascular injury. This cytokine also correlated with the severity of calcification (2) In inflammatory bone destruction, SDF-1 was found to be upregulated, which could possibly enhance fracture healing in osteoporotic patients by recruiting MSCs. And it also improves the vascularization of bone (3) SDF-1 promotes MSCs to repair liver injury, expanded skin, and even cancer (4) Serum SDF-1 can be increased by hypoxemia	[34, 35, 37, 88, 96–104]
BMP2/4/7	It has only been proven in vitro	[82, 89]
FGF	In vivo researches of FGF chemotaxis mainly focus on pulmonary fibrosis	[82, 88, 105, 106]
VEGF	(1) Chemotactic activity of VEGF has been proven in vitro. And VEGF can be released by multiple myeloma and glioma cells to improve vascularization (2) VEGF plays a role in bone regeneration (3) PDGFR-α is required	[82, 89, 107–110]
G-CSF	(1) In vivo chemotactic activity of G-CSF is controversial (2) It may work via CXCR4/SDF-1	[100, 111–113]
TNF-α/IL-1β/IL-6	These cytokines are associated with inflammation and work through the NF-κb pathway. And several researches show that they inhibit instead of promoting migration	[88, 114–118]
IGF-1	Chemotactic activity of IGF-1 is not so assuring. Pretreatment seems more reliable	[89, 119–122]
PTH	PTH can improve osteoporosis in mice and men and spine injuries	[39, 123]

The table shows chemokines of MSCs with a brief introduction of their characters. TGF: transforming growth factor; PDGF: platelet-derived growth factor; SDF: stromal cell-derived factor; BMP: bone morphogenetic protein; FGF: fibroblast growth factor; VEGF: vascular endothelial growth factor; G-CSF: granulocyte colony-stimulating factor; TNF: tumor necrosis factor; IL: interleukin; IGF: insulin-like growth factor; PTH: parathyroid hormone.

Wnt signaling pathways in VC has already been proven by a large number of researches [57, 58], which will be further discussed in the following part. In the indirect coculture study, the activities of canonical and noncanonical Wnt ligands (Wnt5a), receptor tyrosine kinase-like orphan receptor 2 (Ror2), and β-catenin were downregulated [12]. Similarly, how this suppression works remains unknown.

5.4. Inhibition of Apoptosis. Cell apoptosis is regulated by the expression of caspase-3 and the ratio of the antiapoptotic factor Bcl-2 to the proapoptotic factor Bax. This ratio of VSMCs is rescued by MSC-CM in a β-GP-induced VC model [45]. Apoptotic bodies of VSMCs have the capacity to concentrate and crystallize calcium to initiate VC [59]. More directly, bone-targeted overexpression of Bcl-2 in mouse osteoblasts suppressed calcification in vitro [60].

To sum up, the protective role of MSCs in VC is mainly in a paracrine-dependent manner. Autologous cytokines secreted by MSCs regulate VSMC biological behavior in the process of VC. However, further exploration is needed.

6. Possible Mechanisms Determine the Role of Mesenchymal Stem Cells in VC

MSCs differentiate to osteoblast-like cells then promote VC. However, they lead the protective role in a paracrine

manner. That is a brief summary of the role of MSCs in VC. However, it is not clear enough what determines the ultimate effect of VC. The potential factors will be discussed as follows.

6.1. The Microenvironment of the Vessel. Early on, scientists learned the importance of the microenvironment (also called niche) in the fate of stem cells, in both retaining stemness and differentiation. Plenty of studies indicate that differentiated cells could influence MSC differentiation. Direct coculture of MSCs with endothelial cells (ECs) resulted in an increase in α-smooth muscle actin mRNA and protein of MSCs but also a comprehensive disruption of α-smooth muscle actin filament organization [61]. For VC, cell components change a lot. Take VC in atherosclerosis as an example, there are many pathological differentiated cell types, such as foam cells, osteogenic phenotype VSMCs, and ECs with a decrease in physiological vessel cells. Using an in vitro cell-cell coculturing system, Xin et al. observed that MSCs directly interact with normal or calcified VSMCs. Osteosynthesis-inducing medium (OS) treatment did not promote the generation of an osteoblast phenotype in cultured MSCs. However, MSCs exhibited an osteoblast phenotype when MSCs were cocultured in direct contact with calcified VSMCs whether with or without OS treatment [62]. That is completely opposite to the aforementioned indirect coculture research [12].

Regrettably, this study did not give us a contact-related explanation. Instead, the results are reported in a Wnt signaling-dependent manner. LRP5, a receptor of the canonical Wnt pathway, was upregulated, while Ror2, the receptor of the noncanonical pathway, was downregulated in MSCs [62, 63]. Canonical Wnt/β-catenin signaling is a significant pathway in VC. In phosphorus-induced calcification, this signal was upregulated [58]. Another in vitro model of human VSMC calcification was induced by exposure to high glucose. The Wnt signaling molecules including Wnt3a, Wnt7a, and Fzd4 were highly expressed, and the phosphorylation of β-catenin was increased, which can be inhibited by Dkk1, a Wnt signaling inhibitor [57]. As for the downstream genes, many osteogenesis genes, such as osteocalcin type I collagen, Runx2, osteopontin, and autophagy, upregulate type III Na-Pi cotransporters (PiT1), and lymphoid enhancer-binding factor (LEF) has been proven to be the target genes [64–67]. Actually, the Wnt signal was reported earlier in MSC osteogenic transformation in physiological bone and cartilage formation [68–70]. It is not surprising to find a similar effect in VC. When the canonical Wnt signal is suppressed in MSCs by sFRP2, interestingly, MSCs' self-renewal capacity is enhanced, which promotes engraftment and myocardial repair [71]. Taken together, inappropriate activation of the Wnt signal in the microenvironment may result in both VSMC and MSC osteogenesis transformations to facilitate VC.

More recently, one study provides comprehensive evidence that osteoblast-derived small extracellular vesicles in the culture environment were of critical importance. The extracellular vesicles were successfully applied to induce BM-MSC differentiation towards a mineral phenotype [72].

Going through the researches associated with the protective role of MSCs, we found that they all kept the MSCs away from the calcified vascular microenvironment. That means that MSCs can exert the protective effect only when they maintain the ability of stemness. Neither MSC transplantation therapy nor endogenous recruitment can avoid MSCs being affected by the pathological condition. As a result, they facilitate VC (see Figure 1).

6.2. Low Survival Rate of MSCs. It has been reported that less than 1% MSCs survive for more than one week after systemic administration [73, 74], which is a huge challenge in stem cell therapy. The reasons are complicated, one of which is the overload of oxidant stresses. Environmental stress induces excessive production of reactive oxygen species (ROS), which are capable of initiating oxidation and causing a variety of cellular responses, such as DNA damage [75]. Oxidant pressure from hyperlipidemia is a potential common etiology of VC, atherosclerosis, and osteoporosis [76]. After being recruited, MSCs will be continuously exposed to oxidants under the pathological microenvironment and induced to necrosis and apoptosis [77, 78].

However, the story for facilitating VC is quite different. Dead MSCs still have a residual effect to promote VC. Recently, exosomes secreted by osteoblasts or osteoblast-like cells, which are characterized by decreased calcifying inhibitors and increased phosphatidylserine and annexin A6 content, can initiate calcification by acting as crystallization cores [79, 80] and their capacity to concentrate and crystallize calcium as well [59]. That was partly confirmed by Fujita and his collages: apoptosis and necrosis occurred in an osteogenic culture of MSCs and cell death preceded calcification. Spontaneously dead cells by osteogenic culture and exogenously added necrotic cells were surrounded by calcium deposits [81]. Besides, antioxidants (tiron and N-acetylcysteine) inhibited cell death and calcification. This could be partly confirmed by ineffective efferocytosis, which is the main mechanism operating in fibroatheroma [21]. The accumulation of apoptotic bodies established a vicious circle with inflammatory response. However, it has been described that under an in vitro osteogenic microenvironment, MSCs derived from the human arterial wall are able to release exosomes with high affinity for hydroxyapatite crystal, which indicates that viable MSCs facilitate VC as well [21].

Compared with an in vitro experiment, an in vivo model preferably mimics the in-suit environment which is generally harder for MSCs to survive [73, 74]. The residual effect of dead MSCs may partly account for the procalcification effect found in vivo. However, further studies are still needed (see Figure 2).

7. Conclusions

Over the years, it is apparent that VC occurs in a wide range of vascular pathologies and is a tightly regulated process. MSCs, a natural "repairman" and promising stem cell therapy agent, may lose part of their beneficial effects and promote VC [7]. MSCs facilitate VC mainly through

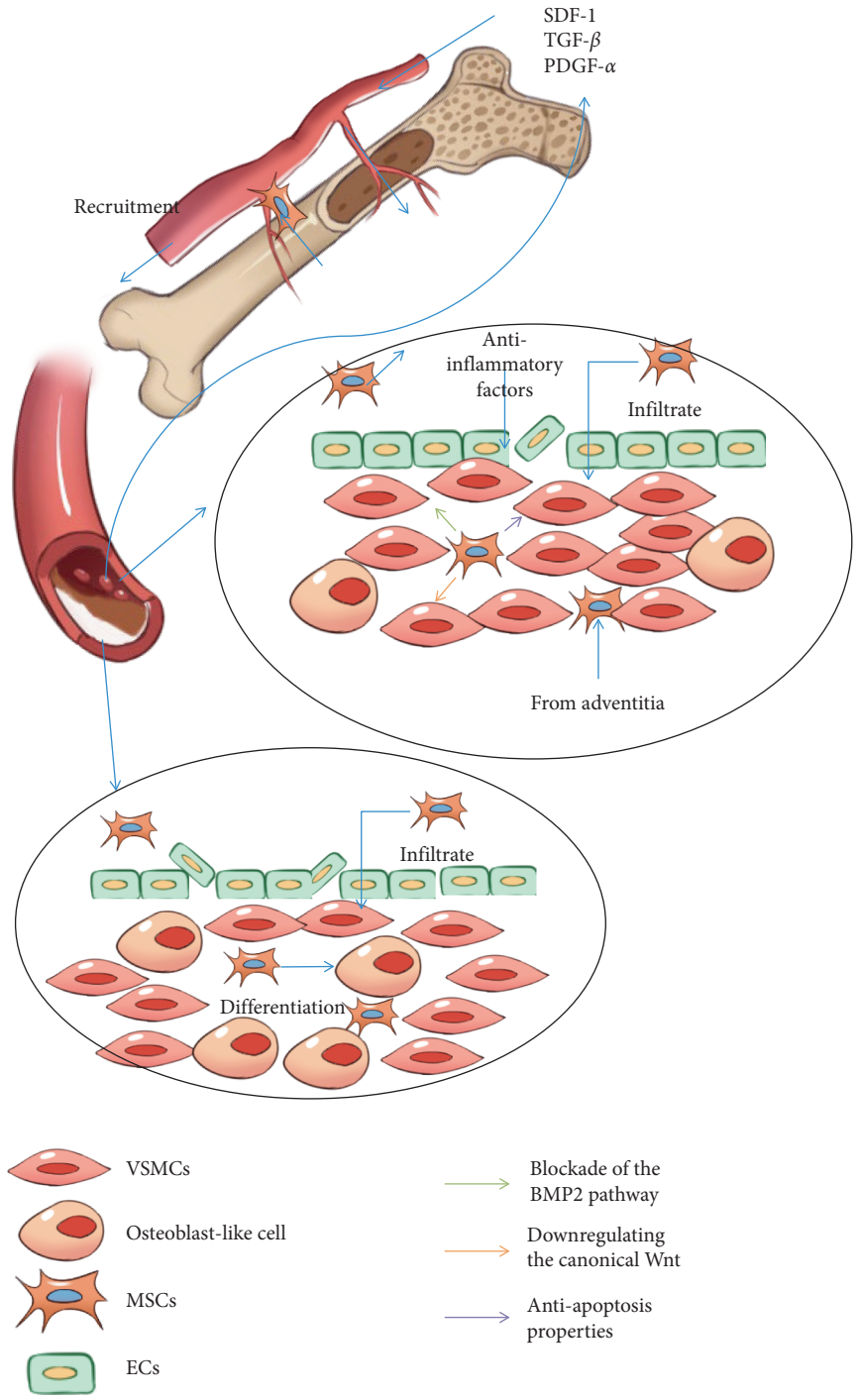

Figure 1: A brief illustration of MSCs and VC and alternation of the microenvironment. In the damaged vessel under the calcification process, SDF-1, PDGF, and TGF-β are released to recruit MSCs from bone marrow and circulation. (a) In this microenvironment, damage of the vessel wall is slight and the effect of oxidative stress and inflammation is very minimal. In addition, fewer VSMCs have been induced to osteoblasts. MSCs are viable and inhibit VSMC osteogenesis differentiation by a paracrine mechanism. (b) In this microenvironment, the vessel is damaged a lot by heavy oxidative stress and inflammation. Several phenotypic transformations of VSMCs have taken place. MSCs tend to undergo apoptosis and differentiate into osteoblast-like cells, which facilitate the VC progress.

osteogenesis differentiation. Even necrotic or apoptotic MSCs have the capacity to concentrate and crystallize calcium as well. However, the protective role only acts through a paracrine mechanism which required high cell vitality. The mechanism remains rarely known. The crosstalk between MSCs and inflammatory mediators has been proven to determine the procalcific remodeling of human atherosclerotic aneurysm [50]. However, not only inflammation but also the alternation of the microenvironment is a driving factor, which impacts the differentiation fate and function of MSCs.

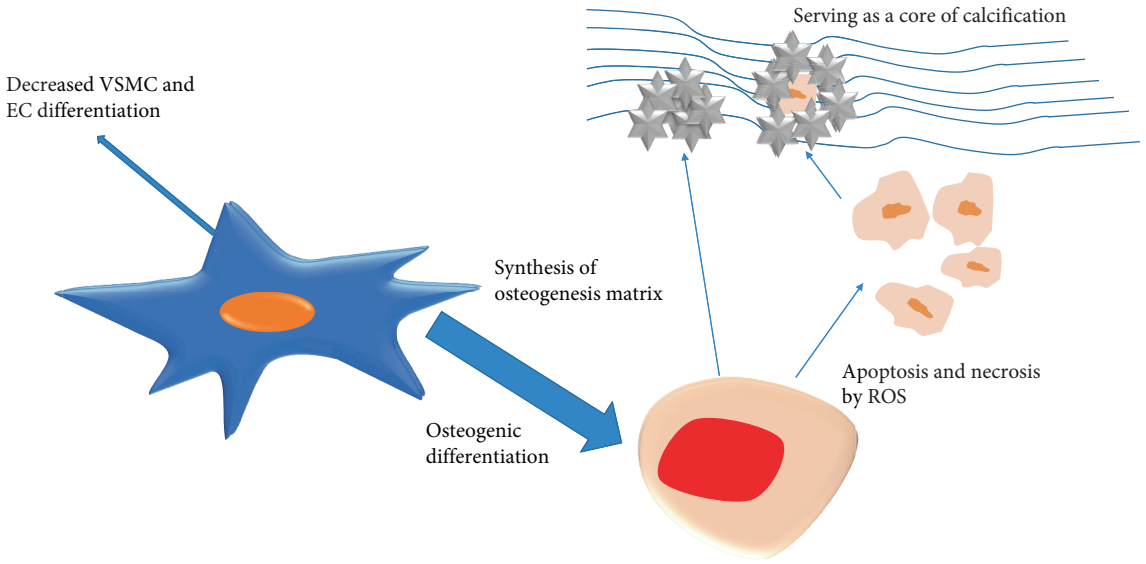

Figure 2: How the MSCs propel the calcification process: in the calcification microenvironment, MSCs are induced to differentiate into osteoblast-like cells, which synthesize the osteogenesis matrix. On the other hand, under adverse condition, MSC apoptosis or necrosis happens. Then, the fragments serve as a core of calcification deposit. Meanwhile, less MSCs differentiate into VSMCs and ECs, which creates a vicious cycle.

The survival rate of MSCs is a huge challenge that not only limits the beneficial effect but also enhances the membrane fraction of necrotic cells and apoptotic bodies. With more clues being discovered, the role of MSCs in VC progression is increasingly clear, which is helpful to illuminate the underlying mechanism of VC.

Conflicts of Interest

The authors declare that they have no conflict of interest.

Acknowledgments

This work was supported in part by the National Natural Science Foundation of China (NSFC) (81870506, 81670676) and Guangzhou Science and Technology Plan Project (201607010075) through Hui Huang.

References

[1] M. Wu, C. Rementer, and C. M. Giachelli, "Vascular calcification: an update on mechanisms and challenges in treatment," *Calcified Tissue International*, vol. 93, no. 4, pp. 365–373, 2013.

[2] P. Lacolley, V. Regnault, P. Segers, and S. Laurent, "Vascular smooth muscle cells and arterial stiffening: relevance in development, aging, and disease," *Physiological Reviews*, vol. 97, no. 4, pp. 1555–1617, 2017.

[3] L. Bessueille and D. Magne, "Inflammation: a culprit for vascular calcification in atherosclerosis and diabetes," *Cellular and Molecular Life Sciences*, vol. 72, no. 13, pp. 2475–2489, 2015.

[4] N. M. Rajamannan and S. Nattel, "Aortic vascular calcification: cholesterol lowering does not reduce progression in patients with familial hypercholesterolemia—or does it?," *Canadian Journal of Cardiology*, vol. 33, no. 5, pp. 594–596, 2017.

[5] C. M. Shanahan, M. H. Crouthamel, A. Kapustin, and C. M. Giachelli, "Arterial calcification in chronic kidney disease: key roles for calcium and phosphate," *Circulation Research*, vol. 109, no. 6, pp. 697–711, 2011.

[6] G. Cianciolo, I. Capelli, M. Cappuccilli, R. Schillaci, M. Cozzolino, and G. La Manna, "Calcifying circulating cells: an uncharted area in the setting of vascular calcification in CKD patients," *Clinical Kidney Journal*, vol. 9, no. 2, pp. 280–286, 2016.

[7] G. P. Fadini, M. Rattazzi, T. Matsumoto, T. Asahara, and S. Khosla, "Emerging role of circulating calcifying cells in the bone-vascular axis," *Circulation*, vol. 125, no. 22, pp. 2772–2781, 2012.

[8] L. Ouyang, K. Zhang, J. Chen, J. Wang, and H. Huang, "Roles of platelet-derived growth factor in vascular calcification," *Journal of Cellular Physiology*, vol. 233, no. 4, pp. 2804–2814, 2018.

[9] M. Dominici, K. le Blanc, I. Mueller et al., "Minimal criteria for defining multipotent mesenchymal stromal cells. The International Society for Cellular Therapy position statement," *Cytotherapy*, vol. 8, no. 4, pp. 315–317, 2006.

[10] M. Crisan, S. Yap, L. Casteilla et al., "A perivascular origin for mesenchymal stem cells in multiple human organs," *Cell Stem Cell*, vol. 3, no. 3, pp. 301–313, 2008.

[11] A. Shafiee, J. Patel, J. S. Lee, D. W. Hutmacher, N. M. Fisk, and K. Khosrotehrani, "Mesenchymal stem/stromal cells enhance engraftment, vasculogenic and pro-angiogenic activities of endothelial colony forming cells in immunocompetent hosts," *Scientific Reports*, vol. 7, no. 1, article 13558, 2017.

[12] M.'e. Zhu, X. Fang, S. Zhou, W. Li, and S. Guan, "Indirect co-culture of vascular smooth muscle cells with bone marrow mesenchymal stem cells inhibits vascular calcification and downregulates the Wnt signaling pathways," *Molecular Medicine Reports*, vol. 13, no. 6, pp. 5141–5148, 2016.

[13] H. J. Cho, H. J. Cho, H. J. Lee et al., "Vascular calcifying progenitor cells possess bidirectional differentiation potentials," *PLoS Biology*, vol. 11, no. 4, article e1001534, 2013.

[14] W. Lu and X. Li, "Vascular stem/progenitor cells: functions and signaling pathways," *Cellular and Molecular Life Sciences*, vol. 75, no. 5, pp. 859–869, 2018.

[15] J. Oswald, S. Boxberger, B. Jorgensen et al., "Mesenchymal stem cells can be differentiated into endothelial cells in vitro," *Stem Cells*, vol. 22, no. 3, pp. 377–384, 2004.

[16] Y. Kashiwakura, Y. Katoh, K. Tamayose et al., "Isolation of bone marrow stromal cell–derived smooth muscle cells by a human SM22α promoter: in vitro differentiation of putative smooth muscle progenitor cells of bone marrow," *Circulation*, vol. 107, no. 16, pp. 2078–2081, 2003.

[17] M. Loibl, A. Binder, M. Herrmann et al., "Direct cell-cell contact between mesenchymal stem cells and endothelial progenitor cells induces a pericyte-like phenotype in vitro," *BioMed Research International*, vol. 2014, Article ID 395781, 10 pages, 2014.

[18] F. Li, X. Guo, and S. Y. Chen, "Function and therapeutic potential of mesenchymal stem cells in atherosclerosis," *Frontiers in Cardiovascular Medicine*, vol. 4, p. 32, 2017.

[19] L. Meesuk, C. Tantrawatpan, P. Kheolamai, and S. Manochantr, "The immunosuppressive capacity of human mesenchymal stromal cells derived from amnion and bone marrow," *Biochemistry and Biophysics Reports*, vol. 8, pp. 34–40, 2016.

[20] J. Gao, K. Zhang, J. Chen et al., "Roles of aldosterone in vascular calcification: an update," *European Journal of Pharmacology*, vol. 786, pp. 186–193, 2016.

[21] L. Zazzeroni, G. Faggioli, and G. Pasquinelli, "Mechanisms of arterial calcification: the role of matrix vesicles," *European Journal of Vascular and Endovascular Surgery*, vol. 55, no. 3, pp. 425–432, 2018.

[22] R. Nicoll and M. Y. Henein, "Arterial calcification: friend or foe?," *International Journal of Cardiology*, vol. 167, no. 2, pp. 322–327, 2013.

[23] M. Alique, R. Ramirez-Carracedo, G. Bodega, J. Carracedo, and R. Ramirez, "Senescent microvesicles: a novel advance in molecular mechanisms of atherosclerotic calcification," *International Journal of Molecular Sciences*, vol. 19, no. 7, 2018.

[24] M. Krajewska-Wlodarczyk and T. Stompor, "Osteoporosis and vascular calcification in rheumatoid arthritis - the role of osteoprotegerin and sclerostin," *Polski merkuriusz lekarski : organ Polskiego Towarzystwa Lekarskiego*, vol. 43, no. 253, pp. 41–47, 2017.

[25] Z. P. Zhao, X. D. Na, H. F. Yang, and J. N. Zhou, "Osteogenic differentiation of murine yolk sac mesenchymal stem cells in vitro," *Zhongguo yi xue ke xue yuan xue bao. Acta Academiae Medicinae Sinicae*, vol. 24, no. 1, pp. 41–44, 2002.

[26] R. Kramann, S. K. Couson, S. Neuss et al., "Exposure to uremic serum induces a procalcific phenotype in human mesenchymal stem cells," *Arteriosclerosis, Thrombosis, and Vascular Biology*, vol. 31, no. 9, pp. e45–e54, 2011.

[27] A. Leszczynska, A. O'Doherty, E. Farrell et al., "Differentiation of vascular stem cells contributes to ectopic calcification of atherosclerotic plaque," *Stem Cells*, vol. 34, no. 4, pp. 913–923, 2016.

[28] B. Jian, N. Narula, Q. Y. Li, E. R. Mohler III, and R. J. Levy, "Progression of aortic valve stenosis: TGF-β1 is present in calcified aortic valve cusps and promotes aortic valve interstitial cell calcification via apoptosis," *The Annals of Thoracic Surgery*, vol. 75, no. 2, pp. 457–465, 2003, discussion 465-6.

[29] D. Liu, W. Cui, B. Liu et al., "Atorvastatin protects vascular smooth muscle cells from TGF-β1-stimulated calcification by inducing autophagy via suppression of the β-catenin pathway," *Cellular Physiology and Biochemistry*, vol. 33, no. 1, pp. 129–141, 2014.

[30] W. Wang, C. Li, L. Pang et al., "Mesenchymal stem cells recruited by active TGFβ contribute to osteogenic vascular calcification," *Stem Cells and Development*, vol. 23, no. 12, pp. 1392–1404, 2014.

[31] F. Zhang, S. Tsai, K. Kato et al., "Transforming growth factor-β promotes recruitment of bone marrow cells and bone marrow-derived mesenchymal stem cells through stimulation of MCP-1 production in vascular smooth muscle cells," *Journal of Biological Chemistry*, vol. 284, no. 26, pp. 17564–17574, 2009.

[32] M. Wan, C. Li, G. Zhen et al., "Injury-activated transforming growth factor β controls mobilization of mesenchymal stem cells for tissue remodeling," *Stem Cells*, vol. 30, no. 11, pp. 2498–2511, 2012.

[33] M. C. Phipps, Y. Xu, and S. L. Bellis, "Delivery of platelet-derived growth factor as a chemotactic factor for mesenchymal stem cells by bone-mimetic electrospun scaffolds," *PLoS One*, vol. 7, no. 7, article e40831, 2012.

[34] T. Takano, Y. J. Li, A. Kukita et al., "Mesenchymal stem cells markedly suppress inflammatory bone destruction in rats with adjuvant-induced arthritis," *Laboratory Investigation*, vol. 94, no. 3, pp. 286–296, 2014.

[35] C. Schmidt-Lucke, F. Escher, S. Van Linthout et al., "Cardiac migration of endogenous mesenchymal stromal cells in patients with inflammatory cardiomyopathy," *Mediators of Inflammation*, vol. 2015, Article ID 308185, 11 pages, 2015.

[36] X. Si, X. Liu, J. Li, and X. Wu, "Transforming growth factor-β1 promotes homing of bone marrow mesenchymal stem cells in renal ischemia-reperfusion injury," *International Journal of Clinical and Experimental Pathology*, vol. 8, no. 10, pp. 12368–12378, 2015.

[37] Q. Jiang, P. Song, E. Wang, J. Li, S. Hu, and H. Zhang, "Remote ischemic postconditioning enhances cell retention in the myocardium after intravenous administration of bone marrow mesenchymal stromal cells," *Journal of Molecular and Cellular Cardiology*, vol. 56, pp. 1–7, 2013.

[38] B. Wu, L. Wang, X. Yang et al., "Norepinephrine inhibits mesenchymal stem cell chemotaxis migration by increasing stromal cell-derived factor-1 secretion by vascular endothelial cells via NE/abrd3/JNK pathway," *Experimental Cell Research*, vol. 349, no. 2, pp. 214–220, 2016.

[39] B. C. Huber, U. Grabmaier, and S. Brunner, "Impact of parathyroid hormone on bone marrow-derived stem cell mobilization and migration," *World Journal of Stem Cells*, vol. 6, no. 5, pp. 637–643, 2014.

[40] J. Liao, X. Chen, Y. Li et al., "Transfer of bone-marrow-derived mesenchymal stem cells influences vascular remodeling and calcification after balloon injury in hyperlipidemic rats," *Journal of Biomedicine & Biotechnology*, vol. 2012, Article ID 165296, 7 pages, 2012.

[41] Y. S. Yoon, J. S. Park, T. Tkebuchava, C. Luedeman, and D. W. Losordo, "Unexpected severe calcification after transplantation of bone marrow cells in acute myocardial infarction," *Circulation*, vol. 109, no. 25, pp. 3154–3157, 2004.

[42] R. Kramann, U. Kunter, V. M. Brandenburg et al., "Osteogenesis of heterotopically transplanted mesenchymal stromal cells in rat models of chronic kidney disease," *Journal of Bone and Mineral Research*, vol. 28, no. 12, pp. 2523–2534, 2013.

[43] R. Kramann, C. Goettsch, J. Wongboonsin et al., "Adventitial MSC-like cells are progenitors of vascular smooth muscle cells and drive vascular calcification in chronic kidney disease," *Cell Stem Cell*, vol. 19, no. 5, pp. 628–642, 2016.

[44] S. Cabbage, N. Ieronimakis, M. Preusch et al., "*Chlamydia pneumoniae* infection of lungs and macrophages indirectly stimulates the phenotypic conversion of smooth muscle cells and mesenchymal stem cells: potential roles in vascular calcification and fibrosis," *Pathogens and Disease*, vol. 72, no. 1, pp. 61–69, 2014.

[45] S. Wang, M. Tong, S. Hu, and X. Chen, "The bioactive substance secreted by MSC retards mouse aortic vascular smooth muscle cells calcification," *BioMed Research International*, vol. 2018, Article ID 6053567, 10 pages, 2018.

[46] S. Wang, S. Hu, J. Wang et al., "Conditioned medium from bone marrow-derived mesenchymal stem cells inhibits vascular calcification through blockade of the BMP2–Smad1/5/8 signaling pathway," *Stem Cell Research & Therapy*, vol. 9, no. 1, p. 160, 2018.

[47] T. Lin, Y. Kohno, J. F. Huang et al., "NFκB sensing IL-4 secreting mesenchymal stem cells mitigate the proinflammatory response of macrophages exposed to polyethylene wear particles," *Journal of Biomedical Materials Research*, vol. 106, no. 10, pp. 2744–2752, 2018.

[48] S. Chen, G. Cui, C. Peng et al., "Transplantation of adipose-derived mesenchymal stem cells attenuates pulmonary fibrosis of silicosis via anti-inflammatory and anti-apoptosis effects in rats," *Stem Cell Research & Therapy*, vol. 9, no. 1, p. 110, 2018.

[49] X. Teng, L. Chen, W. Chen, J. Yang, Z. Yang, and Z. Shen, "Mesenchymal stem cell-derived exosomes improve the microenvironment of infarcted myocardium contributing to angiogenesis and anti-inflammation," *Cellular Physiology and Biochemistry*, vol. 37, no. 6, pp. 2415–2424, 2015.

[50] C. Ciavarella, E. Gallitto, F. Ricci, M. Buzzi, A. Stella, and G. Pasquinelli, "The crosstalk between vascular MSCs and inflammatory mediators determines the pro-calcific remodelling of human atherosclerotic aneurysm," *Stem Cell Research & Therapy*, vol. 8, no. 1, p. 99, 2017.

[51] K. I. Cho, I. Sakuma, I. S. Sohn, S. H. Jo, and K. K. Koh, "Inflammatory and metabolic mechanisms underlying the calcific aortic valve disease," *Atherosclerosis*, vol. 277, pp. 60–65, 2018.

[52] K. Benz, K. F. Hilgers, C. Daniel, and K. Amann, "Vascular calcification in chronic kidney disease: the role of inflammation," *International Journal of Nephrology*, vol. 2018, Article ID 4310379, 7 pages, 2018.

[53] A. Avogaro and G. P. Fadini, "Mechanisms of ectopic calcification: implications for diabetic vasculopathy," *Cardiovascular Diagnosis and Therapy*, vol. 5, no. 5, pp. 343–352, 2015.

[54] Y. Nakagawa, K. Ikeda, Y. Akakabe et al., "Paracrine osteogenic signals via bone morphogenetic protein-2 accelerate the atherosclerotic intimal calcification in vivo," *Arteriosclerosis, Thrombosis, and Vascular Biology*, vol. 30, no. 10, pp. 1908–1915, 2010.

[55] G. Rawadi, B. Vayssiere, F. Dunn, R. Baron, and S. Roman-Roman, "BMP-2 controls alkaline phosphatase expression and osteoblast mineralization by a Wnt autocrine loop," *Journal of Bone and Mineral Research*, vol. 18, no. 10, pp. 1842–1853, 2003.

[56] K. Marinou, C. Christodoulides, C. Antoniades, and M. Koutsilieris, "Wnt signaling in cardiovascular physiology," *Trends in Endocrinology & Metabolism*, vol. 23, no. 12, pp. 628–636, 2012.

[57] J. Y. Yan, Q. Zhou, H. M. Yu, M. L. Hou, and L. H. Lu, "High glucose promotes vascular smooth muscle cell calcification by activating WNT signaling pathway," *Nan fang yi ke da xue xue bao = Journal of Southern Medical University*, vol. 35, no. 1, pp. 29–33, 2015.

[58] L. Yao, Y. T. Sun, W. Sun et al., "High phosphorus level leads to aortic calcification via β-catenin in chronic kidney disease," *American Journal of Nephrology*, vol. 41, no. 1, pp. 28–36, 2015.

[59] D. Proudfoot, J. N. Skepper, L. Hegyi, M. R. Bennett, C. M. Shanahan, and P. L. Weissberg, "Apoptosis regulates human vascular calcification in vitro: evidence for initiation of vascular calcification by apoptotic bodies," *Circulation Research*, vol. 87, no. 11, pp. 1055–1062, 2000.

[60] Y. Nagase, M. Iwasawa, T. Akiyama et al., "Anti-apoptotic molecule Bcl-2 regulates the differentiation, activation, and survival of both osteoblasts and osteoclasts," *Journal of Biological Chemistry*, vol. 284, no. 52, pp. 36659–36669, 2009.

[61] S. G. Ball, A. C. Shuttleworth, and C. M. Kielty, "Direct cell contact influences bone marrow mesenchymal stem cell fate," *The International Journal of Biochemistry & Cell Biology*, vol. 36, no. 4, pp. 714–727, 2004.

[62] H. Xin, F. Xin, S. Zhou, and S. Guan, "The Wnt5a/Ror2 pathway is associated with determination of the differentiation fate of bone marrow mesenchymal stem cells in vascular calcification," *International Journal of Molecular Medicine*, vol. 31, no. 3, pp. 583–588, 2013.

[63] S. Guan, Z. Wang, F. Xin, and H. Xin, "Wnt5a is associated with the differentiation of bone marrow mesenchymal stem cells in vascular calcification by connecting with different receptors," *Molecular Medicine Reports*, vol. 10, no. 4, pp. 1985–1991, 2014.

[64] J. S. Shao, S. L. Cheng, J. M. Pingsterhaus, N. Charlton-Kachigian, A. P. Loewy, and D. A. Towler, "Msx2 promotes cardiovascular calcification by activating paracrine Wnt signals," *The Journal of Clinical Investigation*, vol. 115, no. 5, pp. 1210–1220, 2005.

[65] K. M. Lee, H. A. Kang, M. Park et al., "Interleukin-24 attenuates β-glycerophosphate-induced calcification of vascular smooth muscle cells by inhibiting apoptosis, the expression of calcification and osteoblastic markers, and the Wnt/β-catenin pathway," *Biochemical and Biophysical Research Communications*, vol. 428, no. 1, pp. 50–55, 2012.

[66] S. Rong, X. Zhao, X. Jin et al., "Vascular calcification in chronic kidney disease is induced by bone morphogenetic protein-2 via a mechanism involving the Wnt/β-catenin pathway," *Cellular Physiology and Biochemistry*, vol. 34, no. 6, pp. 2049–2060, 2014.

[67] K. E. Beazley, D. Banyard, F. Lima et al., "Transglutaminase inhibitors attenuate vascular calcification in a preclinical model," *Arteriosclerosis, Thrombosis, and Vascular Biology*, vol. 33, no. 1, pp. 43–51, 2013.

[68] X. X. Xiang, L. Chen, J. H. Wang, Y. B. Zhang, and D. Y. Zhang, "Role of Wnt/β-catenin signaling in aging of mesenchymal stem cells of rats," *Zhejiang da xue xue bao. Yi xue*

ban = Journal of Zhejiang University. Medical Sciences, vol. 40, no. 6, pp. 630–640, 2011.

[69] Z. Saidak, C. Le Henaff, S. Azzi et al., "Wnt/β-catenin signaling mediates osteoblast differentiation triggered by peptide-induced $\alpha5\beta1$ integrin priming in mesenchymal skeletal cells," *Journal of Biological Chemistry*, vol. 290, no. 11, pp. 6903–6912, 2015.

[70] Y. Li, D. Jin, W. Xie et al., "PPAR-γ and Wnt regulate the differentiation of MSCs into adipocytes and osteoblasts respectively," *Current Stem Cell Research & Therapy*, vol. 13, no. 3, pp. 185–192, 2018.

[71] M. P. Alfaro, A. Vincent, S. Saraswati et al., "sFRP2 suppression of bone morphogenic protein (BMP) and Wnt signaling mediates mesenchymal stem cell (MSC) self-renewal promoting engraftment and myocardial repair," *Journal of Biological Chemistry*, vol. 285, no. 46, pp. 35645–35653, 2010.

[72] O. G. Davies, S. C. Cox, R. L. Williams et al., "Annexin-enriched osteoblast-derived vesicles act as an extracellular site of mineral nucleation within developing stem cell cultures," *Scientific Reports*, vol. 7, no. 1, article 12639, 2017.

[73] S. R. Yang, J. R. Park, and K. S. Kang, "Reactive oxygen species in mesenchymal stem cell aging: implication to lung diseases," *Oxidative Medicine and Cellular Longevity*, vol. 2015, Article ID 486263, 11 pages, 2015.

[74] F. Vizoso, N. Eiro, S. Cid, J. Schneider, and R. Perez-Fernandez, "Mesenchymal stem cell secretome: toward cell-free therapeutic strategies in regenerative medicine," *International Journal of Molecular Sciences*, vol. 18, no. 9, 2017.

[75] T. F. Slater, "Free-radical mechanisms in tissue injury," *Biochemical Journal*, vol. 222, no. 1, pp. 1–15, 1984.

[76] A. P. Sage, Y. Tintut, and L. L. Demer, "Regulatory mechanisms in vascular calcification," *Nature Reviews Cardiology*, vol. 7, no. 9, pp. 528–536, 2010.

[77] M. A. Kawashiri, C. Nakanishi, T. Tsubokawa et al., "Impact of enhanced production of endogenous heme oxygenase-1 by pitavastatin on survival and functional activities of bone marrow–derived mesenchymal stem cells," *Journal of Cardiovascular Pharmacology*, vol. 65, no. 6, pp. 601–606, 2015.

[78] X. Bai, J. Xi, Y. Bi et al., "TNF-α promotes survival and migration of MSCs under oxidative stress via NF-κB pathway to attenuate intimal hyperplasia in vein grafts," *Journal of Cellular and Molecular Medicine*, vol. 21, no. 9, pp. 2077–2091, 2017.

[79] I. Perrotta and S. Aquila, "Exosomes in human atherosclerosis: an ultrastructural analysis study," *Ultrastructural Pathology*, vol. 40, no. 2, pp. 101–106, 2016.

[80] M. Liberman and L. C. Marti, "Vascular calcification regulation by exosomes in the vascular wall," in *Exosomes in Cardiovascular Diseases*, vol. 998 of Advances in Experimental Medicine and Biology, pp. 151–160, Springer, Singapore, 2017.

[81] H. Fujita, M. Yamamoto, T. Ogino et al., "Necrotic and apoptotic cells serve as nuclei for calcification on osteoblastic differentiation of human mesenchymal stem cells in vitro," *Cell Biochemistry and Function*, vol. 32, no. 1, pp. 77–86, 2014.

[82] J. Fiedler, N. Etzel, and R. E. Brenner, "To go or not to go: migration of human mesenchymal progenitor cells stimulated by isoforms of PDGF," *Journal of Cellular Biochemistry*, vol. 93, no. 5, pp. 990–998, 2004.

[83] P. Barcellos-de-Souza, G. Comito, C. Pons-Segura et al., "Mesenchymal stem cells are recruited and activated into carcinoma-associated fibroblasts by prostate cancer microenvironment-derived TGF-β1," *Stem Cells*, vol. 34, no. 10, pp. 2536–2547, 2016.

[84] S. J. Zhang, X. Y. Song, M. He, and S. B. Yu, "Effect of TGF-β1/SDF-1/CXCR4 signal on BM-MSCs homing in rat heart of ischemia/perfusion injury," *European Review for Medical and Pharmacological Sciences*, vol. 20, no. 5, pp. 899–905, 2016.

[85] L. Bian, D. Y. Zhai, E. Tous, R. Rai, R. L. Mauck, and J. A. Burdick, "Enhanced MSC chondrogenesis following delivery of TGF-β3 from alginate microspheres within hyaluronic acid hydrogels in vitro and in vivo," *Biomaterials*, vol. 32, no. 27, pp. 6425–6434, 2011.

[86] L. Zhao and B. M. Hantash, "TGF-β1 regulates differentiation of bone marrow mesenchymal stem cells," *Vitamins & Hormones*, vol. 87, pp. 127–141, 2011.

[87] G. Zhen, C. Wen, X. Jia et al., "Inhibition of TGF-β signaling in mesenchymal stem cells of subchondral bone attenuates osteoarthritis," *Nature Medicine*, vol. 19, no. 6, pp. 704–712, 2013.

[88] Y. Naaldijk, A. A. Johnson, S. Ishak, H. J. Meisel, C. Hohaus, and A. Stolzing, "Migrational changes of mesenchymal stem cells in response to cytokines, growth factors, hypoxia, and aging," *Experimental Cell Research*, vol. 338, no. 1, pp. 97–104, 2015.

[89] Y. Mishima and M. Lotz, "Chemotaxis of human articular chondrocytes and mesenchymal stem cells," *Journal of Orthopaedic Research*, vol. 26, no. 10, pp. 1407–1412, 2008.

[90] R. F. Foronjy and S. M. Majka, "The potential for resident lung mesenchymal stem cells to promote functional tissue regeneration: understanding microenvironmental cues," *Cells*, vol. 1, no. 4, pp. 874–885, 2012.

[91] B. Xu, Y. Luo, Y. Liu, B. Y. Li, and Y. Wang, "Platelet-derived growth factor-BB enhances MSC-mediated cardioprotection via suppression of miR-320 expression," *American Journal of Physiology-Heart and Circulatory Physiology*, vol. 308, no. 9, pp. H980–H989, 2015.

[92] C. Ricci and N. Ferri, "Naturally occurring PDGF receptor inhibitors with potential anti-atherosclerotic properties," *Vascular Pharmacology*, vol. 70, pp. 1–7, 2015.

[93] A. Li, X. Xia, J. Yeh et al., "PDGF-AA promotes osteogenic differentiation and migration of mesenchymal stem cell by down-regulating PDGFRα and derepressing BMP-Smad1/5/8 signaling," *PLoS One*, vol. 9, no. 12, article e113785, 2014.

[94] M. Mizuno, H. Katano, K. Otabe et al., "Platelet-derived growth factor (PDGF)-AA/AB in human serum are potential indicators of the proliferative capacity of human synovial mesenchymal stem cells," *Stem Cell Research & Therapy*, vol. 6, no. 1, p. 243, 2015.

[95] T. L. Watts, R. Cui, P. Szaniszlo, V. A. Resto, D. W. Powell, and I. V. Pinchuk, "PDGF-AA mediates mesenchymal stromal cell chemotaxis to the head and neck squamous cell carcinoma tumor microenvironment," *Journal of Translational Medicine*, vol. 14, no. 1, p. 337, 2016.

[96] J. D. Abbott, Y. Huang, D. Liu, R. Hickey, D. S. Krause, and F. J. Giordano, "Stromal cell–derived factor-1α plays a critical role in stem cell recruitment to the heart after myocardial infarction but is not sufficient to induce homing in the

absence of injury," *Circulation*, vol. 110, no. 21, pp. 3300–3305, 2004.

[97] A. T. Askari, S. Unzek, Z. B. Popovic et al., "Effect of stromal-cell-derived factor 1 on stem-cell homing and tissue regeneration in ischaemic cardiomyopathy," *The Lancet*, vol. 362, no. 9385, pp. 697–703, 2003.

[98] D. J. Ceradini, A. R. Kulkarni, M. J. Callaghan et al., "Progenitor cell trafficking is regulated by hypoxic gradients through HIF-1 induction of SDF-1," *Nature Medicine*, vol. 10, no. 8, pp. 858–864, 2004.

[99] S. N. Pal, P. Clancy, and J. Golledge, "Circulating concentrations of stem-cell-mobilizing cytokines are associated with levels of osteoprogenitor cells and aortic calcification severity," *Circulation Journal: Official Journal of the Japanese Circulation Society*, vol. 75, no. 5, pp. 1227–1234, 2011.

[100] S. N. Pal and J. Golledge, "Osteo-progenitors in vascular calcification: a circulating cell theory," *Journal of Atherosclerosis and Thrombosis*, vol. 18, no. 7, pp. 551–559, 2011.

[101] A. Sanghani-Kerai, M. Coathup, S. Samazideh et al., "Osteoporosis and ageing affects the migration of stem cells and this is ameliorated by transfection with CXCR4," *Bone & Joint Research*, vol. 6, no. 6, pp. 358–365, 2017.

[102] G. Ding, L. Wang, H. Xu et al., "Mesenchymal stem cells in prostate cancer have higher expressions of SDF-1, CXCR4 and VEGF," *General Physiology and Biophysics*, vol. 32, no. 2, pp. 245–250, 2013.

[103] S. B. Zhou, J. Wang, C. A. Chiang, L. L. Sheng, and Q. F. Li, "Mechanical stretch upregulates SDF-1α in skin tissue and induces migration of circulating bone marrow-derived stem cells into the expanded skin," *Stem Cells*, vol. 31, no. 12, pp. 2703–2713, 2013.

[104] N. B. Hao, C. Z. Li, M. H. Lu et al., "SDF-1/CXCR4 axis promotes MSCs to repair liver injury partially through trans-differentiation and fusion with hepatocytes," *Stem Cells International*, vol. 2015, Article ID 960387, 10 pages, 2015.

[105] L. Yao, C. J. Liu, Q. Luo et al., "Protection against hyperoxia-induced lung fibrosis by KGF-induced MSCs mobilization in neonatal rats," *Pediatric Transplantation*, vol. 17, no. 7, pp. 676–682, 2013.

[106] X. Chen, C. Shi, X. Meng et al., "Inhibition of Wnt/β-catenin signaling suppresses bleomycin-induced pulmonary fibrosis by attenuating the expression of TGF-β1 and FGF-2," *Experimental and Molecular Pathology*, vol. 101, no. 1, pp. 22–30, 2016.

[107] S. A. Gomes, E. B. Rangel, C. Premer et al., "S-Nitrosoglutathione reductase (GSNOR) enhances vasculogenesis by mesenchymal stem cells," *Proceedings of the National Academy of Sciences of the United States of America*, vol. 110, no. 8, pp. 2834–2839, 2013.

[108] C. Seebach, D. Henrich, K. Wilhelm, J. H. Barker, and I. Marzi, "Endothelial progenitor cells improve directly and indirectly early vascularization of mesenchymal stem cell-driven bone regeneration in a critical bone defect in rats," *Cell Transplantation*, vol. 21, no. 8, pp. 1667–1677, 2012.

[109] C. Schichor, T. Birnbaum, N. Etminan et al., "Vascular endothelial growth factor A contributes to glioma-induced migration of human marrow stromal cells (hMSC)," *Experimental Neurology*, vol. 199, no. 2, pp. 301–310, 2006.

[110] X. Wang, Z. Zhang, and C. Yao, "Angiogenic activity of mesenchymal stem cells in multiple myeloma," *Cancer Investigation*, vol. 29, no. 1, pp. 37–41, 2011.

[111] C.-C. Wu, I.-F. Wang, P.-M. Chiang, L.-C. Wang, C.-K. J. Shen, and K.-J. Tsai, "G-CSF-mobilized bone marrow mesenchymal stem cells replenish neural lineages in Alzheimer's disease mice via CXCR4/SDF-1 chemotaxis," *Molecular Neurobiology*, vol. 54, no. 8, pp. 6198–6212, 2017.

[112] H. Du, H. Naqvi, and H. S. Taylor, "Ischemia/reperfusion injury promotes and granulocyte-colony stimulating factor inhibits migration of bone marrow-derived stem cells to endometrium," *Stem Cells and Development*, vol. 21, no. 18, pp. 3324–3331, 2012.

[113] J. P. Miranda, E. Filipe, A. S. Fernandes et al., "The human umbilical cord tissue-derived MSC population UCX® promotes early motogenic effects on keratinocytes and fibroblasts and G-CSF-mediated mobilization of BM-MSCs when transplanted in vivo," *Cell Transplantation*, vol. 24, no. 5, pp. 865–877, 2015.

[114] X. Fu, B. Han, S. Cai, Y. Lei, T. Sun, and Z. Sheng, "Migration of bone marrow-derived mesenchymal stem cells induced by tumor necrosis factor-α and its possible role in wound healing," *Wound Repair and Regeneration*, vol. 17, no. 2, pp. 185–191, 2009.

[115] Q. Xiao, S. K. Wang, H. Tian et al., "TNF-α increases bone marrow mesenchymal stem cell migration to ischemic tissues," *Cell Biochemistry and Biophysics*, vol. 62, no. 3, pp. 409–414, 2012.

[116] C. B. Sullivan, R. M. Porter, C. H. Evans et al., "TNFα and IL-1β influence the differentiation and migration of murine MSCs independently of the NF-κB pathway," *Stem Cell Research & Therapy*, vol. 5, no. 4, p. 104, 2014.

[117] C. Katanov, S. Lerrer, Y. Liubomirski et al., "Regulation of the inflammatory profile of stromal cells in human breast cancer: prominent roles for TNF-α and the NF-κB pathway," *Stem Cell Research & Therapy*, vol. 6, no. 1, p. 87, 2015.

[118] N. E. Hengartner, J. Fiedler, A. Ignatius, and R. E. Brenner, "IL-1β inhibits human osteoblast migration," *Molecular Medicine*, vol. 19, no. 1, pp. 1–42, 2013.

[119] C. Xinaris, M. Morigi, V. Benedetti et al., "A novel strategy to enhance mesenchymal stem cell migration capacity and promote tissue repair in an injury specific fashion," *Cell Transplantation*, vol. 22, no. 3, pp. 423–436, 2013.

[120] Y. Li, X. Yu, S. Lin, X. Li, S. Zhang, and Y. H. Song, "Insulin-like growth factor 1 enhances the migratory capacity of mesenchymal stem cells," *Biochemical and Biophysical Research Communications*, vol. 356, no. 3, pp. 780–784, 2007.

[121] J. Guo, D. Zheng, W. F. Li, H. R. Li, A. D. Zhang, and Z. C. Li, "Insulin-like growth factor 1 treatment of MSCs attenuates inflammation and cardiac dysfunction following MI," *Inflammation*, vol. 37, no. 6, pp. 2156–2163, 2014.

[122] M. O. Schar, J. Diaz-Romero, S. Kohl, M. A. Zumstein, and D. Nesic, "Platelet-rich concentrates differentially release growth factors and induce cell migration in vitro," *Clinical Orthopaedics and Related Research*, vol. 473, no. 5, pp. 1635–1643, 2015.

[123] D. Sheyn, G. Shapiro, W. Tawackoli et al., "PTH induces systemically administered mesenchymal stem cells to migrate to and regenerate spine injuries," *Molecular Therapy*, vol. 24, no. 2, pp. 318–330, 2016.

Hindawi
Stem Cells International
Volume 2019, Article ID 3894101, 8 pages
https://doi.org/10.1155/2019/3894101

Review Article

One-Carbon Metabolism Links Nutrition Intake to Embryonic Development via Epigenetic Mechanisms

Si Wu,[1] Jun Zhang,[1] Feifei Li,[1] Wei Du,[2] Xin Zhou,[1] Mian Wan,[2] Yi Fan,[2] Xin Xu,[2] Xuedong Zhou,[2] Liwei Zheng,[1] and Yachuan Zhou[2]

[1]*State Key Laboratory of Oral Diseases, National Clinical Research Center for Oral Diseases, Department of Pediatric Dentistry, West China Hospital of Stomatology, Sichuan University, Chengdu, Sichuan 610041, China*
[2]*State Key Laboratory of Oral Diseases, National Clinical Research Center for Oral Diseases, Department of Cariology and Endodontics, West China Hospital of Stomatology, Sichuan University, Chengdu, Sichuan 610041, China*

Correspondence should be addressed to Liwei Zheng; liwei.zheng@scu.edu.cn and Yachuan Zhou; iamyczhou@outlook.com

Received 28 September 2018; Revised 6 January 2019; Accepted 28 January 2019; Published 10 March 2019

Guest Editor: Giuseppina Caretti

Beyond energy production, nutrient metabolism plays a crucial role in stem cell lineage determination. Changes in metabolism based on nutrient availability and dietary habits impact stem cell identity. Evidence suggests a strong link between metabolism and epigenetic mechanisms occurring during embryonic development and later life of offspring. Metabolism regulates epigenetic mechanisms such as modifications of DNA, histones, and microRNAs. In turn, these epigenetic mechanisms regulate metabolic pathways to modify the metabolome. One-carbon metabolism (OCM) is a crucial metabolic process involving transfer of the methyl groups leading to regulation of multiple cellular activities. OCM cycles and its related micronutrients are ubiquitously present in stem cells and feed into the epigenetic mechanisms. In this review, we briefly introduce the OCM process and involved micronutrients and discuss OCM-associated epigenetic modifications, including DNA methylation, histone modification, and microRNAs. We further consider the underlying OCM-mediated link between nutrition and epigenetic modifications in embryonic development.

1. Introduction

Nutrition encompasses the relationships between development and a multitude of processes such as ingestion and digestion of food for metabolism and synthesis of nutrients and is profoundly influenced by various lifestyle factors and eating habits [1]. Different dietary factors like carbohydrates, proteins, lipids, and microelements are all "fundamental materials" for organism development. These nutrient substances and their metabolites not only supply adequate energy for cell activities but also play regulatory roles in various pathways of basal metabolism [2]. Pregnancy is a critical period of cell division and differentiation occurring in utero. The maternal nutritional status greatly influences the fetal development, pregnancy outcome, and further disease development of offspring [3–6]. In the early stages of fetal development, the stem cell fate determination is regulated by epigenetic modification, which is closely related with the metabolic supply from maternal nutrition intake [7]. The remarkable breakthroughs in exploring epigenetic mechanisms have coincided with the focus on the roles of diet and nutrient metabolites in fetal development [8]. Several recent studies reported a potential interplay between gene expression and metabolic microenvironment, which is involved in modulating and regulating the epigenome of cells during early development and stem cell fate determination [9].

The one-carbon metabolism (OCM) is a vital metabolic process involved in the methyl group donation or transfer during cellular activities. These metabolic pathways utilizing one-carbon unit and related micronutrients provide essential signals involved in the interplay between biochemical pathways and epigenetic mechanisms. In this review, we summarize recent studies on the interaction between epigenetics and nutrition underlying one-carbon metabolism, including their

roles in early life development and stem cell fate determination. We also highlight the identification of potential molecular targets, with an update on modulating cell fate as a therapeutic strategy.

2. One-Carbon Metabolism and Related Micronutrients

2.1. One-Carbon Metabolism (OCM). During the process of embryogenesis, metabolites and associated biochemical pathways are essential for cellular activity and stem cell fate determination. Among these metabolic processes, OCM is widely studied for the effect of one-carbon addition, transfer, or removal on cellular activity [10]. OCM is a cyclical network that includes a series of processes such as folate and methionine cycles, nucleotide synthesis, and methyl transferase reactions (Figure 1). Various metabolites in these cycles participate in the methyl (one-carbon units) group transfer and are subsequently involved in major epigenetic and epigenomic mechanisms.

Methionine and folate cycles are entwined and contribute to the methyl group transfers in key methylation reactions that may cause epigenetic changes in cells. Under an ATP-driven reaction, methionine, the immediate source of the methyl groups, is initially converted into S-adenosyl methionine (SAM) by methionine adenosyl transferase (MAT) [11]. SAM then actively contributes the methyl group to DNA, proteins, and other metabolites, via reactions catalyzed by substrate-specific methyltransferases [12]. The S-adenosyl homocysteine (SAH), a byproduct generated from the methylation cycles, is subsequently reversibly cleaved into homocysteine (Hcy) [13, 14]. During these cycles, the released methyl groups become an essential signal participating in cellular methyltransferase reactions feeding into epigenetic mechanisms. Generally, cellular methyltransferases show a higher affinity of binding SAH than SAM. Thus, almost all the SAM-dependent methylation reactions rely on SAH removal [13]. Methionine can be regenerated via the process of folate cycle, which involves remethylation of Hcy by 5-methyltetrahydrofolic acid (5-methyl-THF) to form methionine in the presence of vitamin B_{12} as a cofactor [13]. Notably, 5-methyl-THF is a one-carbon donor playing a role in the methyl group transfers underlying the process of amino acid and vitamin metabolism.

2.2. OCM-Related Micronutrients. Methionine is an essential amino acid and primary methyl donor in the methylation cycle of OCM. Notably, methionine metabolism can be influenced by nutritional deficiencies of relevant cosubstrates and coenzymes derived from vitamin B complex and abnormalities in their metabolism [13]. Vitamin B family consists of eight compounds, which function as coenzymes in synergistic reactions. Among these, vitamin B_9 (folate) is the most studied owing to its crucial role in cellular metabolism during embryonic development. Folate in OCM acts as a coenzyme in the formation of tetrahydrofolate (THF), which is involved in the methyl group transfers. Vitamins B_6 (pyridoxine) and B_{12} (cobalamin) are also indispensable for their functions in the folate cycle as cofactors in OCM. B_{12}, as mentioned above, plays as a cofactor during regeneration of methionine, while B_6 is essential for the transfer of sulfur (thiol) in the transsulfuration pathway of Hcy [15]. Timely and optimal supplementation of vitamin B from food and dietary supplements during the periconceptional period is known to promote neural tube development and protect against birth defects of offsprings [16].

Choline and betaine are important metabolites widely existing in mammals and plants. Under conditions of folate deficiency, choline and betaine provide the methyl groups and catalyze the Hcy conversion into methionine in an alternative pathway [17]. Since the concentrations of choline and betaine were found to be higher in the umbilical cord than in the maternal plasma, they are likely required for fetal development [18]. Moreover, studies with animal models suggested that maternal choline deficiency or supplementation has effects on neuron development during the second trimester of gestation and later development of offspring [19, 20].

The status of folate, cobalamin, choline, and betaine and their interactions during pregnancy have direct effects on OCM and subsequently regulate fetal growth and pregnancy outcome [21]. OCM with its related nutrient substances is ubiquitously present in stem cells during early stage of fetal development. The maternal dietary intake influences the key metabolic reactions in OCM and potentially participates in subsequent DNA synthesis and epigenetic modification via methylation reactions. As a result, OCM influences gene expression and cellular functions such as proliferation, metabolism, pluripotency, and cytodifferentiation and may regulate the growth of the embryo and fetus and even affect future disease development in offsprings.

3. Mechanisms of Epigenetic Modification

Epigenetics involves the study of changes in gene expression without any fundamental alterations in the DNA sequence. The genome can be functionally modified at several levels of regulation without changing the nucleotide sequence that is genetically inherited [22]. The complex epigenetic alterations include DNA methylation, histone modifications, chromatin remodeling, and noncoding RNA (ncRNA) regulation [23, 24]. These epigenetic modifications converge to modulate chromatin structure and transcription programs, allowing or preventing the access of the transcriptional machinery to genomic information [25]. Thus, the expression of gene sequences can be "switched on or off" for timely gene activation or repression during cell lineage determination. Various studies have revealed that the epigenome profiles differed in specific cell types and differentiation stages.

3.1. DNA Methylation. DNA methylation describes a process wherein the methyl groups are added to DNA molecules, like cytosine and adenine. The methylation process does not change the DNA sequence but may affect the activity of a DNA segment. The methylation status of a DNA sequence regulates gene expression by modulating the chromatin structure and consequently regulates the development and maintenance of cellular homeostasis [25, 26]. The pattern of DNA methylation in mammals is mostly erased and then

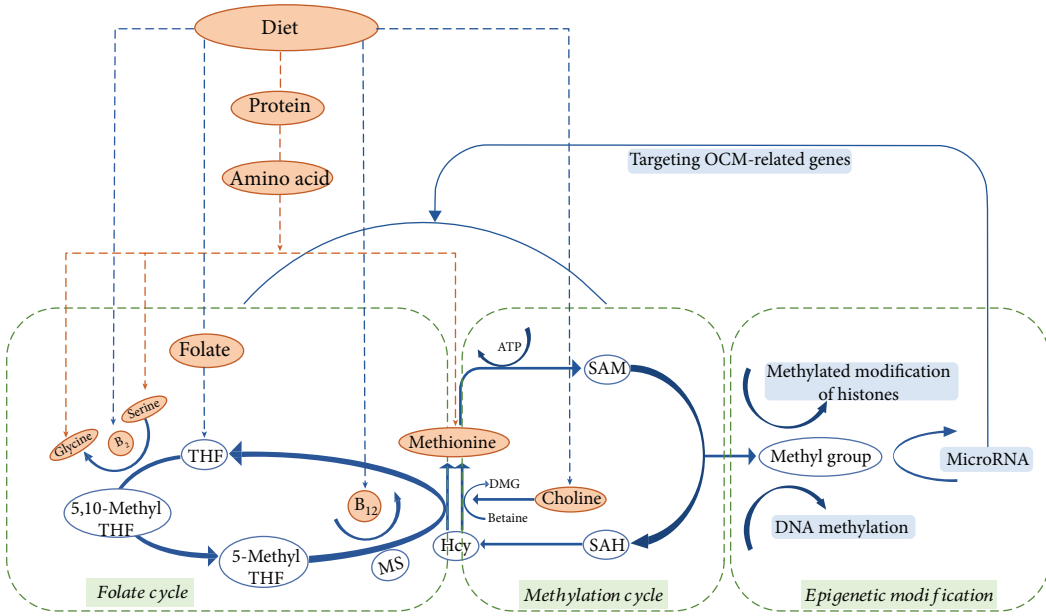

Figure 1: The interplay between one-carbon metabolism (OCM) and epigenetic modifications. Methionine and folate cycles are entwined and contribute to the methyl group transfers that may cause epigenetic changes in cells. Methionine is initially converted into SAM, and then, SAM actively contributes the methyl group to DNA, proteins, and other metabolites, via reactions catalyzed by substrate-specific methyltransferases. SAH, a byproduct generated from the methylation cycles, is subsequently reversibly cleaved into Hcy. Methionine can be regenerated via the process of folate cycle, which involves remethylation of Hcy by 5-methyl-THF to form methionine in the presence of vitamin B_{12} as a cofactor. SAM: S-adenosyl methionine; SAH: S-adenosyl homocysteine; Hcy: homocysteine; THF: tetrahydrofolic acid; 5,10-methyl-THF: 5,10-methylate tetrahydrofolic acid; 5-methyl-THF: 5-methylate tetrahydrofolic acid; B_{12}: vitamin B_{12}; B_2: vitamin B_2; MS: methionine synthase; DMG: dimethylglycine.

reestablished between generations, with the demethylation and remethylation processes occurring each time during early embryogenesis [27]. It should be noted that the DNA methylation at individual genomic regions is a dynamic pattern influenced by nutritional, environmental, and other factors [26, 28]. A family of DNA methyltransferases (DNMTs) catalyzes these methylation reactions [29]. DNMTs, associated with the methylation cycle of OCM, attach the methyl groups to the carbon-5 position of cytosine, resulting in the generation of 5-methylcytosine. These epigenetic processes occur during specific stages of organism development and dynamically change during the lifespan [30].

3.2. Histone Modification. Nucleosomes, the basic structural units of chromatin, are formed by DNA sequences wrapped around histone proteins (H2A, H2B, H3, and H4). The amino-terminal tails of histones can be biochemically modified in multiple ways, including methylation, phosphorylation, acetylation, and ubiquitination [31]. Posttranslational modifications of histone proteins result in distinct landscapes in the cellular epigenome and determine the cell lineage fate by regulating transcriptional and metabolic activities [32]. Studies have uncovered that the histone modification patterns can be diagnostic for the cell type and differentiation stage in the embryos and embryonic stem cells [30]. Among these modifications, methylation of histones can modulate gene transcription depending on how many methyl groups are attached and which amino acids are in the methylated histones. Histone methylation status is mediated by the histone methyltransferase and demethylases, which donate or transfer the methyl groups as part of OCM. These histone-modifying enzymes are modulated by maternal dietary habits and nutritional intake and are linked to the early development of offspring as discussed below [33].

3.3. MicroRNA. Noncoding RNA (ncRNA) is a group of regulatory RNAs that do not code for a protein, but rather function to regulate gene expression at multiple regulatory levels, thereby influencing cellular physiology and development [34, 35]. NcRNAs include long noncoding RNA (lncRNA), microRNA (miRNA), and small interfering RNA (siRNA). Among these, miRNA is widely studied for its function in various cellular activities including proliferation, differentiation, and apoptosis. miRNA is a category of short (~21 nucleotides) ncRNAs that affect gene expression in a posttranscriptional mechanism, wherein the miRNA directly binds to the 3′-untranslated regions (3′-UTRs) of a target mRNA for subsequent repression or degradation [36–38]. Studies have uncovered the expression profiles and regulatory roles of miRNAs during embryogenesis and early life development. Comparative analysis revealed dynamic changes in miRNAs and their targets during embryonic stem cell (ESC) maintenance and differentiation process. Notably, miRNAs were secreted and transferred into the uterine fluid, whose contents were proposed to be involved in a crosstalk between the mother and conceptus. The maternal nutritional environment undoubtedly affected the utero status and the miRNAs of either

maternal or embryo origin, impacting the development of the embryo [39].

4. Metabolites Play a Role in Epigenetic Mechanism

Stem cell fate determination is affected by changes in transcriptional programs, which lead to a defined cell lineage under certain microenvironment stimuli [40]. The important role of epigenetics in driving stem cell fate has been widely investigated at and between different regulatory levels such as chromosomal, transcriptional, and posttranscriptional levels [41–43]. Recent studies reported evidence that the regulation of epigenetics not only affects the chemical modification of DNA and histones but also is closely linked with the nutritional status [44]. An essential role of nutrition and nutrition-related metabolism is generating amino acids and other metabolites in rapidly dividing cells [45]. Furthermore, the metabolite levels in stem cells have a direct influence on the epigenome through histone and DNA modifications and expression of miRNAs [46–48].

Generally, nutrition and micronutrients involved in metabolic pathways can interfere with epigenetic mechanism in different ways: the utilization of the methyl groups from OCM in the (1) DNA methylation and (2) histone modification by shifting the activity of methyl transferase. (3) The metabolic status alters miRNA profiles, and in turn, the OCM-related genes could be regulated by miRNA [49, 50]. For these above reasons, micronutrients and metabolic status, influenced by dietary habits, play an essential role in regulating epigenetic modification and stem cell determination during the early stage of fetal development.

4.1. OCM and DNA Methylation. During embryonic development, epigenetic reprograming occurs with changes in DNA methylation patterns [27]. Evidence indicates that the process of DNA methylation is susceptible to nutritional status and OCM-related micronutrients including methionine, folate, vitamin B_{12}, and vitamin B_6 [51–55].

In humans, micronutrients from diet influence the production of the methyl groups from OCM and subsequently affect the methylation of DNA [21, 56]. Different feeding strategies of female larvae were found to result in two different phenotypes in honeybees. Barchuk et al. [57] found a total of 240 differentially expressed genes that were activated in early larval stages stimulated by different nutrition status. DNA methylation, influenced by the nutritional input, further impacted the honeybee's developmental fate [58]. Among OCM-related micronutrients, methionine is vital for epigenetic reactions to methylate cytosine in CpG islands. High dietary supplementation of methionine would alter mammalian OCM and increase the DNA methylation status, thus potentially regulating the expression of epigenetically labile genes [59]. In the folate cycle of OCM, folate is catabolized to a series of metabolites that serve as the methyl group donors, which feed into the methylation cycle and convert Hcy to methionine (Figure 1). Upon feeding murine offspring with low-folate diet, epigenetic marks were observed to persist into adulthood [60]. Some studies reported that the maternal folate intake can influence the methyl pool in folate-mediated OCM and the patterns of DNA methylation in the placenta [61]. Additionally, other B vitamins also act as cofactors to support methylation reactions [21]. Maternal vitamin B_{12} level in serum was inversely correlated with the global methylation status of offspring at birth [62]. Maternal choline and betaine intake have potential effects against the methylation process in male infants' cord blood [63].

Nutrition can affect the utilization of the methyl groups by shifting the activity of methyltransferases catalyzing the methylation cycle [12]. SAM and SAH levels could indicate transmethylation potential and methylation status to a certain extent. SAM is converted into SAH by DNMT; conversely, a high SAH concentration inhibits the DNMT activity [64]. As described by Yi et al. [65], high affinity of cellular methyltransferases to SAH results in reduced methylation reactions. It was suggested that the deficiency of folate cycle might increase SAH levels and thereby negatively affect the cellular methylation reactions. In addition, glycine N-methyltransferase (GNMT) also regulates the ratio of SAM/SAH in the methylation cycle [66], and its enzymatic activity was further found to be inhibited by the 5-methyl-THF in folate cycle [67, 68].

Thus, transmethylation metabolic pathway is closely related to the methionine and folate-related cycles, which in turn are associated with several micronutrients. If these micronutrient levels are altered, these pathways may cause compensatory changes that influence the DNA methylation status [59, 69]. It was revealed that the dynamic DNA methylation patterns throughout the life period are regulated by OCM process [70, 71].

4.2. OCM and Histone Modification. Methyl deficiency can also influence the regulation of histone modifications by the OCM pathway. The effects of a methyl-deficient diet on histone methylation patterns were found to be similar to that caused by the alternation of DNA methylation resulting in deficiency of the methyl groups [72–74]. Various studies identified that lack of nutrients like methionine, choline, folic acid, and vitamin B_{12} causes aberrant SAM content and impacts the histone modification profiles; as a result, associated epigenomic changes influence the cell activity and lineage fate [75, 76].

The metabolome could regulate epigenetic modifications from preimplantation to postimplantation during embryonic stem cell transition in the early life development. In mouse ESCs, the histone methylation marks can be regulated by threonine deficiency leading to decreased accumulation of SAM [77]. In another study with human ESCs, the depletion of methionine was found to decrease SAM levels, leading to a decrease in H3K4me3 marks and defects in cellular self-renewal [47]. These two studies indicate the crucial role of SAM in regulating ESC differentiation. Mechanistically, these studies focused on threonine and SAM metabolism associated with energy production and acetyl-coA metabolism. The term "methylation index" was used to describe the ratio of SAM to SAH; the influence of SAM/SAH in embryonic stem cells is important part of the interaction between micronutrient and epigenetics. Further studies

identified that aberrant SAM/SAH status caused by different levels of methyl diet directly affected histone modifications. Zhou et al. [78] reported that an imbalanced methyl diet resulted in a decrease in SAM level and an upregulation of histone lysine methyltransferase- (KMT-) 8 level in the livers of mice. However, a methyl-deficient diet caused a decrease in histone H3K9me3, H3K9ac, and H4K20me3 in hepatic tissues [74], as a result of which the cell cycle arrest was released. In intestinal stem cells, deprivation of methionine also resulted in cell proliferation and promoted lineage differentiation [79]. Furthermore, Mentch et al. [80] revealed that methionine metabolism plays a key role in regulating SAM and SAH. This dynamic interplay causes changes in H3K4me3, resulting in altered gene transcription as a feedback to regulate OCM. Certain amounts of methionine were required in the maintenance of hESCs and induced pluripotent stem cells (iPSCs). Methionine deficiency resulted in reduced intracellular SAM and NANOG expression by triggering the p53-p38 signaling pathway, potentiating the differentiation of hESCs and iPSCs into all three germ layers. Notably, a prolonged period of methionine deficiency resulted in cellular apoptosis [47]. These findings suggest that SAM status in OCM plays a key role in maintaining stem cells in an undifferentiated pluripotent status and in regulating their differentiation process. Additionally, the nuclear lysine-specific demethylase 1 (LSD1), a histone demethylase, was identified to be a folate-binding protein with high affinity [81]. It was suggested that folic acid participates in the demethylation of histones and thereby functions in regulating gene expression. However, its relationship with OCM needs to be further investigated.

4.3. OCM and miRNA. In mice fed with a methyl-deficient diet, a total of 74 miRNAs were differentially expressed in the liver, suggesting a relationship between the expression of miRNAs and methyl deficiency [82]. To further study the potential ability of miRNA in regulating OCM, a computational Monte Carlo algorithm was used to identify candidate master miRNAs of 42 OCM-related genes. As a result, miR-22 was identified as a novel and top OCM regulator that targeted OCM genes (MAT2A, MTHFR, MTHFD2, SLC19A1, TCblR, and TCN2) involved in the transportation, distribution, and methylation of folate and vitamin B_{12}. The results also suggested that miR-344-5p/484 and miR-488 function cooperatively as master regulators of the OCM cycle [49]. Using DNA sequencing and by establishing gene network, a total of 48 genes involved in the folate-related OCM pathway were extracted from the KEGG pathway and literature survey. Using this information, a complex database was generated including CpGs, miRNAs, copy number variations (CNVs), and single-nucleotide polymorphisms (SNPs) underlying the OCM pathways (http://slsdb.manipal.edu/ocm/) [83]. Based on these data, recent studies have focused on the potential mechanism between OCM and miRNAs. Song et al. [84] found that the folate exposure of chondrocytes, obtained from individual with osteoarthritis (OA), caused an increase in levels of hydroxymethyltransferase- (HMT-) 2, methyl-CpG-binding protein- (MECP-) 2, and DNMT-3B. Additionally, they reported that miR-373 and miR-370 may, respectively, target MECP-2 and SHMT-2 to directly regulate OCM. Koturbash et al. [85] and Koufaris et al. [86] demonstrated the inhibitory role of miR-29b and miR-22 in regulating the expression of OCM-related genes, including methionine adenosyltransferase I, alpha (Mat1a), and 5,10-methylenetetrahydrofolate reductase (MTHFR). These investigations also showed the role of miR-22 as a regulator in stem cell differentiation and cancer development.

In recent years, the bidirectional analysis of the interplay between miRNA profiles and folate status was examined and the strong interaction between OCM and miRNA expression was shown [87]. In folate-deficient media, cultured mESCs showed differential expression of 12 miRNAs and failed to proliferate and underwent apoptosis. In particular, miR-302a was found to mediate these effects of folate by directly targeting the Lats2 gene [88]. Furthermore, maternal folate supplementation during the late stage of development could restore the folate deficiency-associated defects such as the cerebral layer atrophy and interhemispheric suture defects [89, 90]. These findings suggest that folate deficiency-associatedconsequences might be mediated by miRNAs, indicating their critical roles in mammalian development. Though multiple lines of evidence clearly show the role of miRNAs in regulating OCM and OCM-related genes, there is still a need to elucidate the direct mechanism between nutritional status and functional miRNAs and the potential role of these miRNA as prognostic factors for diseases.

5. Future of Dietary Epigenetic Modulators

Since nearly a century, researchers have identified embryonic cells with stable but epigenetically distinct states of pluripotency [91, 92]. Maternal environment and nutrient status can influence the metabolism of fetus through epigenetic modifications in early stage of fetal development. OCM is a crucial metabolic process involving methyl transfers from micronutrients in a cyclical process. The donation and transfer of the methyl groups link the nutrient status to epigenetic mechanism involved in modulation of cellular activities during early development. Notably, epigenetic mechanisms can also modify metabolism and influence the signaling cascades involved in metabolic regulation [93].

In summary, epigenetic factors and metabolic mechanisms form a complex network regulating the cell fate determination during developmental processes. Detailed investigation on the potential mechanism underlying the effect of maternal dietary factors on epigenome modulations of offspring is needed. Furthermore, improvement of dietary component for achieving favorable effects on the epigenetic pattern of the organism may be a promising therapeutic strategy that should be explored.

Conflicts of Interest

The authors declare that there is no conflict of interests regarding the publication of this paper.

Acknowledgments

This work was supported by the National Natural Science Foundation of China (NSFC) Grant 81800927 to Yachuan Zhou and NSFC Grant 81771033 to Liwei Zheng.

References

[1] A. A. Geraghty, K. L. Lindsay, G. Alberdi, F. McAuliffe, and E. R. Gibney, "Nutrition during pregnancy impacts offspring's epigenetic status—evidence from human and animal studies," *Nutrition and Metabolic Insights*, vol. 8, Supplement 1, pp. 41–47, 2015.

[2] G. Gat-Yablonski, R. Pando, and M. Phillip, "Nutritional catch-up growth," *World Review of Nutrition and Dietetics*, vol. 106, pp. 83–89, 2013.

[3] R. Gabbianelli, "Modulation of the epigenome by nutrition and xenobiotics during early life and across the life span: the key role of lifestyle," *Lifestyle Genomics*, vol. 11, no. 1, pp. 9–12, 2018.

[4] M. H. Vickers, "Early life nutrition, epigenetics and programming of later life disease," *Nutrients*, vol. 6, no. 6, pp. 2165–2178, 2014.

[5] K. M. Godfrey, A. Sheppard, P. D. Gluckman et al., "Epigenetic gene promoter methylation at birth is associated with child's later adiposity," *Diabetes*, vol. 60, no. 5, pp. 1528–1534, 2011.

[6] C. R. Gale, B. Jiang, S. M. Robinson, K. M. Godfrey, C. M. Law, and C. N. Martyn, "Maternal diet during pregnancy and carotid intima–media thickness in children," *Arteriosclerosis, Thrombosis, and Vascular Biology*, vol. 26, no. 8, pp. 1877–1882, 2006.

[7] P. Christian, L. C. Mullany, K. M. Hurley, J. Katz, and R. E. Black, "Nutrition and maternal, neonatal, and child health," *Seminars in Perinatology*, vol. 39, no. 5, pp. 361–372, 2015.

[8] Y. Zhang and T. G. Kutateladze, "Diet and the epigenome," *Nature Communications*, vol. 9, no. 1, p. 3375, 2018.

[9] F. Zenk, E. Loeser, R. Schiavo, F. Kilpert, O. Bogdanović, and N. Iovino, "Germ line–inherited H3K27me3 restricts enhancer function during maternal-to-zygotic transition," *Science*, vol. 357, no. 6347, pp. 212–216, 2017.

[10] E. C. Rush, P. Katre, and C. S. Yajnik, "Vitamin B12: one carbon metabolism, fetal growth and programming for chronic disease," *European Journal of Clinical Nutrition*, vol. 68, no. 1, pp. 2–7, 2014.

[11] G. Wu, "Amino acids: metabolism, functions, and nutrition," *Amino Acids*, vol. 37, no. 1, pp. 1–17, 2009.

[12] O. S. Anderson, K. E. Sant, and D. C. Dolinoy, "Nutrition and epigenetics: an interplay of dietary methyl donors, one-carbon metabolism and DNA methylation," *The Journal of Nutritional Biochemistry*, vol. 23, no. 8, pp. 853–859, 2012.

[13] J. D. Finkelstein, "Metabolic regulatory properties of S-adenosylmethionine and S-adenosylhomocysteine," *Clinical Chemical Laboratory Medicine*, vol. 45, no. 12, pp. 1694–1699, 2007.

[14] J. P. Monteiro, C. Wise, M. J. Morine et al., "Methylation potential associated with diet, genotype, protein, and metabolite levels in the delta obesity vitamin study," *Genes & Nutrition*, vol. 9, no. 3, p. 403, 2014.

[15] B. L. Zaric, M. Obradovic, V. Bajic, M. A. Haidara, M. Jovanovic, and E. R. Isenovic, "Homocysteine and hyperhomocysteinaemia," *Current Medicinal Chemistry*, vol. 25, 2018.

[16] M. Viswanathan, K. A. Treiman, J. Kish-Doto, J. C. Middleton, E. J. L. Coker-Schwimmer, and W. K. Nicholson, "Folic acid supplementation for the prevention of neural tube defects: an updated evidence report and systematic review for the US preventive services task force," *Journal of the American Medical Association*, vol. 317, no. 2, pp. 190–203, 2017.

[17] P. M. Ueland, "Choline and betaine in health and disease," *Journal of Inherited Metabolic Disease*, vol. 34, no. 1, pp. 3–15, 2011.

[18] A. M. Molloy, J. L. Mills, C. Cox et al., "Choline and homocysteine interrelations in umbilical cord and maternal plasma at delivery," *The American Journal of Clinical Nutrition*, vol. 82, no. 4, pp. 836–842, 2005.

[19] J. C. McCann, M. Hudes, and B. N. Ames, "An overview of evidence for a causal relationship between dietary availability of choline during development and cognitive function in offspring," *Neuroscience & Biobehavioral Reviews*, vol. 30, no. 5, pp. 696–712, 2006.

[20] M. C. Fisher, S. H. Zeisel, M. H. Mar, and T. W. Sadler, "Perturbations in choline metabolism cause neural tube defects in mouse embryos in vitro," *The FASEB Journal*, vol. 16, no. 6, pp. 619–621, 2002.

[21] P. Solé-Navais, P. Cavallé-Busquets, J. D. Fernandez-Ballart, and M. M. Murphy, "Early pregnancy B vitamin status, one carbon metabolism, pregnancy outcome and child development," *Biochimie*, vol. 126, pp. 91–96, 2016.

[22] A. D. Goldberg, C. D. Allis, and E. Bernstein, "Epigenetics: a landscape takes shape," *Cell*, vol. 128, no. 4, pp. 635–638, 2007.

[23] S. P. Barros and S. Offenbacher, "Epigenetics: connecting environment and genotype to phenotype and disease," *Journal of Dental Research*, vol. 88, no. 5, pp. 400–408, 2009.

[24] J. Y. Seo, Y. J. Park, Y. A. Yi et al., "Epigenetics: general characteristics and implications for oral health," *Restorative Dentistry & Endodontics*, vol. 40, no. 1, pp. 14–22, 2015.

[25] R. P. Talens, D. I. Boomsma, E. W. Tobi et al., "Variation, patterns, and temporal stability of DNA methylation: considerations for epigenetic epidemiology," *The FASEB Journal*, vol. 24, no. 9, pp. 3135–3144, 2010.

[26] M. F. Fraga, E. Ballestar, M. F. Paz et al., "Epigenetic differences arise during the lifetime of monozygotic twins," *Proceedings of the National Academy of Sciences of the United States of America*, vol. 102, no. 30, pp. 10604–10609, 2005.

[27] K. C. Kim, S. Friso, and S. W. Choi, "DNA methylation, an epigenetic mechanism connecting folate to healthy embryonic development and aging," *The Journal of Nutritional Biochemistry*, vol. 20, no. 12, pp. 917–926, 2009.

[28] J. T. Bell, A. A. Pai, J. K. Pickrell et al., "DNA methylation patterns associate with genetic and gene expression variation in HapMap cell lines," *Genome Biology*, vol. 12, no. 1, article R10, 2011.

[29] S. K. T. Ooi, A. H. O'Donnell, and T. H. Bestor, "Mammalian cytosine methylation at a glance," *Journal of Cell Science*, vol. 122, no. 16, pp. 2787–2791, 2009.

[30] N. L. Vastenhouw and A. F. Schier, "Bivalent histone modifications in early embryogenesis," *Current Opinion in Cell Biology*, vol. 24, no. 3, pp. 374–386, 2012.

[31] L. W. Zheng, B. P. Zhang, R. S. Xu, X. Xu, L. Ye, and X. D. Zhou, "Bivalent histone modifications during tooth development," *International Journal of Oral Science*, vol. 6, no. 4, pp. 205–211, 2014.

[32] T. Kouzarides, "Chromatin modifications and their function," *Cell*, vol. 128, no. 4, pp. 693–705, 2007.

[33] J. S. Butler, E. Koutelou, A. C. Schibler, and S. Y. R. Dent, "Histone-modifying enzymes: regulators of developmental decisions and drivers of human disease," *Epigenomics*, vol. 4, no. 2, pp. 163–177, 2012.

[34] P. Perez, S. I. Jang, and I. Alevizos, "Emerging landscape of non-coding RNAs in oral health and disease," *Oral Diseases*, vol. 20, no. 3, pp. 226–235, 2014.

[35] J. Beermann, M. T. Piccoli, J. Viereck, and T. Thum, "Non--coding RNAs in development and disease: background, mechanisms, and therapeutic approaches," *Physiological Reviews*, vol. 96, no. 4, pp. 1297–1325, 2016.

[36] D. Bayarsaihan, "Epigenetic mechanisms in inflammation," *Journal of Dental Research*, vol. 90, no. 1, pp. 9–17, 2010.

[37] H. Cao, J. Wang, X. Li et al., "MicroRNAs play a critical role in tooth development," *Journal of Dental Research*, vol. 89, no. 8, pp. 779–784, 2010.

[38] A. M. Jevnaker and H. Osmundsen, "MicroRNA expression profiling of the developing murine molar tooth germ and the developing murine submandibular salivary gland," *Archives of Oral Biology*, vol. 53, no. 7, pp. 629–645, 2008.

[39] N. Gross, J. Kropp, and H. Khatib, "MicroRNA signaling in embryo development," *Biology*, vol. 6, no. 4, 2017.

[40] R. Jaenisch and A. Bird, "Epigenetic regulation of gene expression: how the genome integrates intrinsic and environmental signals," *Nature Genetics*, vol. 33, no. 3s, pp. 245–254, 2003.

[41] N. Hussain, "Epigenetic influences that modulate infant growth, development, and disease," *Antioxidants & Redox Signaling*, vol. 17, no. 2, pp. 224–236, 2012.

[42] K. Ohbo and S. Tomizawa, "Epigenetic regulation in stem cell development, cell fate conversion, and reprogramming," *Biomolecular Concepts*, vol. 6, no. 1, pp. 1–9, 2015.

[43] V. Ladopoulos, H. Hofemeister, M. Hoogenkamp, A. D. Riggs, A. F. Stewart, and C. Bonifer, "The histone methyltransferase KMT2B is required for RNA polymerase II association and protection from DNA methylation at the *MagohB* CpG island promoter," *Molecular and Cellular Biology*, vol. 33, no. 7, pp. 1383–1393, 2013.

[44] J. P. Etchegaray and R. Mostoslavsky, "Interplay between metabolism and epigenetics: a nuclear adaptation to environmental changes," *Molecular Cell*, vol. 62, no. 5, pp. 695–711, 2016.

[45] S. Y. Lunt and M. G. Vander Heiden, "Aerobic glycolysis: meeting the metabolic requirements of cell proliferation," *Annual Review of Cell and Developmental Biology*, vol. 27, no. 1, pp. 441–464, 2011.

[46] B. W. Carey, L. W. S. Finley, J. R. Cross, C. D. Allis, and C. B. Thompson, "Intracellular α-ketoglutarate maintains the pluripotency of embryonic stem cells," *Nature*, vol. 518, no. 7539, pp. 413–416, 2015.

[47] N. Shiraki, Y. Shiraki, T. Tsuyama et al., "Methionine metabolism regulates maintenance and differentiation of human pluripotent stem cells," *Cell Metabolism*, vol. 19, no. 5, pp. 780–794, 2014.

[48] K. E. Wellen, G. Hatzivassiliou, U. M. Sachdeva, T. V. Bui, J. R. Cross, and C. B. Thompson, "ATP-citrate lyase links cellular metabolism to histone acetylation," *Science*, vol. 324, no. 5930, pp. 1076–1080, 2009.

[49] N. Stone, F. Pangilinan, A. M. Molloy et al., "Bioinformatic and genetic association analysis of microRNA target sites in one-carbon metabolism genes," *PLoS One*, vol. 6, no. 7, article e21851, 2011.

[50] T. M. Hardy and T. O. Tollefsbol, "Epigenetic diet: impact on the epigenome and cancer," *Epigenomics*, vol. 3, no. 4, pp. 503–518, 2011.

[51] S. Bar-El Dadon and R. Reifen, "Vitamin A and the epigenome," *Critical Reviews in Food Science and Nutrition*, vol. 57, no. 11, pp. 2404–2411, 2017.

[52] A. Chango and I. P. Pogribny, "Considering maternal dietary modulators for epigenetic regulation and programming of the fetal epigenome," *Nutrients*, vol. 7, no. 4, pp. 2748–2770, 2015.

[53] M. Hoang, J. J. Kim, Y. Kim et al., "Alcohol-induced suppression of *KDM6B* dysregulates the mineralization potential in dental pulp stem cells," *Stem Cell Research*, vol. 17, no. 1, pp. 111–121, 2016.

[54] A. V. Majnik and R. H. Lane, "The relationship between early-life environment, the epigenome and the microbiota," *Epigenomics*, vol. 7, no. 7, pp. 1173–1184, 2015.

[55] C. A. Ducsay, R. Goyal, W. J. Pearce, S. Wilson, X. Q. Hu, and L. Zhang, "Gestational hypoxia and developmental plasticity," *Physiological Reviews*, vol. 98, no. 3, pp. 1241–1334, 2018.

[56] D. Watkins and D. S. Rosenblatt, "Lessons in biology from patients with inherited disorders of vitamin B_{12} and folate metabolism," *Biochimie*, vol. 126, pp. 3–5, 2016.

[57] A. R. Barchuk, A. S. Cristino, R. Kucharski, L. F. Costa, Z. L. P. Simões, and R. Maleszka, "Molecular determinants of caste differentiation in the highly eusocial honeybee *Apis mellifera*," *BMC Developmental Biology*, vol. 7, no. 1, p. 70, 2007.

[58] Y. Wang, M. Jorda, P. L. Jones et al., "Functional CpG methylation system in a social insect," *Science*, vol. 314, no. 5799, pp. 645–647, 2006.

[59] R. A. Waterland, "Assessing the effects of high methionine intake on DNA methylation," *The Journal of Nutrition*, vol. 136, no. 6, pp. 1706S–1710S, 2006.

[60] J. A. McKay, K. J. Waltham, E. A. Williams, and J. C. Mathers, "Folate depletion during pregnancy and lactation reduces genomic DNA methylation in murine adult offspring," *Genes & Nutrition*, vol. 6, no. 2, pp. 189–196, 2011.

[61] J. M. Kim, K. Hong, J. H. Lee, S. Lee, and N. Chang, "Effect of folate deficiency on placental DNA methylation in hyperhomocysteinemic rats," *The Journal of Nutritional Biochemistry*, vol. 20, no. 3, pp. 172–176, 2009.

[62] J. A. McKay, A. Groom, C. Potter et al., "Genetic and non-genetic influences during pregnancy on infant global and site specific DNA methylation: role for folate gene variants and vitamin B_{12}," *PLoS One*, vol. 7, no. 3, article e33290, 2012.

[63] C. E. Boeke, A. Baccarelli, K. P. Kleinman et al., "Gestational intake of methyl donors and global LINE-1 DNA methylation in maternal and cord blood: prospective results from a folate-replete population," *Epigenetics*, vol. 7, no. 3, pp. 253–260, 2012.

[64] N. Zhang, "Role of methionine on epigenetic modification of DNA methylation and gene expression in animals," *Animal Nutrition*, vol. 4, no. 1, pp. 11–16, 2018.

[65] P. Yi, S. Melnyk, M. Pogribna, I. P. Pogribny, R. J. Hine, and S. J. James, "Increase in plasma homocysteine associated with parallel increases in plasma *S*-adenosylhomocysteine and lymphocyte DNA hypomethylation," *Journal of Biological Chemistry*, vol. 275, no. 38, pp. 29318–29323, 2000.

[66] Y. Takata, Y. Huang, J. Komoto et al., "Catalytic mechanism of glycine *N*-methyltransferase," *Biochemistry*, vol. 42, no. 28, pp. 8394–8402, 2003.

[67] M. J. Rowling and K. L. Schalinske, "Retinoid compounds activate and induce hepatic glycine *N*-methyltransferase in rats," *The Journal of Nutrition*, vol. 131, no. 7, pp. 1914–1917, 2001.

[68] M. J. Rowling, M. H. McMullen, D. C. Chipman, and K. L. Schalinske, "Hepatic glycine *N*-methyltransferase is up-regulated by excess dietary methionine in rats," *The Journal of Nutrition*, vol. 132, no. 9, pp. 2545–2550, 2002.

[69] M. D. Niculescu and S. H. Zeisel, "Diet, methyl donors and DNA methylation: interactions between dietary folate, methionine and choline," *The Journal of Nutrition*, vol. 132, no. 8, pp. 2333S–2335S, 2002.

[70] R. Ren, A. Ocampo, G. H. Liu, and J. C. Izpisua Belmonte, "Regulation of stem cell aging by metabolism and epigenetics," *Cell Metabolism*, vol. 26, no. 3, pp. 460–474, 2017.

[71] K. Ito and T. Suda, "Metabolic requirements for the maintenance of self-renewing stem cells," *Nature Reviews Molecular Cell Biology*, vol. 15, no. 4, pp. 243–256, 2014.

[72] I. P. Pogribny, V. P. Tryndyak, T. V. Bagnyukova et al., "Hepatic epigenetic phenotype predetermines individual susceptibility to hepatic steatosis in mice fed a lipogenic methyl-deficient diet," *Journal of Hepatology*, vol. 51, no. 1, pp. 176–186, 2009.

[73] I. P. Pogribny, S. A. Ross, V. P. Tryndyak, M. Pogribna, L. A. Poirier, and T. V. Karpinets, "Histone H3 lysine 9 and H4 lysine 20 trimethylation and the expression of Suv4-20h2 and Suv-39h1 histone methyltransferases in hepatocarcinogenesis induced by methyl deficiency in rats," *Carcinogenesis*, vol. 27, no. 6, pp. 1180–1186, 2006.

[74] I. P. Pogribny, V. P. Tryndyak, L. Muskhelishvili, I. Rusyn, and S. A. Ross, "Methyl deficiency, alterations in global histone modifications, and carcinogenesis," *The Journal of Nutrition*, vol. 137, no. 1, pp. 216S–222S, 2007.

[75] N. Shivapurkar and L. A. Poirier, "Tissue levels of S-adenosylmethionine and S-adenosylhomocysteine in rats fed methyl-deficient, amino acid-defined diets for one to five weeks," *Carcinogenesis*, vol. 4, no. 8, pp. 1051–1057, 1983.

[76] I. P. Pogribny, S. J. James, and F. A. Beland, "Molecular alterations in hepatocarcinogenesis induced by dietary methyl deficiency," *Molecular Nutrition & Food Research*, vol. 56, no. 1, pp. 116–125, 2012.

[77] N. Shyh-Chang, J. W. Locasale, C. A. Lyssiotis et al., "Influence of threonine metabolism on *S*-adenosylmethionine and histone methylation," *Science*, vol. 339, no. 6116, pp. 222–226, 2013.

[78] W. Zhou, S. Alonso, D. Takai et al., "Requirement of RIZ1 for cancer prevention by methyl-balanced diet," *PLoS One*, vol. 3, no. 10, article e3390, 2008.

[79] Y. Saito, K. Iwatsuki, H. Hanyu et al., "Effect of essential amino acids on enteroids: methionine deprivation suppresses proliferation and affects differentiation in enteroid stem cells," *Biochemical and Biophysical Research Communications*, vol. 488, no. 1, pp. 171–176, 2017.

[80] S. J. Mentch, M. Mehrmohamadi, L. Huang et al., "Histone methylation dynamics and gene regulation occur through the sensing of one-carbon metabolism," *Cell Metabolism*, vol. 22, no. 5, pp. 861–873, 2015.

[81] Z. Luka, F. Moss, L. V. Loukachevitch, D. J. Bornhop, and C. Wagner, "Histone demethylase LSD1 is a folate-binding protein," *Biochemistry*, vol. 50, no. 21, pp. 4750–4756, 2011.

[82] A. Starlard-Davenport, V. Tryndyak, O. Kosyk et al., "Dietary methyl deficiency, microRNA expression and susceptibility to liver carcinogenesis," *World Review of Nutrition and Dietetics*, vol. 101, pp. 123–130, 2010.

[83] M. K. Bhat, V. P. Gadekar, A. Jain, B. Paul, P. S. Rai, and K. Satyamoorthy, "1-CMDb: a curated database of genomic variations of the one-carbon metabolism pathway," *Public Health Genomics*, vol. 20, no. 2, pp. 136–141, 2017.

[84] J. Song, D. Kim, C. H. Chun, and E. J. Jin, "miR-370 and miR-373 regulate the pathogenesis of osteoarthritis by modulating one-carbon metabolism via SHMT-2 and MECP-2, respectively," *Aging Cell*, vol. 14, no. 5, pp. 826–837, 2015.

[85] I. Koturbash, S. Melnyk, S. J. James, F. A. Beland, and I. P. Pogribny, "Role of epigenetic and miR-22 and miR-29b alterations in the downregulation of *Mat1a* and *Mthfr* genes in early preneoplastic livers in rats induced by 2-acetylaminofluorene," *Molecular Carcinogenesis*, vol. 52, no. 4, pp. 318–327, 2013.

[86] C. Koufaris, G. N. Valbuena, Y. Pomyen et al., "Systematic integration of molecular profiles identifies miR-22 as a regulator of lipid and folate metabolism in breast cancer cells," *Oncogene*, vol. 35, no. 21, pp. 2766–2776, 2016.

[87] E. L. Beckett, M. Veysey, and M. Lucock, "Folate and microRNA: bidirectional interactions," *Clinica Chimica Acta*, vol. 474, pp. 60–66, 2017.

[88] Y. Liang, Y. Li, Z. Li et al., "Mechanism of folate deficiency-induced apoptosis in mouse embryonic stem cells: cell cycle arrest/apoptosis in G1/G0 mediated by microRNA-302a and tumor suppressor gene *Lats2*," *The International Journal of Biochemistry & Cell Biology*, vol. 44, no. 11, pp. 1750–1760, 2012.

[89] A. Geoffroy, R. Kerek, G. Pourié et al., "Late maternal folate supplementation rescues from methyl donor deficiency-associated brain defects by restoring Let-7 and miR-34 pathways," *Molecular Neurobiology*, vol. 54, no. 7, pp. 5017–5033, 2017.

[90] R. Kerek, A. Geoffroy, A. Bison et al., "Early methyl donor deficiency may induce persistent brain defects by reducing Stat3 signaling targeted by miR-124," *Cell Death & Disease*, vol. 4, no. 8, article e755, 2013.

[91] H. Sperber, J. Mathieu, Y. Wang et al., "The metabolome regulates the epigenetic landscape during naive-to-primed human embryonic stem cell transition," *Nature Cell Biology*, vol. 17, no. 12, pp. 1523–1535, 2015.

[92] W. Zhou, M. Choi, D. Margineantu et al., "HIF1α induced switch from bivalent to exclusively glycolytic metabolism during ESC-to-EpiSC/hESC transition," *The EMBO journal*, vol. 31, no. 9, pp. 2103–2116, 2012.

[93] C. C. Wong, Y. Qian, and J. Yu, "Interplay between epigenetics and metabolism in oncogenesis: mechanisms and therapeutic approaches," *Oncogene*, vol. 36, no. 24, pp. 3359–3374, 2017.

Hindawi
Stem Cells International
Volume 2019, Article ID 4067162, 10 pages
https://doi.org/10.1155/2019/4067162

Review Article

Mitochondrial Role in Stemness and Differentiation of Hematopoietic Stem Cells

Luena Papa, Mansour Djedaini, and Ronald Hoffman

Division of Hematology/Oncology, Tisch Cancer Institute, Icahn School of Medicine at Mount Sinai, New York, NY 10029, USA

Correspondence should be addressed to Luena Papa; Luena.Papa@mssm.edu

Received 26 September 2018; Accepted 24 December 2018; Published 6 February 2019

Guest Editor: Viviana Moresi

Quiescent and self-renewing hematopoietic stem cells (HSCs) rely on glycolysis rather than on mitochondrial oxidative phosphorylation (OxPHOS) for energy production. HSC reliance on glycolysis is considered an adaptation to the hypoxic environment of the bone marrow (BM) and reflects the low energetic demands of HSCs. Metabolic rewiring from glycolysis to mitochondrial-based energy generation accompanies HSC differentiation and lineage commitment. Recent evidence, however, highlights that alterations in mitochondrial metabolism and activity are not simply passive consequences but active drivers of HSC fate decisions. Modulation of mitochondrial activity and metabolism is therefore critical for maintaining the self-renewal potential of primitive HSCs and might be beneficial for ex vivo expansion of transplantable HSCs. In this review, we emphasize recent advances in the emerging role of mitochondria in hematopoiesis, cellular reprograming, and HSC fate decisions.

1. Introduction

Hematopoiesis is a complex process that allows sustained production of each of the blood cell lineages throughout the lifespan of an individual. Vast numbers of adult mature blood cells are constantly generated from hematopoietic stem cells (HSCs) through a series of lineage-committed progenitor cells [1]. HSCs replenish the hematopoietic system with more committed progenitor and differentiated cells while they sustain long-term hematopoiesis. The balance between self-renewal (ability to generate themselves) and differentiation is central to blood cell homeostasis [2]. Cells in both states are characterized by distinct gene expression profiles, epigenetic landscapes, and developmental potentials [3]. Importantly, HSCs and committed progenitors as well as differentiated blood cells differ drastically in both their metabolic profiles and mitochondrial functions. Metabolic cues and mitochondrial DNA content, mass, and activity have been reported to vary within different stages of hematopoiesis [4–6].

Mitochondria are very complex and highly dynamic organelles. They are the major source of adenosine-5′-triphosphate (ATP) production through oxidative phosphorylation and sustained electron transport chain (ETC) activity. Mitochondrial OxPHOS is fueled by the tricarboxylic acid (TCA) cycle that converts pyruvate to acetyl-CoA. In addition, mitochondria serve as biosynthetic and signaling organelles [7]. The intermediates generated from the TCA cycle are essential for heme, amino acid, and nucleotide biosynthesis as well as for histone acetylation. Mitochondria are also the sites for fatty acid oxidation and steroid metabolism [8]. Besides their fundamental role in energy production and metabolism, mitochondria possess other important functions including calcium homeostasis, regulation of cellular and intracellular signaling, inflammation, and apoptosis, all of which are consistent with the notion that mitochondria act as a signaling organelle [9, 10]. These processes are impacted and regulated by reactive oxygen species (ROS), the by-products of OxPHOS activity. While mitochondrial OxPHOS activity is the most efficient pathway for energy

production, glycolysis is another energy-generating pathway. During glycolysis, glucose is converted to pyruvate and then anaerobically to lactate. Importantly, glycolysis is preferentially utilized by HSCs [4, 11]. The potential benefit of the reduced need for mitochondrial functions in HSCs is the limitation of ROS levels. HSCs are particularly vulnerable to oxidative stress and high levels of ROS [12, 13]. Excessive ROS levels drive the exit of HSCs from quiescence, impair their multilineage differentiation capacity, and induce uncontrolled proliferation and sustained cumulative damage, ultimately leading to HSC exhaustion and loss of self-renewal potential [13–15].

Quiescent HSCs predominantly reside in regions of the bone marrow (BM) cavity termed niches, which provide a unique landscape with a low oxygen tension [16, 17]. As a consequence, the dependency of HSCs on glycolysis has been proposed to reflect their adaptation to low oxygen levels as well as their relatively low demands for energy [5, 12, 18]. During HSC differentiation and maturation, however, a rapid switch from glycolysis to mitochondrial OxPHOS and ATP generation occurs [4, 12, 19, 20]. This switch allows differentiating cells to meet their altered and higher metabolic and energy requirements associated with differentiation [11, 21]. An increase not only in mitochondrial activity but also in mitochondrial mass, membrane potential, and ROS levels accompanied by profound alterations in the mitochondrial ultrastructure characterizes the transition from quiescence to proliferation, from a primitive stem-like state to a differentiated state [12, 21–26]. By contrast, ex vivo reprograming of more differentiated cells into HSCs with the use of chromatin-modifying agents is associated with a reverse metabolic switch. In this review, we will discuss whether the alterations in the mitochondrial profile and function are simply passive consequences of changes in the status of HSCs or are in fact critical drivers of the transition from a stem cell to more differentiated cells. Moreover, we will review the recent evidence that emphasizes the role of mitochondria during reprograming of more committed cells to HSCs followed by their ex vivo expansion, a process that substantially increases the numbers of functional human HSCs that have potential therapeutic applications.

2. Mitochondrial Oxidative Phosphorylation versus Glycolysis in Determining HSC Fate Decisions

HSCs display unique properties and functions that distinguish them from more committed progenitors and mature blood cells. HSCs are predominantly quiescent, and their metabolic wiring and reliance on glycolysis are distinct from those of committed progenitors and the other cells in the BM that encompass primarily lineage-differentiated cells [4, 5, 27]. Unlike their progeny, HSCs accumulate high levels of 1,6-bisphosphate and other products of the final ATP-producing step of glycolysis. Such an increase in the levels of glycolytic by-products correlates with high pyruvate kinase (PDK) activity [22], which is dependent on hypoxia-inducible factor 1α (HIF1α). In turn, HIF1α drives and regulates a metabolic program that limits the engagement of the TCA cycle and sustains glycolysis as a main source of energy [28].

Enhanced mitochondrial activity is detrimental to the functional identity of HSCs and maintenance of their numbers. Loss of mitochondrial carrier homolog 2 (MTCH2) enhances OxPHOS activity and intracellular ROS levels, triggering the entry of HSCs into the cell cycle and loss of their self-renewal potential [29]. By contrast, lowering mitochondrial activity by chemically uncoupling the mitochondrial ETC sustains the self-renewal potential of HSCs in ex vivo cultures that normally induce differentiation [30].

In spite of the high preference for glycolysis, mitochondria in HSCs are not completely inactive. In fact, HSCs residing in the BM depend on mitochondrial activity and metabolism for their differentiation and survival. Suppression of OxPHOS activity in HSCs upon the loss of Ptpmt1, a PTEN-like mitochondrial phosphatase, impairs the early differentiation of HSCs and results in defective hematopoiesis [21]. Moreover, the mouse mutant, SDHD-ESR, that carries an inducible deletion of the *SdhD* gene, which encodes for one of the subunits of the mitochondrial complex II, is characterized by impaired survival of both HSCs and progenitors belonging to different lineages [31]. Of interest is also a recent study, which revealed that the complete disruption of mitochondrial respiration due to loss of the mitochondrial complex III subunit Rieske iron-sulfur protein (RISP) in fetal mouse HSCs leads to depletion of HSC numbers and their multilineage repopulation capacity [32]. Whereas RISP-null fetal HSCs have defects in their differentiation capacity, the RISP-null adult HSCs are characterized by loss of quiescence and entry into the cell cycle that is associated with lethality [32]. Collectively, these studies suggest that the self-renewing HSCs rely heavily, but not solely, on glycolysis, therefore emphasizing the importance of limited mitochondrial activity and metabolism in hematopoiesis and HSC fate decisions.

While the metabolic switch from glycolysis to mitochondrial OxPHOS activity and metabolism is required to meet the robust energy and metabolic demands imposed by differentiation, the precise mechanism underlying this switch remains elusive. It is likely that this metabolic rewiring is more complex than a simple switch from one form of energy production to another one. Instead, it might be the result of a series of events that occur before the onset of the well-known "metabolic switch." Importantly, these events might engage mechanisms that not only impact but also act in concert with this "metabolic switch" to coordinate and control the balance between HSC self-renewal and differentiation.

3. Mitochondrial Mass and Membrane Potential in HSC Fate

The role of mitochondria in HSC fate decisions and function is not merely limited to the metabolic switch but involves concomitant alterations of the mitochondrial features and properties. Distinctive mitochondrial membrane potential and mass between HSCs and cells at different stages of

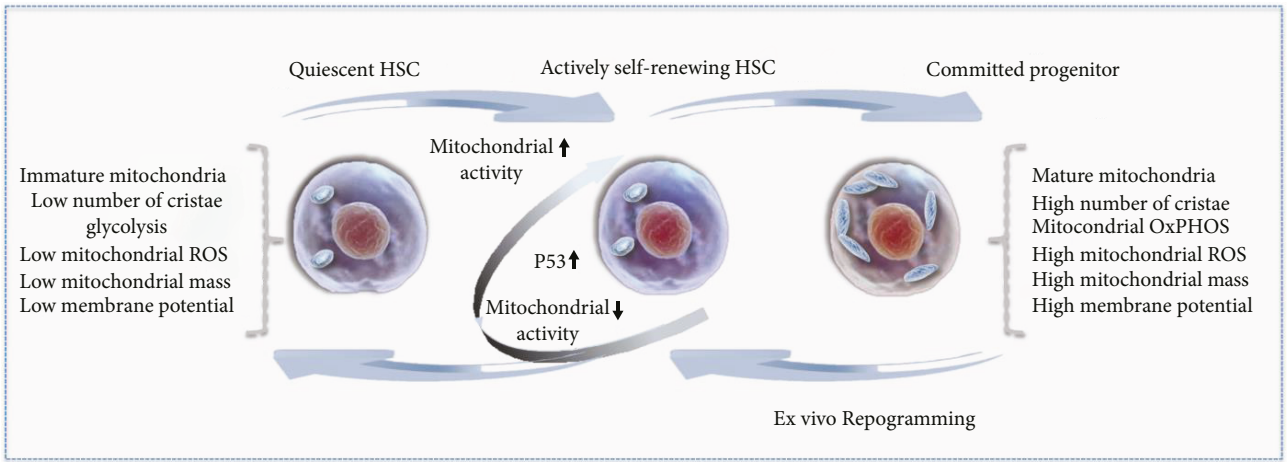

Figure 1: Mitochondrial regulation of HSCs. HSCs exhibit an immature mitochondrial network with globular mitochondria and primitive cristae. They rely heavily on glycolysis and display a low metabolic profile and OxPHOS activity accompanied by low mitochondrial ROS levels, mass, and membrane potential. During transition from quiescent to active cycling, HSCs increase their mitochondrial activity and potential to meet the increased demands of cycling cells for energy and metabolic bioproducts. During active cycling and divisions, suppression of the mitochondrial activity and activation of the p53 pathway are however required for HSCs to retain their self-renewing potential. By contrast, more committed progenitors display a mature mitochondrial network with the tubular mitochondria filled with a high number of regular cristae. Moreover, they exhibit high mitochondrial OxPHOS activity accompanied by high membrane potential, ROS generation, and mass. Ex vivo reprograming of more committed progenitors to actively dividing HSCs and their expansion are tightly linked to remodeling of a primitive mitochondrial network with low mitochondrial OxPHOS activity, increased glycolysis, and activation of the p53 pathway.

hematopoiesis have been reported. Indeed, both low mitochondrial activity and membrane potential mark the self-renewing murine and human HSCs [30, 33, 34] (Figure 1). Such HSCs possess significantly greater long-term multilineage reconstituting capacity in both primary and secondary NSG mice as compared to the same subpopulation of phenotypically defined HSCs that display a high mitochondrial membrane potential, indicative of mitochondrial bioenergetics [30]. Remarkably, these long-term HSCs have a lower mitochondrial mass as opposed to the more committed progenitors [30]. This evidence is consistent with findings indicating that a blockade in HSC differentiation by TSC1-mediated mTOR pathway inhibition is accompanied by a decrease in the mitochondrial mass [35]. By contrast, the loss of self-renewal capacity of HSCs due to lack of MTCH2 is related to an increase in both OxPHOS activity and mitochondrial size/volume [29].

The role and extent of mitochondrial membrane potential and mass on murine HSC self-renewal and commitment are similar to those observed during ex vivo studies performed with human umbilical cord blood-derived $CD34^+$cells (UCB-$CD34^+$) [34, 36]. The subpopulation of UCB-$CD34^+$ cells enriched in cells with long-term repopulating potential exhibits low levels of both mitochondrial mass and membrane potential as opposed to more differentiated cells [26]. Interestingly, the loss of CD34 expression in human mobilized HSCs undergoing commitment correlates with an increase in the mitochondrial content [37]. Unlike differentiation, cellular reprograming of UCB-$CD34^+$ cells into functional HSCs and acquisition of the CD90 phenotype triggered by treatment with a histone deacetylase inhibitor, valproic acid (VPA), are accompanied by a significant decline in mitochondrial mass and DNA content [36, 38]. Importantly, the reduction in mitochondrial mass is concomitant with a decrease in both mitochondrial OxPHOS activity and membrane potential [36] (Figure 1). Within the pool of ex vivo-expanded HSCs under normoxic conditions, cells expressing higher levels of both CD34 and CD90 exhibit lower mitochondrial mass compared to cells expressing low levels of both of these markers that phenotypically define functional HSCs [36].

Recently, the evidence that HSCs contain a low mitochondrial mass compared to progenitors and to mature cells has been challenged. A new study indicated that the mitochondrial mass in HSCs is underestimated due to artifacts caused by the efflux of MitoTracker Green, a commonly used dye to measure mitochondrial mass [39]. Intriguingly, another report revealed that both *in vivo* initiation and *in vitro* initiation of HSC division upon hematopoietic stress involve enhanced mitochondrial membrane potential and activity induced by increased Ca_2^+ flux [33] (Figure 1). While the amount of mitochondrial content in HSCs warrants further investigation, it is plausible that a parallel increase in both mitochondrial mass and potential may transiently precede the entry of HSCs to the cell cycle. To this end, however, it should be emphasized that following initiation of HSC divisions, retention of the self-renewing capacity of dividing HSCs requires suppression of the mitochondrial potential [33].

It is also important to reinforce at this point that even under normoxic condition HSCs display highly reduced mitochondrial activity as opposed to lineage-committed progenitors [4, 40]. In this regard, autophagy that is essential for HSC self-renewal potential acts primarily as a gatekeeper of

metabolic activity [40–42]. HSCs undergo active autophagy, which limits the number of active mitochondria and therefore reduces not only the mitochondrial mass but also, and more importantly, the mitochondrial activity of HSCs [33, 40, 41]. Although this view has been challenged due to the heterogeneity of HSCs used in the majority of studies, a recent report has reinforced the emerging role of autophagy [41]. In fact, the self-renewal potential of purified $Tie2^+$ HSCs that were identified to be at the top of the HSC hierarchy by both single-cell analysis and cell transplantation depends on activation of autophagy and particularly mitophagy [41].

It appears that the activation of autophagy is not balanced by enhanced mitochondrial biogenesis. In support of this notion is the evidence that mTOR pathway inhibition contributes to HSC quiescence not only by promoting autophagy but also by repressing mitochondrial biogenesis [35, 43–47]. In fact, the maintenance of HSC self-renewal relies on the repression of mitochondrial biogenesis and metabolic activity [25, 35, 48]. Conversely, transition of HSCs from quiescence to active proliferation is intrinsically related to enhanced mitochondrial biogenesis [49]. Mitochondrial metabolic fitness during this transition is tightly monitored by the mitochondrial unfolded protein response (UPR^{mt}), which is currently emerging as one of the main mitochondrial quality control mechanisms for HSC self-renewal. Interestingly, one of the key elements of the UPR^{mt}, SIRT7, protects the HSC pool challenged by stress by suppressing mitochondrial biogenesis [50]. This evidence underlines the remarkable ability of HSCs to activate multiple mechanisms and tightly control mitochondrial metabolic activity, which appears to be not simply a hallmark but rather a critical determinant of HSC maintenance and functional identity.

4. Multifaceted ROS and Their Role in HSC Fate

HSC fate decision with regard to self-renewal or commitment is monitored and regulated by ROS, a by-product of the bioenergetic metabolism. Although critical for physiological processes including activation of signal transduction pathways and fighting pathogens, excessive ROS can impair cellular functions by causing oxidative damage to lipids, proteins, RNA, and DNA. While the mitochondria are the major sources of ROS generation, they are also the main targets of ROS leading to vicious cycles of mitochondrial damage and energetic catastrophe. As discussed above, such damage and a complete failure in mitochondrial activity eventually lead to HSC exhaustion and impaired differentiation. Excessive ROS contribute to HSC aging and senescence, and at even higher levels, ROS induce HSC cell death [51].

Although evidence points towards the need for a tight control of ROS levels to prevent tissue damage and cell death, it is becoming clear that ROS might function as a rheostat that regulates cell fate decisions. At low levels, ROS maintain quiescence and the long-term repopulating capacity of HSCs [46]. At moderate levels, however, ROS act as second messengers and govern changes in cell fate. A limited elevation in ROS levels is necessary to drive HSC differentiation [14, 52]. Moderate levels of ROS are needed for hematopoiesis during both embryonic development and adult homeostasis [53]. Enhanced ROS levels are also required for proliferation of HSCs and progenitor cells during recovery from bone marrow injuries [54]. Thus, at different concentrations, ROS exert different roles. In fact, differential modulation of ROS levels by MCL-1 and BID, both members of the BCL-2 family of apoptotic proteins, can lead to HSC self-renewal, hematopoietic differentiation, or cell death [55, 56]. Suppression of high mitochondrial ROS levels by ATM-mediated BID phosphorylation regulates HSC self-renewal and quiescence. In a steady state, loss of BID phosphorylation and its increased association with mitochondria induce ROS generation at levels that are sufficient to drive HSCs into active proliferation and cell cycle progression, but not to cell death [55]. However, upon stress, loss of BID phosphorylation results in an immense generation of ROS ultimately causing exhaustion of the HSC pool [55, 56]. These findings are consistent with a report indicating that low levels of ROS can be used to enrich for highly primitive and quiescent HSCs capable of establishing long-term engraftment in murine models [14]. Conversely, HSCs with high ROS levels demonstrate remarkable exhaustion following serial transplantations [14, 55, 57]. Thus, these studies collectively address the intriguing puzzle of the need for low ROS levels in the maintenance of HSC self-renewal and integrity, but the absolute necessity for a limited ROS elevation was during hematopoietic development and stress.

4.1. Balanced ROS Regulation in HSCs by Coordinated Activity of Redox Signaling, Metabolism, and Epigenome. Regulation of ROS levels in HSCs is highly complex and involves regulation of both HSC metabolic activity and their antioxidant defense mechanisms [5, 58, 59]. Several lines of evidence indicate that MEIS1 (myeloid ecotropic viral integration site 1 homolog) regulates both of these processes by activating HIF1α and HIF2α [28, 58, 59], both of which drive cellular metabolism towards anaerobic glycolysis instead of mitochondrial respiration [4, 28, 46, 60]. Although the role of HIF1α and HIF2α in HSC function [61, 62] has been recently challenged, HSC maintenance by MEIS1 and its role in limiting oxidative stress have been well established using numerous mouse models [58, 59, 63, 64]. In addition to MEIS1, several other molecular pathways have been reported to act as central hubs that integrate metabolism with redox signaling and epigenetic modification. These pathways, which include class O of forkhead box (FoxOs) family proteins, sirtuin family members (SIRTs), p53 (TP53), the nuclear factor-kappa B (NF-κB), mTOR, and epigenetic regulators such as histone deacetylases (HDACs), are tightly interconnected. Together, they control, in a coordinated manner, the equilibrium between quiescence, active cycling, and differentiation of HSCs [15, 22, 65, 66]. Of great interest in this regard are the sirtuins, which have emerged as stress-responsive enzymes that govern cellular adaptations by altering the acetylome [67]. SIRT1 contributes to the maintenance of HSCs by limiting high levels of ROS through FOXO activation and decreased p53 activity [68–74]. It is likely that following metabolic stress, SIRT1 mitigates high ROS levels in HSCs by also activating a rapid induction of

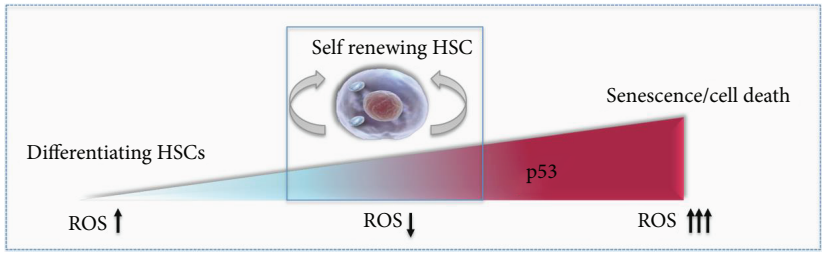

Figure 2: Effect of different levels of p53 in HSCs. Adequate p53 level and activity regulate the quiescent and self-renewing potential of HSCs by reducing ROS levels (boxed area). Lack of p53 impairs the quiescent state and self-renewing potential of HSCs and compromises the functional fitness of HSCs. Decreased p53 expression levels and activity promote differentiation of HSCs. Upon high levels of oxidative stress and ROS, increased p53 activity leads to senescence or cell death.

FOXO3A-dependent autophagy [75, 76]. In addition, SIRT1 retains both the genomic landscape and the epigenetic landscape of adult HSCs by promoting polycomb-specific repressive histone modification [77]. Notably, polycomb proteins, in particular BMI-1, which is a master epigenetic regulator of HSC self-renewal and fate, control mitochondrial ROS generation, further linking ROS with the epigenome and the fate of HSCs [78, 79].

The orchestration of the redox status of HSCs is monitored by the antioxidant defense mechanism, which relies on the activity of the scavenger antioxidant enzymes such as MnSOD. Sirtuin family proteins, primarily SIRT3, are required to retain the regenerative capacity of aged HSCs and to limit ROS production by enhancing MnSOD activity [80]. The long-term reconstitution capacity and premature aging of HSCs are also impacted by deficiencies in other redox sensors including thioredoxin-interacting protein (TXNIP) [65, 81]. The capability of TXNIP to regulate the aging of HSCs is attributed to its direct interaction and inhibition of the p38 MAPK pathway [81]. Whereas p38 activation by ROS limits the lifespan of HSCs [52], inhibition of p38 restores the long-term reconstitution capacity of HSCs. Moreover, p38 activation has been shown to deplete human HSCs and to be associated with the development of aplastic anemia in man [14, 52, 82]. In addition, TXNIP acts to retain the HSC pool by switching the function of p53 from serving as a prooxidant to an antioxidant [65]. Indeed, p53 is required for the maintenance of quiescent HSCs [83], and loss of p53 impairs the long-term repopulating capacity and functional identity of HSCs in serial transplantation assays [84] (Figure 2). Remarkably, a recent report demonstrated that suppression of Ca_2^+-mediated mitochondrial functions contributes to the maintenance of self-renewing murine HSCs during cell divisions through upregulation of p53-related genes [33]. At the same time, another study by our group revealed that the antioxidant activity of p53 is essential for the successful ex vivo reprograming and expansion of primitive HSCs from more committed UCB-CD34$^+$cells with VPA treatment [36]. To prevent excessive ROS generation, cells undergoing reprograming with VPA treatment mount a cellular antioxidant defense that relies on the activity of the p53-MnSOD axis. Notably, this defense mechanism acts in concert with a remodeled primitive mitochondrial network, which exhibits reduced OxPHOS activity [36]. Consistent with this decrease is the suppression of p38 activity as well as the upregulation of MEIS1 [36]. Together, these events underscore the array of coordinated mechanisms that control ROS levels and limit mitochondrial functions required for cellular reprograming of human functional HSCs and their ex vivo expansion. Collectively, these studies point towards the complex and unique regulation of HSC fate decisions dictated by mitochondrial function and the dynamic changes in ROS levels.

5. Mitochondrial Dynamics in HSCs

Mitochondrial bioenergetics and structure are tightly linked. Mitochondrial dynamics, including the modulation in mitochondrial ultrastructure, has been suggested to play a fundamental role in mitochondrial metabolism and, therefore, in determining stem cell fate [85, 86]. Emerging evidence indicates that massive remodeling of the mitochondria and particularly cristae, which are highly dynamic compartments where the OxPHOS complexes reside, might reflect changes in the energetic state of the cell [85, 87]. Consistent with a reliance on glycolysis and limited mitochondrial OxPHOS activity, human HSCs as well as human and mouse embryonic stem cells (ESCs) contain rare mitochondria with immature, globular morphology and poorly developed cristae [37, 88–90]. During differentiation, mitochondrial maturation results in the appearance of more mature, elongated, and tubular mitochondria with well-developed cristae that reflects increased mitochondrial activity [91–93]. Indeed, impairment of HSC long-term reconstitution capacity due to the loss of imprinting at the Dlk1-glt2 locus is linked to enhanced mitochondrial activity and ROS levels, as well as increased folds of cristae [25]. Consistent with this, the loss of MITCH2, which primes mitochondrial OxPHOS and increases mitochondrial size/volume, results in accelerated differentiation to progenitor cells, loss of quiescence, and eventual HSC exhaustion [29].

Mitochondrial dynamics and morphology are orchestrated by the mitochondrial fission/fusion machinery that relies on the activity of shaping proteins such as optic atrophy (OPA1), mitofusin-1 and mitofusin-2 (Mfn1 and Mfn2), and dynamin-related protein 1 (Drp1). Indeed, the shape of mitochondria is continuously defined by antagonistic and balanced activities of fusion and fission proteins [94]. Aberrations in the mitochondrial fission/fusion machinery accompanied by a shift towards fusion favor the generation

of abundant, large, and highly interconnected mitochondrial networks that are beneficial to metabolically active cells [85]. Such enlargement of mitochondria is due to decreased mitochondrial translocation of Drp-1, which is a master regulator of mitochondrial fragmentation [94]. Interestingly, the increase in mitochondrial size and the impairment of HSC function and numbers are due to loss of MITCH2, which is associated with a decreased association of Drp1 with mitochondria [29]. However, another study demonstrated that the fusion protein, Mfn2, which increases the buffering of intracellular $Ca2^{+}$, is also required for the maintenance of the lymphoid potential of HSCs, suggesting that mitochondrial dynamics influences HSC fate through numerous mechanisms [95].

The current understanding of mitochondrial architecture in HSCs and the role of fission/fusion in retaining of HSC self-renewal potential is very limited. A better understanding has been achieved by studies performed during reprograming of somatic cells into induced pluripotent stem cells (iPSs). During reprograming to iPCs, mitochondria undergo significant remodeling accompanied by an early wave of mitochondrial fragmentation due to increased fission and Drp1 activity [96]. In fact, mitochondrial fragmentation is required during the reprograming process to a pluripotent state [91, 92, 96–98]. Consistent with this, a study by our group revealed that cellular reprograming of HSCs from more committed UCB-$CD34^{+}$ cells is accompanied by a profound remodeling of the mitochondrial network comprised of morphologically small and globular mitochondria [36]. This cellular reprograming encompasses not only mitochondrial morphological changes but also a shift from OxPHOS activity to glycolysis (Figure 1). While the mechanism for such remodeling during HSC reprograming remains unknown, these data underlie the tight linkage between the mitochondrial ultrastructure and ROS generation, membrane potential, and mass in human primitive HSCs.

6. Conclusion and Perspectives

HSC reliance on glycolysis has been perceived as an adaptation to the hypoxic niche of the BM until now. Current evidence emphasized in this review, however, suggests that hypoxia might not be the only cause of limited mitochondrial metabolism in HSCs. In fact, numerous studies highlight the plasticity of mitochondria and their profound role in controlling the self-renewal and maintenance of HSCs. Important cues regarding the mechanisms and roles of mitochondria as drivers of HSC fate might be applied to improve efforts aimed at manipulation and ex vivo expansion of HSCs from UCBs. Ex vivo-expanded HSCs have potential therapeutic benefits in regenerative medicine to be used as allogeneic grafts for transplantation and/or gene therapy for monogenetic inherited blood disorders.

The use of UCBs for bone marrow transplantation is restricted due to the limited number of HSCs within a single unit. Several ex vivo strategies including the aryl hydrocarbon receptor antagonist (SR-1), pyrimidoindole derivative (UM-171), and VPA are currently utilized to overcome this limitation and expand to a great degree the numbers of transplantable HSCs [36, 38, 99, 100].

Ex vivo HSC cultures have been reported to induce stress. Such stress can impact mitochondrial function and activity, compromising therefore the characteristics of primary and clinically relevant HSCs. Overcoming this stress by limiting mitochondrial potential and activity presents an exciting target by which to expand the numbers of cycling HSCs while they retain their self-renewal and primitive characteristics. Remarkably, VPA treatment in ex vivo cultures has been reported to trigger both the acquisition and retention of a transcriptome and primitive mitochondrial profile with low activity, characteristic of primary functional HSCs [36, 38]. Both the acquisition and maintenance of a primitive HSC status were influenced by the antioxidant effect of the p53 pathway, which interestingly is reported to be enriched and activated during HSC self-renewing divisions [33, 36] (Figures 1 and 2). Thus, manipulation of both mitochondrial activity and the antioxidant p53 activity open new perspectives for the robust expansion of the self-renewing HSCs in ex vivo cultures. Such manipulations might be also beneficial for autologous HSC gene therapy and have the potential to overcome the loss of functional HSCs associated with gene editing. An adequate regulation of p53 activity and level also has the potential to preserve the functional fitness of HSCs with a youthful gene expression signature, both of which are lost during aging [101, 102]. Certainly, further understanding of the molecular mechanisms orchestrated by mitochondria in maintaining primary HSCs and determining their fate decisions will be essential to accelerate their application in regenerative medicine and transplantation settings.

Conflicts of Interest

The authors have declared that no conflict of interest exists.

Acknowledgments

This work was supported by New York State Stem Cell Science grant C030136 to RH. We would like to thank Dr. Christoph Schaniel and Bartek Jablonski for their feedback and revision of the manuscript.

References

[1] S. H. Orkin and L. I. Zon, "Hematopoiesis: an evolving paradigm for stem cell biology," *Cell*, vol. 132, no. 4, pp. 631–644, 2008.

[2] J. Seita and I. L. Weissman, "Hematopoietic stem cell: self-renewal versus differentiation," *Wiley Interdisciplinary Reviews: Systems Biology and Medicine*, vol. 2, no. 6, pp. 640–653, 2010.

[3] H. Cedar and Y. Bergman, "Epigenetics of haematopoietic cell development," *Nature Reviews Immunology*, vol. 11, no. 7, pp. 478–488, 2011.

[4] K. Takubo, G. Nagamatsu, C. I. Kobayashi et al., "Regulation of glycolysis by Pdk functions as a metabolic checkpoint for cell cycle quiescence in hematopoietic stem cells," *Cell Stem Cell*, vol. 12, no. 1, pp. 49–61, 2013.

[5] T. Simsek, F. Kocabas, J. Zheng et al., "The distinct metabolic profile of hematopoietic stem cells reflects their location in a hypoxic niche," *Cell Stem Cell*, vol. 7, no. 3, pp. 380–390, 2010.

[6] Y. H. Wang, W. J. Israelsen, D. Lee et al., "Cell-state-specific metabolic dependency in hematopoiesis and leukemogenesis," *Cell*, vol. 158, no. 6, pp. 1309–1323, 2014.

[7] J. R. Cantor and D. M. Sabatini, "Cancer cell metabolism: one hallmark, many faces," *Cancer Discovery*, vol. 2, no. 10, pp. 881–898, 2012.

[8] M. B. Hock and A. Kralli, "Transcriptional control of mitochondrial biogenesis and function," *Annual Review of Physiology*, vol. 71, no. 1, pp. 177–203, 2009.

[9] N. Urao and M. Ushio-Fukai, "Redox regulation of stem/progenitor cells and bone marrow niche," *Free Radical Biology & Medicine*, vol. 54, pp. 26–39, 2013.

[10] M. Khacho and R. S. Slack, "Mitochondrial dynamics in the regulation of neurogenesis: from development to the adult brain," *Developmental Dynamics*, vol. 247, no. 1, pp. 47–53, 2018.

[11] L. Kohli and E. Passegue, "Surviving change: the metabolic journey of hematopoietic stem cells," *Trends in Cell Biology*, vol. 24, no. 8, pp. 479–487, 2014.

[12] T. Suda, K. Takubo, and G. L. Semenza, "Metabolic regulation of hematopoietic stem cells in the hypoxic niche," *Cell Stem Cell*, vol. 9, no. 4, pp. 298–310, 2011.

[13] K. Ito, A. Hirao, F. Arai et al., "Regulation of oxidative stress by ATM is required for self-renewal of haematopoietic stem cells," *Nature*, vol. 431, no. 7011, pp. 997–1002, 2004.

[14] Y. Y. Jang and S. J. Sharkis, "A low level of reactive oxygen species selects for primitive hematopoietic stem cells that may reside in the low-oxygenic niche," *Blood*, vol. 110, no. 8, pp. 3056–3063, 2007.

[15] Z. Tothova and D. G. Gilliland, "FoxO transcription factors and stem cell homeostasis: insights from the hematopoietic system," *Cell Stem Cell*, vol. 1, no. 2, pp. 140–152, 2007.

[16] J. A. Spencer, F. Ferraro, E. Roussakis et al., "Direct measurement of local oxygen concentration in the bone marrow of live animals," *Nature*, vol. 508, no. 7495, pp. 269–273, 2014.

[17] S. J. Morrison and D. T. Scadden, "The bone marrow niche for haematopoietic stem cells," *Nature*, vol. 505, no. 7483, pp. 327–334, 2014.

[18] C. Piccoli, F. Agriesti, R. Scrima, F. Falzetti, M. di Ianni, and N. Capitanio, "To breathe or not to breathe: the haematopoietic stem/progenitor cells dilemma," *British Journal of Pharmacology*, vol. 169, no. 8, pp. 1652–1671, 2013.

[19] N. Shyh-Chang, G. Q. Daley, and L. C. Cantley, "Stem cell metabolism in tissue development and aging," *Development*, vol. 140, no. 12, pp. 2535–2547, 2013.

[20] D. Klimmeck, J. Hansson, S. Raffel, S. Y. Vakhrushev, A. Trumpp, and J. Krijgsveld, "Proteomic cornerstones of hematopoietic stem cell differentiation: distinct signatures of multipotent progenitors and myeloid committed cells," *Molecular & Cellular Proteomics*, vol. 11, no. 8, pp. 286–302, 2012.

[21] W. M. Yu, X. Liu, J. Shen et al., "Metabolic regulation by the mitochondrial phosphatase PTPMT1 is required for hematopoietic stem cell differentiation," *Cell Stem Cell*, vol. 12, no. 1, pp. 62–74, 2013.

[22] Z. Tothova, R. Kollipara, B. J. Huntly et al., "FoxOs are critical mediators of hematopoietic stem cell resistance to physiologic oxidative stress," *Cell*, vol. 128, no. 2, pp. 325–339, 2007.

[23] X. Xu, S. Duan, F. Yi, A. Ocampo, G. H. Liu, and J. C. Izpisua Belmonte, "Mitochondrial regulation in pluripotent stem cells," *Cell Metabolism*, vol. 18, no. 3, pp. 325–332, 2013.

[24] A. Wanet, T. Arnould, M. Najimi, and P. Renard, "Connecting mitochondria, metabolism, and stem cell fate," *Stem Cells and Development*, vol. 24, no. 17, pp. 1957–1971, 2015.

[25] P. Qian, X. C. He, A. Paulson et al., "The Dlk1-Gtl2 locus preserves LT-HSC function by inhibiting the PI3K-mTOR pathway to restrict mitochondrial metabolism," *Cell Stem Cell*, vol. 18, no. 2, pp. 214–228, 2016.

[26] D. Romero-Moya, C. Bueno, R. Montes et al., "Cord blood-derived CD34+ hematopoietic cells with low mitochondrial mass are enriched in hematopoietic repopulating stem cell function," *Haematologica*, vol. 98, no. 7, pp. 1022–1029, 2013.

[27] M. R. Warr and E. Passegue, "Metabolic makeover for HSCs," *Cell Stem Cell*, vol. 12, no. 1, pp. 1–3, 2013.

[28] K. Takubo, N. Goda, W. Yamada et al., "Regulation of the HIF-1alpha level is essential for hematopoietic stem cells," *Cell Stem Cell*, vol. 7, no. 3, pp. 391–402, 2010.

[29] M. Maryanovich, Y. Zaltsman, A. Ruggiero et al., "An MTCH2 pathway repressing mitochondria metabolism regulates haematopoietic stem cell fate," *Nature Communications*, vol. 6, no. 1, p. 7901, 2015.

[30] N. Vannini, M. Girotra, O. Naveiras et al., "Specification of haematopoietic stem cell fate via modulation of mitochondrial activity," *Nature Communications*, vol. 7, no. 1, article 13125, 2016.

[31] J. A. Bejarano-García, Á. Millán-Uclés, I. V. Rosado et al., "Sensitivity of hematopoietic stem cells to mitochondrial dysfunction by SdhD gene deletion," *Cell Death & Disease*, vol. 7, no. 12, article e2516, 2016.

[32] E. Ansó, S. E. Weinberg, L. P. Diebold et al., "The mitochondrial respiratory chain is essential for haematopoietic stem cell function," *Nature Cell Biology*, vol. 19, no. 6, pp. 614–625, 2017.

[33] T. Umemoto, M. Hashimoto, T. Matsumura, A. Nakamura-Ishizu, and T. Suda, "Ca2+–mitochondria axis drives cell division in hematopoietic stem cells," *The Journal of Experimental Medicine*, vol. 215, no. 8, pp. 2097–2113, 2018.

[34] F. Notta, S. Doulatov, E. Laurenti, A. Poeppl, I. Jurisica, and J. E. Dick, "Isolation of single human hematopoietic stem cells capable of long-term multilineage engraftment," *Science*, vol. 333, no. 6039, pp. 218–221, 2011.

[35] C. Chen, Y. Liu, R. Liu et al., "TSC-mTOR maintains quiescence and function of hematopoietic stem cells by repressing mitochondrial biogenesis and reactive oxygen species," *The Journal of Experimental Medicine*, vol. 205, no. 10, pp. 2397–2408, 2008.

[36] L. Papa, E. Zimran, M. Djedaini et al., "Ex vivo human HSC expansion requires coordination of cellular reprogramming with mitochondrial remodeling and p53 activation," *Blood Advances*, vol. 2, no. 20, pp. 2766–2779, 2018.

[37] C. Piccoli, R. Ria, R. Scrima et al., "Characterization of mitochondrial and extra-mitochondrial oxygen consuming reactions in human hematopoietic stem cells. Novel evidence of the occurrence of NAD(P)H oxidase activity," *The Journal*

of Biological Chemistry, vol. 280, no. 28, pp. 26467–26476, 2005.

[38] P. Chaurasia, D. C. Gajzer, C. Schaniel, S. D'Souza, and R. Hoffman, "Epigenetic reprogramming induces the expansion of cord blood stem cells," *The Journal of Clinical Investigation*, vol. 124, no. 6, pp. 2378–2395, 2014.

[39] M. J. de Almeida, L. L. Luchsinger, D. J. Corrigan, L. J. Williams, and H. W. Snoeck, "Dye-independent methods reveal elevated mitochondrial mass in hematopoietic stem cells," *Cell Stem Cell*, vol. 21, no. 6, pp. 725–729.e4, 2017.

[40] T. T. Ho, M. R. Warr, E. R. Adelman et al., "Autophagy maintains the metabolism and function of young and old stem cells," *Nature*, vol. 543, no. 7644, pp. 205–210, 2017.

[41] K. Ito, R. Turcotte, J. Cui et al., "Self-renewal of a purified Tie2+ hematopoietic stem cell population relies on mitochondrial clearance," *Science*, vol. 354, no. 6316, pp. 1156–1160, 2016.

[42] M. Nguyen-McCarty and P. S. Klein, "Autophagy is a signature of a signaling network that maintains hematopoietic stem cells," *PLoS One*, vol. 12, no. 5, article e0177054, 2017.

[43] C. Chen, Y. Liu, Y. Liu, and P. Zheng, "The axis of mTOR-mitochondria-ROS and stemness of the hematopoietic stem cells," *Cell Cycle*, vol. 8, no. 8, pp. 1158–1160, 2009.

[44] A. Joshi and M. Kundu, "Mitophagy in hematopoietic stem cells: the case for exploration," *Autophagy*, vol. 9, no. 11, pp. 1737–1749, 2013.

[45] X. Liu, Y. Zhang, M. Ni et al., "Regulation of mitochondrial biogenesis in erythropoiesis by mTORC1-mediated protein translation," *Nature Cell Biology*, vol. 19, no. 6, pp. 626–638, 2017.

[46] A. Ludin, S. Gur-Cohen, K. Golan et al., "Reactive oxygen species regulate hematopoietic stem cell self-renewal, migration and development, as well as their bone marrow microenvironment," *Antioxidants & Redox Signaling*, vol. 21, no. 11, pp. 1605–1619, 2014.

[47] J. T. Rodgers, K. Y. King, J. O. Brett et al., "mTORC1 controls the adaptive transition of quiescent stem cells from G0 to G(Alert)," *Nature*, vol. 510, no. 7505, pp. 393–396, 2014.

[48] C. Mantel, S. Messina-Graham, and H. E. Broxmeyer, "Upregulation of nascent mitochondrial biogenesis in mouse hematopoietic stem cells parallels upregulation of CD34 and loss of pluripotency: a potential strategy for reducing oxidative risk in stem cells," *Cell Cycle*, vol. 9, no. 10, pp. 2008–2017, 2010.

[49] M. Mohrin, A. Widjaja, Y. Liu, H. Luo, and D. Chen, "The mitochondrial unfolded protein response is activated upon hematopoietic stem cell exit from quiescence," *Aging Cell*, vol. 17, no. 3, article e12756, 2018.

[50] M. Mohrin, J. Shin, Y. Liu et al., "Stem cell aging. A mitochondrial UPR-mediated metabolic checkpoint regulates hematopoietic stem cell aging," *Science*, vol. 347, no. 6228, pp. 1374–1377, 2015.

[51] K. Naka, T. Muraguchi, T. Hoshii, and A. Hirao, "Regulation of reactive oxygen species and genomic stability in hematopoietic stem cells," *Antioxidants & Redox Signaling*, vol. 10, no. 11, pp. 1883–1894, 2008.

[52] K. Ito, A. Hirao, F. Arai et al., "Reactive oxygen species act through p38 MAPK to limit the lifespan of hematopoietic stem cells," *Nature Medicine*, vol. 12, no. 4, pp. 446–451, 2006.

[53] J. M. Harris, V. Esain, G. M. Frechette et al., "Glucose metabolism impacts the spatiotemporal onset and magnitude of HSC induction in vivo," *Blood*, vol. 121, no. 13, pp. 2483–2493, 2013.

[54] D. Lewandowski, V. Barroca, F. Duconge et al., "In vivo cellular imaging pinpoints the role of reactive oxygen species in the early steps of adult hematopoietic reconstitution," *Blood*, vol. 115, no. 3, pp. 443–452, 2010.

[55] M. Maryanovich, G. Oberkovitz, H. Niv et al., "The ATM-BID pathway regulates quiescence and survival of haematopoietic stem cells," *Nature Cell Biology*, vol. 14, no. 5, pp. 535–541, 2012.

[56] M. Maryanovich and A. Gross, "A ROS rheostat for cell fate regulation," *Trends in Cell Biology*, vol. 23, no. 3, pp. 129–134, 2013.

[57] M. Hu, H. Zeng, S. Chen et al., "SRC-3 is involved in maintaining hematopoietic stem cell quiescence by regulation of mitochondrial metabolism in mice," *Blood*, vol. 132, no. 9, pp. 911–923, 2018.

[58] F. Kocabas, J. Zheng, S. Thet et al., "Meis1 regulates the metabolic phenotype and oxidant defense of hematopoietic stem cells," *Blood*, vol. 120, no. 25, pp. 4963–4972, 2012.

[59] Z. Unnisa, J. P. Clark, J. Roychoudhury et al., "Meis1 preserves hematopoietic stem cells in mice by limiting oxidative stress," *Blood*, vol. 120, no. 25, pp. 4973–4981, 2012.

[60] W. W. Wheaton and N. S. Chandel, "Hypoxia. 2. Hypoxia regulates cellular metabolism," *American Journal of Physiology-Cell Physiology*, vol. 300, no. 3, pp. C385–C393, 2011.

[61] M. Vukovic, C. Sepulveda, C. Subramani et al., "Adult hematopoietic stem cells lacking Hif-1α self-renew normally," *Blood*, vol. 127, no. 23, pp. 2841–2846, 2016.

[62] A. V. Guitart, C. Subramani, A. Armesilla-Diaz et al., "Hif-2α is not essential for cell-autonomous hematopoietic stem cell maintenance," *Blood*, vol. 122, no. 10, pp. 1741–1745, 2013.

[63] R. Ariki, S. Morikawa, Y. Mabuchi et al., "Homeodomain transcription factor Meis1 is a critical regulator of adult bone marrow hematopoiesis," *PLoS One*, vol. 9, no. 2, article e87646, 2014.

[64] M. E. Miller, P. Rosten, M. E. Lemieux, C. Lai, and R. K. Humphries, "Meis1 is required for adult mouse erythropoiesis, megakaryopoiesis and hematopoietic stem cell expansion," *PLoS One*, vol. 11, no. 3, article e0151584, 2016.

[65] H. Jung, M. J. Kim, D. O. Kim et al., "TXNIP maintains the hematopoietic cell pool by switching the function of p53 under oxidative stress," *Cell Metabolism*, vol. 18, no. 1, pp. 75–85, 2013.

[66] Y. Chen, K. Liu, Y. Shi, and C. Shao, "The tango of ROS and p53 in tissue stem cells," *Cell Death and Differentiation*, vol. 25, no. 4, pp. 637–639, 2018.

[67] C. L. Brooks and W. Gu, "How does SIRT1 affect metabolism, senescence and cancer?," *Nature Reviews Cancer*, vol. 9, no. 2, pp. 123–128, 2009.

[68] H. Vaziri, S. K. Dessain, E. N. Eaton et al., "hSIR2(SIRT1) functions as an NAD-dependent p53 deacetylase," *Cell*, vol. 107, no. 2, pp. 149–159, 2001.

[69] J. Wang and J. Chen, "SIRT1 regulates autoacetylation and histone acetyltransferase activity of TIP60," *The Journal of Biological Chemistry*, vol. 285, no. 15, pp. 11458–11464, 2010.

[70] J. Wang, H. Fivecoat, L. Ho, Y. Pan, E. Ling, and G. M. Pasinetti, "The role of Sirt1: at the crossroad between promotion of longevity and protection against Alzheimer's disease

neuropathology," *Biochimica et Biophysica Acta (BBA) - Proteins and Proteomics*, vol. 1804, no. 8, pp. 1690–1694, 2010.

[71] P. Rimmelé, C. L. Bigarella, R. Liang et al., "Aging-like phenotype and defective lineage specification in SIRT1-deleted hematopoietic stem and progenitor cells," *Stem Cell Reports*, vol. 3, no. 1, pp. 44–59, 2014.

[72] K. Matsui, S. Ezoe, K. Oritani et al., "NAD-dependent histone deacetylase, SIRT1, plays essential roles in the maintenance of hematopoietic stem cells," *Biochemical and Biophysical Research Communications*, vol. 418, no. 4, pp. 811–817, 2012.

[73] L. Li and R. Bhatia, "Role of SIRT1 in the growth and regulation of normal hematopoietic and leukemia stem cells," *Current Opinion in Hematology*, vol. 22, no. 4, pp. 324–329, 2015.

[74] K. Miyamoto, K. Y. Araki, K. Naka et al., "Foxo3a is essential for maintenance of the hematopoietic stem cell pool," *Cell Stem Cell*, vol. 1, no. 1, pp. 101–112, 2007.

[75] X. Ou, M. R. Lee, X. Huang, S. Messina-Graham, and H. E. Broxmeyer, "SIRT1 positively regulates autophagy and mitochondria function in embryonic stem cells under oxidative stress," *Stem Cells*, vol. 32, no. 5, pp. 1183–1194, 2014.

[76] M. R. Warr, M. Binnewies, J. Flach et al., "FOXO3A directs a protective autophagy program in haematopoietic stem cells," *Nature*, vol. 494, no. 7437, pp. 323–327, 2013.

[77] S. K. Singh, C. A. Williams, K. Klarmann, S. S. Burkett, J. R. Keller, and P. Oberdoerffer, "Sirt1 ablation promotes stress-induced loss of epigenetic and genomic hematopoietic stem and progenitor cell maintenance," *The Journal of Experimental Medicine*, vol. 210, no. 5, pp. 987–1001, 2013.

[78] J. Liu, L. Cao, J. Chen et al., "Bmi1 regulates mitochondrial function and the DNA damage response pathway," *Nature*, vol. 459, no. 7245, pp. 387–392, 2009.

[79] L. Arranz, A. Urbano-Ispizua, and S. Mendez-Ferrer, "Mitochondria underlie different metabolism of hematopoietic stem and progenitor cells," *Haematologica*, vol. 98, no. 7, pp. 993–995, 2013.

[80] K. Brown, S. Xie, X. Qiu et al., "SIRT3 reverses aging-associated degeneration," *Cell Reports*, vol. 3, no. 2, pp. 319–327, 2013.

[81] H. Jung, D. O. Kim, J. E. Byun et al., "Thioredoxin-interacting protein regulates haematopoietic stem cell ageing and rejuvenation by inhibiting p38 kinase activity," *Nature Communications*, vol. 7, no. 1, article 13674, 2016.

[82] A. Verma, D. K. Deb, A. Sassano et al., "Cutting edge: activation of the p38 mitogen-activated protein kinase signaling pathway mediates cytokine-induced hemopoietic suppression in aplastic anemia," *Journal of Immunology*, vol. 168, no. 12, pp. 5984–5988, 2002.

[83] Y. Liu, S. E. Elf, Y. Miyata et al., "p53 regulates hematopoietic stem cell quiescence," *Cell Stem Cell*, vol. 4, no. 1, pp. 37–48, 2009.

[84] J. Chen, F. M. Ellison, K. Keyvanfar et al., "Enrichment of hematopoietic stem cells with SLAM and LSK markers for the detection of hematopoietic stem cell function in normal and Trp53 null mice," *Experimental Hematology*, vol. 36, no. 10, pp. 1236–1243, 2008.

[85] S. Cogliati, J. A. Enriquez, and L. Scorrano, "Mitochondrial cristae: where beauty meets functionality," *Trends in Biochemical Sciences*, vol. 41, no. 3, pp. 261–273, 2016.

[86] H. Zhang, K. J. Menzies, and J. Auwerx, "The role of mitochondria in stem cell fate and aging," *Development*, vol. 145, no. 8, 2018.

[87] Y. Tang, B. Luo, Z. Deng et al., "Mitochondrial aerobic respiration is activated during hair follicle stem cell differentiation, and its dysfunction retards hair regeneration," *PeerJ*, vol. 4, article e1821, 2016.

[88] S. Chung, P. P. Dzeja, R. S. Faustino, C. Perez-Terzic, A. Behfar, and A. Terzic, "Mitochondrial oxidative metabolism is required for the cardiac differentiation of stem cells," *Nature Clinical Practice Cardiovascular Medicine*, vol. 4, Supplement 1, pp. S60–S67, 2007.

[89] J. R. Hom, R. A. Quintanilla, D. L. Hoffman et al., "The permeability transition pore controls cardiac mitochondrial maturation and myocyte differentiation," *Developmental Cell*, vol. 21, no. 3, pp. 469–478, 2011.

[90] C. T. Chen, Y. R. V. Shih, T. K. Kuo, O. K. Lee, and Y. H. Wei, "Coordinated changes of mitochondrial biogenesis and antioxidant enzymes during osteogenic differentiation of human mesenchymal stem cells," *Stem Cells*, vol. 26, no. 4, pp. 960–968, 2008.

[91] S. Varum, A. S. Rodrigues, M. B. Moura et al., "Energy metabolism in human pluripotent stem cells and their differentiated counterparts," *PLoS One*, vol. 6, no. 6, article e20914, 2011.

[92] A. Prigione, B. Fauler, R. Lurz, H. Lehrach, and J. Adjaye, "The senescence-related mitochondrial/oxidative stress pathway is repressed in human induced pluripotent stem cells," *Stem Cells*, vol. 28, no. 4, pp. 721–733, 2010.

[93] Y. M. Cho, S. Kwon, Y. K. Pak et al., "Dynamic changes in mitochondrial biogenesis and antioxidant enzymes during the spontaneous differentiation of human embryonic stem cells," *Biochemical and Biophysical Research Communications*, vol. 348, no. 4, pp. 1472–1478, 2006.

[94] B. Westermann, "Mitochondrial fusion and fission in cell life and death," *Nature Reviews Molecular Cell Biology*, vol. 11, no. 12, pp. 872–884, 2010.

[95] L. L. Luchsinger, M. J. de Almeida, D. J. Corrigan, M. Mumau, and H. W. Snoeck, "Mitofusin 2 maintains haematopoietic stem cells with extensive lymphoid potential," *Nature*, vol. 529, no. 7587, pp. 528–531, 2016.

[96] J. Prieto, M. León, X. Ponsoda et al., "Early ERK1/2 activation promotes DRP1-dependent mitochondrial fission necessary for cell reprogramming," *Nature Communications*, vol. 7, no. 1, article 11124, 2016.

[97] C. D. L. Folmes, T. J. Nelson, A. Martinez-Fernandez et al., "Somatic oxidative bioenergetics transitions into pluripotency-dependent glycolysis to facilitate nuclear reprogramming," *Cell Metabolism*, vol. 14, no. 2, pp. 264–271, 2011.

[98] C. D. L. Folmes, P. P. Dzeja, T. J. Nelson, and A. Terzic, "Mitochondria in control of cell fate," *Circulation Research*, vol. 110, no. 4, pp. 526–529, 2012.

[99] J. E. Wagner Jr, C. G. Brunstein, A. E. Boitano et al., "Phase I/II trial of stemregenin-1 expanded umbilical cord blood hematopoietic stem cells supports testing as a stand-alone graft," *Cell Stem Cell*, vol. 18, no. 1, pp. 144–155, 2016.

[100] I. Fares, J. Chagraoui, B. Lehnertz et al., "EPCR expression marks UM171-expanded CD34(+) cord blood stem cells," *Blood*, vol. 129, 2017.

[101] M. Dumble, L. Moore, S. M. Chambers et al., "The impact of altered p53 dosage on hematopoietic stem cell dynamics during aging," *Blood*, vol. 109, no. 4, pp. 1736–1742, 2007.

[102] Z. Feng, W. Hu, A. K. Teresky, E. Hernando, C. Cordon-Cardo, and A. J. Levine, "Declining p53 function in the aging process: a possible mechanism for the increased tumor incidence in older populations," *Proceedings of the National Academy of Sciences*, vol. 104, no. 42, pp. 16633–16638, 2007.

Hindawi
Stem Cells International
Volume 2019, Article ID 1516746, 7 pages
https://doi.org/10.1155/2019/1516746

Research Article

Oral Plaque from Type 2 Diabetic Patients Reduces the Clonogenic Capacity of Dental Pulp-Derived Mesenchymal Stem Cells

Antonella Bordin,[1] **Francesca Pagano**,[1] **Eleonora Scaccia**,[1] **Matteo Saccucci**,[2] **Iole Vozza**,[2] **Noemi Incerti**,[1] **Antonella Polimeni**,[2] **Elena Cavarretta**,[1] **Isotta Chimenti**,[1] **and Elena De Falco**[1]

[1]*Department of Medical Surgical Sciences and Biotechnologies, Sapienza University of Rome, C.so della Repubblica 79, 04100 Latina, Italy*
[2]*Department of Oral and Maxillo-Facial Sciences, Sapienza University of Rome, Rome, Italy*

Correspondence should be addressed to Elena De Falco; elena.defalco@uniroma1.it

Received 25 September 2018; Accepted 3 December 2018; Published 14 January 2019

Academic Editor: Alexandra Harvey

Type 2 diabetes (T2D) is a major metabolic disease and a key epigenetic risk factor for the development of additional clinical complications. Among them, periodontitis (PD), a severe inflammatory disease ascribable to a dysregulated physiology and composition of the oral microbiota, represents one of the most relevant complications. Periodontitis can impact the structure of the tooth and likely the stem and progenitor cell pool, which actively contributes to the periodontal microenvironment and homeostasis. Modifications of the oral plaque play a key role in the etiopathogenesis of PD caused by T2D. However, to what extent the biology of the progenitor pool is affected has still to be elucidated. In this short report, we aimed to explore the biological effects of oral plaque derived from T2D patients with PD in comparison to non-diabetic patients with PD. Oral plaque samples were isolated from T2D and non-diabetic subjects with PD. Dental pulp stem cells (DPSCs), derived from the premolar tooth, were conditioned for 21 days with oral plaque samples and tested for their clonogenic ability. Cultures were also induced to differentiate towards the osteogenic lineage, and ALP and osteocalcin gene expression levels were evaluated by real-time qPCR. Results have shown that the number of clones generated by DPSCs exposed to T2D oral plaque was significantly lower compared to controls (ctl). The multivariate analysis confirmed that the decreased clonogenesis was significantly correlated only with T2D diagnosis. Moreover, the effect of T2D oral plaque was specific to DPSCs. Indicators of osteogenic differentiation were not significantly affected. This study provides a new biological insight into the effects ascribable to T2D in PD.

1. Introduction

Type 2 diabetes (T2D) is a very common metabolic disease caused by resistance to insulin and consequent systemic hyperglycaemia. The pathological effects induced by T2D are chronic and exhibit multifaceted features, as they imply profound alterations in both the endocrine asset and metabolic/physiological functions of several biological systems [1–3], including the oral microenvironment [4, 5]. In this regard, periodontitis (PD), a severe inflammatory disorder of the periodontium caused by oral bacterial challenge, is a complication of T2D [6]. In fact, patients affected by T2D are more susceptible to PD. The periodontium is a highly vascularised system, and oral plaque possesses intrinsic biological properties such as the pivotal chemotactic ability for immune cells [7]. Type 2 diabetes severely impairs the architecture of periodontal tissue and interferes with basic cellular functions such as phagocytosis, migration, and more importantly the innate immune response provided by the epithelial mucosa of the periodontium. Importantly, the unbalanced inflammatory and dysmetabolic state in T2D significantly affects the composition of the bacterial film in the oral plaque, therefore impairing periodontal integrity and function [8]. This scenario is further exacerbated by modifications both in macro and microcirculation of the periodontium, ascribable to T2D due to the increase in glycation

end-products (AGEs), oxidative stress and deregulation of the endothelial barrier [8]. Intriguingly, PD and diabetes mutually influence each other in a bidirectional fashion: diabetes increases proinflammatory levels of soluble mediators, therefore reinforcing periodontal inflammation; in turn, PD influences the glycaemic index in diabetic patients [9]. Moreover, epidemiological studies have demonstrated that PD is strictly associated with increased cardiovascular risk as a direct consequence of endothelial dysfunction following changes of oral plaque [10]. Notably, T2D-induced oral plaque modifications are not limited to the sole periodontium, but they could likely affect defined cell populations of dental origin and mainly progenitors of mesenchymal origin, which reside in the tooth canal opening in the periodontium. Dental pulp stem cells (DPSCs) have been defined as adult progenitor cells of ectodermal origin, exhibiting mesenchymal features [11–13], including clonogenic and self-renewal capacity, mesodermal-like differentiation, and mainly osteogenic, mineralization, and regeneration capabilities [14, 15]. Interestingly, transplanted DPSCs in streptozotocin-induced diabetic mouse models have confirmed the ability of DPSCs both to enhance glucose tolerance in a paracrine manner [16, 17] and to restore vascular function [18, 19]. Dental pulp stem cells have been also reported as effective candidates to generate insulin-producing cells [20–22], parallel to a peculiar and attractive feature of anti-inflammatory and nociceptive soluble mediator-based secretion [21]. Importantly, the progression of PD in the presence of T2D is certainly dependent on the plaque-host relationship, which may vary between individuals. To date, biological and molecular mechanisms underlying the interplay between DPSC properties and alterations of the oral microenvironment caused by T2D are still to be addressed. Here, we investigate the effects of T2D-related oral dysbiosis and its potential biological consequences that might involve DPSCs, responsible for the dental stemness homeostasis and regenerative properties. Accordingly, we hypothesize a direct biological effect of T2D oral plaque on DPSC function and differentiation beyond the sole involvement of the periodontium. We found that oral plaque obtained from T2D patients with PD significantly reduced the clonogenic ability of DPSCs compared to that obtained from nondiabetic patients with PD, without impacting osteogenic differentiation, analysed by the expression of both alkaline phosphatase (ALP) and osteocalcin, known to represent specific markers of the osteoblast lineage [23] and to be involved in the mineralization of the extracellular matrix and therefore in osteogenesis [24]. Notably, the decrease in clonogenic potential of DPSCs was independent of the main specific clinical features of diabetic patients, such as age and sex.

2. Materials and Methods

2.1. Isolation, Culture, and Characterization of Dental Pulp Stem Cells (DPSCs) by Flow Cytometry. Dental pulp stem cells (DPSCs) were obtained from explants of dental pulp from one subject undergoing tooth extraction for orthodontic treatment and according to previous reports [15, 25]. Briefly, the premolar tooth was kept in a physiological solution after extraction and then in milk. Afterwards, the pulp was collected, chopped in a petri dish containing PBS and 1% penicillin/streptomycin, and left to adhere for 2 hours at 37°C in 5% CO_2 in the incubator. Afterwards, PBS was removed and replaced by complete media composed of DMEM-low glucose supplemented with 20% FBS and 1% penicillin/streptomycin (all Gibco). After 72 hours, nonadherent cells were removed and fresh complete media were added. DPSCs were expanded up to the third passage by trypsinization and subcultured at 4000 cells/cm^2 in complete media. Cell growth and viability were monitored by trypan blue exclusion assay. Cultures were characterized by flow cytometry analysis. At passage 3, DPSCs were trypsinized and resuspended in FACS buffer (PBS/2% foetal bovine serum) for immunophenotype assessment. Cells were stained with indirectly or directly conjugated primary antibodies against CD44, CD105, CD117, CD90 (all Abcam, Cat. N. ab44967, ab6124, ab23894, and ab5506), CD34 (Miltenyi Biotec, Calderara di Reno, Bologna, Italy, Cat. N. 130-081-001), and CD73 (BioLegend, San Diego, CA, USA, Cat. 344005). Cells were incubated with primary antibodies for 30 minutes, followed by staining with secondary antibodies (only if indirectly conjugated) [11–13, 26]. Data was acquired by cytofluorimeter (FACSAria II, BD, San Jose, CA, USA) and analysed by Diva Software (v6.1.1, BD, San Jose, CA, USA). This study was approved by the Ethical Committee of Policlinico Umberto I, Rome, Italy (protocol number 4336, 02/02/2017). Experiments were conducted in accordance with the 1964 Helsinki Declaration regarding the study involving human participants. Informed consent was obtained from all subjects before the surgical procedure. Subjects were all deidentified by employing a code (from B-F (T2D) and from G-I (ctl)). The clinical features of all patients are reported in Table 1. Subcutaneous adipose stromal cells (ASCs, primary cell lines 55P and 56P) were isolated as previously described [11, 27], according to the approved protocol (Ethical Committee of "Sant'Andrea" Hospital in Rome, Ref. 49_2013/28.01.2016).

Table 1: Clinical features of patients.

	Age	Sex	Smoker
Donor DPSCs			
1	16	M	No
Donor oral plaque			
T2D-B	52	M	No
T2D-C	91	F	No
T2D-D	79	M	No
T2D-E	94	F	No
T2D-F	94	M	No
Ctl-G	22	M	No
Ctl-H	53	M	No
Ctl-I	82	F	No

2.2. Oral Plaque Isolation. Oral plaque was isolated as previously reported [7]. Briefly, single plaque samples were firstly spun at 400g for 5 minutes at 4°C in order to concentrate the

plaque. Afterwards, the pellet was weighed for the following data normalization and mechanically homogenised using a pestle in ice. The plaque was then diluted in 1 ml of sterile PBS and centrifuged at 4°C and 600g for 15 minutes. The supernatant was then collected and filtered by using a 0.45 μm mesh. Oral plaque suspensions were freshly used.

2.3. Clonogenic and Osteogenic Differentiation Assay. Cultures were conditioned with oral plaque from diabetic and ctl patients, by seeding DPSCs at a low density (10 cells/cm^2) in complete media, as previously described [11–13, 26], then supplemented with an equal amount of oral plaque-derived suspensions (volume ratio 1 : 1) for 21 days. Fresh oral plaque suspensions were replaced every 3 days. At the end of the incubation time, cells were fixed with 4% paraformaldehyde for 1 hour at room temperature and then stained with Giemsa (Sigma) in order to identify nuclear and/or cytoplasmic morphology of colony-forming units (CFU). The number of clones was quantified by an optical microscope and then normalized to the amount (mg) of the oral plaque seeded [11–13, 26]. For osteogenic differentiation tests, DPSCs were cultured for 21 days in a StemPro® Osteogenesis Differentiation Kit (5×10^3 cells/cm^2, Gibco, Cat. N. A10072-01) [12, 13] supplemented with an equal amount of oral plaque-derived suspensions (volume ratio 1 : 1). Afterwards, calcium deposition was analysed incubating the cells for 1 hour at room temperature with a 2% Alizarin red solution at pH 4.1-4.3 (Sigma, St. Louis, USA, Cat. N. A5533) [13, 26].

2.4. Real-Time PCR. Total RNA was isolated (RNeasy kit, Qiagen), and c-DNA was obtained and amplified by the SensiMix SYBR Hi-ROX Kit (Bioline, London, UK). Templates were amplified by the 7900HT Fast Real-Time PCR System (Applied Biosystems, Cheshire, UK) for 40 cycles according to the following protocol: 95°C for 15 seconds, 56-58°C for 15 seconds, and 72°C for 15 seconds. Primer sequences used were the following: forward—GATGTG GAGTATGAGAGTGAC and reverse—GGTCAAGGGTC AGGAGTTC (ALP), forward—TGAAAGCCGATGTGGT CAG and reverse—CAGCGAGGTAGTGAAGAGAC (osteocalcin), and forward—ACAGTCAGCCGCATCTTC and reverse—GCCCAATACGACCAAATCC (GAPDH). GAPDH was considered a housekeeping gene. The reaction products were analysed by SDS 2.1.1 software (Applied Biosystems, Cheshire, UK).

2.5. Statistical Analysis. Statistical analysis was performed by using GraphPad Prism 5 software (San Diego, USA). Comparison between two groups was performed by t-test. Multivariable linear regression analyses were conducted to adjust for potential confounders, and computation was performed with SPSS 20 (IBM). A p value < 0.05 has been considered statistically significant. Data are presented as mean ± standard error, unless specified.

3. Results

In order to test the influence of T2D patient-derived oral plaque on DPSC biology in the presence of PD, we have firstly isolated and characterized the primary cell line of DPSCs from the premolar tooth. Flow cytometry analysis showed that DPSCs exhibited a mesenchymal stem cell-like immunophenotype [11–13, 26] with high expression of stromal markers such as CD44, CD90 and CD73 and a moderate and low positivity for CD105 and CD117, respectively (Figure 1(a)). The expression of CD34 (hematopoietic marker) was undetectable. The DPSC cultures were expanded up to the third passage, when they exhibited the highest number of doubling viable cells (Figure 1(b), $p < 0.0001$ and $p < 0.01$, passage 3 vs. passages 1 and 2, respectively). In order to evaluate their clonogenic ability, cells were then cultured at a low density for 21 days by supplementing the culture media with oral plaque preparations obtained from T2D patients ($N = 5$) with PD. Cultures supplemented with oral plaque from non-diabetic individuals with PD were used as ctl ($N = 3$). The clinical features of subjects enrolled in this study are displayed in Table 1. Smoking, surgical interventions, and infections have been considered exclusion criteria. Results showed a striking and significant decrease in the number of clones generated by DPSCs when conditioned with oral plaque derived from T2D patients with PD compared to ctl (Figure 1(c), $p < 0.0001$). Since the average age of donors in the two groups appeared to differ, we performed a multivariable linear regression analysis to adjust for this potential confounder. The multivariable regression analysis indicated a significant association between the presence of T2D and decreased clonogenesis independently of the age of the patient (Table 2). Afterwards, we induced DPSC differentiation into the mesodermal lineage, by priming the cultures for 21 days towards the osteogenic phenotype in the presence of both types of oral plaque, and we quantified the expression of the main osteogenic genes including ALP and osteocalcin [28]. Results showed that T2D oral plaque did not significantly affect the osteogenic differentiation, although a trend of ALP to increase in cultures supplemented with oral plaque samples derived from T2D patients with respect to ctl was observed (Figure 1(d)).

Finally, in order to verify whether the effect of T2D oral plaque was specific to DPSCs, we tested the samples on two distinct human primary subcutaneous ASC lines (55P and 56P). Results have shown that the number of CFU was not significantly affected by T2D oral plaque (Figure 2), therefore suggesting a specific effect mainly related to the dental microenvironment.

4. Discussion

In this study, we have shown that oral plaque derived from T2D patients with PD impacts negatively on the clonogenic ability of DPSCs, highlighting a potential biological mechanism by which diabetes may contribute to periodontal damage. To the best of our knowledge, the direct effect of T2D-derived plaque on DPSCs has never been addressed. Our set of diabetic patients has developed PD, whose etiopathogenesis is linked to a wide range of alterations triggered in the mouth. These include changes of the periodontal microbiota with respect to healthy individuals [28], associated in particular with the increase in defined pathogens

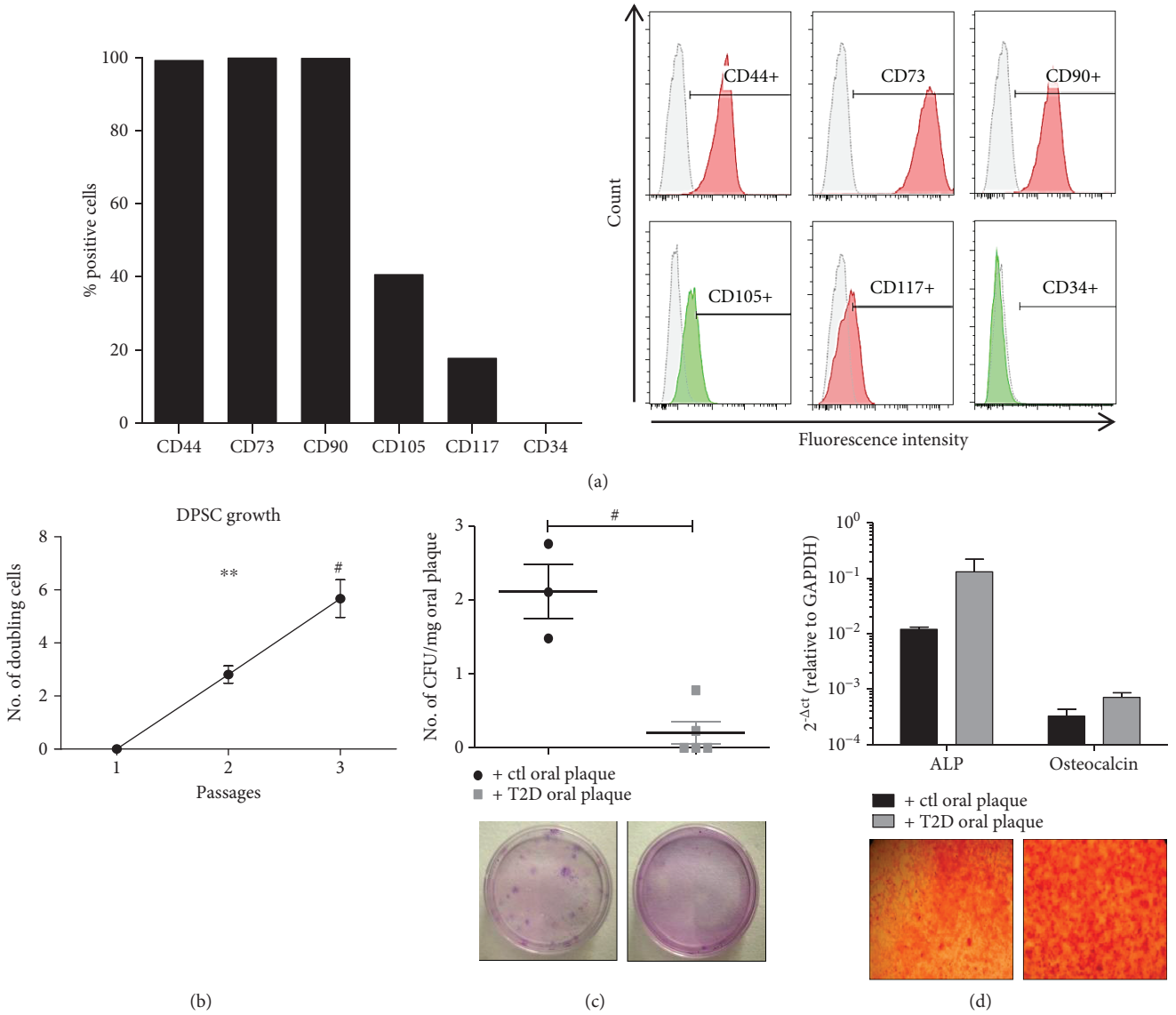

Figure 1: (a) Flow cytometry analysis of DPSCs after isolation. The graph shows that DPSC cultures exhibit a mesenchymal-like immunophenotype with positivity to the main stromal markers and negativity to the hematopoietic marker CD34. Representative cytofluorimetric histograms are displayed on the right (red and green histograms and APC and FITC fluorochromes, respectively). (b) Cell growth profile of DPSCs. The graph displays that the number of doubling cells is significantly increased at higher passages. Results were normalized to passage 1. $^{**}p < 0.01$, $^{\#}p < 0.0001$. (c) The graph shows that the number of clones generated by DPSCs in the presence of T2D oral plaque is significantly lower compared to that in controls (ctls). The number of CFU was normalized to the amount of oral plaque (mg). Below the graph, representative optical images of CFU stained with Giemsa are shown. $^{\#}p < 0.0001$. (d) Osteogenic differentiation of DPSCs. The graph displays the gene expression levels of ALP and osteocalcin which are unaltered between the two treatments. Below the graph, representative optical images of osteogenic differentiation of DPSCs stained with Alizarin red. Magnification: 10x.

Table 2: Multivariable linear regression analysis for the association of the normalized CFU yield (CFU/mg) and diabetes, adjusted for age.

Independent variable	Regression coefficient	p
T2D	-1.74	0.01
Age	-0.006	0.54

[29–31], known to antagonize the immune response in patients with PD [32]. Although we did not identify the nature of the biofilm in our oral plaque samples, it is plausible that the microbiological profile has been profoundly modified in diabetic patients [8, 33, 34]. Notably, the number of CFU generated by DPSCs was negatively affected by oral plaque from this set of T2D patients, despite the absence of significant statistical correlations with clinical parameters and potential inter-patient variability, known to play a role in the progression of PD even in relation to the oral microenvironment [28].

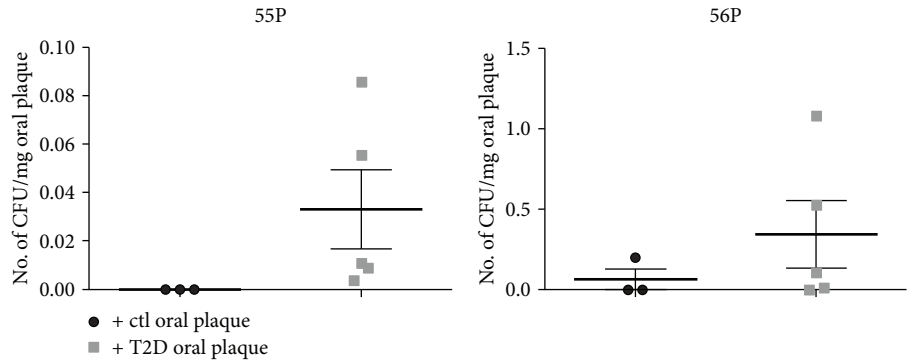

Figure 2: The graphs display the number of clones (CFU) generated from two distinct primary lines (55P and 56P) derived from subcutaneous adipose tissue and stimulated with ctl and T2D oral plaque, highlighting that there is no significant difference between the treatments. The number of CFU was normalized to the amount of oral plaque (mg).

Intriguingly, when subcutaneous ASCs (stromal cells of different tissue origin from DPSCs) are similarly treated with T2D oral plaque, the effect is not reproducible in our conditions, indicating that the ability of T2D to decrease the clonogenic efficiency is specific to DPSCs and likely restricted to the dental microenvironment.

The low number of subjects enrolled in this study certainly represents a limitation. Nevertheless, we cannot rule out that the alterations of the oral plaque mediated by diabetes with regard to the intrinsic properties of DPSCs represent a priming and sufficient event able to transversely affect individuals at any age and gender, therefore highlighting non-cumulative effects over the time. Additionally, we have detected a trend towards increased osteogenic differentiation in the presence of T2D oral plaque (although not statistically significant). This result is only apparently discrepant from the majority of the studies in literature, showing that diabetes severely compromises osteogenic differentiation [28, 35, 36]. However, our result should be interpreted in the light of the clonogenesis result. In fact, normally, the biological events related to the clonogenic and differentiation properties are mutually exclusive and strictly dependent on the tissue of origin [11, 23]. In the majority of adult progenitor populations, including DPSCs, the balance between these two processes is finely tuned, and pathological insults as T2D are able to deregulate both phases. Thus, the modifications of the oral plaque caused by diabetes are likely to shift the ability of DPSCs to select the proliferative clones towards a main tendency to differentiate, therefore exhausting the original multipotent and stromal stem cell pool. From a clinical point of view, this effect would result in a deregulated ossification and in the inability of patients to exploit their own stem cell pool to trigger regeneration upon pathological conditions. Accordingly, DPSCs represent the responsible population for periodontal homeostasis, able to actively respond to different damages, by enhancing the repairing process [15]. Notably, periodontal therapy (especially the intensive kind) in diabetic patients in combination with glycaemia control is able to successfully restore a suitable periodontal microenvironment [33, 37, 38], therefore confirming the reversible epigenetic nature of T2D. Thus, it is also plausible that hyperglycaemia consequent to insulin resistance (the hallmark of T2D patients) may represent the key stimulus to change both the composition of the oral plaque and the biological features of DPSCs.

5. Conclusions

Our study strengthens the involvement of DPSCs in T2D-mediated PD. The finding that oral plaque may represent the direct biological modality by which diabetes impairs the dental pulp stem and progenitor cell pool could be of clinical significance.

Data Availability

The data used to support the findings of this study are available from the corresponding author upon request.

Conflicts of Interest

The authors declare no conflicts of interest to disclose.

Acknowledgments

We thank "Fondazione Roma" for the continuous support. This work was supported by the Department of Medical-Surgical Sciences and Biotechnologies, Sapienza University of Rome.

References

[1] F. Angelini, F. Pagano, A. Bordin et al., "The impact of environmental factors in influencing epigenetics related to oxidative states in the cardiovascular system," *Oxidative Medicine and Cellular Longevity*, vol. 2017, Article ID 2712751, 18 pages, 2017.

[2] G. Frati, L. Schirone, I. Chimenti et al., "An overview of the inflammatory signalling mechanisms in the myocardium underlying the development of diabetic cardiomyopathy," *Cardiovascular Research*, vol. 113, no. 4, pp. 378–388, 2017.

[3] Y. Zheng, S. H. Ley, and F. B. Hu, "Global aetiology and epidemiology of type 2 diabetes mellitus and its

complications," *Nature Reviews Endocrinology*, vol. 14, no. 2, pp. 88–98, 2018.

[4] R. A. DeFronzo, E. Ferrannini, L. Groop et al., "Type 2 diabetes mellitus," *Nature Reviews Disease Primers*, vol. 1, article 15019, 2015.

[5] G. G. Nascimento, F. R. M. Leite, P. Vestergaard, F. Scheutz, and R. Lopez, "Does diabetes increase the risk of periodontitis? A systematic review and meta-regression analysis of longitudinal prospective studies," *Acta Diabetologica*, vol. 55, no. 7, pp. 653–667, 2018.

[6] D. F. Kinane, P. G. Stathopoulou, and P. N. Papapanou, "Periodontal diseases," *Nature Reviews Disease Primers*, vol. 3, article 17038, 2017.

[7] R. L. Miller, L. E. A. Folke, and C. R. Umana, "Chemotactic ability of dental plaque upon autologous or heterologous human polymorphonuclear leukocytes," *Journal of Periodontology*, vol. 46, no. 7, pp. 409–414, 1975.

[8] R. S. Levine, "Obesity, diabetes and periodontitis – a triangular relationship?," *British Dental Journal*, vol. 215, no. 1, pp. 35–39, 2013.

[9] C. M. M. L. Santos, R. Lira-Junior, R. G. Fischer, A. P. P. Santos, and B. H. Oliveira, "Systemic antibiotics in periodontal treatment of diabetic patients: a systematic review," *PLoS One*, vol. 10, no. 12, article e0145262, 2015.

[10] A. Saremi, R. G. Nelson, M. Tulloch-Reid et al., "Periodontal disease and mortality in type 2 diabetes," *Diabetes Care*, vol. 28, no. 1, pp. 27–32, 2005.

[11] C. Siciliano, A. Bordin, M. Ibrahim et al., "The adipose tissue of origin influences the biological potential of human adipose stromal cells isolated from mediastinal and subcutaneous fat depots," *Stem Cell Research*, vol. 17, no. 2, pp. 342–351, 2016.

[12] C. Siciliano, I. Chimenti, A. Bordin et al., "The potential of GMP-compliant platelet lysate to induce a permissive state for cardiovascular transdifferentiation in human mediastinal adipose tissue-derived mesenchymal stem cells," *BioMed Research International*, vol. 2015, Article ID 162439, 10 pages, 2015.

[13] C. Siciliano, M. Ibrahim, G. Scafetta et al., "Optimization of the isolation and expansion method of human mediastinal-adipose tissue derived mesenchymal stem cells with virally inactivated GMP-grade platelet lysate," *Cytotechnology*, vol. 67, no. 1, pp. 165–174, 2015.

[14] N. Nuti, C. Corallo, B. M. F. Chan, M. Ferrari, and B. Gerami-Naini, "Multipotent differentiation of human dental pulp stem cells: a literature review," *Stem Cell Reviews*, vol. 12, no. 5, pp. 511–523, 2016.

[15] E. Ledesma-Martinez, V. M. Mendoza-Nunez, and E. Santiago-Osorio, "Mesenchymal stem cells derived from dental pulp: a review," *Stem Cells International*, vol. 2016, Article ID 4709572, 12 pages, 2016.

[16] M. M. Kanafi, Y. B. Rajeshwari, S. Gupta et al., "Transplantation of islet-like cell clusters derived from human dental pulp stem cells restores normoglycemia in diabetic mice," *Cytotherapy*, vol. 15, no. 10, pp. 1228–1236, 2013.

[17] T. Izumoto-Akita, S. Tsunekawa, A. Yamamoto et al., "Secreted factors from dental pulp stem cells improve glucose intolerance in streptozotocin-induced diabetic mice by increasing pancreatic β-cell function," *BMJ Open Diabetes Research & Care*, vol. 3, no. 1, article e000128, 2015.

[18] M. Omi, M. Hata, N. Nakamura et al., "Transplantation of dental pulp stem cells improves long-term diabetic polyneuropathy together with improvement of nerve morphometrical evaluation," *Stem Cell Research & Therapy*, vol. 8, no. 1, p. 279, 2017.

[19] I. Datta, N. Bhadri, P. Shahani et al., "Functional recovery upon human dental pulp stem cell transplantation in a diabetic neuropathy rat model," *Cytotherapy*, vol. 19, no. 10, pp. 1208–1224, 2017.

[20] Y. Li, S. Zhao, X. Nan et al., "Repair of human periodontal bone defects by autologous grafting stem cells derived from inflammatory dental pulp tissues," *Stem Cell Research & Therapy*, vol. 7, no. 1, p. 141, 2016.

[21] M. K. Marei and R. M. El Backly, "Dental mesenchymal stem cell-based translational regenerative dentistry: from artificial to biological replacement," *Frontiers in Bioengineering and Biotechnology*, vol. 6, p. 49, 2018.

[22] V. Govindasamy, V. S. Ronald, A. N. Abdullah et al., "Differentiation of dental pulp stem cells into islet-like aggregates," *Journal of Dental Research*, vol. 90, no. 5, pp. 646–652, 2011.

[23] G. Mori, G. Brunetti, A. Oranger et al., "Dental pulp stem cells: osteogenic differentiation and gene expression," *Annals of the New York Academy of Sciences*, vol. 1237, no. 1, pp. 47–52, 2011.

[24] H. S. Ching, N. Luddin, I. A. Rahman, and K. T. Ponnuraj, "Expression of odontogenic and osteogenic markers in DPSCs and SHED: a review," *Current Stem Cell Research & Therapy*, vol. 12, no. 1, pp. 71–79, 2017.

[25] L. Spath, V. Rotilio, M. Alessandrini et al., "Explant-derived human dental pulp stem cells enhance differentiation and proliferation potentials," *Journal of Cellular and Molecular Medicine*, vol. 14, no. 6B, pp. 1635–1644, 2010.

[26] C. Siciliano, I. Chimenti, M. Ibrahim et al., "Cardiosphere conditioned media influence the plasticity of human mediastinal adipose tissue-derived mesenchymal stem cells," *Cell Transplantation*, vol. 24, no. 11, pp. 2307–2322, 2015.

[27] R. Businaro, E. Scaccia, A. Bordin et al., "Platelet lysate-derived neuropeptide y influences migration and angiogenesis of human adipose tissue-derived stromal cells," *Scientific Reports*, vol. 8, no. 1, article 14365, 2018.

[28] E. Lalla and P. N. Papapanou, "Diabetes mellitus and periodontitis: a tale of two common interrelated diseases," *Nature Reviews Endocrinology*, vol. 7, no. 12, pp. 738–748, 2011.

[29] R. L. Mandell, J. Dirienzo, R. Kent, K. Joshipura, and J. Haber, "Microbiology of healthy and diseased periodontal sites in poorly controlled insulin dependent diabetics," *Journal of Periodontology*, vol. 63, no. 4, pp. 274–279, 1992.

[30] J. L. Ebersole, S. C. Holt, R. Hansard, and M. J. Novak, "Microbiologic and immunologic characteristics of periodontal disease in Hispanic Americans with type 2 diabetes," *Journal of Periodontology*, vol. 79, no. 4, pp. 637–646, 2008.

[31] D. Haubek, O. K. Ennibi, K. Poulsen, M. Vaeth, S. Poulsen, and M. Kilian, "Risk of aggressive periodontitis in adolescent carriers of the JP2 clone of *Aggregatibacter (Actinobacillus) actinomycetemcomitans* in Morocco: a prospective longitudinal cohort study," *The Lancet*, vol. 371, no. 9608, pp. 237–242, 2008.

[32] N. Bostanci, R. P. Allaker, G. N. Belibasakis et al., "*Porphyromonas gingivalis* antagonises *Campylobacter rectus* induced cytokine production by human monocytes," *Cytokine*, vol. 39, no. 2, pp. 147–156, 2007.

[33] T. S. Miranda, M. Feres, B. Retamal-Valdés, P. J. Perez-Chaparro, S. S. Maciel, and P. M. Duarte, "Influence of glycemic control on the levels of subgingival periodontal pathogens in patients with generalized chronic periodontitis and type 2 diabetes," *Journal of Applied Oral Science*, vol. 25, no. 1, pp. 82–89, 2017.

[34] E. A. Babaev, I. P. Balmasova, A. M. Mkrtumyan et al., "Metagenomic analysis of gingival sulcus microbiota and pathogenesis of periodontitis associated with type 2 diabetes mellitus," *Bulletin of Experimental Biology and Medicine*, vol. 163, no. 6, pp. 718–721, 2017.

[35] J. A. F. Silva, M. Lorencini, J. R. R. Reis, H. F. Carvalho, V. H. A. Cagnon, and D. R. Stach-Machado, "The influence of type I diabetes mellitus in periodontal disease induced changes of the gingival epithelium and connective tissue," *Tissue & Cell*, vol. 40, no. 4, pp. 283–292, 2008.

[36] A. N. Gurav, "Management of diabolical diabetes mellitus and periodontitis nexus: are we doing enough?," *World Journal of Diabetes*, vol. 7, no. 4, pp. 50–66, 2016.

[37] C. M. Silva-Boghossian, S. R. P. Orrico, D. Gonçalves, F. O. B. Correa, and A. P. V. Colombo, "Microbiological changes after periodontal therapy in diabetic patients with inadequate metabolic control," *Brazilian Oral Research*, vol. 28, no. 1, pp. 1–9, 2014.

[38] H. P. C. Artese, P. L. Longo, G. H. Gomes, M. P. A. Mayer, and G. A. Romito, "Supragingival biofilm control and systemic inflammation in patients with type 2 diabetes mellitus," *Brazilian Oral Research*, vol. 29, no. 1, pp. 1–7, 2015.